Supplementary Information for:

Genetically Encoded Fragment-Based Discovery of Glycopeptide Ligands for Carbohydrate-Binding Proteins

Simon Ng, Edith Lin, Pavel I. Kitov, Katrina F. Tjhung, Oksana O. Gerlits, Lu Deng, Brian Kasper, Amika Sood, Beth M. Paschal, Ping Zhang, Chang-Chun Ling, John S. Klassen, Christopher J. Noren, Lara K. Mahal, Robert J. Woods, Leighton Coates, Ratmir Derda*

*Corresponding author: ratmir@ualberta.ca

Table of Contents (click on topic)

Abbreviation

bp	Base pair
BSA	Bovine serum albumin
ConA	Concanavalin A
DC-SIGN	Dendritic cell-specific intercellular adhesion molecule-3-grabbing non-integrin
DEPBT	3-(Diethoxyphosphoryloxy)-1,2,3-benzotriazin-4(3*H*)-one
DIC	*N,N′*-Diisopropylcarbodiimide
DIPEA	*N*,*N*-Diisopropylethylamine
DMAP	4-Dimethylaminopyridine
DMF	Dimethyl formamide
DMSO	Dimethyl sulfoxide
dsDNA	Double-stranded DNA
EDTA	Ethylenediaminetetraacetic acid
eq.	Equivalent
ESI	Electrospray ionization
Fmoc	Fluorenylmethyloxycarbonyl
h	Hour
HBTU	2-(1*H*-Benzotriazole-1-yl)-1,1,3,3-tetramethyluronium hexafluorophosphate
HOAt	1-Hydroxy-7-azabenzotriazole
HEPES	4-(2-Hydroxyethyl)piperazine-1-ethanesulfonic acid
HPLC	High-performance liquid chromatography
HRMS	High-resolution mass spectrometry
MeCN	Acetonitrile
min	Minute
MOPS	3-Morpholinopropane-1-sulfonic acid
MQ	Milli-Q
PBS	Phosphate buffered saline
PCR	Polymerase chain reaction
PDB	The Protein Data Bank
RP	Reversed phase
rpm	Revolutions per minute
RT	Room temperature
s	Second
STD	Saturation-transfer difference
ssDNA	Single-stranded DNA
tBu	*tert*-Butyl
TFA	Trifluoroacetic acid
TIPS	Triisopropylsilane

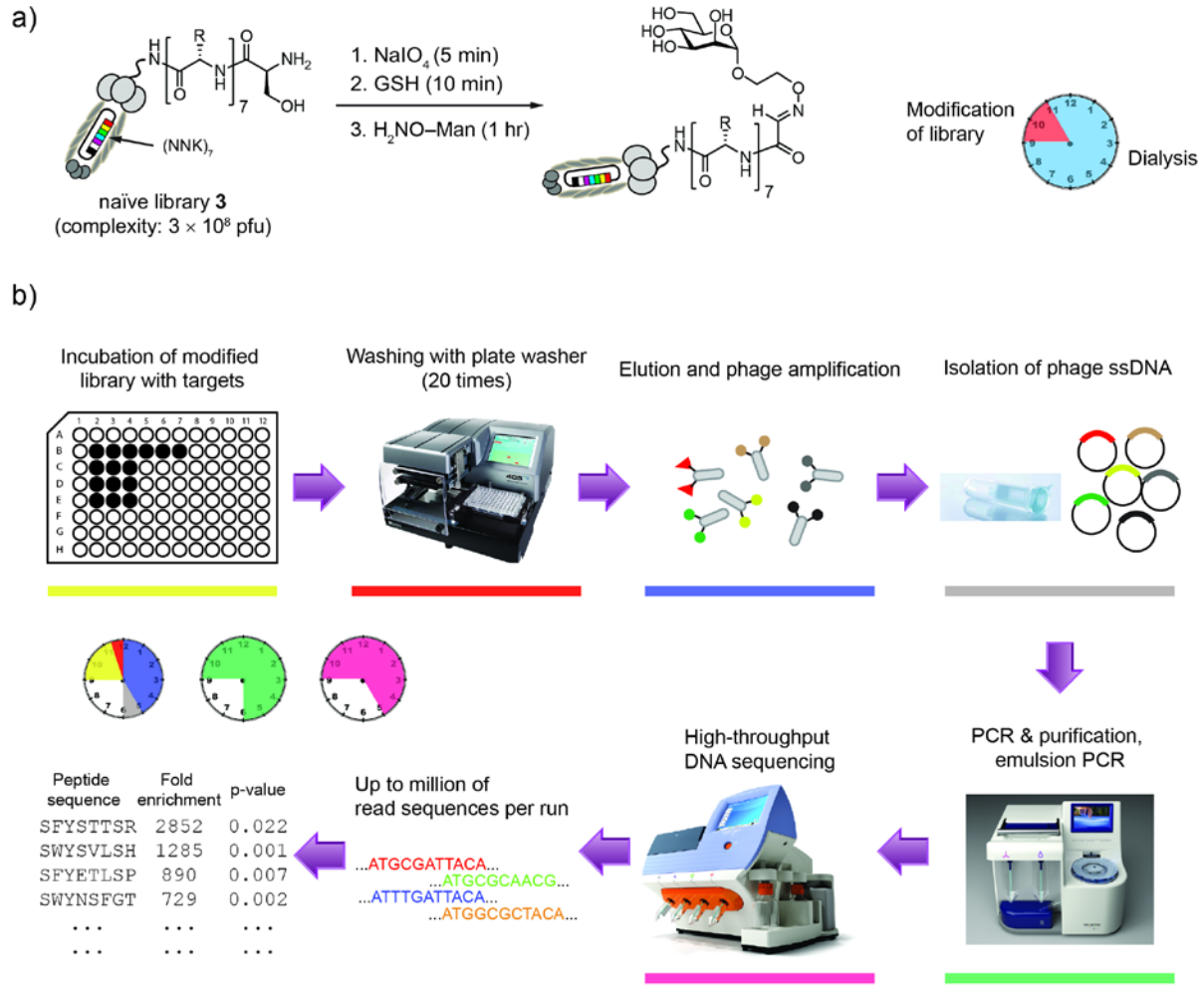

Figure S1. Overview of the workflow of ligand search.
The entire ligand search could be accomplished within a week. a) Modification of phage library and subsequent purification by dialysis required a day. b) Incubation of the modified library with targets on 96-well plate (yellow, 2 h); washing of plate (red, 0.5 h); elution and phage amplification (blue, 5 h); isolation of phage ssDNA (grey, 1 h); PCR of library DNA with 15-barcoded primers, E-Gel purification and template preparation on Ion OneTouch™ 2 System (green, one day); DNA sequencing with Ion PGM™ System (magenta, one day).

K_D ± S.D. (μM)	IC_{50} ± S.E. (μM)	86 Hit peptide sequences	Rank in **A** screen	Log(mean fraction)	Ratio of **A**/**B**	Ratio of **A**/**C**	Ratio of **A**/**D**
29.2		**SAWEAYWY**	1	-1.31	197	11	12
42.6	34.4	**SFYSTTSR**	2	-1.38	2852	12	1984
14.1	15.2	**SWYSVLSH**	5	-1.72	1285	963	894
15.9	14.2	**SFYETLSP**	7	-1.88	890	666	619
	15.2	**SWYNSFGT**	9	-1.97	729	546	507
		STYAWLDV	12	-2.25	547	57	6
		SLYDMNPL	14	-2.28	359	269	33
23.9		**SFYLGSDI**	16	-2.32	326	40	12
55.2		**SYWEFTSL**	19	-2.34	308	97	9
		SFYDQTYL	21	-2.36	293	220	204
20.9	16.1 ± 0.4	**SYYHNPNA**	39	-2.62	163	122	20
		SWYSHTLK	68	-2.94	78	58	54
11.1		**SYYDLMQT**	87	-3.06	59	44	41
		SYYSTSLA	89	-3.07	57	43	40
		SQSHWWQA	98	-3.1	54	7	6
		SSLALQMP	107	-3.12	51	38	36
		SWLTTHDT	108	-3.12	51	38	17
		SFYARSHS	119	-3.15	48	36	33
		SYYETNRI	120	-3.17	46	34	32
		SLPMHIKI	126	-3.19	44	17	31
		SFYDRFNS	137	-3.24	39	29	27
		STQGVGSD	142	-3.25	38	28	26
		SMMSKATT	150	-3.3	22	33	24
17.2	10.9 ± 0.2	**SFYDTIPD**	171	-3.35	30	23	21
		SWFQPLNL	189	-3.41	27	20	19
		SWYQITAS	196	-3.43	25	19	17
		SWYSVHQP	214	-3.47	23	17	16
		SWYSSPLY	233	-3.5	22	16	15
		SWYRDMDV	236	-3.51	21	16	15
		SWYSTIRT	273	-3.57	18	14	13
		SRGPAHQY	288	-3.59	17	13	12
		SIELFPYK	289	-3.59	17	13	12
		SWYASIPI	294	-3.6	17	13	12
		SWYSLMDK	296	-3.6	17	13	12
		SWFESALT	298	-3.61	17	13	12
		SWYHLNSA	299	-3.61	17	13	12
		STPFYVRY	300	-3.61	17	13	12
		SWLQMARD	314	-3.63	16	12	11
		SWYTLPSQ	325	-3.65	15	11	11
		SWYRTPVI	345	-3.67	15	11	10
		SWYMTQPG	346	-3.67	15	11	10
		SWYDHATT	354	-3.68	14	11	10
		SWYDSLPD	356	-3.68	14	11	10
		SWYSFRTP	363	-3.69	14	10	10
		SYYDRPYS	370	-3.69	14	10	10
		SWYEQTSR	373	-3.69	14	10	10
		SFYAVQPA	379	-3.7	14	10	10
		SWYLDHSD	381	-3.7	14	10	9
		SKVTDPYS	382	-3.7	13	10	9
		SWYHAMLP	394	-3.72	13	10	9
		SYYDRASN	396	-3.72	13	10	9
		SPYSIPSA	402	-3.72	13	10	8
		SWYHQVHP	410	-3.72	13	10	9
		SYYESSLF	442	-3.76	12	9	8
		SYYESLSH	446	-3.76	12	9	8
		SWYALPRT	455	-3.77	12	9	8
		SWYHRTPI	456	-3.77	11	9	8
		SWYSTLAA	470	-3.79	11	8	8
		SWYGARPQ	473	-3.79	11	8	8
		SSWPALYG	484	-3.8	11	8	7
		SWYASATA	487	-3.81	11	8	7
		SRTIPHTD	494	-3.82	10	8	7
		SWYSQLLV	500	-3.83	10	8	7
		SWYEVARV	510	-3.84	10	7	7
		SWYADTRT	516	-3.85	10	7	7
		SWYQVVHP	521	-3.85	10	7	7
		SWYMNPLT	523	-3.85	9	7	7
		SWYADALV	528	-3.86	9	7	7
		SWYSEPMT	532	-3.86	9	7	6
		SWYAYPPD	533	-3.86	9	7	6
		SWYETPSA	566	-3.89	9	6	6
		SWYNLTAS	568	-3.89	9	6	6
		SWYKNPMS	594	-3.92	8	6	6
		SWYDTSHP	599	-3.92	8	6	6
		SYYEMYPS	611	-3.93	8	6	5
		SWYEVVSN	613	-3.94	8	6	5
		SYYEQVTL	614	-3.94	8	6	5
		SWYDDPFH	626	-3.94	8	6	5
		SWYDTLAG	633	-3.94	8	6	5
		SSSSDFPY	644	-3.96	8	6	5
		STLTGELV	654	-3.96	7	6	5
		SWYSHNTN	659	-3.96	7	6	5
		SNPDPYTP	661	-3.96	7	6	5
		SPSIPTPI	669	-3.97	7	6	5
		SWYAVPHN	671	-3.97	7	5	5

Table S1. Complete list of peptide sequences identified from three sets of volcano plot.
From the first round of selection using Man-X_7 library, a total of 86 peptide sequences was identified and they reside at the "intersection" of three pair-wise volcano analysis (see Figure 2B).

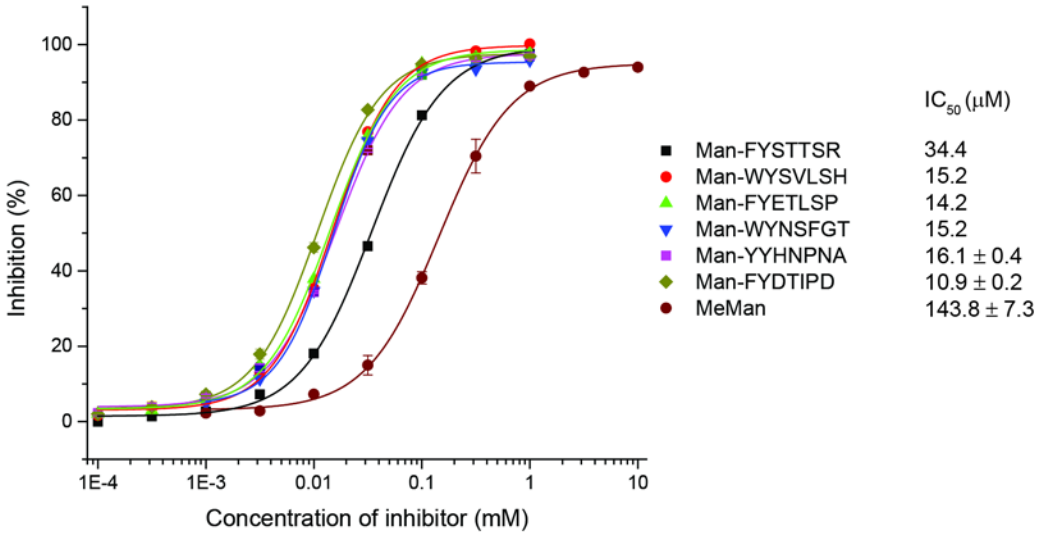

Figure S2. Inhibition curves of Man-X_7 conjugates.

Inhibitions of ConA (200 μg/mL) binding to the dextran-coated surface (CM5 chip) were measured with surface plasmon resonance using Man-X_7 conjugates or methyl α-D-mannopyranoside (MeMan) as the inhibitor. IC_{50} values with standard error were measured in three independent experiments.

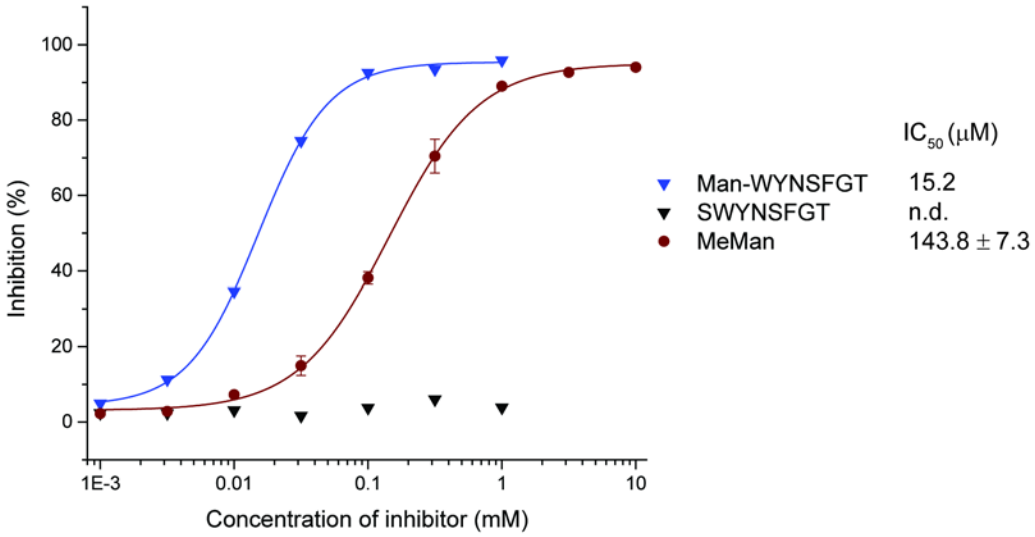

Figure S3. Inhibition curves of Man-WYNSFGT and SWYNSFGT.
Inhibitions of ConA (200 μg/mL) binding to the dextran-coated surface (CM5 chip) were measured with surface plasmon resonance using Man-X_7 conjugate, Ser-X_7 or MeMan as the inhibitor. IC_{50} of SWYNSFGT was not determined (n.d.) due to insignificant inhibition even with inhibitor concentration as high as 1 mM. IC_{50} values with standard error were measured in three independent experiments.

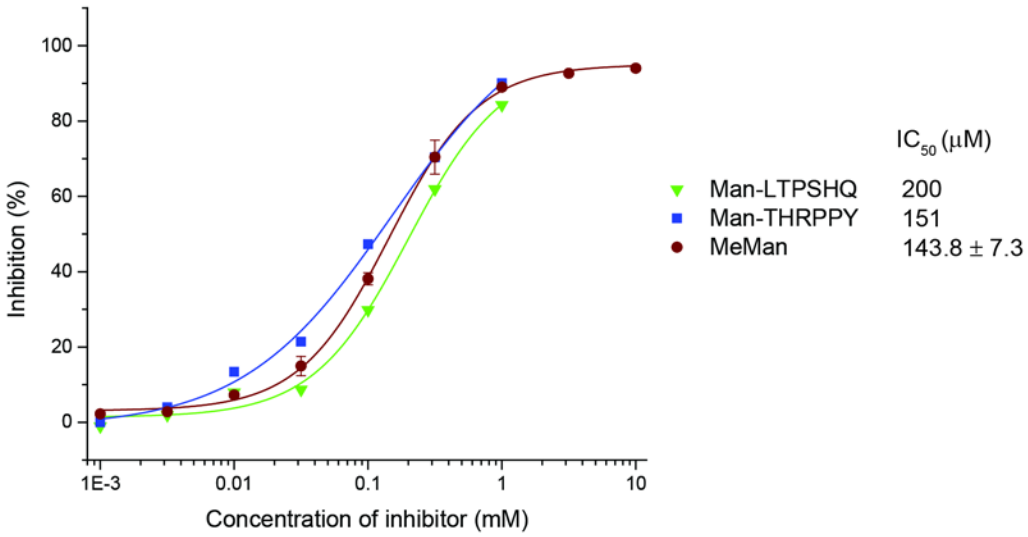

Figure S4. Inhibition curves of control ligands.

Inhibitions of ConA (200 μg/mL) binding to the dextran-coated surface (CM5 chip) were measured with surface plasmon resonance using Man-X_6 conjugates or MeMan as the inhibitor. These conjugates have IC_{50} values similar to that of MeMan suggested that the inhibition mainly stem from the mannopyranosyl moiety and is independent of the peptide moiety. IC_{50} values with standard error were measured in three independent experiments.

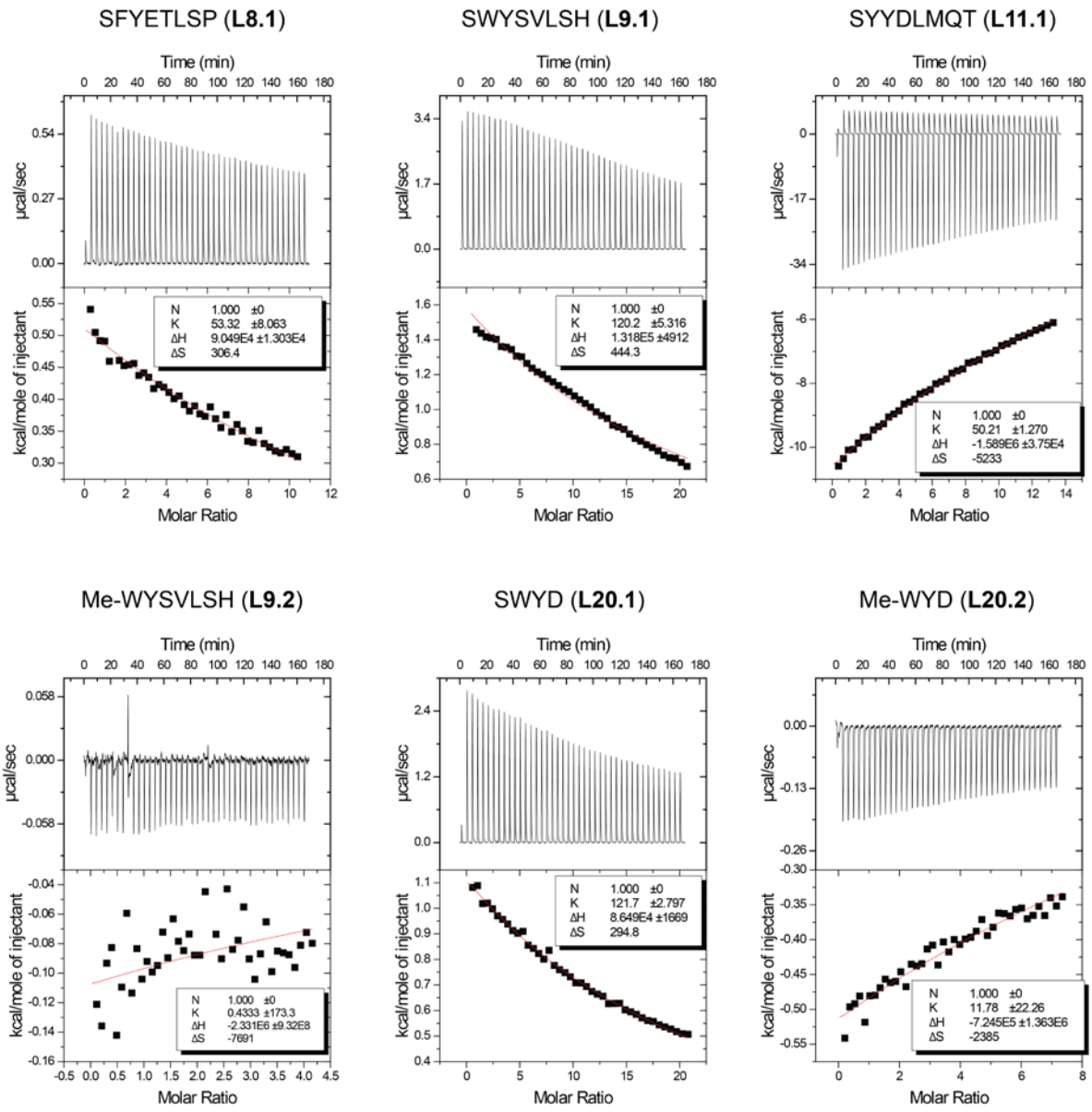

Figure S5. Raw ITC data of peptide fragments.

Raw data obtained for 42 injections of ligands (2 mM for **L9.2**, **L20.2**; 5 mM for **L8.1**; and 10 mM for **L9.1**, **L11.1** and **L20.1**) into a solution of ConA (0.1 mM–0.20 mM) at 4-min intervals and 30 °C. The integrated curve showed experimental points (■) and the best fit (–) to the points by a nonlinear least-squares regression algorithm. The fitting were performed by fixing the stoichiometry of binding to one. It is important to note that, the determination of *K*a, ΔH and ΔS in these experiments are inaccurate since they were performed with *c* values much lower than one, because the preparation of ConA with concentration >>1 mM is difficult due to solubility issue. In these cases, it is safe to assume that the K_D values of these peptide fragments are much greater than 1 mM.

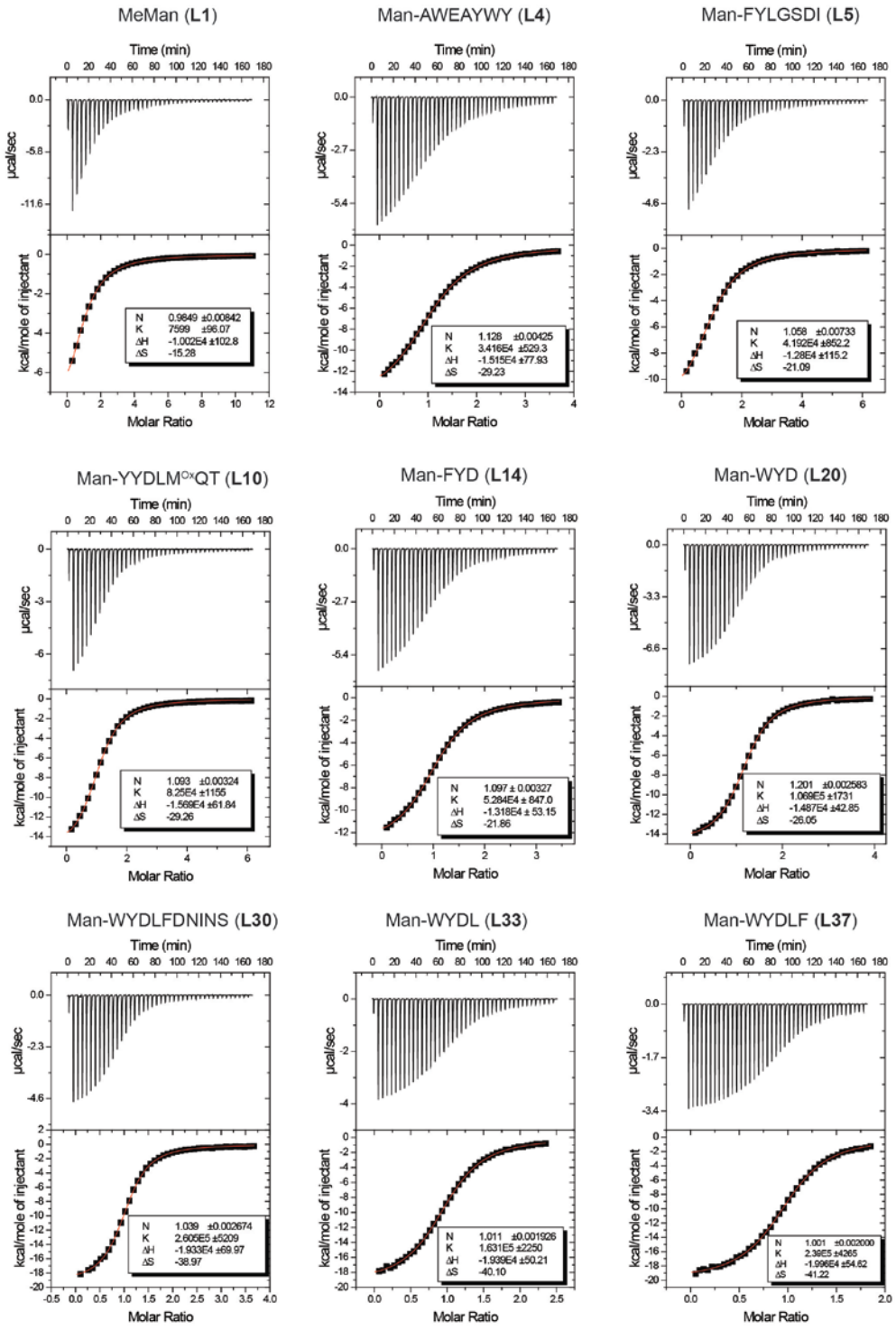

Figure S6. Examples of raw ITC data of ConA binders.

Selected examples of raw data obtained for 42 injections of ligands (2 mM for **L4**, **L5**, **L10**, **L14**, and **L20**; 1 mM for **L30**, **L33** and **L37**; and 10 mM for **L1**) into a solution of ConA (0.07 mM–0.30 mM) at 4-min intervals and 30 °C. The integrated curve showed experimental points (■) and the best fit (–) to the points by a nonlinear least-squares regression algorithm.

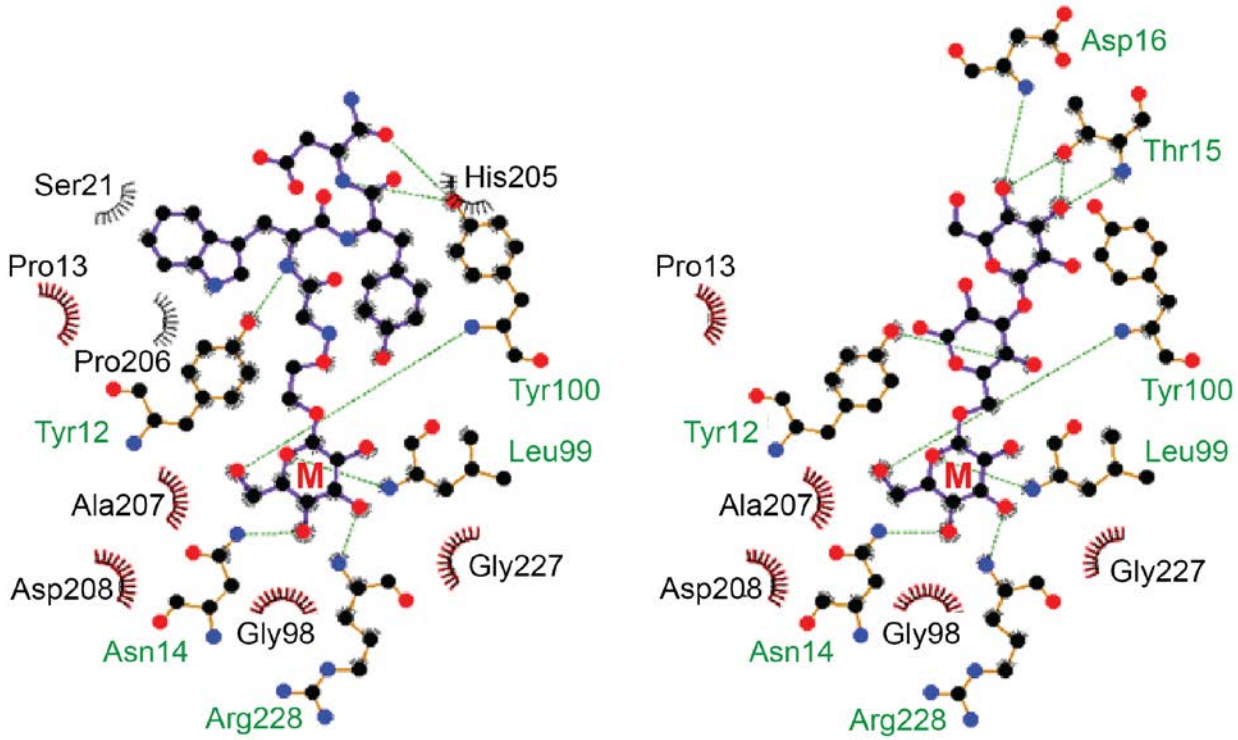

Figure S7. Contact analysis of ConA bound to Man-WYD and to Man3.
The two equivalent Man residues (labeled with "M"), originated from Man-WYD (left) or Man3 (right), displayed equivalent hydrogen-bonding patterns (Arg228 NH to O3, Asn14 side chain NH to O4, Leu99 NH to O5, and Tyr100 NH to O6). In contrast to Man3, the Man-WYD forms few additional hydrogen bonds, and prefers to van der Waals contacts with the protein surface. This is as shown by a higher contact area of synthetic ligand (662 Å) compared to the trisaccharide Man3 (204 Å).

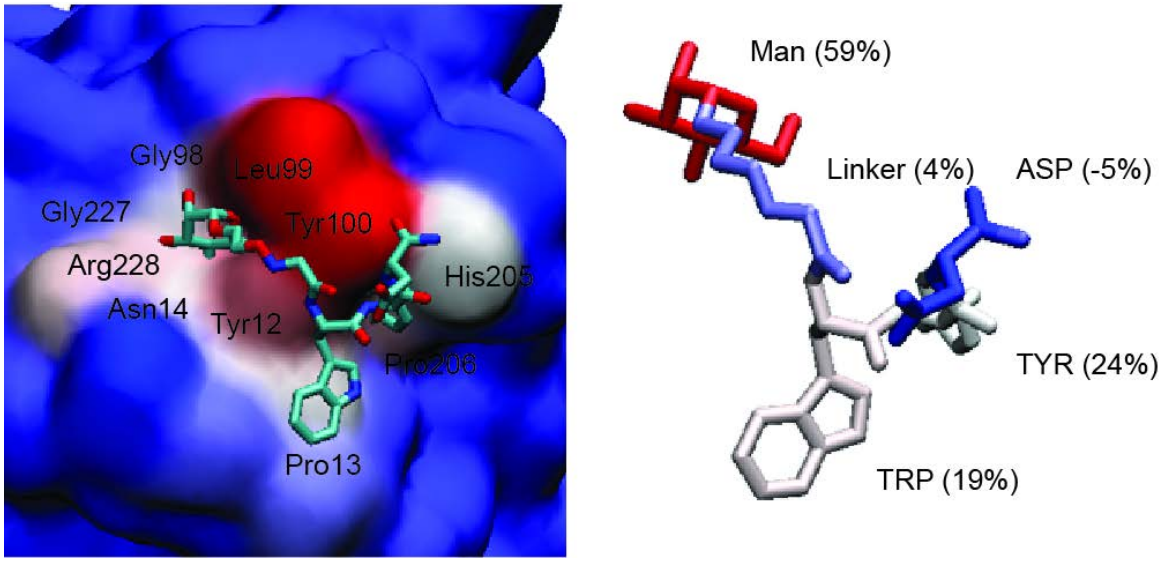

Figure S8. Binding free energy analysis of ConA bound to Man-WYD.
Strength of interaction energies scaled from red (strongest) to blue (weakest) in the protein (left) and in the ligand, with percent contribution shown in parentheses (right).

Table S2. Binding free energy analysis estimated by MD simulation.
Average per-residue binding energy[a] contributions for key[b] residues in the protein and the ligand

Residue	van der Waals	Electrostatic	Polar Desolvation	Nonpolar Desolvation	Total
Protein					
Tyr100	-3.9	-2.9	3.6	-0.4	-3.6
Leu99	-2.5	-2.1	1.4	-0.3	-3.5
Asp208	1.1	-9.4	5.5	0.0	-2.9
Tyr12	-4.1	-1.4	3.3	-0.5	-2.7
Pro206	-0.3	-4.3	2.4	-0.1	-2.3
Gly98	-1.1	-2.8	1.8	-0.1	-2.2
Arg228	-1.1	-10.0	9.3	-0.1	-2.0
Pro13	-2.3	-0.2	0.9	-0.3	-1.8
Asn14	-0.3	-3.1	1.9	-0.1	-1.5
His205	-2.7	-2.4	4.0	-0.3	-1.5
Gly227	-0.9	-1.1	0.7	-0.1	-1.5
Ala207	-0.8	0.5	-0.5	0.0	-0.8
Ser21	-0.8	-0.3	0.8	-0.2	-0.5
Thr97	-0.4	0.1	-0.2	0.0	-0.5
Ligand					
Man	-8.2	-43.0	37.3	-1.6	-15.5
TYR	-6.4	-7.7	9.0	-1.2	-6.2
TRP	-5.8	-3.6	5.4	-1.0	-4.9
Linker	-2.9	11.2	-8.7	-0.3	-1.0
ASP	-0.5	42.2	-40.3	-0.1	1.3

[a] In kcal/mol
[b] Residues that contribute greater than 0.5 kcal/mol to the total binding energy.

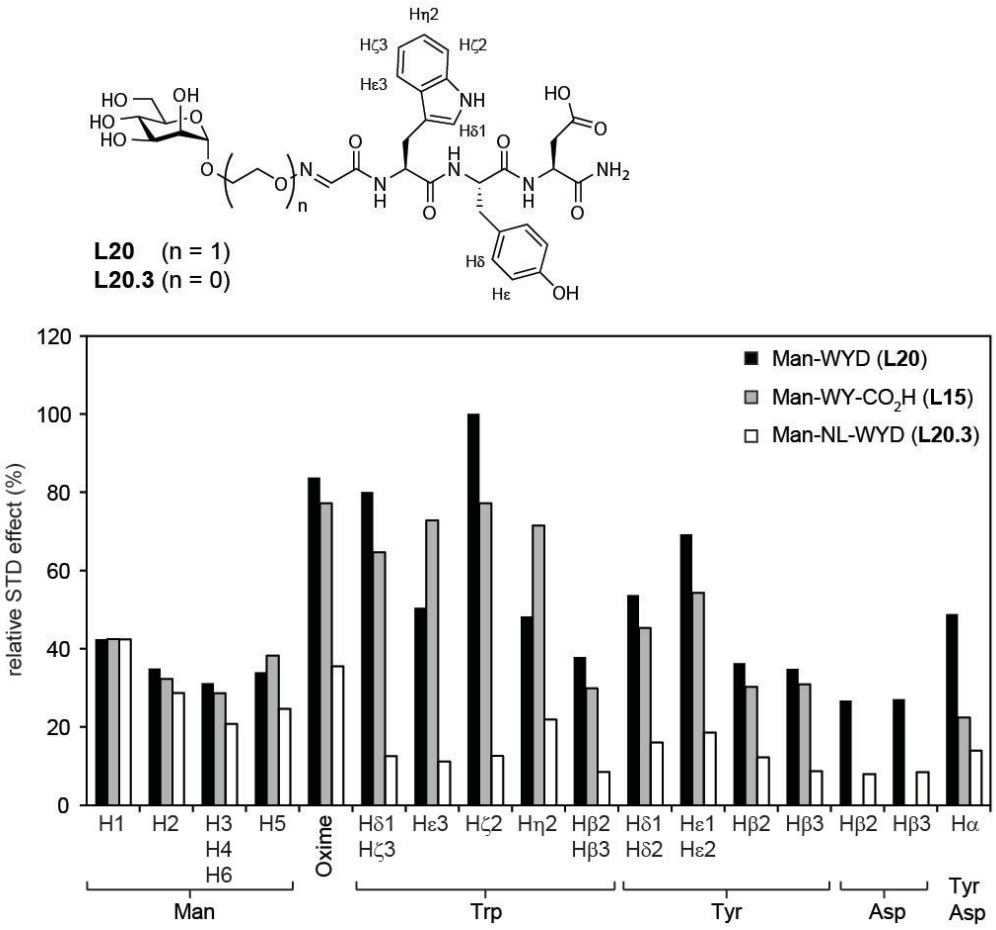

Figure S9. STD-NMR analysis of interaction between ConA and three glycopeptides.
We hypothesized that oxime functionality might be involved in molecular recognition. STD-NMR[1] detected significant contacts between ConA and the protons of the oxime, as well as Tyr and Trp of **L20** and **L15.** Both oxime and the aromatic rings play significant roles in the interaction of the ligand with the protein (Figure 3). The same protons in the control ligand (**L20.3**) exhibited much weaker signal in the STD-NMR, and, thus, significantly less contact with the protein. These results were in-line with the ITC measurements and crystallographic data. The shortened linker ablates the geometry necessary for synergistic binding. To facilitate the ligand comparison, Man H1 of **L20.3** was set as the reference and normalized to 42% (same for **L20** and **L15**). The relative STD effects for other protons were then calculated based on this reference proton. The STD effect of Trp Hα was not determined due to the complete attenuation of its signals by WATERGATE W5 sequence.[2]

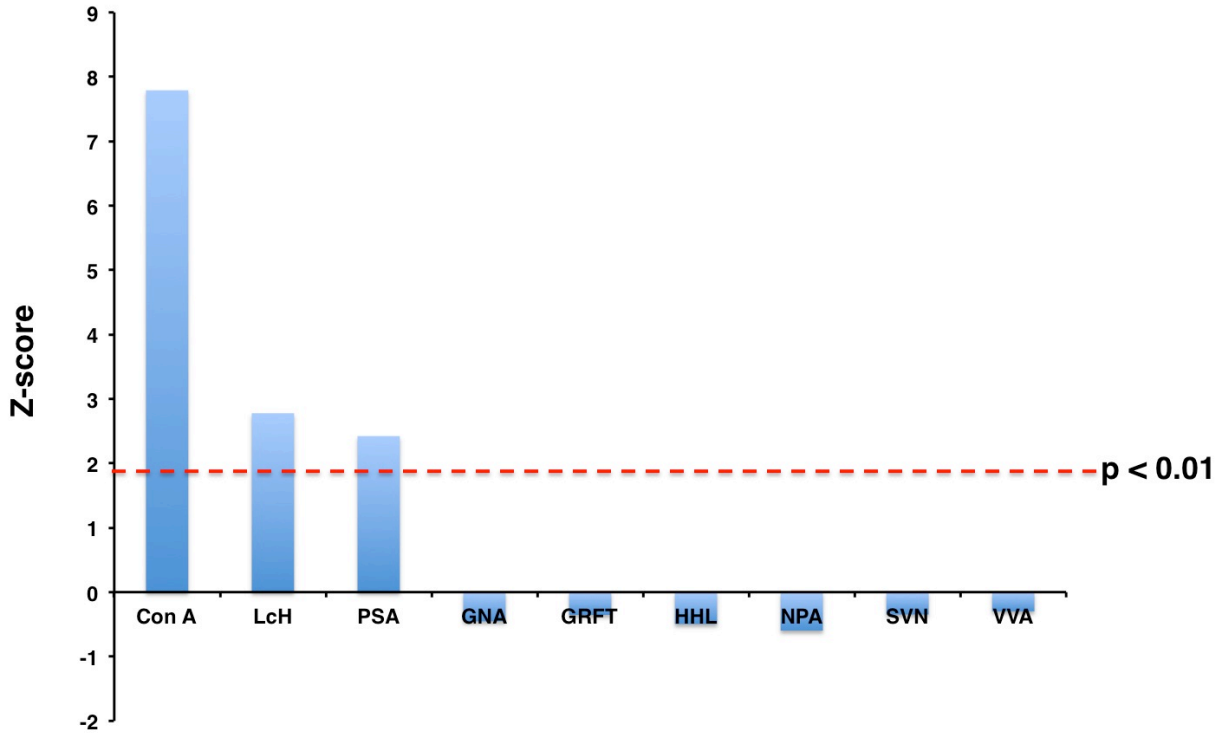

Figure S10. Lectin microarray analysis.
Z-scores for mannose-binding lectins from a lectin microarray incubated with 1.85 μM Cy3-labeled Man-WYK-OH are shown. The $p < 0.01$ cutoff is indicated (red dashed line, Z=1.95). Of the 85 lectins tested, only ConA, LcH, and PSA met this significance threshold, while other mannose-binding proteins (GNA, GRFT, HHL, NPA, SVN, and VVA, see Table S3 for details) did not.

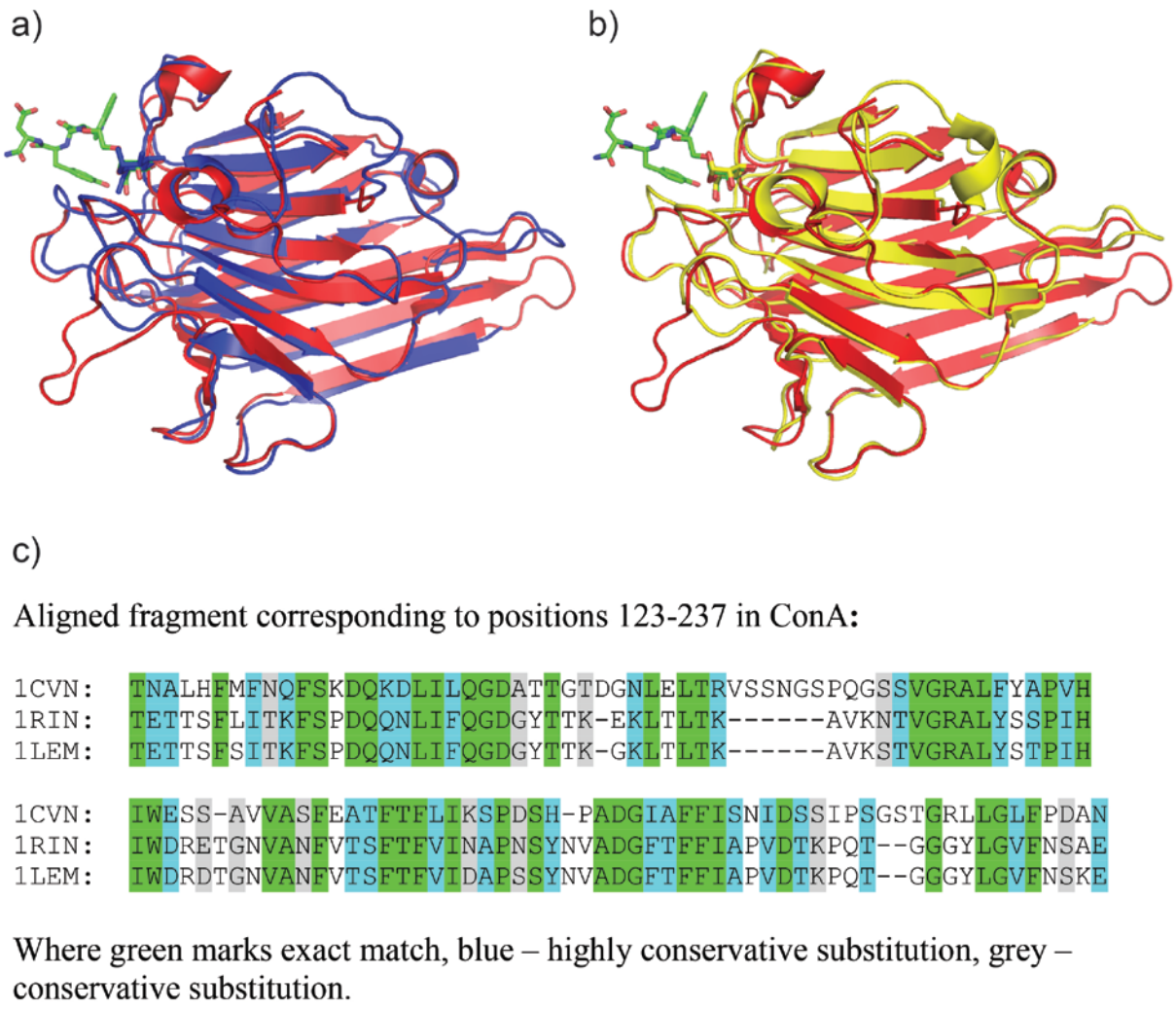

Figure S11. Sequence and structure homology of ConA/LcH or ConA/PSA.

a) Superimposition of Man-WYD–ConA complex (red, PDB: 4CZS) with the Glc–LcH complex (blue, PDB: 1LEM), generated by aligning the protein backbone atoms (RMSD = 0.81 Å). b) Superimposition of Man-WYD:ConA complex (red, PDB: 4CZS) with the Man–PSA complex (yellow, PDB: 1RIN), generated by aligning the protein backbone atoms (RMSD = 0.76 Å). c) Multiple sequence alignment of ConA (PDB: 1CVN), PSA (PDB: 1RIN), and LcH (PDB: 1LEM) using Clustal Omega from EMBL-EBI.[3]

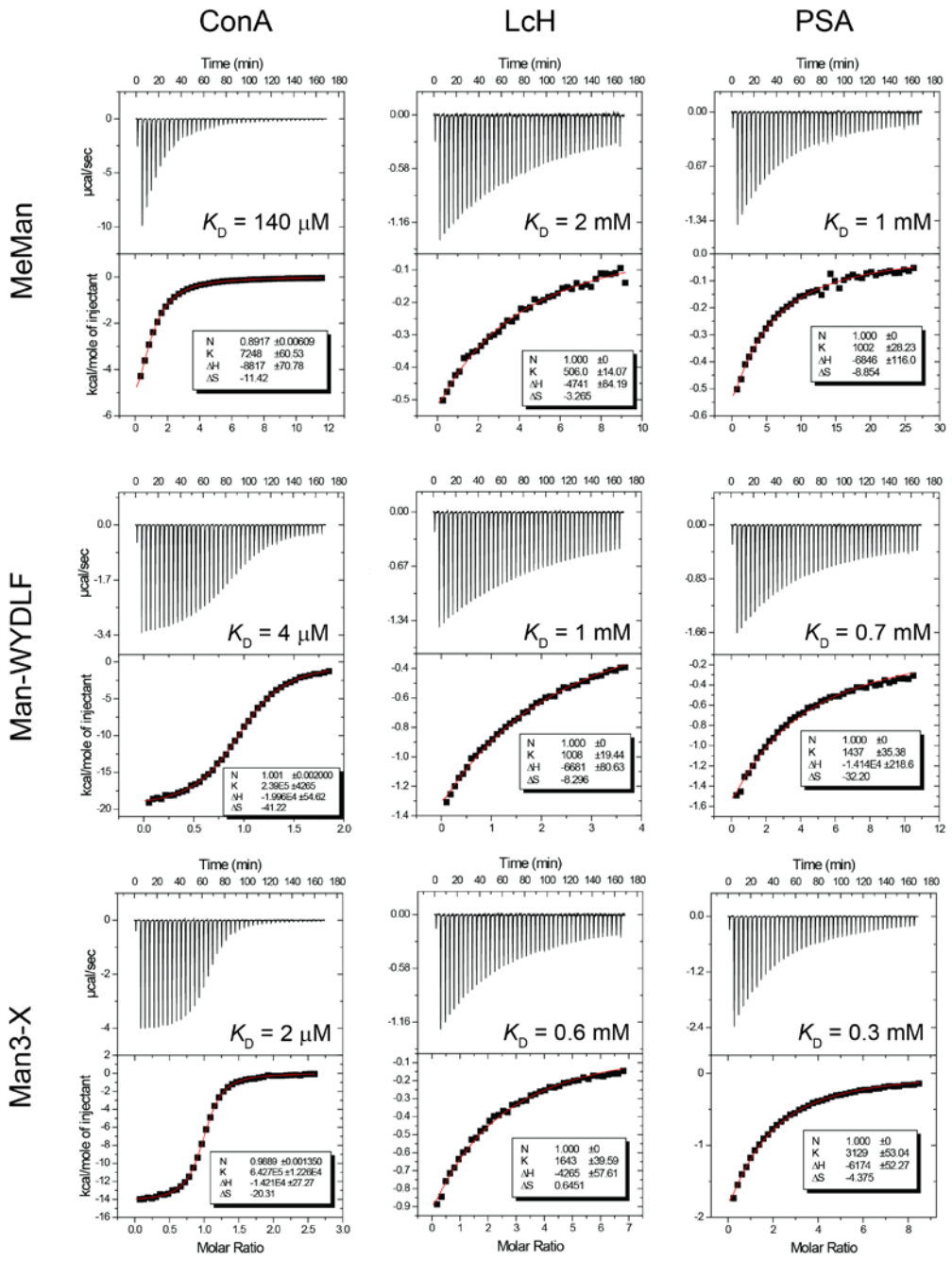

Figure S12. Raw ITC data of MeMan, Man-WYDLF, and Man3-X binding to ConA, LcH and PSA. Raw data obtained for 42 injections of ligands (10 mM for MeMan; 1–4 mM for Man-WYDLF; 1–5 mM for Man3-X) into a solution of ConA (0.19 mM), LcH (0.24 mM) or PSA (0.09 mM) at 4-min intervals and 30 °C. The integrated curve showed experimental points (■) and the best fit (–) to the points by a nonlinear least-squares regression algorithm. The stoichiometry parameter, N, was fixed at 1.0 for $c \leq 1$ but allowed to float freely for $c > 1$. The K_D of MeMan binding to ConA, LcH or PSA measured on our hands at 30 °C correlate linearly with the literature values measured at 19 °C, i.e., ConA: 140 µM vs. 83 µM,[4] LcH: 2 mM vs. 1.2 mM,[4] and PSA: 1 mM vs. 0.5 mM.[4]

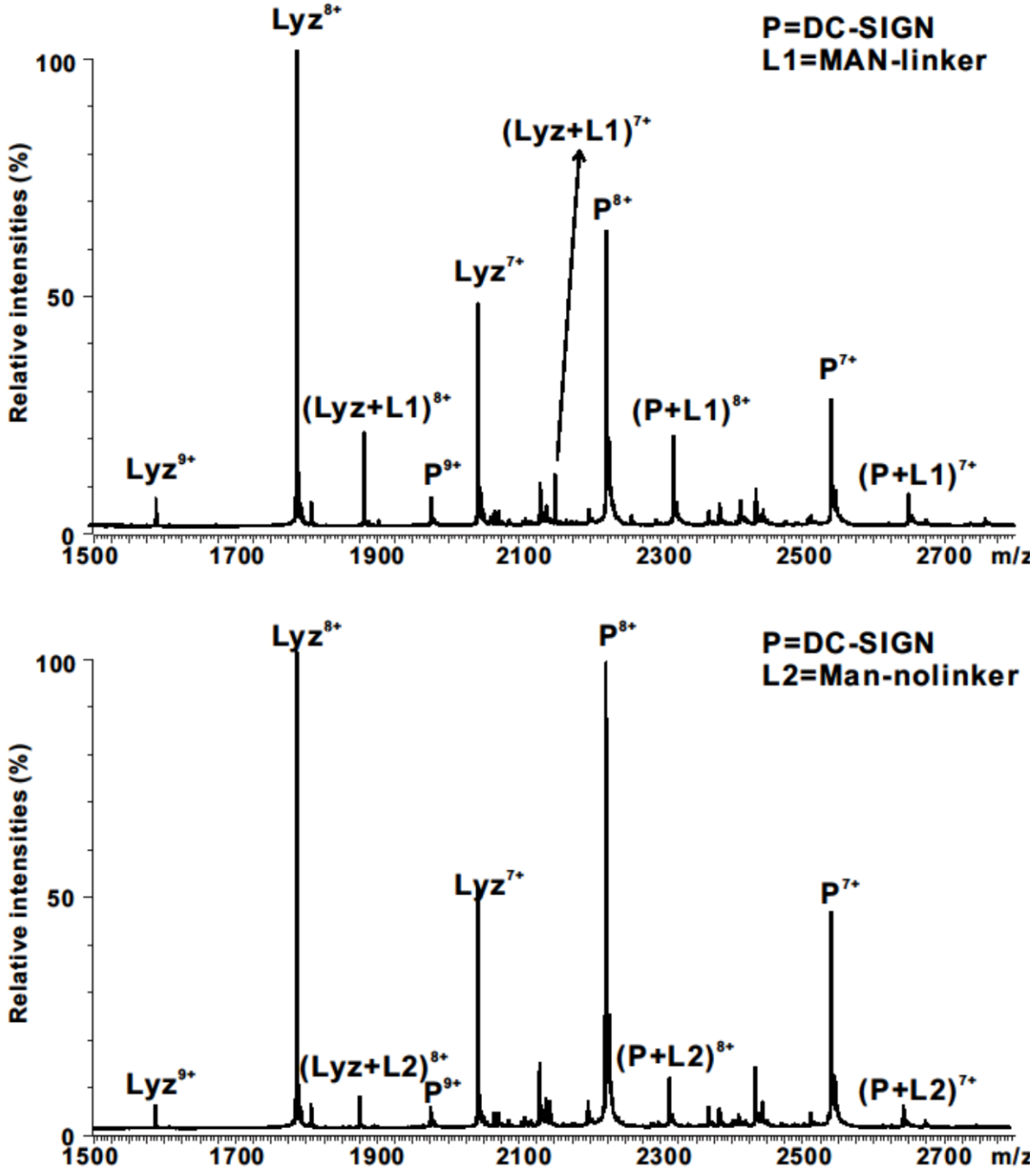

Figure S13. ESI-MS binding measurement for DC-SIGN.

The mass spectra of ESI-MS binding measurement for DC-SIGN. Top spectrum: Man-WYD (**L20**); bottom spectrum: Man-NL-WYD (**L20.3**). The measured K_D of **L20** and **L20.3** are 600 ± 7 μM and 1890 ± 40 μM respectively.

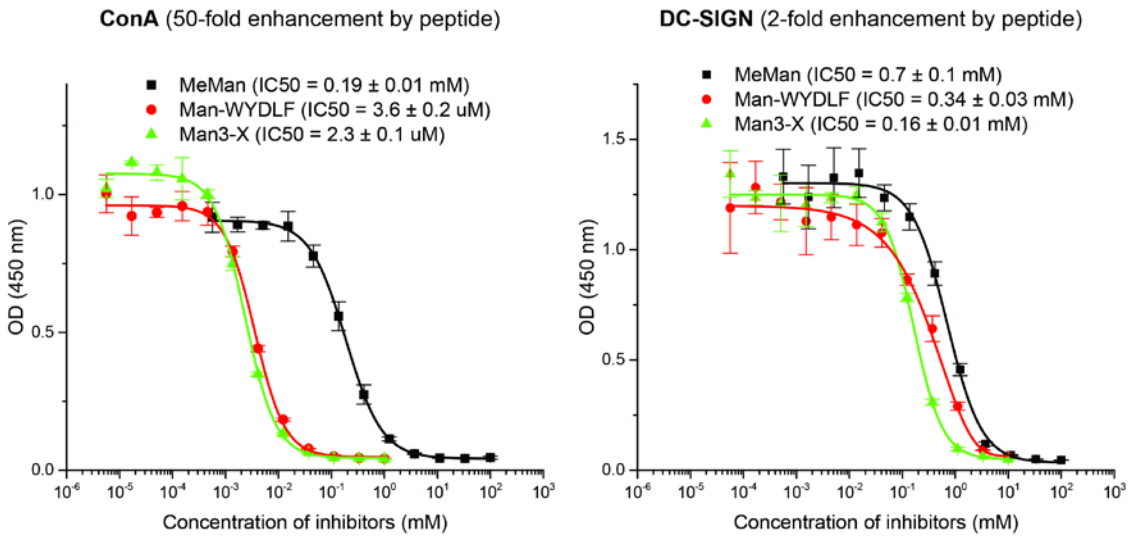

Figure S14. Inhibition curves of ConA and DC-SIGN mediated by MeMan, Man-WYDLF and Man3-X.

MeMan, Man-WYDLF, and Man3-X competitively inhibit the binding of glycoprotein probe, horseradish peroxidase (HRP), which contains trimannoside core, to immobilized ConA (left panel) or immobilized tetrameric extracellular domain of DC-SIGN (right panel). The monosaccharide couples synergistically with the peptide fragment and decreases the half maximal inhibitory concentration (IC_{50}) by more than 50-fold for ConA but only 2-fold for DC-SIGN. The results indicate a selective activity enhancement of the peptide fragment for ConA. The absorbance at 450 nm (OD = optical density) is a mean value measured in three independent wells with the error represents one standard deviation of the mean.

a)

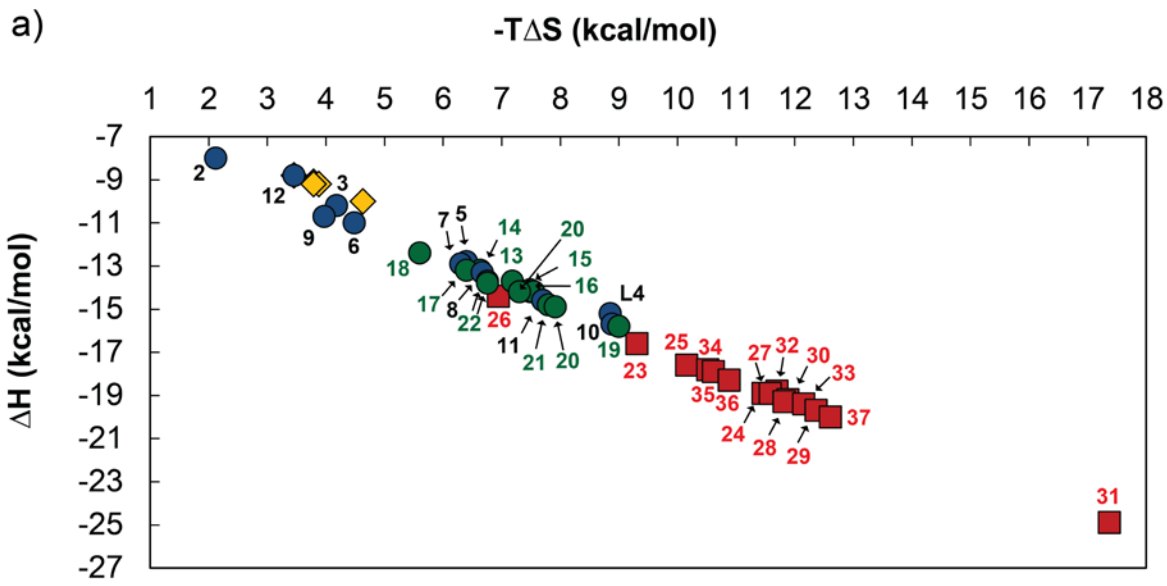

b)

	Ligand	K_D		Ligand	K_D		Ligand	K_D
L1	MeMan	137.4 ± 6.1	**L13**	Man-YYD	20.1	**L23**	Man-WYDANHSKPL	6.0
L2	Man-YWEFTSL	55.2	**L14**	Man-FYD	18.9	**L24**	Man-WYDRQETRFR	4.6
L3	Man-FYSTTSR	42.6	**L15**	Man-WY-OH	17.1 ± 0.4	**L25**	Man-WYDLHHSRTR	4.5
L4	Man-AWEAYWY	29.2	**L16**	Man-WYS	14.3	**L26**	Man-WYDLYHPVQH	4.3
L5	Man-FYLGSDI	23.9	**L17**	Man-WYA	13.5	**L27**	Man-WYELLDDDIT	5.3
L6	Man-YYHNPNA	20.9	**L18**	Man-WYH	12.7	**L28**	Man-WYDQFPPLHQ	5.1
L7	Man-FYDTIPD	17.2	**L19**	Man-WY	12.0	**L29**	Man-WYDNFDTIFA	5.0
L8	Man-FYETLSP	15.9	**L20**	Man-WYD	10.0 ± 0.9	**L30**	Man-WYDLFDNINS	3.8
L9	Man-WYSVLSH	14.1	**L21**	Man-WYE	9.6	**L31**	Man-WYDRFPPHES	3.7
L10	Man-YYDLM^{ox}QT	12.0	**L22**	Man-WYG-OH	9.8 ± 1.1	**L32**	Man-WYDR	7.5
L11	Man-YYDLMQT	11.1				**L33**	Man-WYDL	6.1
L12	Man-HTHDSVE	151.5				**L34**	Man-WYDFF	5.8
						L35	Man-WYEIF	5.3
						L36	Man-WYDRF	4.9
						L37	Man-WYDLF	4.2

Figure S15. Summary of thermodynamic data and affinity.

a) Enthalpy and entropy of the binding of glycopeptides and MeMan to ConA measured with ITC. Orange diamonds (◆) are MeMan (n = 5). Blue circles (●) are ligands selected from first round. Green circles (●) are truncations of ligands from the first round. Red squares (■) are ligands selected from second round (affinity maturation) and their truncations. b) Summarized table of the K_D of ligand interaction with ConA derived from the ITC data.

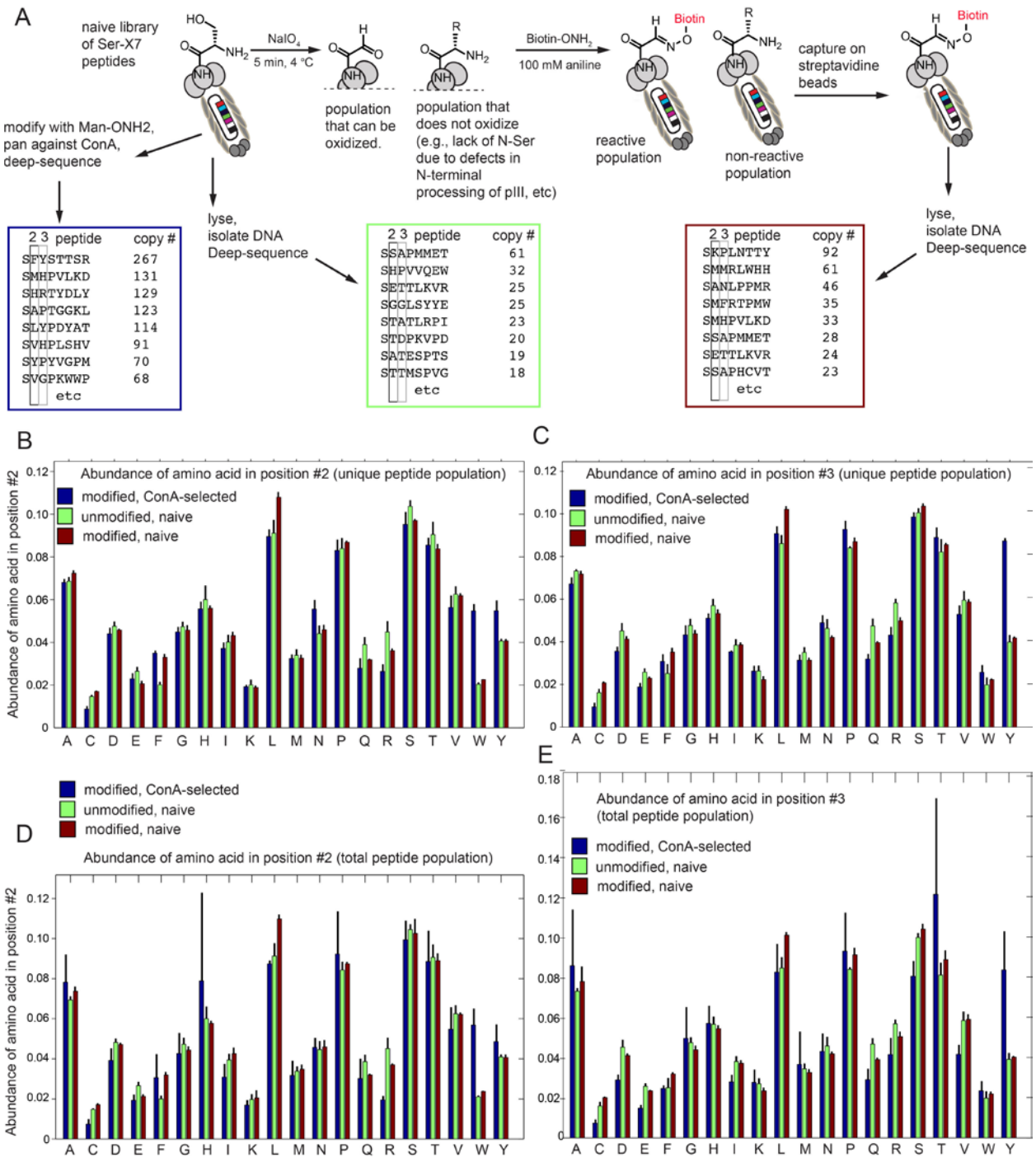

Figure S16. Positional abundance of amino acids in phage-displayed peptide libraries.
(A) To demonstrate that the enrichment of a specific amino acid in a specific location does not result from sequence bias in chemically-modified libraries, we compared amino acid composition in a population selected against ConA (blue) to naïve population (green) and biotin-modified population (crimson). The population selected against ConA was obtained as described in the main text. To analyze the sequences present in the chemically-modified population, we oxidized the library, ligated aminooxy biotin (AOB), captured the biotinylated phage on streptavidin-coated beads and deep-sequenced the captured population

(ca. 10^8 clones). In these conditions, all biotin-modified phage should be captured and sequenced irrespective of their displayed peptides. To sequence naïve library, we isolated and deep-sequenced DNA from 10^9 clones in naïve library (number of independently processed and deep-sequenced replicates: n=6 for ConA-selected library, n=3 for naïve, n=3 for biotin-modified naïve)

(B-C) The height of each bar is proportional to the average positional abundance of 2^{nd} (B) and 3^{rd} (C) amino acids in a population of unique sequences. Error bar is equal to one standard deviation. (C-D) The height of bars describes the same average positional abundance in a population of total sequences (each unique sequence was multiplied by its copy number). As anticipated from our selection, W and Y are abundant in 2^{nd} (B, D) and 3^{rd} (C, E) positions respectively in the ConA-selected library (blue). On the other hand, naïve non-modified and biotin-modified libraries exhibit no differences in positional abundance with one, minor exception: Leucine in position 2 is more abundant in modified library (crimson L-bar in B and D) compared to naïve library.

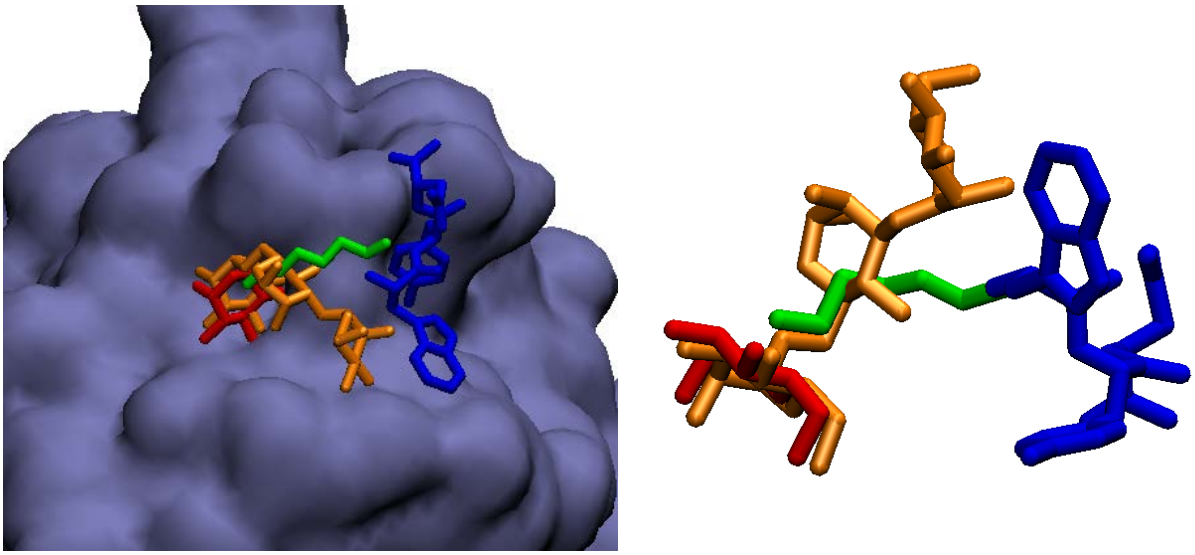

Figure S17. Comparison of the ligand-binding modes.

Left, superimposition of the ConA-trimannoside (α-Man-(1→3)-[α-Man-(1→6)]-α-Man, orange) complex (PDB ID: 1CVN) with the present crystal structure of the glycopeptide ligand (red: Man, green: linker, blue: peptide), generated by aligning the protein backbone atoms. Right, overlay of the endogenous and synthetic ligands.

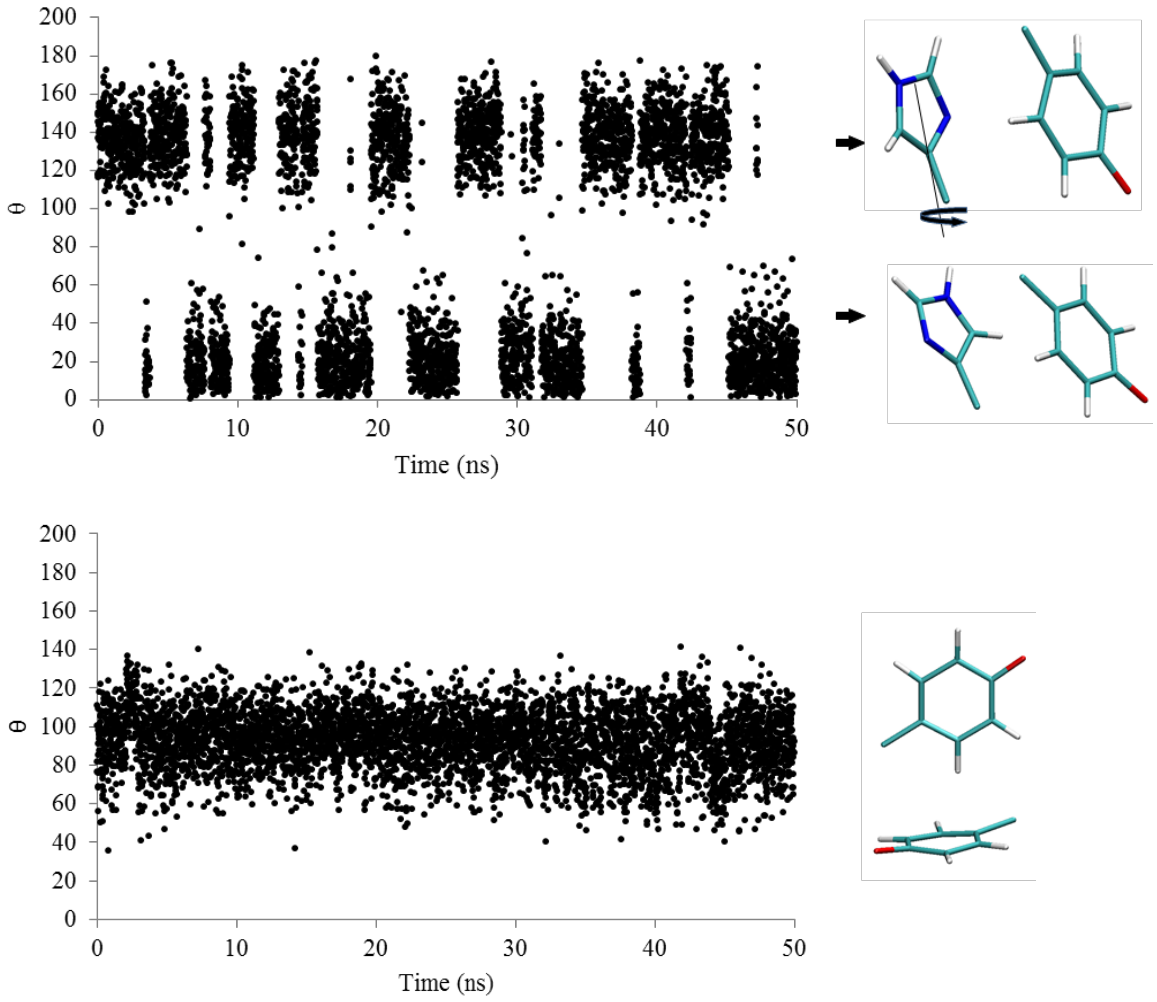

Figure S18. MD simulation of aromatic stacking between Man-WYD and ConA.
Aromatic stacking between His205 in the protein (blue) and TYR in the ligand (top), and Tyr100 in the protein (blue) and TYR in the ligand (bottom).

Table S3. List of 85 lectins printed on microarray.

Abbreviation	Lectin source	Print conc. µg/ml	Inhibitory mono-saccharide	Rough specificity
AAA	*Anguilla anguilla*	1000	Fuc	α-Fuc
AAL	*Aleuria aurantia*	500	Fuc	Fuc
AOL	*Aspergillus oryzae*	1000	Fuc	Fucα1-6 (core fucosylation), Fucα1,2Gal
UEA-I	*Ulex europaaeus I*	500	Fuc	Fucα1-2Galβ1-4GlcNAc
PTLII	*Psophocarpus tetragonolobus*	1000	Gal	β-GalNAc, Type II Blood H
TJA-II	*Trichosanthes japonica*	500	Lac	Fuca1-2Galb1-3/4GlcNAc, GalNAcβ1-4Galβ1
PSA	*Pisum sativum*	500	Man	Man
CCA	*Cancer antennarius*	1000	Lac	9-O-Acetyl NeuAc and 4-O-Acetyl NeuAc
LFA	*Limax flavus*	500	Lac	α -NeuAc (O-glycans)
LPA	*Limulus polphemus*	500	Lac	α -NeuAc
MAA	*Maackia amurensis*	500	Lac	NeuAcα2-3LacNAc
MAL-I	*Maackia amurensis - I*	1000	Lac	NeuAcα2-3LacNAc
MAL-II	*Maackia amurensis - II*	1000	Lac	NeuAcα2-3LacNAc
PSL	*Polyporus Squamosus*	500	Lac	NeuAcα-2-6LacNAc
SNA	*Sambucus nigra*	500	Lac	NeuAcα-2-6, (Lac core)
TJA-I	*Trichosanthes japonica*	1000	Lac	NeuAca2-6LacNAc or 6-Sulfo LacNAc.
PHA-L	*Phaseolus vulgaris-L*	500	Gal	Complex triantennary N-linked glycans
ECA	*Erythrina cristagalli*	500	Gal	GalNAcβ1-4GlcNAc, Galβ1-4GlcNAc
RCA	*Ricinus communis agglutinin B*	1000	Lac	Terminal β-Gal, terminal LacNAc
PHA-E	*Phaseolus vulgaris-E*	500	Lac	Complex N-linked (bisecting GlcNAc)
CA	*Colchicum autumnale*	1000	Gal	Terminal β-Gal, α- and β-GalNac
BPA	*Bauhinia purpurea*	500	Gal	Galβ1-3 or GalNAcβ1-4 more weakly
APA	*Abrus precatorius*	500	Gal	Gal β-1,3GalNAc (TF antigen) > Gal
GS-I	*Griffonia simplicifolia I*	1000	Gal	α-Gal, some GalNAc
APP	*Aegopodium podagraria*	500	GalNAc	GalNAc>Lacose>Galactose
BDA	*Bryonia dioica*	500	Gal	GalNAc
Blackbean	*Black bean*	1000	Lac	GalNAc
CAA	*Caragana arborescens*	500	Gal	GalNAc/Gal (monosaccharides best)
CSA	*Cystisus scoparius*	500	Gal	β-GalNAc, terminal
IRA	*Iris Hybrid*	1000	Gal	GalNAc(GalNAc α-1,3)Gal>GalNAc>Gal
VVA	*Vicia villosa*	500	Gal	α-Linked terminal GalNAc, GalNAcα-1,3 Gal

WFA	*Wisteria floribunda*	500	Gal	GalNAc
ASA	*Allium sativum*	1000	Man	Mannose
AMA	*Allium moly*	1000	Man	D-Mannose
Calsepa	*Calystegia sepium*	500	Man	Man/maltose
Con A	*Canavalia ensiformis*	1000	Man	Branched and terminal mannose [High-Man, Manα-1,6 (Manα-1,3) Man]
CVN	*Cyanovirin*	1000	Man	α-1,2 Mannose
GNA	*Galanthus nivalis*	1000	Man	Terminal α-1,3mannose
GRFT	*Griffithsin*	1000	Man	Mannose,GlcNAc
HHL	*Hippeastrum Hybrid*	1000	Man	α-1,3 Mannose and α-1,6 mannose
NPA	*Narcissus pseudonarcissus*	1000	Man	Terminal and internal Man
MNA-M	*Moringa M*	500	Man	Branched and terminal mannose
SVN	*Scytovirin*	500	Man	α-1,2 Mannose
TL	*Tulipa sp.*	1000	GlcNAc	Man3 core, bi- and tri-antennary complex-type N-glycan, GalNAc
PMA	*Polugonatum mulitiflorum*	500	Man	Mannan
UDA	*Uritica dioica*	1000	GlcNAc	GlcNAc β-1,4 GlcNAc oligomers and high mannose epitopes
VVA (man)	*Vicia villosa*	500	Man	Man
VFA	*Vicia faba*	500	Man	Man>Glc>GlcNAC
LcH	*Lens culinaris*	500	Man	Complex
Jacalin, AIA	*Artocarpus integrifolia*	500	Gal	O-glycosidically linked oligosaccharides, preferring the structure galactosyl (β-1,3) N-acetylgalactosamine
EEL	*Eunonymus europaeus*	1000	Lac	Blood group B antigen, Gal α-1,3 Gal
MPL	*Maclura pomifera*	1000	Gal	Gal β-1,3 GalNAc, GalNAc
GHA	*Glechoma hederacea*	500	Gal	multivalent GalNAc α-Ser/Thr
PNA	*Arachis hyogaea*	500	Gal	Terminal Gal β-OR
ACA	*Amaranthus Caudatus*	1000	Lac	Gal β-1,3 GalNAc (the T antigen)
DBA	*Dolichos biflorus*	500	Gal	GalNAc α-OR (GalNAcα-1,3 GalNAc) and Blood group A antigen,
SBA	*Glycine max*	500	Gal	α- or β-Linked terminal GalNAc, GalNAc α-1,3 Gal
SJA	*Sophora japonica*	500	Gal	GalNAc
HPA	*Helix pomatia*	500	Gal	α -Linked terminal GalNAc
SNA-II	*Sambucus nigra*	500	Gal	GalNAc linked alpha to C-2, C-3 or C-6 hydroxyl gropup of galactose
PTLI	*Psophocarpus tetragonolobus*	1000	Gal	α-GalNAc, A-antigen
PTA	*Psophocarpus tetragonolobus*	500	Gal	Gal
LBA	*Phaseolus lunatus*	1000	Gal	GalNAc α-1,3 [Fuc α-1,2]Gal
DSA	*Datura stramonium*	500	Lac	GlcNAc β-1,4 GlcNAc oligomers and LacNAc (Gal β 1-4 GlcNAc)
GS-II	*Griffonia*	500	GlcNAc	terminal GlcNAc

	simplicifoia			
UEA-II	*Ulex europaaeus II*	1000	GlcNAc	Oligomers of β-1,4 GlcNAc
RPA	*Robinia pseudoacacia*	500	GlcNAc	Complex
LEA	*Lycopersicon esculentum*	500	GlcNAc	β-1,4GlcNAc oligomers
STA	*Solanus tuberosum*	500	GlcNAc	GlcNAc oligomers, LacNAc
WGA	*Triticum vulgare*	1000	GlcNAc	β-GlcNAc, sialic acid, GalNAc
Cholera Toxin	*Cholera Toxin from Vibrio cholerae*	2000	Lac	glycolipid
MOA	*Marasmium oreades*	500	Gal	Gal α-1,3 Gal and Gal α-1,3 Gal β-1,4GlcNAc
MNA-G	*Morniga sp.*	1000	Gal	GalNAc α, Tn antigen
Lotus	*Lotus tetragonolobus*	500	Fuc	Terminal α-Fuc, Lewis x
IAA	*Iberis amara*	500	GalNAc	GalNAc
Ricin B Chain		500	Gal	β-Gal
GS-I	*Griffonia simplicifolia I*	1000	Gal	α-Gal, some GalNAc
DC-SIGN		100	Man	High Mannose
PA-IL[†]	*Pseudomonas Aeruginosa*	500	Gal	Terminal α-Gal
7LE	antibody	100		Lewis a
SPM110	antibody	100		Sialyl Lewis a
LeX P12	antibody	100		Lewis x
LeX R&D	antibody	100		Lewis x
Lewis Y	antibody	100		Lewis Y
Lewis Y IgM	antibody	100		Lewis Y

Materials and general information

PBS contains 10 mM sodium phosphate dibasic, 2 mM potassium phosphate monobasic, 137 mM sodium chloride and 2.7 mM potassium chloride with pH of 7.4 after preparation. ConA from *Canavalia ensiformis* (Jack bean) was purchased from Sigma-Aldrich. ConA (2.5–10 mg, monomeric MW = 26500 Da) was dissolved in HEPES buffer (1.0 mL, 50 mM HEPES, 150 mM NaCl, 1 mM $CaCl_2$, pH 7.2). After incubating for overnight at 4 °C, the ConA mixture was centrifuged for 2 min at 14000 rpm and syringe-filtered (0.22 μm). The final subunit concentration of ConA solution was determined by UV absorbance at 280 nm (A_{280} = 1.37 × [mg/mL ConA]).[5] LcH from *Lens culinaris* (lentil) and PSA from *Pisum sativum* (pea) were purchased from Medicago. The monomeric MW of LcH and PSA are 24500 and 23500 Da respectively.[4] The final subunit concentrations of LcH or PSA solution were determined by UV absorbance at 280 nm (A_{280} = 1.26 × [mg/mL LcH] or A_{280} = 1.50 × [mg/mL PSA]).[4] Horseradish peroxidase (HRP) was purchased from Sigma-Aldrich. All solutions used for phage work are sterilized either by autoclave or by filter sterilization (0.22 μm)

1. Solid-phase peptide synthesis

Standard Fmoc-protected amino acids, HBTU, Rink Amide AM resin, and Wang resin were purchased from ChemPrep. Poly-Prep® chromatography columns (10 mL) were purchased from Bio-Rad. Vacuum manifold was the product of Promega.

2. RP-HPLC

RP-HPLC were performed on Waters HPLC system equipped with a Waters 1525 EF binary pump, a Waters FlexInject manual injector (dual mode) and a Waters 2489 tunable UV detector. SymmetryPrep™ C18 semi-preparative column (19 × 50 mm, particle size 5 μm, pore size 100 Å) was used for all the purification at a typical flow rate of 12 mL/min. For analytical run, Symmetry® C18 analytical column (4.6 × 75 mm, particle size 3.5 μm, pore size 100 Å) was used at a typical flow rate of 1 mL/min. HPLC traces were monitored with UV detection at 220 nm and 280 nm.

3. Synthesis

2-(aminooxy)ethyl α-D-mannopyranoside was synthesized as described previously.[6] *O*-α-D-mannopyranosyl oxyamine was synthesized according the literature method.[7] Product purification was accomplished with automated chromatography machine (CombiFlash® Rf, Teledyne Isco, Inc.). ^{1}H NMR spectra were acquired on Agilent/Varian VNMRS 500 MHz and 600 MHz spectrometers in $CDCl_3$ (referenced to residual $CHCl_3$ at δ_H 7.26 ppm), CD_3OD (referenced to residual CD_2HOD at δ_H 3.3 ppm), or in D_2O (referenced to external acetone at δ_H 2.225 ppm). Chemical shift (δ) is reported in ppm and coupling constants (*J*) are given in Hz. The following abbreviations classify the multiplicity: s = singlet, d = doublet, t = triplet, m = multiplet or unresolved, br = broad signal. HRMS (ESI) spectra were recorded on Agilent 6220 oaTOF mass spectrometer using either positive or negative ionization mode.

Detailed procedures for ligands search

1. Generation of Man-X_7 and Me-X_7 phage-displayed peptide library

N-SerX_7 phage-displayed peptide library **3** (complexity: 3×10^8 pfu) was generated according to the referred protocol.[8] Prior to the chemical modification, the phage library was dialyzed extensively (4 °C, 10K MWCO) against two changes of PBS (5 L) to remove the storage buffer which contains 50% (v/v) glycerol. The phage library (1 mL, ~4×10^{12} pfu/mL) was oxidized with 0.06 mM sodium periodate (by adding 10 μL of 6 mM solution in MQ water) at 4 °C for 5 min. The oxidation was quenched with 0.5 mM glutathione (by adding 10 μL of 50 mM solution in MQ water) at RT for 10 min. To monitor the oxidation, a small portion of the oxidized library was treated with aminooxy-biotin and captured with biotin-capture assay as described in a previously published method.[6] Typically, 60% of the fractions of phage library were successfully oxidized.

The oxidized library was distributed into two separate portions of 0.75 mL and 0.25 mL, and they were treated with 1 mM 2-(aminooxy)ethyl α-D-mannopyranoside (by adding 0.75 mL of 2 mM solution in 200 mM anilinium acetate buffer, pH 4.7) and 1 mM methoxylamine (by adding 0.25 mL of 2 mM solution in 200 mM anilinium acetate buffer, pH 4.7) respectively. The reaction mixtures were incubated for 1 h at RT, after which, the excess of reagents were removed by dialysis (4 °C, 10K MWCO) against two changes of PBS (5 L) to yield the Man-X_7 library **1** and Me-X_7 library **2**. To quantify the reaction efficiency, right after the oxime ligation, a small portion of the library was treated with aminooxy-biotin and captured with biotin-capture assay as described in a previously published method.[6] Typically, 55% of the fractions of phage library were successfully modified with the reagents.

2. Selection of chemically-modified phage library against ConA

12 wells of a 96-well polystyrene plate were coated with a solution of ConA (100 μL, 100 μg/mL) in PBS for overnight at 4 °C. These wells plus an additional three empty wells were blocked with a solution of 2% (w/v) BSA in PBS (300 μL) for 1 h at RT. The Man-X_7 library **1** (0.9 mL), Me-X_7 library **2** (0.3 mL), and *N*-Ser-X_7 library **3** (0.3 mL) were blocked with an equal volume of 2× blocking solution (4% (w/v) BSA in PBS) for 1 h at RT. After blocking, the plate was rinsed with washing solution (3 × 300 μL, 0.1% (v/v) Tween-20 in PBS) using 405™ Touch Microplate Washer (BioTek). The selection of Man-X_7 library **1** against ConA (denote as screen **A**) was performed in six replicates. The control selections, i.e., Man-X_7 against BSA (**B**), Me-X_7 against ConA (**C**), and *N*-Ser-X_7 against ConA (**D**), were performed as triplicate in parallel with screen **A**. Specifically, the solutions of library **1**, **2**, or **3** were added into the corresponding wells (200 μL/well, ~1×10^{11} pfu/well). After incubating for 1 h at RT, the unbound phage was rinsed with the washing solution (20 × 300 μL) using the plate washer. Phage remained on the well was eluted for 9 min at RT by adding 200 μL of glycine elution buffer (0.2 M glycine-HCl, pH 2.2, 1 mg/ml BSA). The elution buffer was transferred into a 1.5-mL microcentrifuge tube and immediately neutralized with 50 μL of 1 M Tris-HCl (pH 9.1). An additional washing solution (200 μL) was added to the well to recover the remaining phage and subsequently combined with the eluate. Up to this point, the selections yielded 15 different eluates (0.45 mL per sample).

3. Phage Amplification and PCR of library DNA

The eluted phage was amplified separately by adding the eluates (15 × 0.45 mL) into 3 mL of ER2738 culture (1:100 dilution of overnight culture). The phage and bacterial mixtures were incubated for 4.5 h at

37 °C with vigorous shaking. The cultures were centrifuged (15 min, 4700 rpm) at 4 °C to pellet the bacterial cells. The supernatants (~3.4 mL) containing the amplified phage were poured into a fresh tube. The ssDNA of the amplified phage was extracted using QIAprep spin M13 kit (Qiagen, #27704) according to manufacturer's instructions. 15 reverse barcoded primers were designed with adapters compatible with Ion Torrent sequencing.[9] The library DNA was subjected to PCR amplification with the barcoded primers flanking the variable region. Briefly, the library DNA (15 samples, 50 ng each) was amplified in a total volume of 50 μL with 1× Phusion® buffer, 50 μM each dNTPs, 500 μM $MgCl_2$, 1 μM forward primer, 1 μM reverse barcoded primer, and one unit Phusion® High-Fidelity DNA Polymerase. PCR was performed using the following thermo cycler program: a) 98 °C 30 s, b) 98 °C 10 s, c) 60 °C 20 s, d) 72 °C 30 s, e) repeat b)–d) for 34 cycles (total 35 cycles), f) 72 °C 5 min, g) 4 °C hold. The dsDNA fragments from the PCR were quantified by running at 2% (w/v) agarose gel in Tris-Borate-EDTA buffer at 100 volts for ~45 min using a low molecular weight DNA ladder as a standard (NEB, #N3233S). The dsDNA fragments (15 samples, 40 ng per sample) were pooled together and purified on E-Gel® SizeSelect™ 2% agarose gel (Invitrogen, #G6610-02). The desired band corresponding to 121 bp with reference to the ladder was collected with RNAse-free water and the concentration was determined by Qubit® Fluorimeter (Invitrogen, #Q32851) using manufacturer's protocol.

4. DNA template preparation and Ion Torrent sequencing

Ion PGM™ Template OT2 200 Kit (Life Technologies) was used to prepare the DNA template for sequencing. Briefly, the pooled and purified dsDNA fragments were hybridized onto Ion Sphere Particles (ISPs) and amplified by emulsion PCR using Ion OneTouch™ 2 System according to manufacturer's protocol. The fraction of ISPs loaded with the DNA template was determined with Qubit® Fluorimeter (Invitrogen) according to manufacturer's protocol. The ISPs loaded with the DNA template were enriched and deposited in Ion 316™ chip. The DNA sequencing was performed on Ion PGM™ System using Ion PGM™ Sequencing 200 Kit v2. The FASTQ file generated from the sequencing data was processed by in-house MATLAB script that identified the barcodes and constant flanking regions, and extracted the reads of the correct length (24 bp only) corresponding to the $TCT(NNK)_7$ structure.

5. Volcano plot and generation of sequence logos

This plot identified sequences isolated from **A** screen that increased significantly in abundance against sequences isolated from the control selection. The copy number of each sequence is normalized through dividing the copy number by the total number of reads in each replicate. Sequences not observed in a specific replicate were assigned a copy number of zero. For volcano analysis, the ratio of each sequence was calculated through dividing the mean fraction of the particular sequence in **A** screen by that in the control screen (e.g., **B**, **C**, or **D**). Since the denominator must not be a zero when taking the ratio, sequences with zero copy number found in all three replicates are assigned with 0.3 copy number before taking the normalization. Significance of the ratio was assessed using one-tailed, unequal variance Student *t*-test. The ratio is considered to be statistically significant if the calculated *p*-value ≤ 0.05. Only sequences with ratio ≥ 5 and *p*-value ≤ 0.05 were included in the set **A**/**B**, **A**/**C**, and **A**/**D**. The volcano plot was generated using in-house MATLAB script. Sequence LOGO was generated using the MATLAB function *seqlogo* with *StartatValue* set as 2 and *EndatValue* set as 8 (define the range of position to be considered in the sequence).[10]

Affinity maturation from Man-WY[D/E]X_7 library

1. Generation of N-SerWY[D/E]X_7 phage-displayed peptide library

Library preparation was adapted from *Noren et al.*[8] with minor modifications. An oligonucleotide library was designed to code for the amino acid sequence SWY[D/E], followed by a 7-mer variable region $(NNK)_7$ and GGG linker. The oligonucleotide also includes a KpnI restriction enzyme recognition site (underlined) at the 5' end, followed by the pIII leader sequence of phage M13KE and a fixed Ser. At the 3' end, there is an EagI site (underlined). The oligo sequence corresponding to the **anti-sense** strand is as follows:

3'-GGGCCCATGGAAAGATAAGAGTGAGAAGAACCATGCTN(NNM)$_7$CCACCTCCAAGCCGGCCCGCG-5'
S W Y D/E X_7 G G G

where K = G or T, M = A or C, and N = G, T, A, or C.

In a 0.2-mL PCR tube, 200 pmoles of single-stranded oligonucleotide library and 3 molar equivalents of extension primer (5'- CATGCCCGGGTACCTTTCTATTCTC-3') were combined in 100 mM NaCl to a final volume of 50 μL. In a thermal cycler, fragments were annealed using a program that begins with an initial temperature of 95 °C and cools to 4 °C over 90 min. Extension of the annealed duplex was achieved by adding 20 μL of Klenow fragment reaction buffer, 50 μM dNTPs (final concentration), 15 U Klenow fragment (#EP0051, Thermo Scientific) and DNase-free water to a 1.5-mL microcentrifuge tube, to a final volume of 150 μL. The reaction mixture was incubated for 15 min at 37 °C. The extended library oligonucleotide was purified by ethanol precipitation by adding 20 μL of 3 M sodium acetate, 400 μL of 100% ethanol and 1 μL glycogen. The mixture was incubated for 2 h at -20 °C and centrifuged at 14,000 rpm for 10 min at 4 °C, followed by a washing step using 500 μL of 70% ethanol and a final centrifugation step at 14,000 rpm for 10 min at 4 °C. The sample was re-suspended in 25 μL DNase-free water or TE buffer. The digestion of the library duplex was performed using KpnI and EagI FastDigest restriction enzymes (#FD0524 and #FD0334, Thermo Scientific) and the reaction was set up according to manufacturer instructions. A 2% E-Gel® SizeSelect™ Gel was used to purify oligonucleotide digests. M13KE vector was also digested using KpnI and EagI FastDigest enzymes as per manufacturer instructions and purified by 0.7% agarose gel extraction. For the ligation step, 50 ng of M13KE cut vector and library duplex were combined at a molar ratio of 1:30 in a 0.2-mL PCR tube with 1 μL of 400 U T4 DNA Ligase, 2 μL of 10× Ligase Buffer and DNase-free water to a final volume of 20 μL and incubated overnight at 16 °C. Transformation of bacterial cells was performed by electroporation of ethanol precipitation purified DNA (see above) into TG1 electrocompetent cells (Lucigen) according to manufacturer's specifications. After transformation, cells were incubated at 37 °C for 45 min to generate the inoculating culture that was added to 25 mL of LB media and further amplified at 37 °C for 4.5 h. Viral particles were collected by PEG/NaCl precipitation from supernatant of culture, titered and stored in PBS and 50% glycerol for further experiments.

2. Modification, panning and sequencing

The modification of the library was exactly the same as described above. 50% of the fractions of phage library were successfully modified with 2-(aminooxy)ethyl α-D-mannopyranoside. Both modified and non-modified libraries were subjected to affinity selection using the procedure as described above. After the elution of bound phage, it was amplified and subjected to a second round of modification and affinity selection. Eventually, the isolated phage DNA was obtained and sequenced by Ion Torrent. The same analysis was applied to narrow down the hits.

Surface plasmon resonance (SPR)

Buffer was sterile-filtered before use. All ligands were pre-dissolved in a 5% volume of DMF followed by the addition of HEPES buffer (50 mM HEPES, 150 mM NaCl, 1 mM $CaCl_2$, pH 7.2). Solution of ConA tetramer (0.4 mg/mL) was prepared using the same buffer. The measurements were recorded on BIAcore 2000 instrument using CM5 chip (carboxylated dextran) as the binding target for ConA. To perform the competitive inhibition, ConA (0.4 mg/mL) was mixed with an equal volume of inhibitor and this mixture (50 μL) was injected (10 μL/min). Inhibitor concentrations of 0, 0.0001, 0.0003, 0.001, 0.003, 0.01, 0.03, 0.1, 0.3, and 1 mM were tested. Two more data points (3 and 10 mM) were included for inhibition with MeMan. The solution of inhibitor in the absence of ConA was injected each time before the injection of the ConA/inhibitor mixture of the same concentration. The response values were used for subtraction to account for the bulk effect caused by the inhibitor itself. The chip was regenerated after each injection with the regeneration buffer (6 M guanidinium chloride). Bound ConA response values were assessed during the equilibrium binding portion of the curve (280 s after injection). The corrected response value (R_{max}) of bound ConA in the absence of inhibitor was set as 0% inhibition. The degree of inhibition by the inhibitor was calculated with the equation $R_{max}-R_{inh}/R_{max}$, where R_{inh} is the corrected response value given by the bound ConA in the presence of certain concentration of inhibitor.

Isothermal titration calorimetry (ITC)

ITC were performed using a Microcal VP-ITC instrument. Ligands were pre-dissolved in a small amount of DMF followed by the addition of HEPES buffer (50 mM HEPES, 150 mM NaCl, 1 mM $CaCl_2$, pH 7.2). The final solvent was HEPES buffer containing 2% (v/v) DMF. In the case, where ligands have poor solubility in the prepared buffer, up to 5% (v/v) DMF was used. The ConA solution was prepared with the same buffer as the ligand. All solutions were degassed with MicroCal ThermoVac unit prior to use. All titrations were carried out at 30 °C. An initial injection of 2 μL followed by a total of 41 injections of ligand solution (7 μL) were added at intervals of 4 min into the solution of ConA (cell volume = 1.44 mL) while stirring at 300 rpm. Typically, the initial concentrations of ConA and ligands were 0.05−0.30 mM and 2 mM respectively, unless otherwise specified. The quantity $c = K_a M$, where M is the initial macromolecule concentration, is of importance in ITC. All experiments were performed with c values in the range of $1 < c < 100$, except for the ligands with $K_a \leq 1000\ M^{-1}$, where preparation of ConA with concentration > 1 mM is difficult due to solubility issue. In the case where heat of dilution is significant, titration data obtained by making identical injection of ligand into the buffer without ConA was subtracted from the titration data obtained in the presence of ConA. The data point produced by the first injection was discarded prior to curve fitting in order to account for the diffusion effect during the equilibration process. The experimental data were fitted to a non-interacting one-site binding model using Origin software supplied by Microcal, with ΔH (enthalpy change), K_a (association constant) and n (number of binding sites per monomer) as adjustable parameters. Free energy change (ΔG) and entropy contributions (TΔS) were determined from the standard equation: $\Delta G = \Delta H - T\Delta S = -RT \ln K_a$, where T is the absolute temperature and R = 1.987 cal mol^{-1} K^{-1}.

For ITC measurements of ligand binding to LcH or PSA, exactly the same protocol was used as described above.

Protein Crystallization

Jack bean concanavalin A, type V, used for crystallization trials, was purchased from Sigma-Aldrich, St. Louis, Missouri, USA. Prior to crystallization, a sample of ConA (20 mg/mL) in 1 M NaCl, 50 mM NaOAc at pH 5.0, 1 mM $CaCl_2$, 1 mM $MnCl_2$ was incubated at 42 °C for 2 hours and dialyzed against three changes of 0.1 M NaCl, 20 mM Tris pH 7, 1 mM $CaCl_2$, 1 mM $MnCl_2$. For crystallization trials, ConA was concentrated to 14-15 mg/mL. About 1 hour prior to crystallization the solution of ConA was combined with the stock solution of Man-WYD in DMSO at a molar ratio of 1:10 (ConA : ligand). Initial crystals were obtained from QIAGEN's the JCSG Core II Suite, condition #34: 0.1 M HEPES pH 6.5, 10 % (w/v) PEG 6000. Diffraction quality co-crystals were grown at 20 °C in sitting drop microbridges using well solutions consisting of 0.1 M HEPES pH 6.5 and 10-16 % PEG 6000.

X-ray Data collection

Prior to data collection crystals were placed in a cryoprotectant solution composed of 75% well solution and 25% glycerol and then flash cooled by immersion in liquid nitrogen. X-ray diffraction data were collected at 100K over a range of 100° (1° steps) using an ADSC Quantum 315r detector at the Advanced Photon Source (APS) on the ID19 beamline SBC-CAT to 1.73 Å resolution. Reduction of the X-ray data was performed using the XDS[11] and the CCP4 suite.[12] Refinement was completed using the *phenix.refine* program in the *PHENIX* suite[13] and the resulting structure analyzed with molprobity.[14]

X-ray data collection (110K)

PDB accession code	4CZS
Unit-cell parameters (Å)	a = 60.00, b = 62.76, c = 124.83 $\alpha = 90$ $\beta = 96.10°$ $\gamma = 90°$
Space group	$P2_1$
No. of unique reflections	7,632
Resolution range (Å)	45.48–1.73 (1.78–1.73)
Multiplicity	3.01 (2.55)
I/σ(I)	11.87 (2.32)
R_{merge} (%)	6.2 (47.2)
Data completeness (%)	98.4 (97.1)

Crystallographic refinement

R_{factor} (%)	19.16
R_{free} (%)	23.74
RMSDBonds (Å)	0.008
RMSDAngles (°)	1.328

Ramachandran plot

Outliers (%)	0.00
Favored (%)	97.6
Rotamer Outliers (%)	2.89

MD analysis

Comparison of the ligand-binding mode

A crystal structure of the ConA protein bound to trimannoside (PDB ID: 1CVN) has been reported at 2.3 Å resolution. The mannopyranosyl (Man) residue of the synthetic ligand used in the present study and Man-240 (the 1,6-linked Man) in the endogenous ligand, bind to the protein at the same site (Figure 3B) and in the same $^4C_1$ conformation (Figure S17). These two Man residues displayed equivalent hydrogen-bonding patterns (Arg228 NH to O3, Asn14 side chain NH to O4, Leu99 NH to O5, and Tyr100 NH to O6). In contrast to the endogenous trimannoside, the synthetic ligand forms few additional hydrogen bonds, and prefers to van der Waals contacts with the protein surface (Figure S7). This is as shown by a higher contact area of synthetic ligand (662 Å) compared to the trisaccharide Man3 (204 Å).

A number of structural studies show that a conserved water molecule plays an important role in facilitating the ConA-carbohydrate interaction, by forming hydrogen bonds with ARG 228, ASP 16, ASP 14 and MAN 241.[15] A crystallized water molecule is present at the same location in the present protein structure, but because of the absence of MAN 241 in the synthetic ligand, this water does not mediate hydrogen bond formation with the ligand.

To examine the stabilities and strengths of these interactions, and to study the dynamics of the ligand in the binding pocket of the protein, a 50 ns molecular dynamics (MD) simulation was performed with the AMBER/GLYCAM force field and explicit water. The ligand-protein complex remained stable over the course of the simulation (average backbone RMSD = 0.69 (0.03) Å, average ligand displacement RMSD = 1.62 (0.32) Å).

Key interactions between protein and ligand

1. Hydrogen bonds

The MAN residue forms two stable hydrogen bonds with ASN 14 and ASP 208. TYR in the ligand also participates in the hydrogen bonding with PRO 206. The bonds with ASP 208 and PRO 206 are not present in the crystal structure, whereas the hydrogen bonds of MAN with LEU 100, ARG 228 and TYR 100, which exist in the crystal structure, are not formed during the MD simulation.

Table S4. Intermolecular hydrogen bonds[a] between protein and ligand

Donor		Acceptor				
Residue	Atom	Residue	Atom	MD Occupancy[b]	MD Distance[c]	X-ray
MAN	O4	ASN 14	Nδ2	100	2.9 (0.1)	2.98
ASP 208	Oδ2	MAN	O4	100	2.6 (0.1)	2.52
PRO 206	O	TYR (ligand)	OH	100	2.7 (0.1)	2.45
MAN	O3	ARG 228	N	100	3.0 (0.1)	2.88
MAN	O6	TYR 100	N	99	3.1 (0.1)	3.22
MAN	O5	LEU 99	N	97	3.2 (0.2)	2.93

[a] Based on a distance cut-off of 3.5Å.

[b] In percent of total simulation.

[c] Average distance in Å.

2. Hydrophobic interactions

HIS 205 in the protein interacts with TYR in the ligand via parallel displaced aromatic stacking. The histidine ring flips through the simulation maintaining this interaction, but it might not be strong enough to prevent it from flipping. TYR 100 in the protein also interacts with TYR in the ligand via CH/π interaction. This interaction can provide binding energy of 3.54 kcal/mol, as estimated by QM calculation at MP2/aug-cc-pVQZ, between two benzene rings in this conformation.[16] These interactions were characterized by the angle (θ) between the normals to the ring planes, and the distance (R) between their centroids (Figure S18).[17] For a stacking conformation, θ should be around 180° or 0°, and for CH/π, it should be around 90°. In case of HIS 205 the average θ over the flipped and non-flipped arrangement is 138° and 21° at an average distance of 4.8 Å, while with TYR 100, the average θ is 93° at 5.1 Å.

Binding free energy analysis

The results from the binding free energy analysis were sorted and ranked on the basis of the per-residue total energy contributions (see Figure S8 and Table S2). Using this information, the residues significant to the ligand binding were identified. Residues involved in hydrogen bonds and hydrophobic interactions are amongst the top contributors, and stabilize the binding mainly via electrostatic and van der Waals interactions respectively. TYR 100 was involved in a hydrogen bond with the ligand in the crystal structure, but that bond does not exist during the simulation and largely its contribution to binding is through van der Waals. Most of the high ranked residues are hydrophobic which suggests that the binding interaction could mainly be non-polar. With regard to the ligand, the Man residue appears to contribute over 50% of the interaction energy, with the remainder coming principally from the TYR and TRP residues.

Method for MD simulation

1. Preparation of protein and ligand structures

Antechamber was used to develop GAFF charges and force field parameters for the linker; ff12SB[18] parameters were employed for the amino acids and GLYCAM06j parameters for the sugar (see Figure below). The complex was solvated in a truncated octahedral box of 9837 TIP3P water molecules with counter ions (Na^+) added to neutralize the charge, using the tLEAP module of AMBER. All histidine residues were considered neutral with hydrogen at the ε-position. The crystalized water molecules were retained and appropriate hydrogen atoms were added using a tool provided by AMBERTOOLS called protonator.

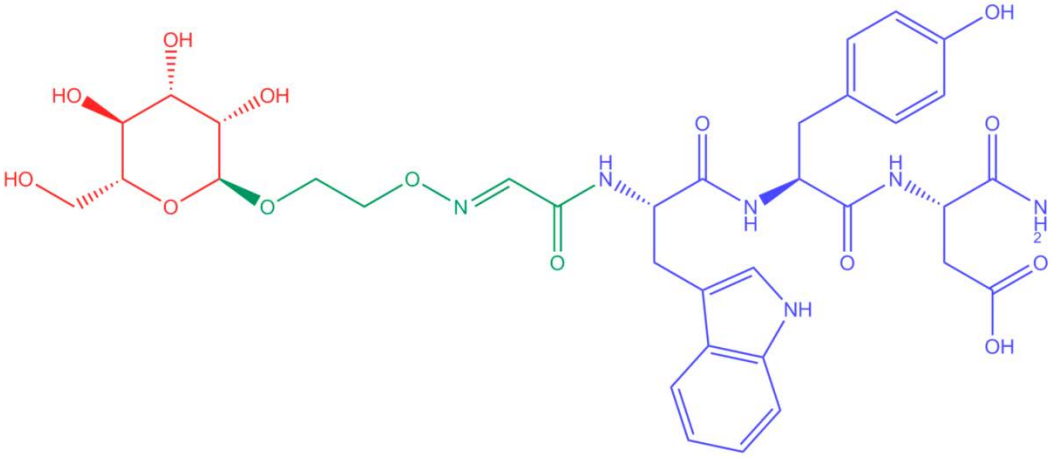

Figure. Components of the ligand colored according to the source of the force field parameters: GLYCAM06j (red), GAFF (green), and AMBER12SB (blue).

2. Energy Minimization

All simulations were performed with a cutoff for non-bonded interactions of 10 Å. To remove bad contacts, the system was minimized in two steps. Firstly, the energy of the water and ions was minimized while keeping all protein atoms restrained (500 kcal/mol $Å^2$). This was followed by energy minimization of the entire system. Each minimization was comprised of an initial phase of steepest descent method for 5000 steps, followed by conjugate gradient for 20000 steps using AMBER12. The resulting minimized structure was subjected to MD simulation performed with the pmemd.cuda version of AMBER12.[19]

3. MD Simulation

All the bonds involving hydrogen were constrained using the SHAKE algorithm,[20] enabling an integration time step of 2 fs. Long-range electrostatic interactions were treated with the Particle-Mesh Ewald algorithm.[21] The systems were heated from 5 K to 300 K over a span of 50 ps, under nVT conditions employing the Langevin thermostat using a collision frequency of 1.0 ps^{-1}. The simulation was then continued for 50 ns under nPT conditions with weak restraints on the backbone atoms (10 kcal/mol $Å^2$).

4. Data Analysis

Ligand contact areas were computed with NACCESS.[22] Binding free energies were calculated using single trajectory Molecular Mechanics-Generalized Born Solvation Area (MM-GBSA) method, and the solvation energies were approximated with an implicit solvent (igb=2).[23] For this analysis all the water

molecules and ions were removed from the complex, and average energy values were computed over an ensemble of 5000 snapshots, collected every 10 ps from MD trajectory. The MM-GBSA energy was decomposed to obtain per-residue contribution, in terms of van der Waals and electrostatic energies, and nonpolar and polar solvation free energies, and the residues were sorted on the basis of mean total energy binding contribution.

1D STD-NMR experiments

The experiments were conducted on Agilent/Varian VNMRS 600 MHz spectrometer at a probe temperature of 300 K. The NMR samples were prepared by pre-dissolving the ligand in a small amount of DMSO-d_6 (14 μL), followed by the addition of ConA in deuterated PBS (686 μL). Deuterated PBS was prepared from 1× PBS (pH 7.4) by two cycles of lyophilization and redissolution in D_2O. The final samples contained ligand/ConA in a ratio of 40:1 (2 mM ligand, 0.05 mM ConA). The NMR experiments involved the selective saturation of protein resonances at 0.2 ppm (30 ppm for reference spectra) using a cascade of 20 Gaussian-shaped pulses (50-ms duration, 1-ms delay between each pulse) resulting in a total saturation time of 1.02 s. WATERGATE W5 sequence[2] was used to suppress the residual HDO signal. A 30-ms $T_{1\rho}$ filter was applied to suppress protein background. STD-NMR spectra were obtained by subtracting the saturated spectra from the reference spectra *via* phase cycling. The integral regions of the reference spectra were copied to the STD-NMR spectra to guarantee identical boundaries and unbiased ratio of the particular integrals. Relative STD effects were calculated according to the equation $\boldsymbol{E}_{STD} = (\boldsymbol{I}_0 - \boldsymbol{I}_{sat})/\boldsymbol{I}_0 = \boldsymbol{I}_{STD}/\boldsymbol{I}_0$ by comparing the intensity of the signals in the STD-NMR spectrum ($\boldsymbol{I}_{STD}$) with intensity of the signals in a reference spectrum ($\boldsymbol{I}_0$). Control STD experiments using the free ligand (Man-WYD) were performed under the same experimental conditions to verify true ligand binding. No signal was present in the STD-NMR spectra, indicating that the effects observed in the presence of the protein were due to true saturation transfer with negligible artifacts. The reference spectra and STD-NMR spectra of Man-WYD and Man-NL-WYD were shown at the following page.

Control: Man-WYD (**L20**) in the absence of ConA

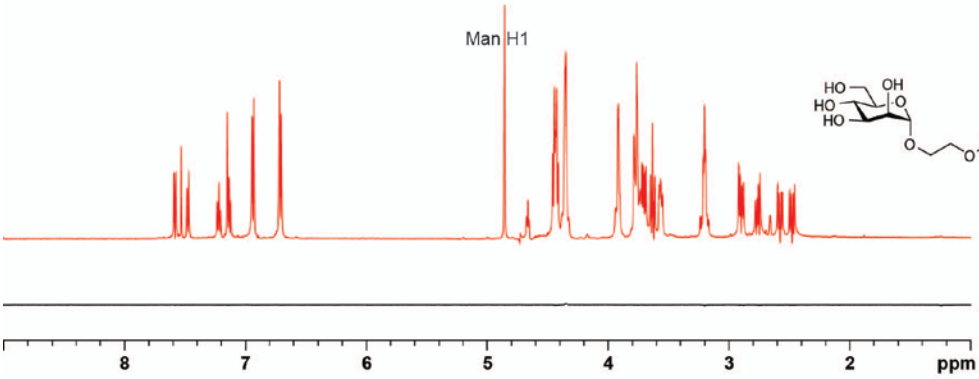

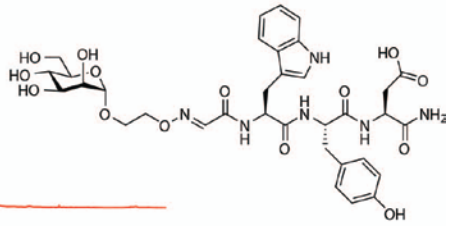

Man-WYD (**L20**) in the presence of ConA

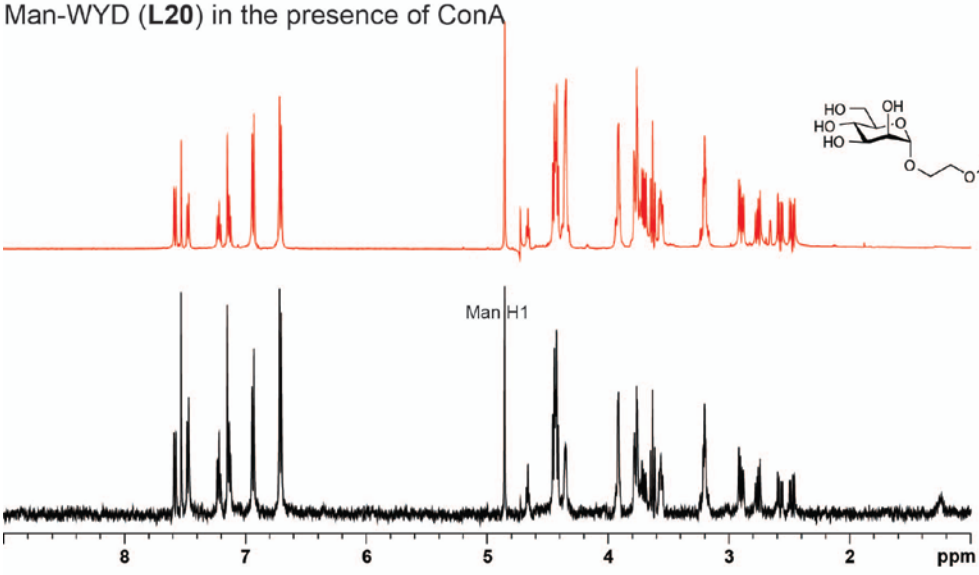

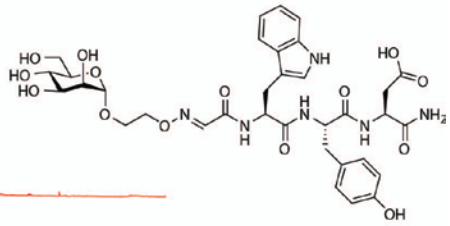

Man-NL-WYD (**L20.3**) in the presence of ConA

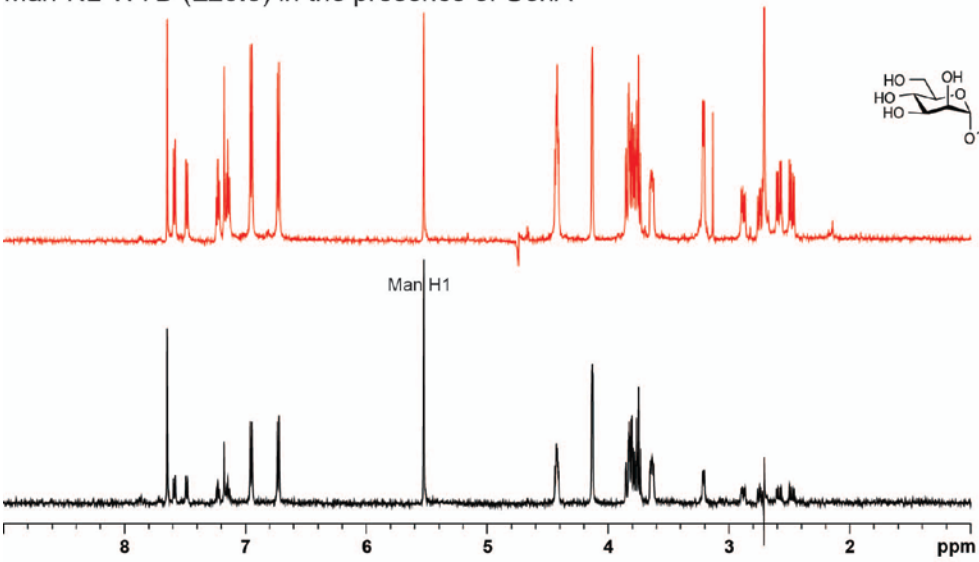

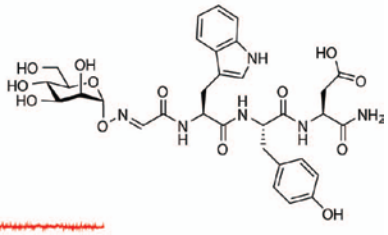

Red traces: reference spectra
Black traces: STD-NMR spectra

Lectin microarray printing and analysis

Lectin arrays were printed according to the method described in literature.[24] Briefly, lectins were printed using Nano-Plotter non-contact piezoelectric printer at 100 volts onto Nexterion H slides at 45% humidity and 13˚C. For a printlist see Table S3. Slides were blocked with 25 mM ethanolamine in 100 mM sodium borate (pH 8.0) for one hour with gentle rocking. Man-WYK-OH labeled with Cy3 were diluted by serial dilutions (3.33µM, 2.50µM, 1.88µM, 1.41µM, and 1.05µM, 100 µL total volume) in nano-pure water and then analyzed as previously described.[24] In brief, samples were incubated on the arrays for two hours followed by five washes with 0.1 M NaH_2PO_4, 0.15 M NaCl, 0.01% Tween 20 (pH 7.2). The slides were dried by spinning and scanned using GenePix 4300a slide scanner at PMT of 450 at 532nm with 100% power. Signals were tested for outliers by Grubbs tests (critical value of 1.15). Data was subjected to Z-score transformation[25] and a significance cutoff of Z=1.95 ($p < 0.01$) was applied to look for significant signals.

ESI-MS binding measurement

1. Sample preparation

Monomeric carbohydrate-recognition domain of dendritic cell-specific intercellular adhesion molecule-3-grabbing non-integrin (DC-SIGN, MW 17 802 Da) was a gift from Professor Kurt Drickamer (Imperial College, London). Chicken egg white lysozyme (Lyz, MW 14 315 Da) was purchased from Sigma-Aldrich Canada (Oakville, ON, Canada). Protein stock solutions were prepared by exchanging protein into 100 mM ammonium acetate using Vivaspin 500 centrifugal concentrators with a 10 kDa MW cut-off (Sartorius Steddin Biotech, Gottingen, Germany). The protein concentrations were measured using Pierce™ BCA Protein Assay Kit. The ESI solutions containing 8.5 μM DC-SIGN, 5 μM Lyz, 50 μM Man-WYD (**L20**) or Man-NL-WYD (**L20.3**) and 10 mM ammonium acetate were prepared from the stock solutions. Lyz was added to the ESI solutions to act as a reference protein,[26] so that nonspecific binding during the ESI process could be corrected.

2. Mass spectrometry

Binding measurements were performed on a Synapt G2-S quadrupole-ion mobility separation-time-of-flight (Q-IMS-TOF) mass spectrometer (Waters UK Ltd., Manchester, UK) equipped with a nanoflow ESI source. ESI was performed using nanoESI tips pulled from borosilicate glass capillaries (1.0 mm o.d., 0.78 mm i.d.) using a P-97 micropipette puller (Sutter Instruments, Novato, CA, USA). Mass spectra were obtained in positive ion mode using cesium iodide (concentration 30 ng μL^{-1}) for calibration. A capillary voltage of 1.1 kV under positive mode was applied to carry out nanoESI. A cone voltage of 30 V was used and the source block temperature was maintained at 80 °C. Other important voltages for ion transmission, that is the injection voltages into the trap and transfer ion guides, were maintained at 5 and 2 V, respectively. Argon was used in the trap and transfer ion guides at a pressure of 2.22×10^{-2} mbar and 3.36×10^{-2} mbar, respectively. Data acquisition and processing were carried out using MassLynx (ver. 4.1).

Inhibition studies of ConA and DC-SIGN by competitive binding assay

Tetrameric extracellular domain of dendritic cell-specific intercellular adhesion molecule-3-grabbing non-integrin (DC-SIGN) was a gift from Professor Kurt Drickamer (Imperial College, London). The competitive binding assay involves the binding of immobilized lectins, i.e., ConA or DC-SIGN, to horseradish peroxidase (HRP), a glycoprotein containing trimannoside epitope, under the competition of the studied inhibitors, i.e., MeMan, Man-WYDLF, or Man3-X. Buffer used in the experiment was a solution of 50 mM MOPS, 150 mM NaCl, and 2mM $CaCl_2$ (pH 7.4). A solution of ConA or DC-SIGN (10 μg/mL) dissolved in the buffer was used to coat a polystyrene plate (Costar #3369) to have a final volume of 50 μL/well. The plate was sealed with a membrane and kept in fridge for overnight. In a separate non-binding surface plate (Corning #3641), a 3-fold serial dilution was performed for the solutions of the inhibitor dissolved in the buffer. The diluted solutions were then mixed with an equal volume of the solution of HRP (2 μg/mL) dissolved in the same buffer. The coating solution of lectin was aspirated using 405™ Touch Microplate Washer (BioTek) and subsequently washed with the washing solution (10 × 300 μL, the same buffer containing 0.1% (v/v) Tween-20). The mixture of the inhibitor and HRP probe was transferred accordingly onto the plate coated with the lectin to have a final volume of 50 μL/well. The plate was incubated at RT for 1 h. Then, the plate was washed with the washing solution (10 × 300 μL) and the TMB substrate (50 μL) was added to each well. After 5 min incubation for ConA-coated well or 10 min incubation for DC-SIGN-coated well, 1 M phosphoric acid (50 μL) was added to quench the colorimetric assay. The color developed was read at 450 nm with 96-wells plate reader. The data was fitted with logistic function using Origin software to determine the half maximal inhibitory concentration (IC_{50}) of the studied inhibitor.

Synthesis of carboxymethylthiopropyl α-D-mannopyranoside

1. Methoxycarbonylmethylthiopropyl 2,3,4,6-tetra-O-acetyl-α-D-mannopyranoside

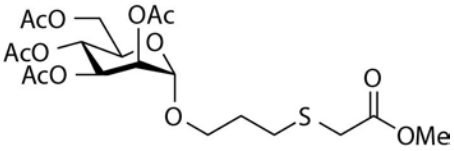

A solution of allyl 2,3,4,6-tetra-O-acetyl-α-D-mannopyranoside (900 mg, 2.3 mmol) and methyl thioglycolate (0.31 mL, 1.5 eq.) in CH_2Cl_2 (20 mL) was irradiated with UV lamp at 254 nm for 1 h then concentrated. Chromatograpy of the residue on silica gel in CH_2Cl_2-MeOH (50:50) gave the title compound (980 mg, 85%): ^{1}H NMR (500 MHz, $CDCl_3$) δ = 5.35 (dd, 1 H, $J_{2,3}$ = 3.3 Hz, $J_{3,4}$ 9.8 Hz, H-3), 5.29 (t, 1 H, H-4), 5.26 (dd, 1H, $J_{1,2}$ = 1.7 Hz, H-2), 4.84 (d, 1 H, H-1), 4.30 (dd, 1 H, $J_{6a,6b}$ = 12.2, $J_{5,6a}$ = 5.2 Hz, H-6a), 4.14 (dd, 1H, $J_{5,6b}$ = 2.20 Hz, H-6b), 3.97 - 4.04 (m, 1 H, H-5), 3.84 (dt, 1 H, *J* = 9.8, *J* = 6.3 Hz, CH_2), 3.77 (s, 3 H, OMe), 3.57 (dt, 1 H, *J* = 9.8, *J* = 6.0 Hz, CH_2), 3.26 (s, 2 H, CH_2), 2.75 (t, 2 H, CH_2S), 2.18 (s, 3 H, OAc), 2.13 (s, 3 H, OAc), 2.07 (s, 3 H, OAc), 2.01 (s, 3 H, OAc), 1.95 (dq, *J* = 13.39, *J* = 6.97 Hz, 2 H, CH_2). ^{13}C NMR (125 MHz, $CDCl_3$) δ = 170.79 (CO), 170.64 (CO), 170.04 (CO), 169.86 (CO), 169.71(CO), 97.64 (C-1), 69.58 (C-2), 69.09 (C-5), 68.61 (C-3), 66.43 (CH_2), 66.18 (C-4), 62.49 (C-6), 52.41 (OMe), 33.38 (CH_2), 29.28 (CH_2), 28.50 (CH_2), 20.89 (OAc), 20.76 (OAc), 20.71 (OAc), 20.69 (OAc).

2. Carboxymethylthiopropyl α-D-mannopyranoside

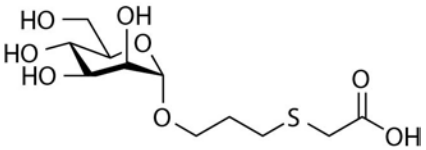

To a solution of above compound (800 mg, 1.62 mmol) in dry MeOH (5 mL), 1 M NaOMe (1 mL) was added. After 1 h incubation, the mixture was concentrated, taken up in water (5 mL), and 2 M NaOH (1 mL) was added. After overnight incubation the mixture was treated with Dowex (H^+) and filtered. The supernatant was freeze-dried. Chromatography of the residue on silica gel in CH_2Cl_2-MeOH (50-100%) afforded the title compound (355 mg, 67%): ^{1}H NMR (498 MHz, D_2O) δ = 4.82 (d, 1 H, $J_{1,2}$ = 1.5 Hz, H-1), 3.90 (dd, 1 H, $J_{2,3}$ = 3.3, H-2), 3.87-3.54 (m, 7 H, H-3, H-4, H-5, H-6a, H-6b, CH_2), 3.36 (s, 2 H, CH_2), 2.65 - 2.75 (m, 2 H, CH_2), 1.82 - 1.95 (m, 2 H, CH_2). ^{13}C NMR (126 MHz, D_2O) δ = 175.00 (CO), 99.77 (C-1), 72.80, 70.62, 70.10, 66.76, 66.04 (CH_2), 60.93 (C-6), 33.39 (CH_2), 28.75 (CH_2), 28.07 (CH_2).

Synthesis of Man3-X (X = 6-azidohexyl)

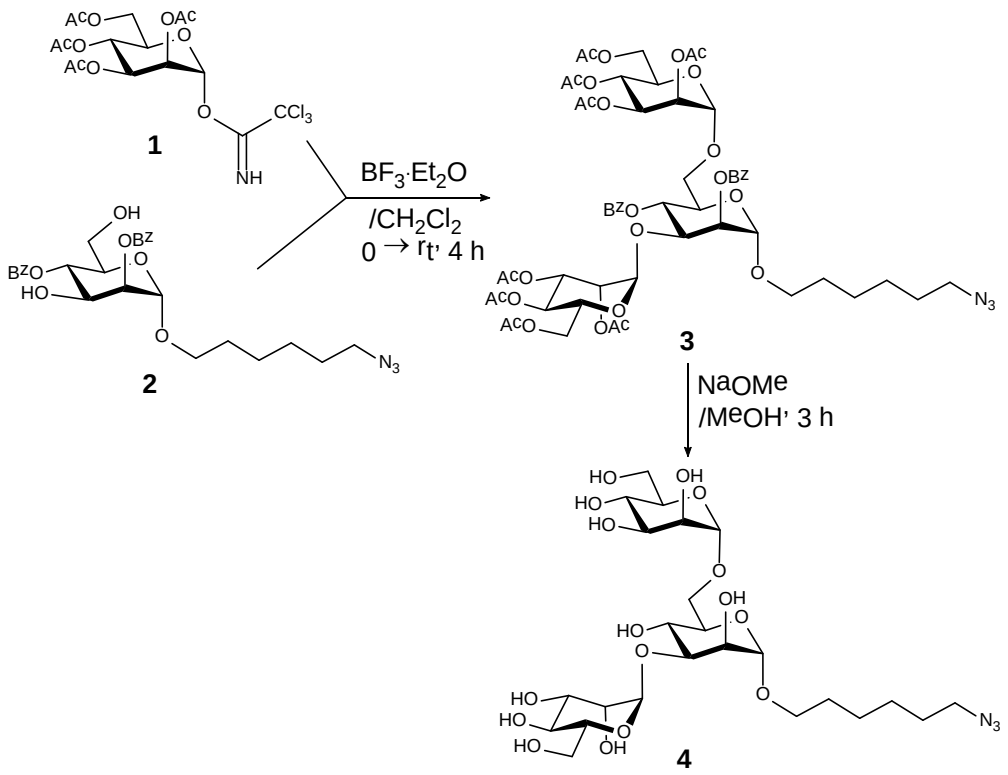

6-Azidohexyl O-(2,3,4,6-tetra-O-acetyl-α-D-mannopyranosyl)-(1→6)-[(2,3,4,6-tetra-O-acetyl-α-D-mannopyranosyl)-(1→3)]-2,4-di-O-benzoyl-α-D-mannopyranoside (3)

A mixture of diol **2** (102 mg, 0.20 mmol), imidate **1** (315 mg, 0.64 mmol) and 4 Å molecular sieves (0.4 g) in anhydrous dichloromethane (4 mL) was stirred for 2 hours under argon. The mixture was cooled to 0 °C and $BF_3{\cdot}Et_2O$ (60 μL, 0.47 mmol) was added drop wise. The reaction mixture was allowed to warm up to room temperature slowly and stirred overnight. Triethylamine (0.7 mL) was added, and the solid was filtered off and the obtained solution was concentrated under reduced pressure. The residue was purified by column chromatography on silica gel using a gradient of ethyl acetate – hexane (10→35 %) as the eluent to yield compound **3** as a colorless foam (133 mg, 57% yield). $[\alpha]_D^{25}$: + 5.8 (*c* 0.43, $CHCl_3$). ^1H NMR (400 MHz, $CDCl_3$) δ = 8.17 – 8.11 (m, 2H, Bz), 8.07 – 8.02 (m, 2H, Bz), 7.65 – 7.51 (m, 4H, Bz), 7.45 (m, 2H, Bz), 5.61 (dd, *J* = 10.0, 10.0 Hz, 1H, H-4_Man_B), 5.49 (dd, *J* = 3.4, 1.7 Hz, 1H, H-2_Man_B), 5.33 (dd, *J* = 10.1, 3.4 Hz, 1H, H-3_Man_C), 5.28 – 5.19 (m, 2H, H-2_Man_C + H-4_Man_C), 5.14 – 5.05 (m, 2H, H-3_Man_A + H-4_Man_A), 5.03 - 4.99 (m, 2H, H-1_Man_A + H-1_Man_B), 4.87 (dd, *J* = 2.9, 2.0 Hz, 1H, H-2_Man_A), 4.79 (d, *J* = 1.6 Hz, 1H, H-1_Man_C), 4.45 (dd, *J* = 9.7, 3.4 Hz, 1H, H-3_Man_B), 4.22 – 3.94 (m, 7H, H-5_Man_A + H-5_Man_B + H-5_Man_C + H-6a_Man_A + H-6b_Man_A + H-6a_Man_C + H-6b_Man_C), 3.90 (dd, *J* = 10.7, 7.1 Hz, 1H, H-6a_Man_B), 3.79 (ddd, *J* = 9.7, 9.7, 6.7 Hz, 1H, OC*H*aHbCH$_2$), 3.59 (dd, *J* = 10.6, 1.9 Hz, 1H, H-6b_Man_B), 3.53 (ddd, *J* = 9.7, 9.7, 6.4 Hz, 1H, OCHa*H*bCH$_2$), 3.30 (t, *J* = 6.9 Hz, 2H, CH_2N_3), 2.11 (s, 3H, Ac), 2.11 (s, 3H, Ac), 2.04 (s, 3H, Ac), 1.97 (s, 3H, Ac), 1.94 (s, 3H, Ac), 1.90 (s, 3H, Ac), 1.87 (s, 3H, Ac), 1.82 (s, 3H, Ac), 1.75 – 1.59 (m, 4H, OCHaHbCH_2 + CH_2CH$_2$N$_3$), 1.51 – 1.38 (m, 4H,

C*H*$_2$C*H*$_2$CH$_2$CH$_2$N$_3$). ^{13}C NMR (100 MHz, $CDCl_3$) δ = 170.56 (CO), 169.91 (CO), 169.73 (CO), 169.69 (CO), 169.50 (CO), 169.19 (CO), 169.05 (CO), 166.00 (CO), 165.33 (CO), 133.63, 133.57, 129.97, 129.89, 129.14, 128.78, 128.51 (Bz), 99.55 (C-1_Man_B), 97.16 (C-1_Man_A), 97.13 (C-1_Man_C), 75.97 (C-3_Man_B), 71.92 (C-2_Man_B), 69.42, 69.36, 69.29, 69.25, 68.90, 68.67, 68.53, 68.26, 68.12 (O*C*HaHb), 66.66 (C-6_Man_B), 65.90, 65.88 (C-4_Man_A, C-4_Man_C), 62.27, 62.13 (C-6_Man_A, C-6_Man_C), 51.32 (CH_2N_3), 29.21 (CH_2), 28.73 (CH_2), 26.49 (CH_2), 25.70 (CH_2), 20.82 (Ac), 20.71 (Ac), 20.64 (2 × Ac), 20.59 (Ac), 20.56 (Ac), 20.45 (2 × Ac). HRMS m/z calc'd for $C_{54}H_{71}N_4O_{26}Na$ ($M+NH_4^+$): 1191.4357; found: 1191.4316.

6-Azidohexyl O-(α-D-mannopyranosyl)-(1→6)-[(α-D-mannopyranosyl)-(1→3)]-α-D-mannopyranoside (4, Man3-X)

Compound **4** (100 mg) was dissolved in anhydrous methanol (10 mL), and a 1.5 M solution of NaOMe in MeOH (0.5 mL) was added. The mixture was stirred at room temperature for 3 hrs. The solution was neutralized with Amberlite IR-120 (H^+) resin, and evaporated under reduced pressure. The residue was dissolved in deionized H_2O, purified by HPLC on a reverse phase C18-bond silica gel column using a gradient of MeOH - H_2O (0 → 40%) as the eluent. The desired trisaccharide **4** was obtained as a fluffy colorless solid after freeze-drying (48.0 mg, 90% yield). $[\alpha]_D^{25}$: + 96.5 (*c* 0.49, H_2O). ^{1}H NMR (600 MHz, D_2O) δ = 5.13 (d, *J* = 1.6 Hz, 1H), 4.92 (d, *J* = 1.6 Hz, 1H), 4.85 (d, *J* = 1.6 Hz, 1H), 4.11 (dd, *J* = 2.1, 2.1 Hz, 1H), 4.09 (dd, *J* = 3.4, 1.7 Hz, 1H), 4.04 – 3.99 (m, 2H), 3.94 – 3.87(m, 5H), 3.87 – 3.82 (m, 2H), 3.81 – 3.65 (m, 9H), 3.59 (ddd, *J* = 9.9, 9.9, 6.0 Hz, 1H), 3.36 (t, *J* = 6.6 Hz, 2H), 1.72 – 1.59 (m, 4H), 1.49 – 1.37 (m, 4H). ^{13}C NMR (150 MHz, D_2O) δ = 102.34, 99.85, 99.35, 78.55, 73.30, 72.66, 71.02, 70.60, 70.32, 70.02, 69.95, 69.68, 67.94, 66.75, 66.70, 65.74, 65.29, 61.02, 60.92, 51.10, 28.34, 27.88, 25.63, 24.97. HRMS m/z calc'd for $C_{24}H_{43}N_3O_{16}Na$ ($M+Na^+$): 652.2541; found: 652.2522

Synthesis of Man-peptide conjugates

1. Solid-phase peptide synthesis

The procedure of peptide synthesis was adapted from the literature.[27] Briefly, Rink Amide AM resin (200 mg, 0.91 mmol g^{-1}, 0.18 mmol) was weighed into a Poly-Prep® chromatography column. The column was set up on a vacuum manifold. The manifold was equipped with a three-way stopcock that allows draining of the solvent by vacuum filtration and agitation of the resin by nitrogen bubbling.[28] CH_2Cl_2 (3 mL) was added to the dried resin for swelling. After 15 min, the solvent was drained by vacuum filtration. The resin was washed with DMF (3 mL) and then deprotected with 20% (v/v) piperidine in DMF (3 mL) for 1 min. The deprotection was repeated for another 10 min using fresh 20% (v/v) piperidine in DMF (3 mL). The resin was washed with DMF (4 × 3 mL). Fmoc-protected amino acid (0.73 mmol, 4 eq.) and HBTU (276 mg, 0.73 mmol, 4 eq.) dissolved in DMF (3 mL) were added to the resin. After 30 s agitation, DIPEA (0.25 mL, 1.46 mmol, 8 eq.) was added to the mixture. After 30 min agitation, the reagents were removed by vacuum filtration and the resin was washed with DMF (4 × 3 mL). The Fmoc-deprotection, amide coupling, and washing steps were repeated consecutively to elongate the sequence up to Fmoc-Ser(tBu)-OH, the *N*-terminal residue. After Fmoc-deprotection, the resin was washed with DMF (5 × 3 mL), followed by CH_2Cl_2 (5 × 3 mL). The resin was left on the manifold for 10 min to dry under the vacuum. A cleavage cocktail (2 mL) containing TFA/H_2O/phenol/TIPS [85/5/5/5 (v/v/w/v)] was added to the dried resin. The column was left on a rocker for 2 h to cleave the peptide. The flow through from the column was collected and the resin was rinsed with TFA (1 mL). The combined cleavage mixture was added dropwise to cold diethyl ether (20 mL) in a centrifuge tube. The mixture was incubated on ice for 30 min. The precipitates were centrifuged for 5 min at 3000 rpm. Supernatant was decanted and the precipitates were washed with cold diethyl ether (10 mL). The centrifugation and washing steps were repeated for another two cycles. The precipitates were air-dried and then left under vacuum for overnight. Typical yield: 50–150 mg.

The procedure described above produced the *C*-terminal peptide amides. To generate peptides with carboxylic acid at the *C*-terminus, Wang resin was used instead. The procedure is similar as described above, except for the loading of the first amino acid. After swelling of Wang resin (300 mg, 0.59 mmol/g, 0.18 mmol) with CH_2Cl_2 (3 mL) for 15 min, the resin was resuspended in 9:1 (v/v) CH_2Cl_2/DMF (3.6 mL/0.4 mL). Fmoc-protected amino acid (0.53 mmol, 3 eq.) and HOAt (72 mg, 0.53 mmol, 3 eq.) dissolved in a minimum amount of DMF were added to the resin. The mixture was agitated for 30 s. DIC (0.08 mL, 0.53 mmol, 3 eq.) was added to the resin followed by DMAP (2 mg, 0.02 mmol, 0.1 eq.) dissolved in a minimum amount of DMF. After 2 h of agitation, the unreacted hydroxyl groups were capped with acetic anhydride (0.03 mL, 0.35 mmol, 2 eq.) in the presence of pyridine (0.03 mL, 0.35 mmol, 2 eq.). The mixture was agitated for 30 min. The reagents were removed and the resin was washed with DMF (4 × 3 mL). Fmoc-deprotection, subsequent coupling of the amino acid, cleavage of peptide, and ether precipitation are identical as described for Rink Amide Am resin.

2. Purification of crude peptide

Crude peptide (40 mg) was dissolved in DMF (0.25 mL) and 0.1% aqueous TFA (0.25 mL). The solution was injected into a semi-preparative RP-HPLC system. A gradient of solvent A (MQ water, 0.1% (v/v) TFA) and solvent B (MeCN, 0.1% (v/v) TFA) was run at a flow rate of 12 mL/min as shown below. The fractions corresponding to the main peak were collected. MeCN was removed by evaporation under reduced pressure. The aqueous solution was lyophilized to yield the peptide as white powder (20–32 mg).

Time (min)	Eluent B (%)
0	5
2	5
26	35
27	100
29	100
30	5

3. Representative example of synthesis of Man-peptide conjugates

SYWD (5.7 mg, 10 μmol, 1 eq.) was dissolved in DMF (0.25 mL) followed by the addition of 200 mM MOPS (0.25 mL, pH 7.0). The solution was added to a 1.5-mL microcentrifuge tube containing sodium periodate (2.6 mg, 12 μmol, 1.2 eq.). The reaction mixture was incubated for 10 min at RT. To quench the oxidation, the solution was added to glutathione (37 mg, 120 μmol, 12 eq.) and mixed rapidly to ensure the dissolution of glutathione. After incubation for 10 min at RT, 2-(aminooxy)ethyl *α*-D-mannopyranoside (2.6 mg, 11 μmol, 1.1 eq.) dissolved in 200 mM anilinium acetate (0.25 mL, pH 4.7) was added to the quenched solution. The oxime ligation was carried out for 30 min at RT. The reaction mixture was injected into a semi-preparative RP-HPLC system. HPLC purification was carried out as described above for crude peptide to yield the product as a white fluffy powder (40–70% isolated yield) after lyophilization. The purity of the product was determined with an analytical RP-HPLC system (flow rate: 1 mL/min) using a gradient of solvent A (MQ water, 0.1% (v/v) TFA) and solvent B (MeCN, 0.1% (v/v) TFA) as shown below. The product was further characterized with HRMS (ESI).

Time (min)	Eluent B (%)
0	5
2	5
16	40
17	100
19	100
20	5

Man-WYD (**L20**)

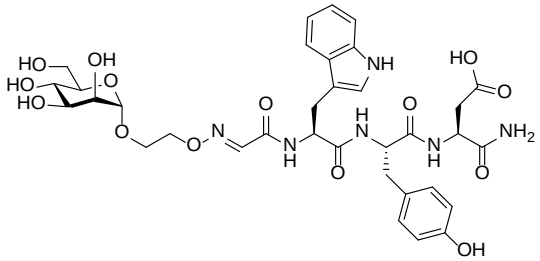

White fluffy powder (5.0 mg, 66% isolated yield): ^{1}H NMR (600MHz , deuterated PBS + 0.1% (v/v) DMSO-d_6) δ = 7.61 (d, *J* = 7.9 Hz, 1 H), 7.56 (s, 1 H), 7.50 (d, *J* = 7.9 Hz, 1 H), 7.24 (t, *J* = 7.9 Hz, 1 H), 7.20 – 7.13 (m, 2 H), 6.96 (d, *J* = 8.1 Hz, 2 H), 6.74 (d, *J* = 8.1 Hz, 2 H), 4.88 (br. d, 1 H), 4.69 (t, *J* = 6.9 Hz, 1 H), 4.50 – 4.42 (m, 2 H), 4.41 – 4.33 (m, 2 H), 3.98 – 3.91 (m, 2 H), 3.83 - 3.75 (m, 3 H), 3.75 – 3.70 (m, 1 H), 3.66 (t, *J* = 9.6 Hz, 1 H), 3.62 – 3.56 (m, 1 H), 3.29 – 3.17 (m, 2 H), 2.92 (dd, *J* = 7.4, 13.9

Hz, 1 H), 2.79 (dd, *J* = 7.4, 13.9 Hz, 1 H), 2.60 (dd, *J* = 6.7, 16.0 Hz, 1 H), 2.50 (dd, *J* = 6.7, 16.0 Hz, 1 H); HRMS (ESI) calcd for $C_{34}H_{41}N_6O_{14}$ $[M-H]^-$ *m/*z = 757.2686, found 757.2691.

4. Synthesis of Me-peptide conjugates

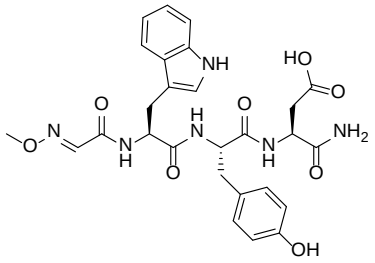

The synthesis and purification are identical to that of Man-peptides, other than the use of methoxylamine instead of 2-(aminooxy)ethyl *α*-D-mannopyranoside during the oxime ligation. Me-WYSVLSH (6.7 mg, 69% isolated yield) and Me-WYD (3.1 mg, 55% isolated yield) were obtained as a white fluffy powder. The purity of the products was determined with an analytical RP-HPLC system as described above. The products were further characterized with HRMS (ESI).

5. Synthesis of Man-NL-WYD (L20.3)

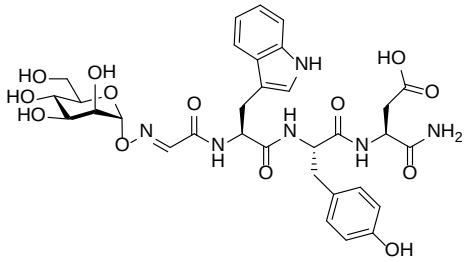

The synthesis and purification are identical to that of Man-peptides, other than the use of *O*-α-D-mannopyranosyl oxyamine instead of 2-(aminooxy)ethyl α-D-mannopyranoside during the oxime ligation. The product was obtained as a white fluffy powder (4.3 mg, 60% isolated yield): ^{1}H NMR (500MHz, D_2O + 0.1% (v/v) DMSO-d_6) δ = 7.65 (s, 1 H), 7.60 (d, *J* = 7.9 Hz, 1 H), 7.49 (d, *J* = 7.9 Hz, 1 H), 7.24 (t, *J* = 7.9 Hz, 1 H), 7.21 (s, 1 H), 7.16 (t, *J* = 7.9 Hz, 1 H), 6.93 (d, *J* = 8.4 Hz, 2 H), 6.74 (d, *J* = 8.4 Hz, 2 H), 5.53 (br. d, 1 H), 4.68 (t, *J* = 7.1 Hz, 1 H), 4.50 (t, *J* = 7.2 Hz, 1 H), 4.42 (t, *J* = 7.2 Hz, 1 H), 4.14 (dd, *J* = 1.9, 3.2 Hz, 1 H), 3.90 – 3.72 (m, 4 H), 3.68 – 3.60 (m, 1 H), 3.29 – 3.17 (m, 2 H), 2.86 – 2.72 (m, 3 H), 2.61 (dd, *J* = 7.2, 17.0 Hz, 1 H); HRMS (ESI) calcd for $C_{32}H_{37}N_6O_{13}$ $[M-H]^-$ *m/*z = 713.2424, found 713.2430.

6. Synthesis of Man-allyl-WYD (L20.4)

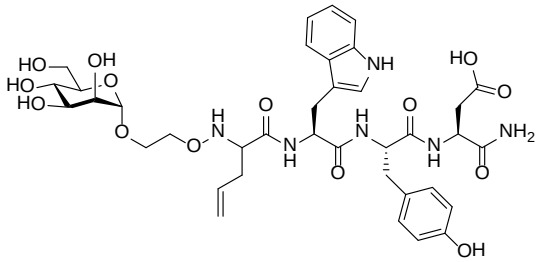

To a mixture of allyl bromide (12 μL, 132 μmol, 20 eq.) and indium (3 mg, 26 μmol, 4 eq.), a solution of Man-WYD **L20** (5 mg, 6.6 μmol, 1 eq.) dissolved in DMF/H_2O/MeOH (200 μL, 1:1:2) was added. The mixture was agitated for 2 h at RT, after which, the solid was filtered. The filtrate was injected into a semi-preparative RP-HPLC system. HPLC purification was carried out as described above for crude peptide to yield the product as a white fluffy powder (2 mg, 38% isolated yield): ^{1}H NMR (500MHz, D_2O + 0.1% (v/v) DMSO-d_6) δ = 7.62 (d, *J* = 7.7 Hz, 1 H), 7.48 (d, *J* = 8.3 Hz, 1 H), 7.26 – 7.20 (m, 2 H), 7.15 (t, *J* = 7.7 Hz, 1 H), 7.01 (d, *J* = 8.4 Hz, 2 H), 6.79 (d, *J* = 8.4 Hz, 2 H), 5.49 – 5.37 (m, 1 H), 5.03 – 4.92 (m, 2 H), 4.77 (br. d, 1 H), 4.71 – 4.65 (m, 1 H), 4.56 (t, *J* = 6.4 Hz, 1 H), 4.46 (t, *J* = 7.2 Hz, 1 H), 3.89 – 3.79 (m, 2 H), 3.75 – 3.69 (m, 2 H), 3.69 – 3.51 (m, 6 H), 3.51 – 3.44 (m, 1 H), 3.24 (dd, *J* = 7.2, 14.9 Hz, 1 H), 3.13 (dd, *J* = 7.2, 14.9 Hz, 1 H), 2.93 – 2.77 (m, 3 H), 2.71 – 2.65 (m, 1 H), 2.12 (t, *J* = 6.9 Hz, 2 H); HRMS (ESI) calcd for $C_{37}H_{47}N_6O_{14}$ $[M–Na]^-$ *m/*z = 799.3156, found 799.3163.

7. Synthesis of Man-SL-WYD (L20.5)

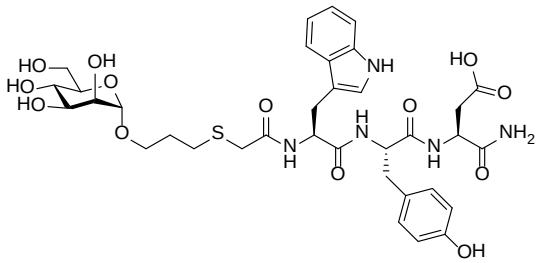

The whole synthesis was carried out on resin as described above for solid-phase peptide synthesis. Briefly, Rink Amide AM resin (100 mg, 0.91 mmol g^{-1}, 0.09 mmol) was weighed into a Poly-Prep® chromatography column. After the swelling of the resin and Fmoc-deprotection, the resin was coupled with Fmoc-Asp(OtBu)-OH. The cycles of Fmoc-deprotection, amide coupling and washing step were repeated consecutively for Fmoc-Tyr(tBu)-OH and Fmoc-Trp(Boc)-OH. After the final Fmoc-deprotection, carboxymethylthiopropyl α-D-mannopyranoside (74 mg, 0.18 mmol, 2 eq.) and DEPBT (54 mg, 0.18 mmol, 2 eq.) dissolved in DMF was added to the resin. After 30 s agitation, DIPEA (0.06 mL, 0.36 mmol, 4 eq.) was added to the mixture and the mixture was agitated for 2 h. The resin was washed with DMF (5 × 3 mL), followed by CH_2Cl_2 (5 × 3 mL). The resin was left on the manifold for 10 min to dry under the vacuum. A cleavage cocktail (1 mL) containing TFA/H_2O/phenol/TIPS [85/5/5/5 (v/v/w/v)] was added to the dried resin. The column was left on a rocker for 2 h to cleave the peptide. The flow through from the column was collected and the resin was rinsed with TFA (1 mL). The combined cleavage mixture was added dropwise to cold diethyl ether (20 mL) in a centrifuge tube. The mixture was incubated on ice for 30 min. The precipitates were centrifuged for 5 min at 3000 rpm. Supernatant was decanted and the precipitates were washed with cold diethyl ether (10 mL). The centrifugation and

washing steps were repeated for another two cycles. The precipitates were air-dried and then left under vacuum for overnight. The crude solid was dissolved in DMF (0.25 mL) and 0.1% aqueous TFA (0.25 mL). The solution was injected into a semi-preparative RP-HPLC system. HPLC purification was carried out as described above for crude peptide to yield the product as to yield the product as white powder (35 mg, 50% isolated yield): HRMS (ESI) calcd for $C_{35}H_{44}N_5O_{13}S$ $[M-H]^-$ *m/*z = 774.2662, found 774.2656.

8. Synthesis of Man-WYK(Cy3)-OH

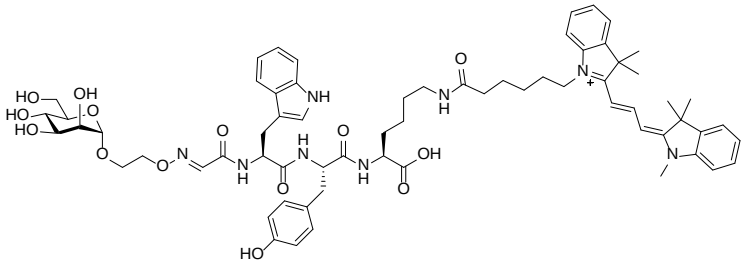

To a solution of Man-WYK-OH (4 mg, 5.2 μmol, 1 eq.) in DMSO/100 mM $NaHCO_3$ (400 μL, 1:1, pH 8.35), a solution of Cyanine3 NHS ester (3 mg, 5.2 μmol, 1 eq.) in DMSO (100 μL) was added. After three hours of reaction, the mixture was purified on semi-preparative RP-HPLC system. A gradient of solvent A (MQ water, 0.1% (v/v) TFA) and solvent B (MeCN, 0.1% (v/v) TFA) was run at a flow rate of 12 mL/min as shown below. The fractions corresponding to the main peak were collected. MeCN was removed by evaporation under reduced pressure. The aqueous solution was lyophilized to yield the product as red powder (4 mg, 58% isolated yield). HRMS (ESI) calcd for $C_{66}H_{83}N_8O_{14}$ $[M]^+$ *m/*z = 1211.6023, found 1211.6005.

Time (min)	Eluent B (%)
0	5
2	5
26	100
27	100
29	100
30	5

HPLC purity and HRMS spectra of synthesized ligands

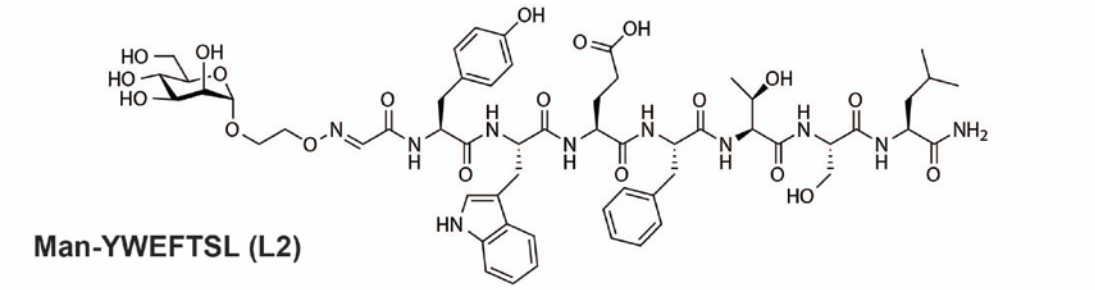

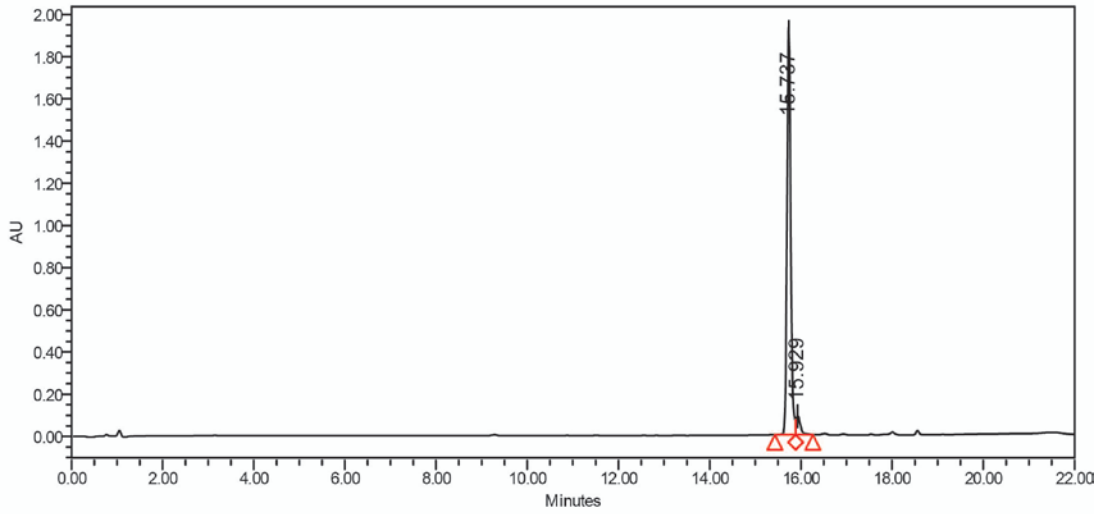

Peak Results

	RT	Area	Height	% Area
1	15.737	1111421	1918960	94.72
2	15.929	619860	88725	5.28

User Spectra

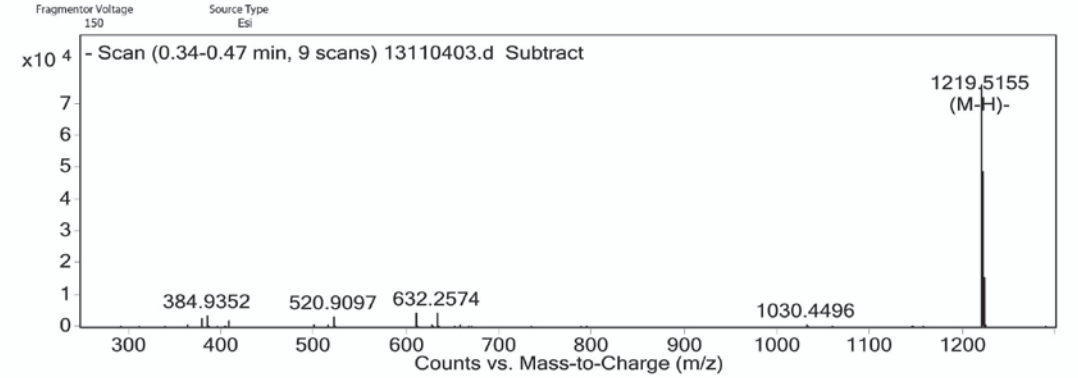

Formula Calculator Results

Formula	Ion Species	m/z	Calc. m/z	Diff (mDa)	Diff (ppm)	DBE	Ion	Score
C57 H76 N10 O20	C57 H75 N10 O20	1219.5155	1219.5165	0.88	0.72	25	(M-H)-	95.55

--- End Of Report ---

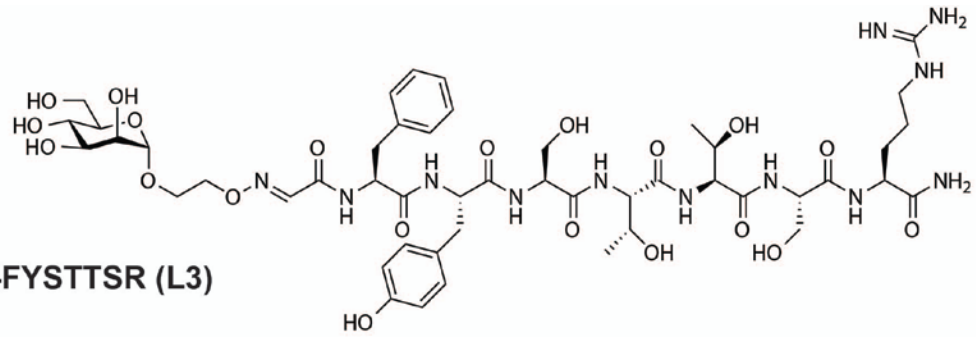

Man-FYSTTSR (L3)

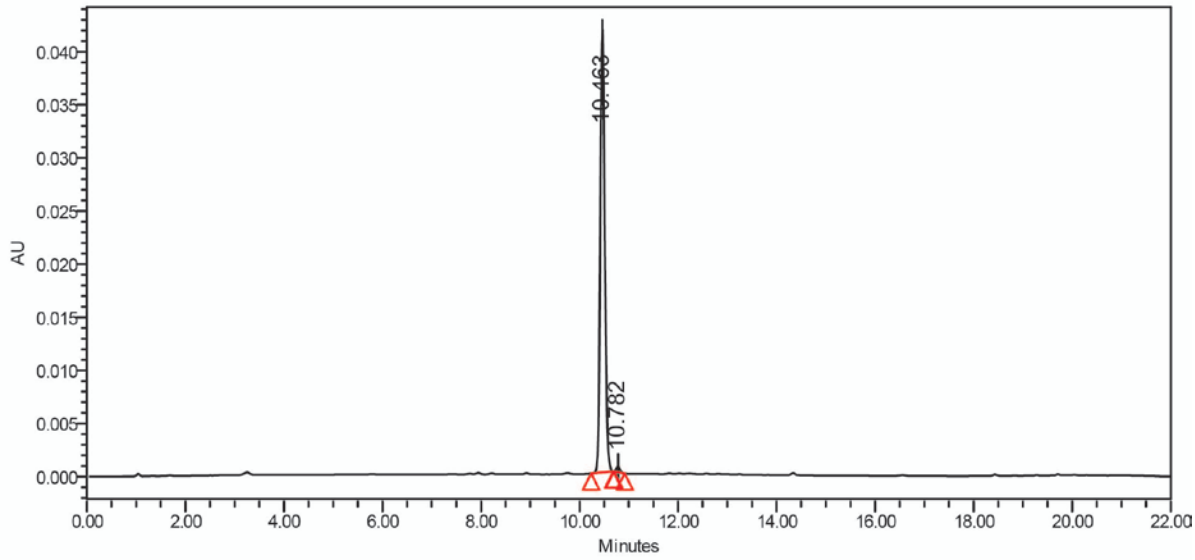

Peak Results

	RT	Area	Height	% Area
1	10.463	266395	41582	98.95
2	10.782	2833	542	1.05

User Spectra

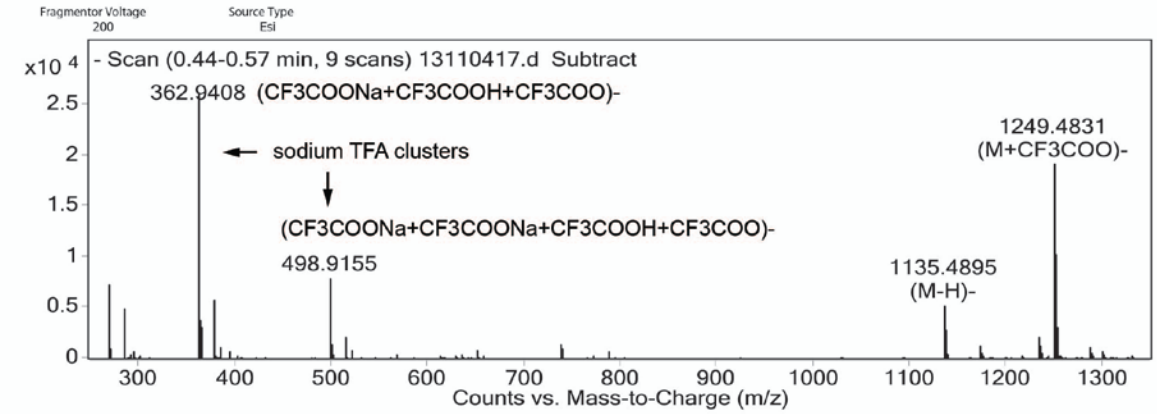

Formula Calculator Results

Formula	Ion Species	m/z	Calc. m/z	Diff (mDa)	Diff (ppm)	DBE	Ion	Score
C48 H72 N12 O20	C48 H71 N12 O20	1135.4895	1135.4913	1.89	1.66	19	(M-H)-	92.27
C48 H72 N12 O20	C50 H72 F3 N12 O22	1249.4831	1249.4842	1.11	0.98	19	(M+CF3COO)-	93.95

--- End Of Report ---

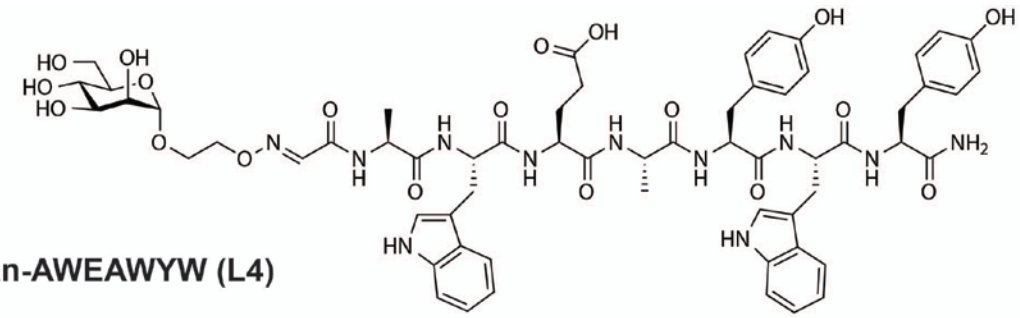

Man-AWEAWYW (L4)

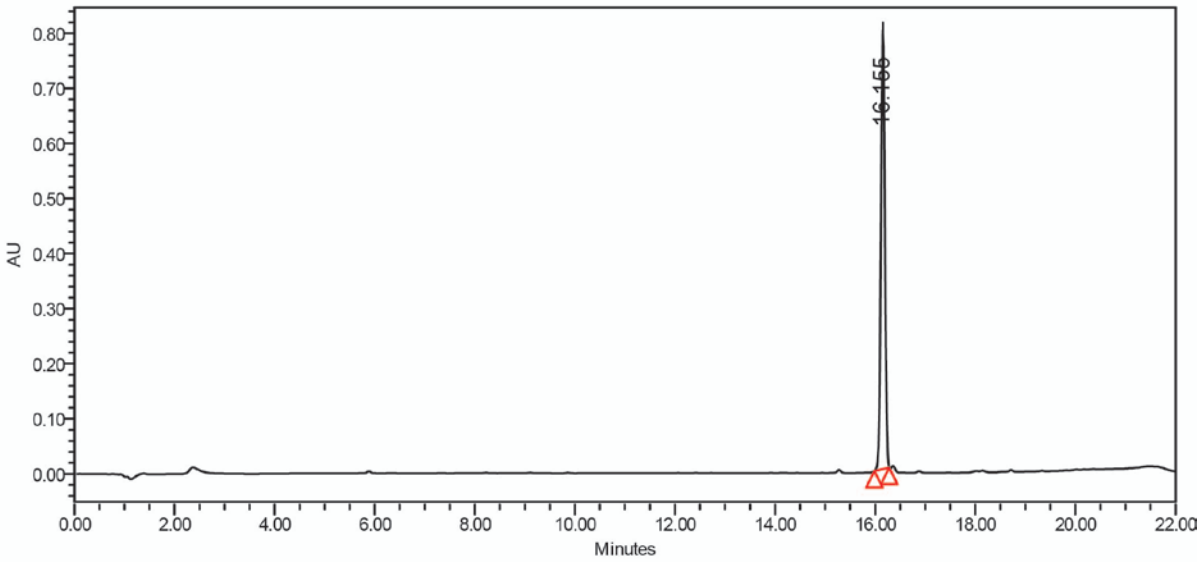

Peak Results

	RT	Area	Height	% Area
1	16.155	4480182	795606	100.00

User Spectra

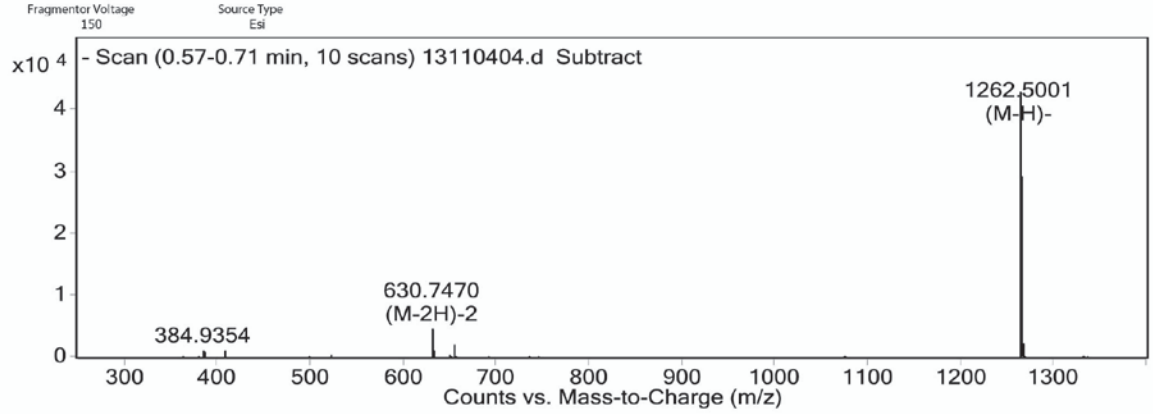

Formula Calculator Results

Formula	Ion Species	m/z	Calc. m/z	Diff (mDa)	Diff (ppm)	DBE	Ion	Score
C61 H73 N11 O19	C61 H72 N11 O19	1262.5001	1262.5011	1.01	0.8	31	(M-H)-	94.45
C61 H73 N11 O19	C61 H71 N11 O19	630.747	630.7469	0.06	0.05	31	(M-2H)-2	99.46

--- End Of Report ---

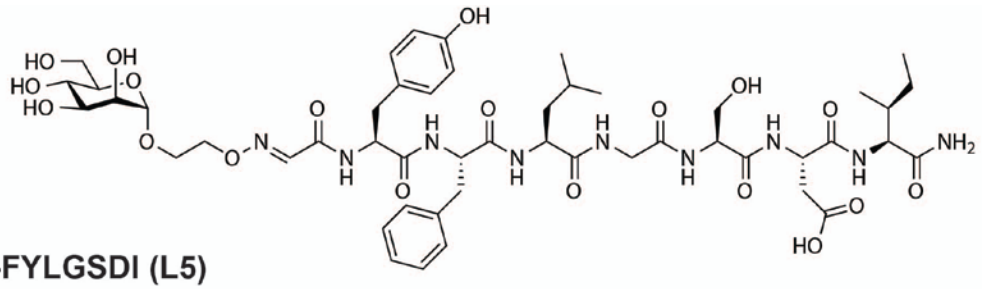

Man-FYLGSDI (L5)

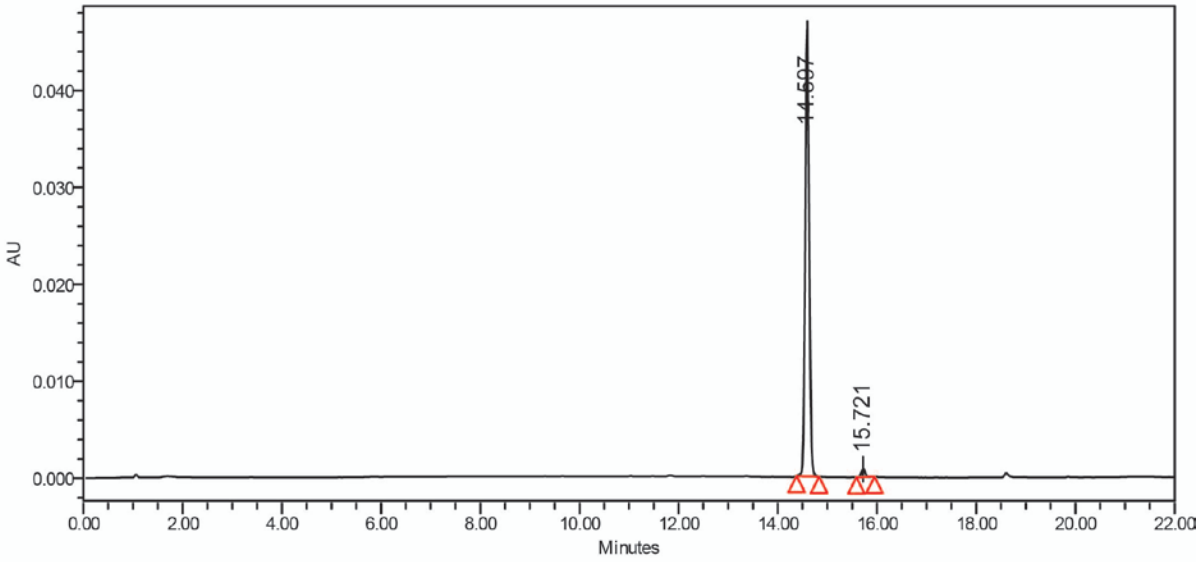

Peak Results

	RT	Area	Height	% Area
1	14.597	253573	45834	98.25
2	15.721	4525	829	1.75

User Spectra

Fragmentor Voltage 150 Source Type Esi

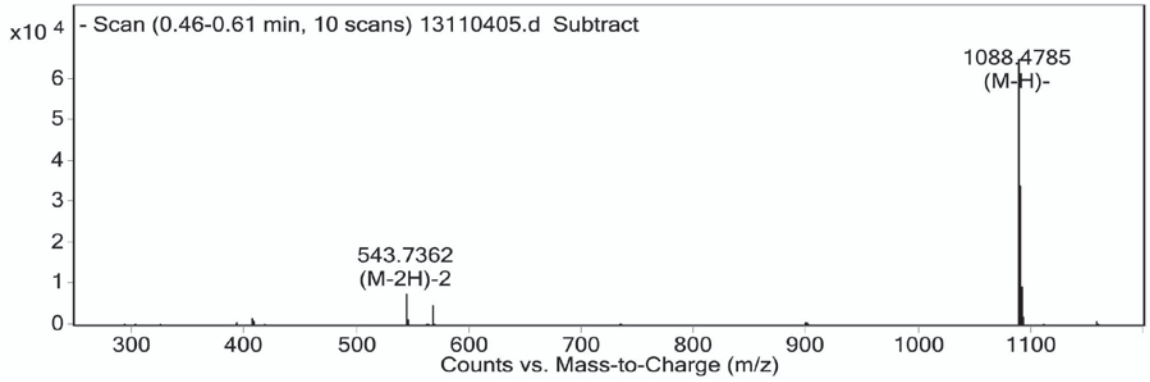

Formula Calculator Results

Formula	Ion Species	m/z	Calc. m/z	Diff (mDa)	Diff (ppm)	DBE	Ion	Score
C49 H71 N9 O19	C49 H70 N9 O19	1088.4785	1088.4793	0.77	0.71	19	(M-H)-	95.19
C49 H71 N9 O19	C49 H69 N9 O19	543.7362	543.736	-0.27	-0.25	19	(M-2H)-2	99.21

--- End Of Report ---

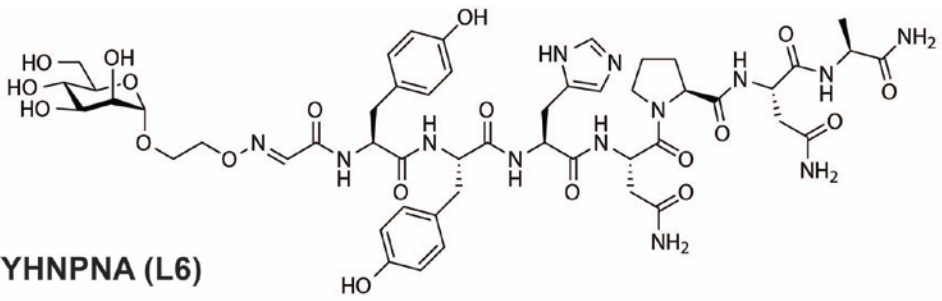

Man-YYHNPNA (L6)

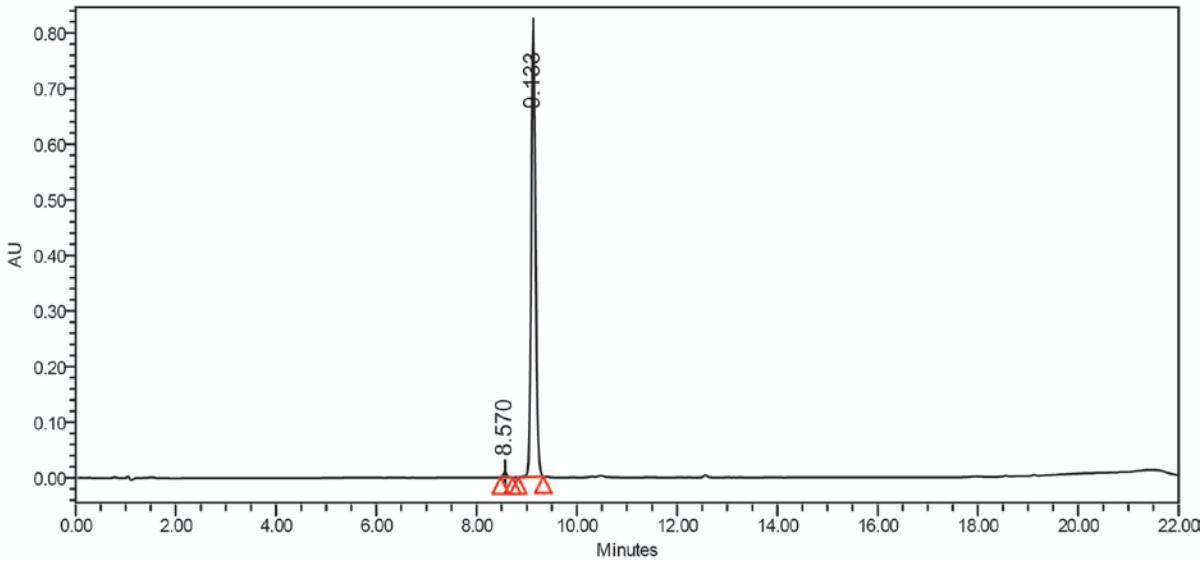

Peak Results

	RT	Area	Height	% Area
1	8.570	46334	8413	0.94
2	9.133	4861914	797620	99.06

User Spectra

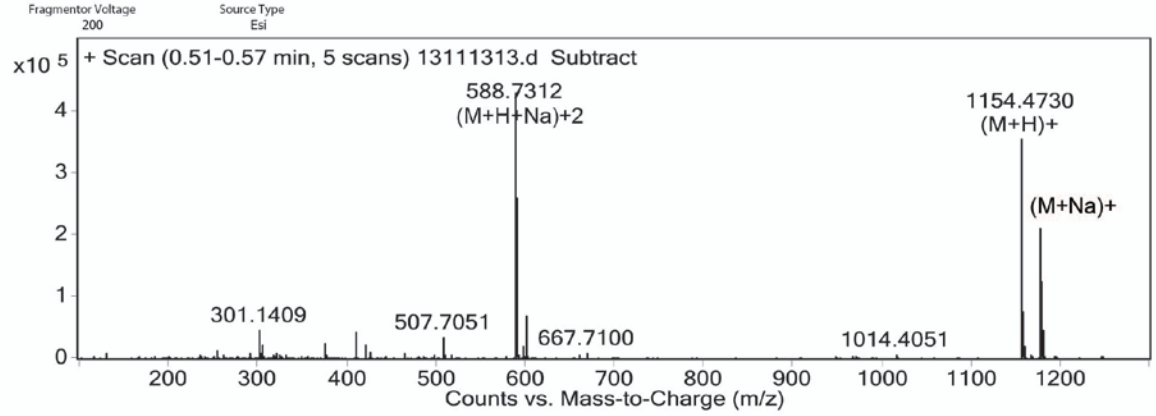

Formula Calculator Results

Formula	Ion Species	m/z	Calc. m/z	Diff (mDa)	Diff (ppm)	DBE	Ion	Score
C50 H67 N13 O19	C50 H68 N13 O19	1154.473	1154.4749	1.89	1.64	24	(M+H)+	95.19
C50 H67 N13 O19	C50 H67 N13 Na O19	1176.4552	1176.4568	1.64	1.42	24	(M+Na)+	96.38

--- End Of Report ---

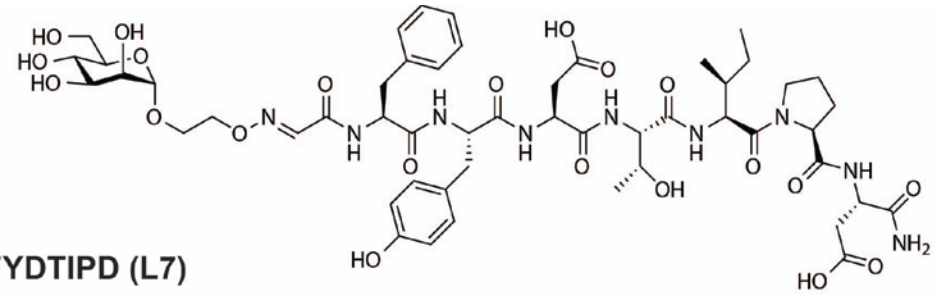

Man-FYDTIPD (L7)

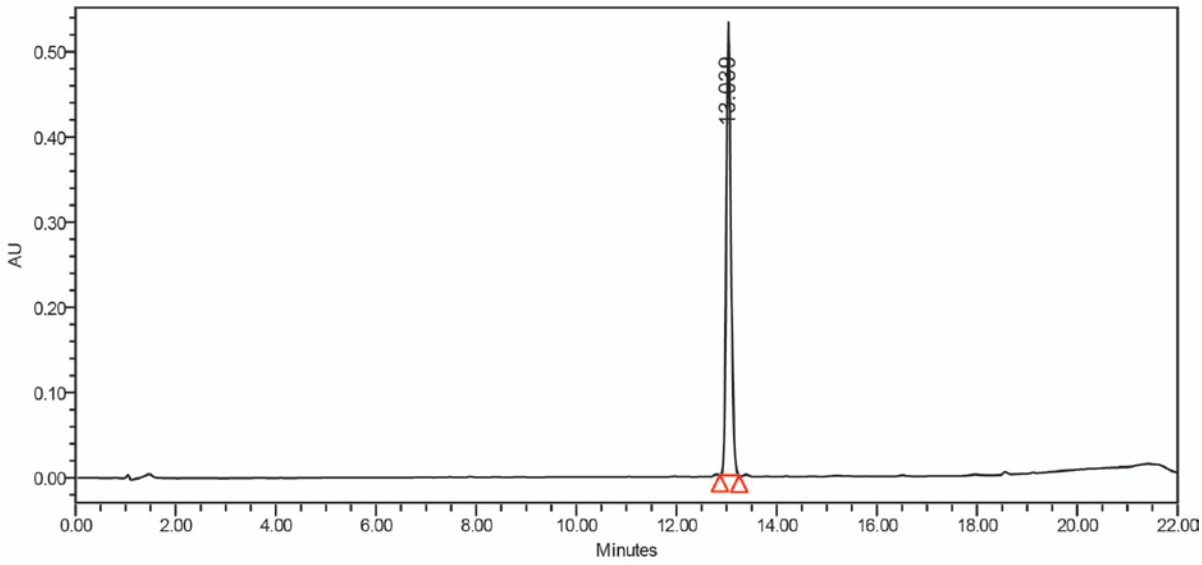

Peak Results

	RT	Area	Height	% Area
1	13.039	3443559	522726	100.00

User Spectra

Fragmentor Voltage 150 Source Type Esi

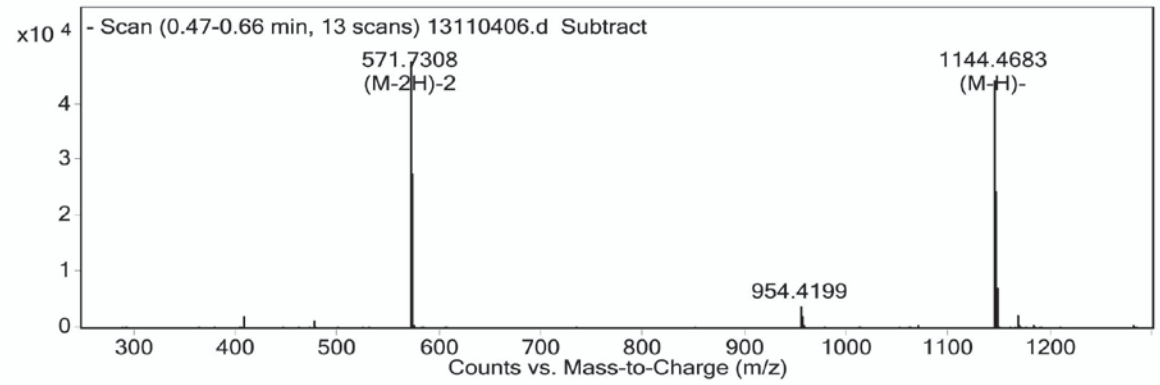

Formula Calculator Results

Formula	Ion Species	m/z	Calc. m/z	Diff (mDa)	Diff (ppm)	DBE	Ion	Score
C51 H71 N9 O21	C51 H69 N9 O21	571.7308	571.7309	0.19	0.17	21	(M-2H)-2	98.54
C51 H71 N9 O21	C51 H70 N9 O21	1144.4683	1144.4692	0.79	0.69	21	(M-H)-	95.11

--- End Of Report ---

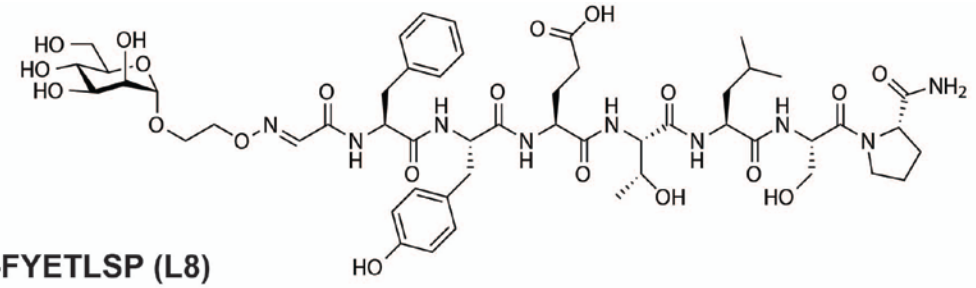

Man-FYETLSP (L8)

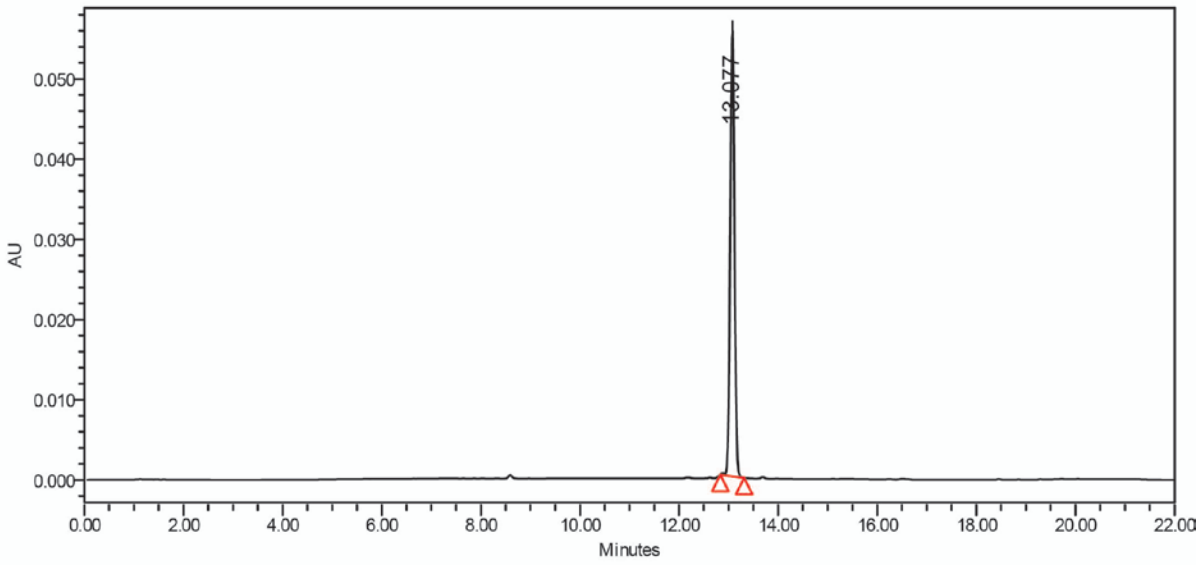

Peak Results

	RT	Area	Height	% Area
1	13.077	339489	55754	100.00

User Spectra

Fragmentor Voltage 150 Source Type Esi

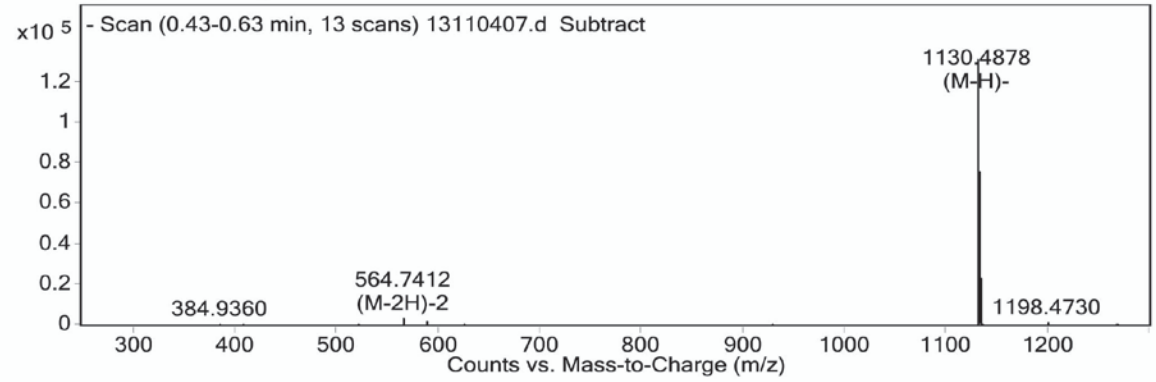

Formula Calculator Results

Formula	Ion Species	m/z	Calc. m/z	Diff (mDa)	Diff (ppm)	DBE	Ion	Score
C51 H73 N9 O20	C51 H71 N9 O20	564.7412	564.7413	0.37	0.33	20	(M-2H)-2	99.44
C51 H73 N9 O20	C51 H72 N9 O20	1130.4878	1130.4899	1.85	1.63	20	(M-H)-	91.24

--- End Of Report ---

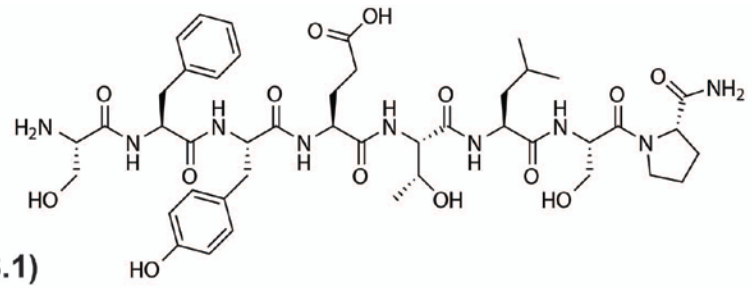

SFYETLSP (L8.1)

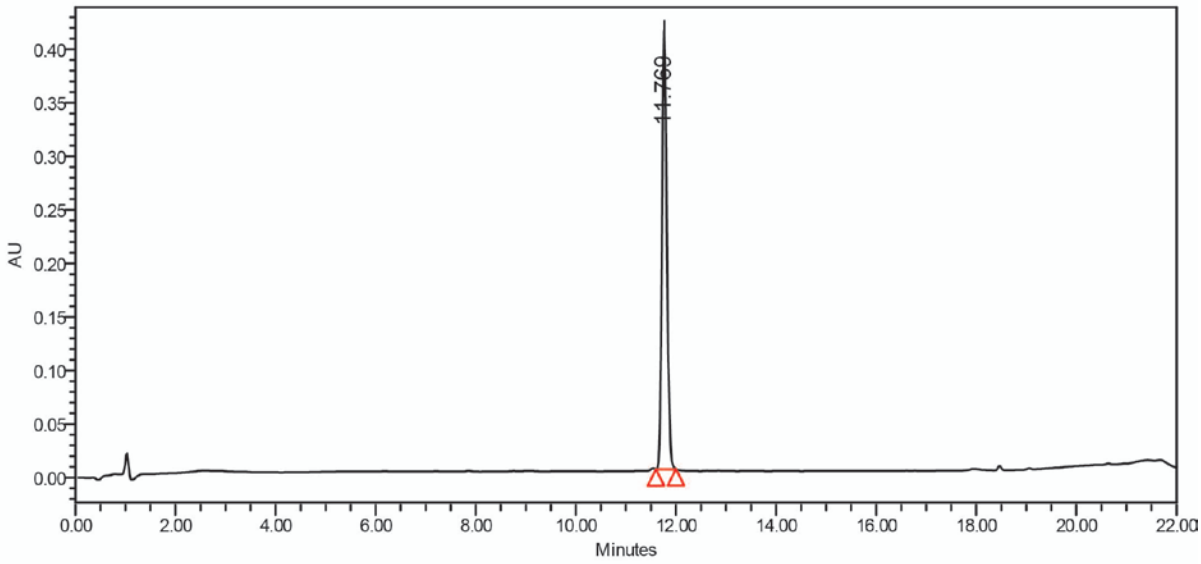

Peak Results

	RT	Area	Height	% Area
1	11.76	2796601	408733	100.00

User Spectra

Fragmentor Voltage 150 Source Type Esi

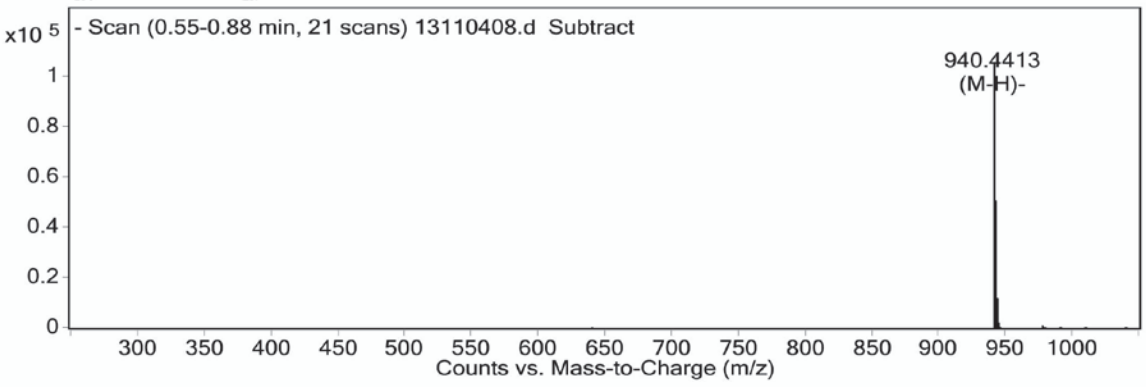

Formula Calculator Results

Formula	Ion Species	m/z	Calc. m/z	Diff (mDa)	Diff (ppm)	DBE	Ion	Score
C44 H63 N9 O14	C44 H62 N9 O14	940.4413	940.4422	0.75	0.8	18	(M-H)-	94.8

--- End Of Report ---

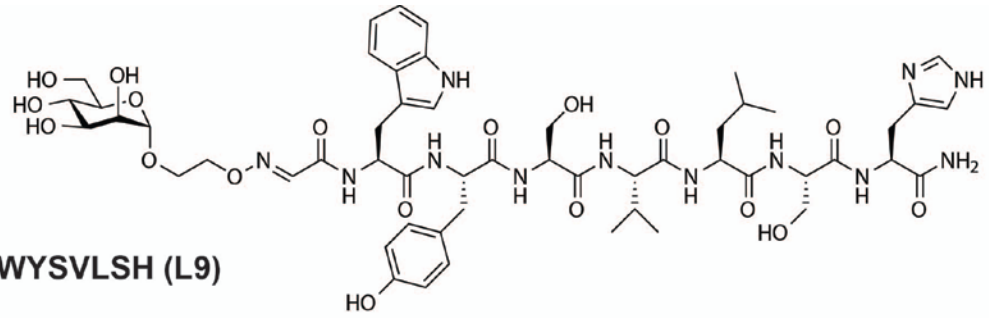

Man-WYSVLSH (L9)

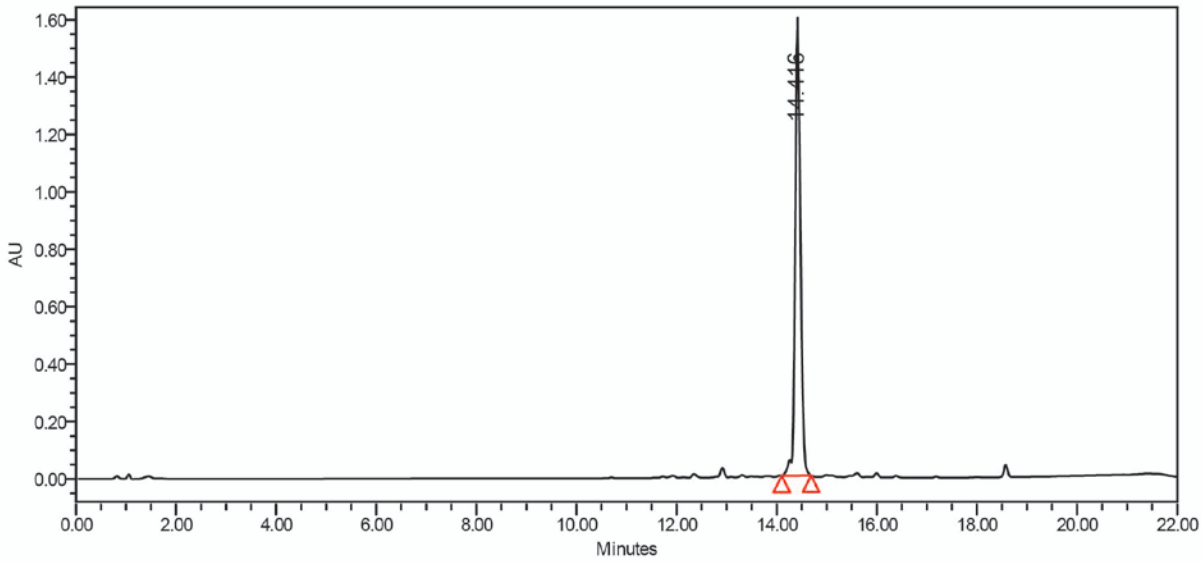

Peak Results

	RT	Area	Height	% Area
1	14.416	1168120(	1548779	100.00

User Spectra

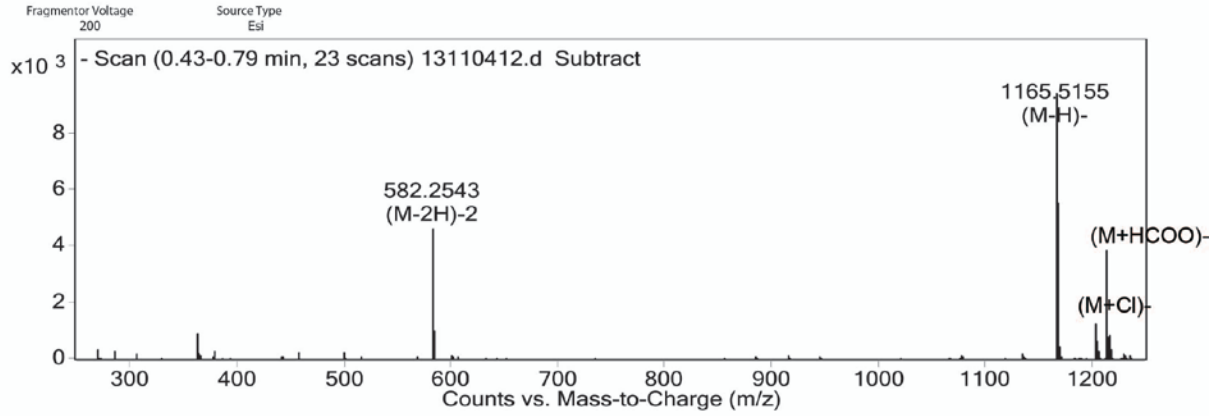

Formula Calculator Results

Formula	Ion Species	m/z	Calc. m/z	Diff (mDa)	Diff (ppm)	DBE	Ion	Score
C53 H74 N12 O18	C53 H72 N12 O18	582.2543	582.2549	1.16	1	23	(M-2H)-2	98.03
C53 H74 N12 O18	C53 H73 N12 O18	1165.5155	1165.5171	1.68	1.44	23	(M-H)-	93.7

--- End Of Report ---

SWYSVLSH (L9.1)

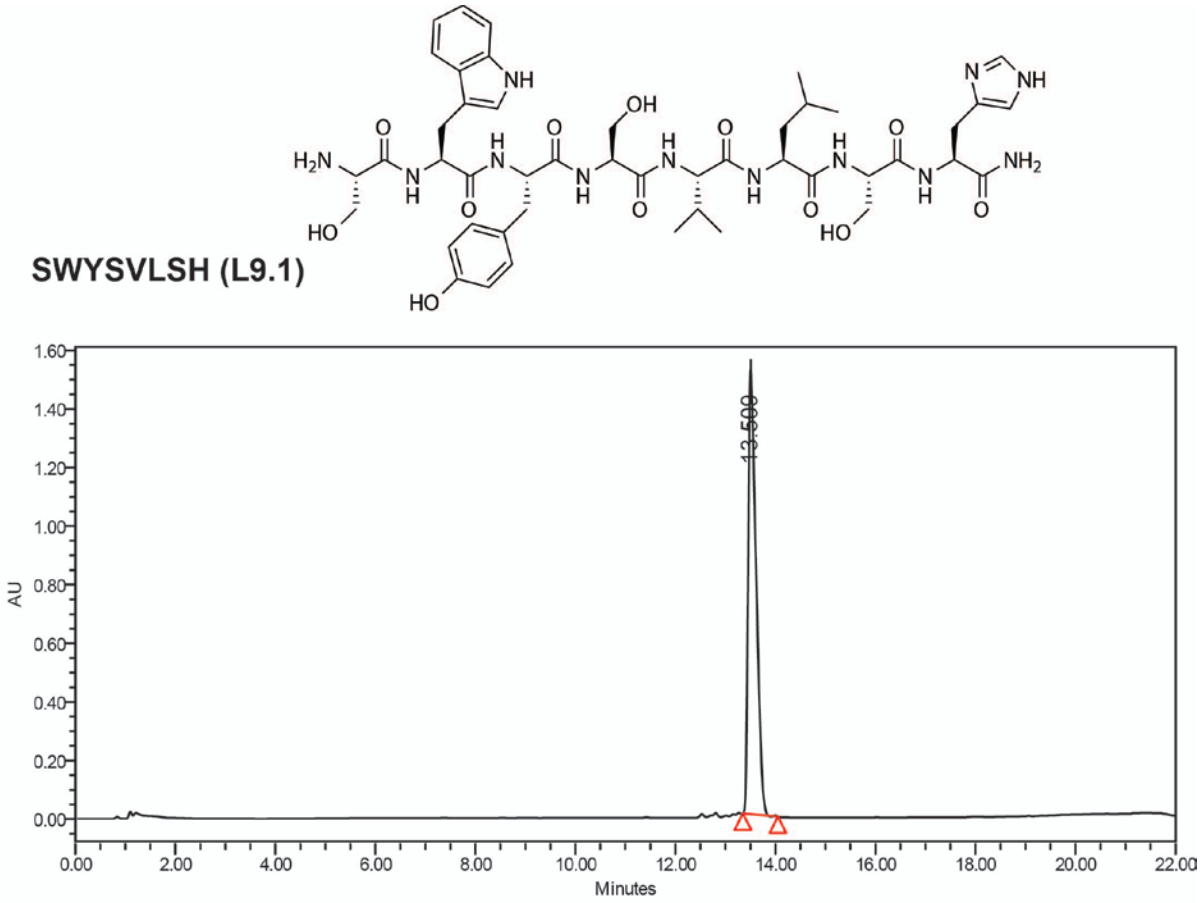

Peak Results

	Name	RT	Area	Height	% Area
1		13.509	16673459	1532418	100.00

User Spectra

Fragmentor Voltage 175 Source Type Esi

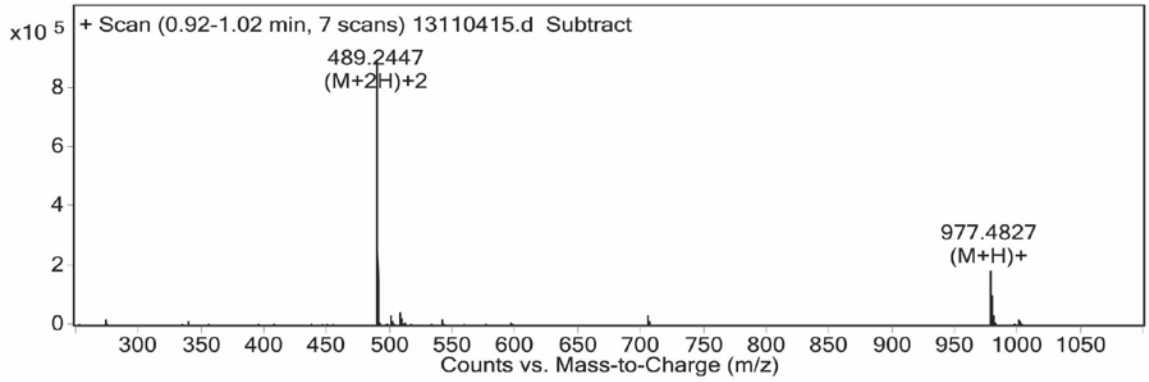

Formula Calculator Results

Formula	Ion Species	m/z	Calc. m/z	Diff (mDa)	Diff (ppm)	DBE	Ion	Score
C46 H64 N12 O12	C46 H66 N12 O12	489.2447	489.2456	1.95	2	21	(M+2H)+2	91.65
C46 H64 N12 O12	C46 H65 N12 O12	977.4827	977.4839	1.3	1.33	21	(M+H)+	96.71

--- End Of Report ---

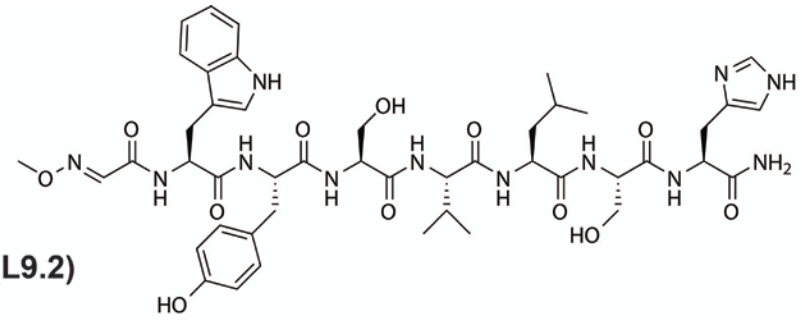

Me-WYSVLSH (L9.2)

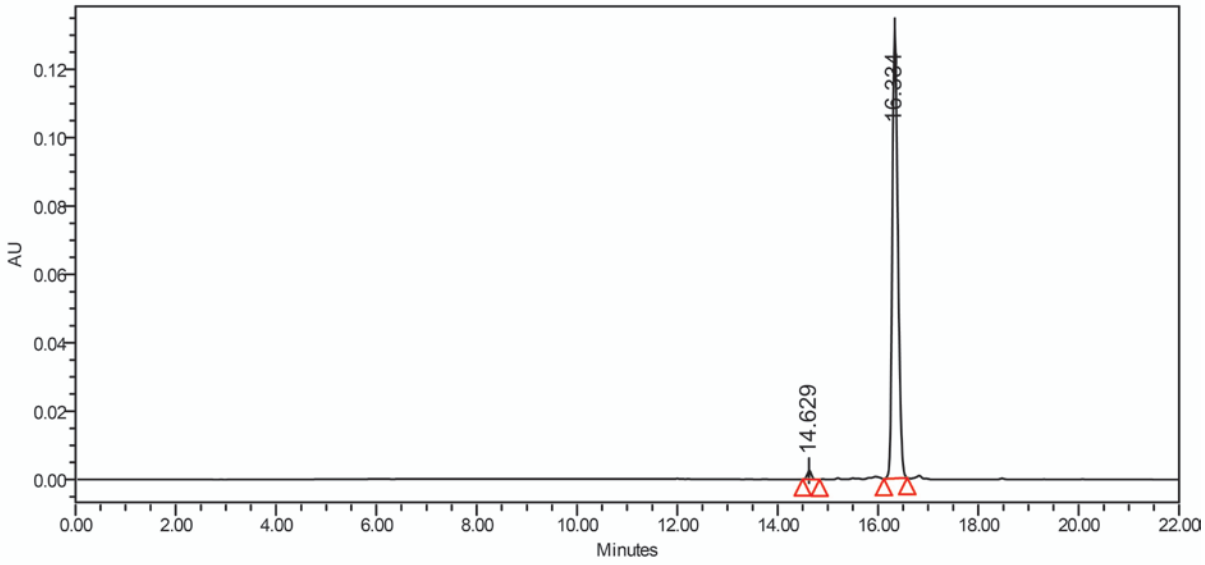

Peak Results

	RT	Area	Height	% Area
1	14.629	14068	2516	1.40
2	16.334	993766	131135	98.60

User Spectra

Fragmentor Voltage 150 Source Type Esi

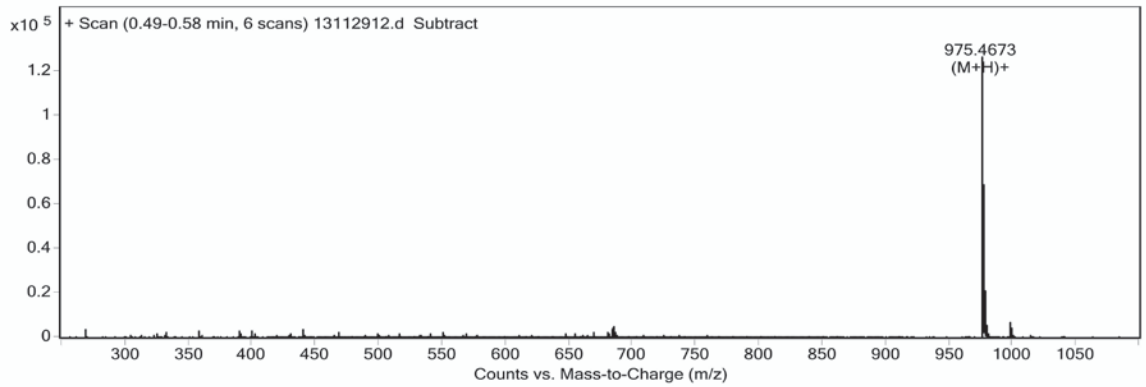

Formula Calculator Results

Formula	Ion Species	m/z	Calc. m/z	Diff (mDa)	Diff (ppm)	DBE	Ion	Score
C46 H62 N12 O12	C46 H63 N12 O12	975.4673	975.4683	1	1.03	22	(M+H)+	97.13
C46 H62 N12 O12	C46 H62 N12 Na O12	997.4521	997.4502	-1.75	-1.8	22	(M+Na)+	87.27

--- End Of Report ---

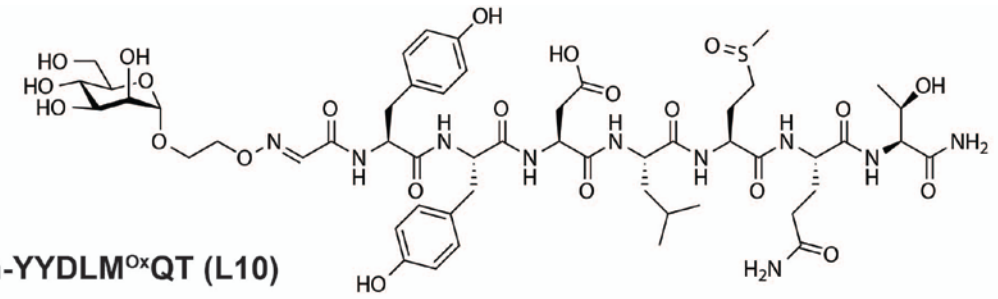

Man-YYDLM^{Ox}QT (L10)

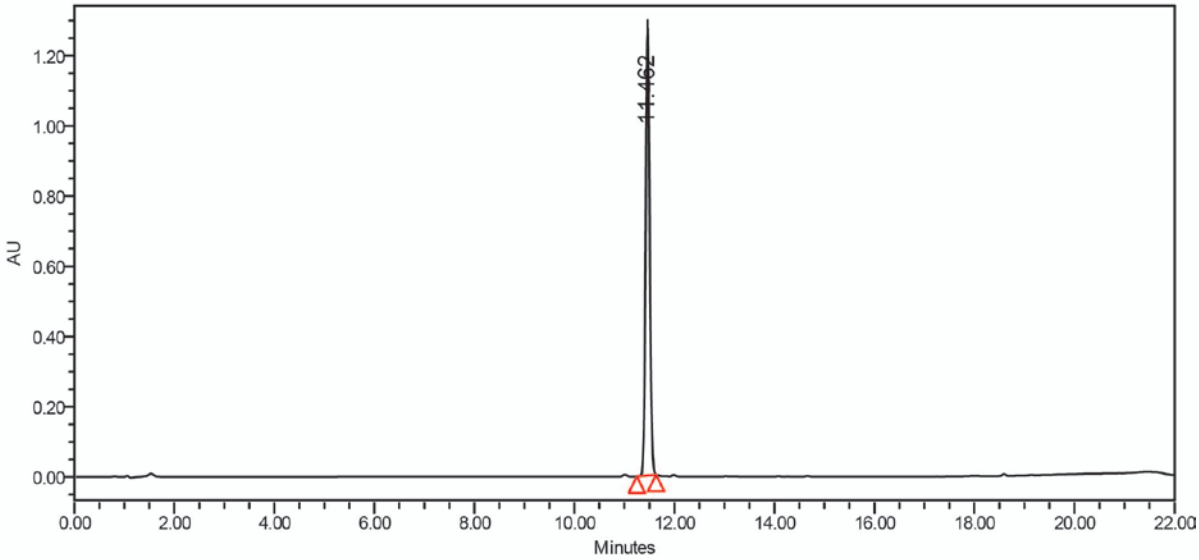

Peak Results

	RT	Area	Height	% Area
1	11.462	7305602	1269968	100.00

User Spectra

Fragmentor Voltage 150 Source Type Esi

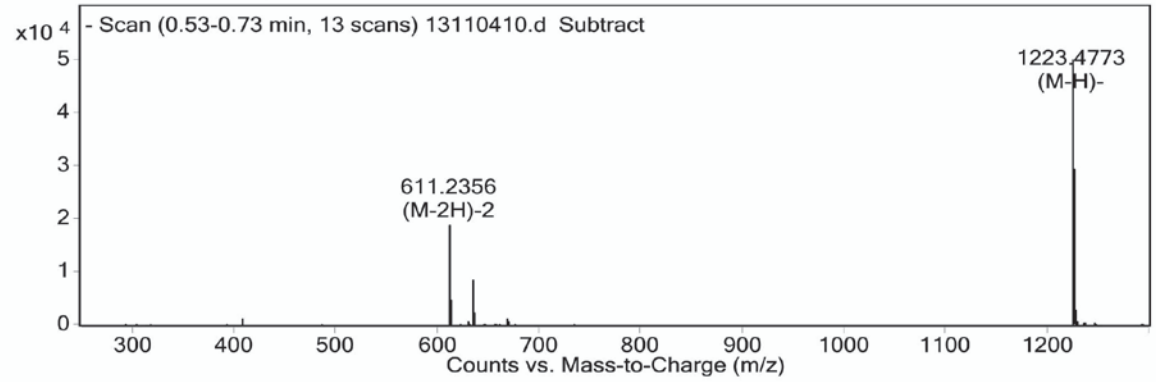

Formula Calculator Results

Formula	Ion Species	m/z	Calc. m/z	Diff (mDa)	Diff (ppm)	DBE	Ion	Score
C52 H76 N10 O22 S	C52 H74 N10 O22 S	611.2356	611.2355	-0.22	-0.18	20	(M-2H)-2	99.09
C52 H76 N10 O22 S	C52 H75 N10 O22 S	1223.4773	1223.4784	0.97	0.79	20	(M-H)-	95.24

--- End Of Report ---

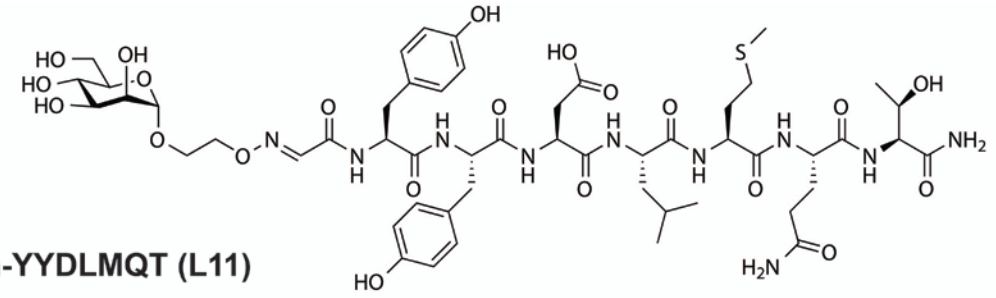

Man-YYDLMQT (L11)

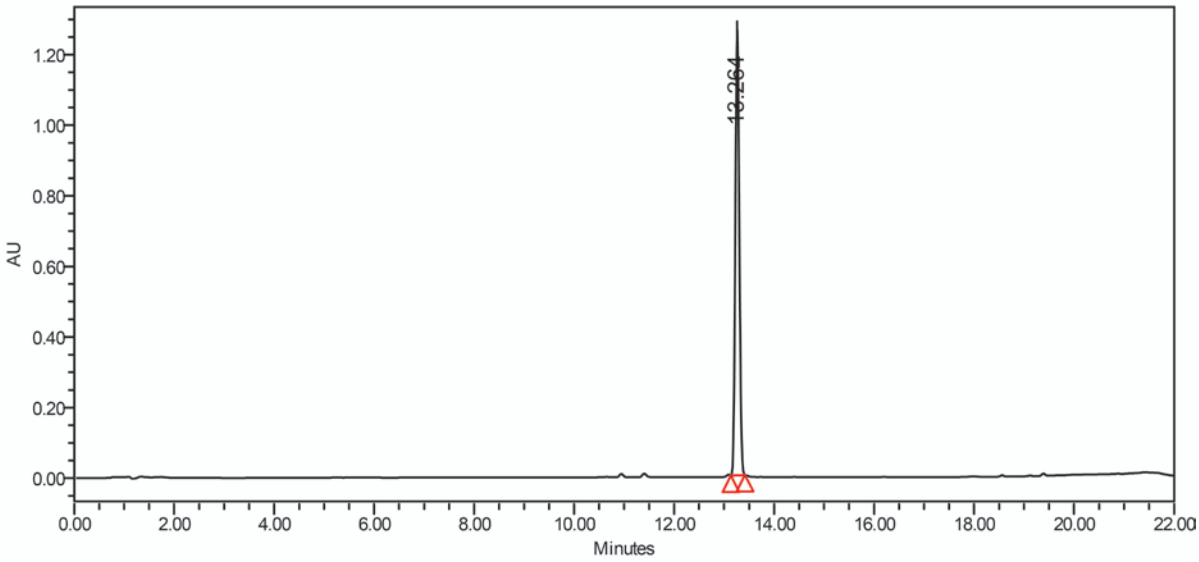

Peak Results

	RT	Area	Height	% Area
1	13.264	7061286	1255459	100.00

User Spectra

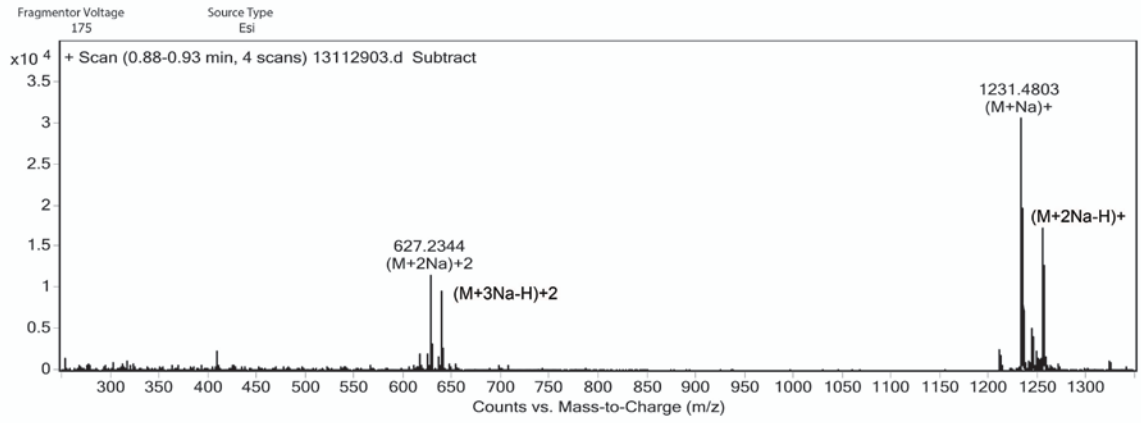

Formula Calculator Results

Formula	Ion Species	m/z	Calc. m/z	Diff (mDa)	Diff (ppm)	DBE	Ion	Score
C52 H76 N10 O21 S	C52 H77 N10 O21 S	1209.499	1209.498	-0.44	-0.36	20	(M+H)+	88.58
C52 H76 N10 O21 S	C52 H76 N10 Na O21 S	1231.4803	1231.4799	-0.32	-0.26	20	(M+Na)+	99.3
C52 H74 N10 Na2 O21 S	C52 H75 N10 Na2 O21 S	1253.4618	1253.4619	-0.06	-0.05	20	(M+2Na-H)+	95.27
C52 H73 N10 Na3 O21 S	C52 H75 N10 Na3 O21 S	638.2253	638.2256	0.68	0.54	20	(M+3Na-H)+2	96.54
C52 H76 N10 O21 S	C52 H76 N10 Na2 O21 S	627.2344	627.2346	0.15	0.12	20	(M+2Na)+2	96.76

--- End Of Report ---

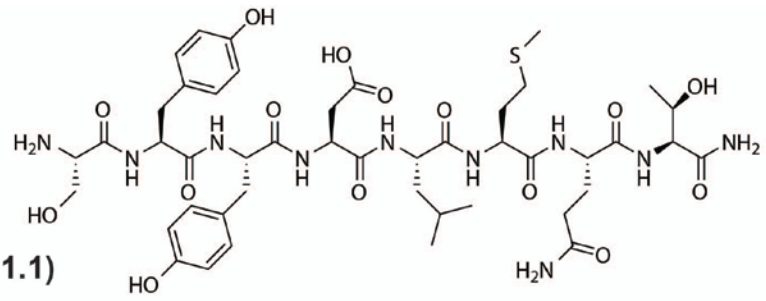

SYYDLMQT (L11.1)

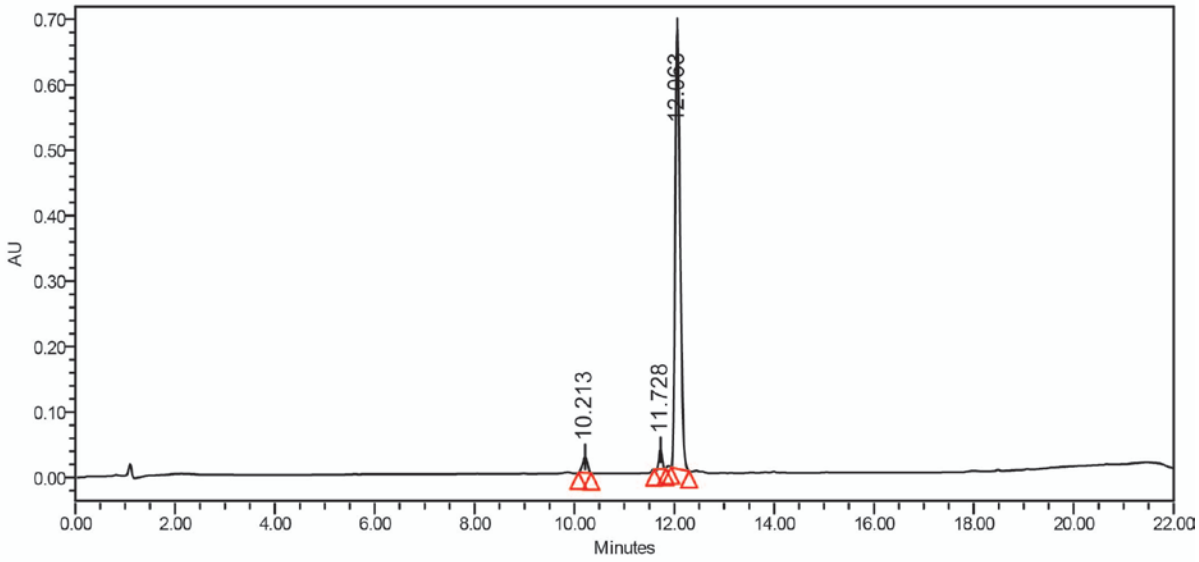

Peak Results

	RT	Area	Height	% Area
1	10.213	165724	24203	3.28
2	11.728	137695	29513	2.72
3	12.063	4750259	671777	94.00

User Spectra

Fragmentor Voltage 150 Source Type Esi

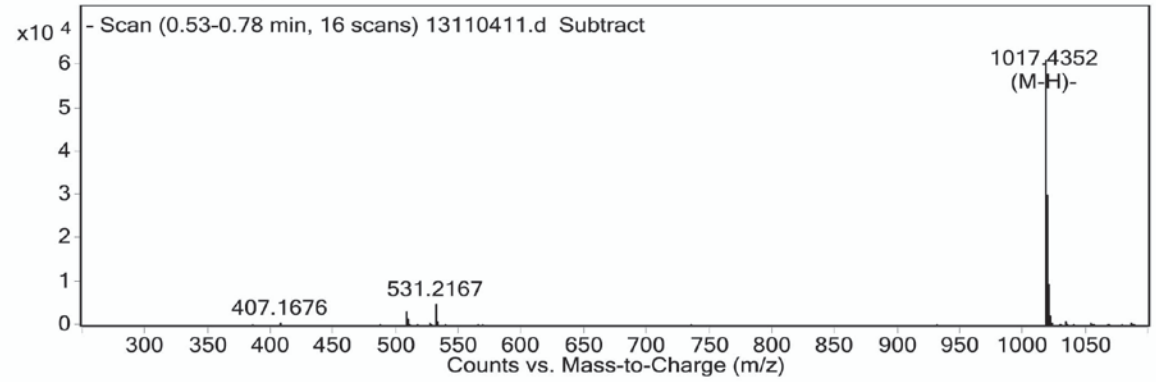

Formula Calculator Results

Formula	Ion Species	m/z	Calc. m/z	Diff (mDa)	Diff (ppm)	DBE	Ion	Score
C45 H66 N10 O15 S	C45 H65 N10 O15 S	1017.4352	1017.4357	0.49	0.48	18	(M-H)-	95.18
C45 H66 N10 O15 S	C45 H64 N10 O15 S	508.2139	508.2142	0.53	0.52	18	(M-2H)-2	99.33

--- End Of Report ---

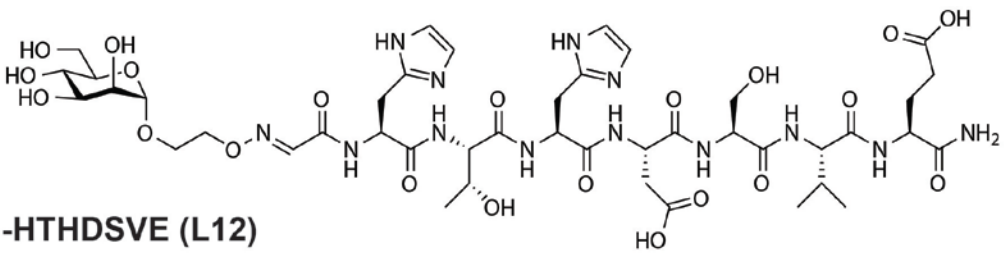

Man-HTHDSVE (L12)

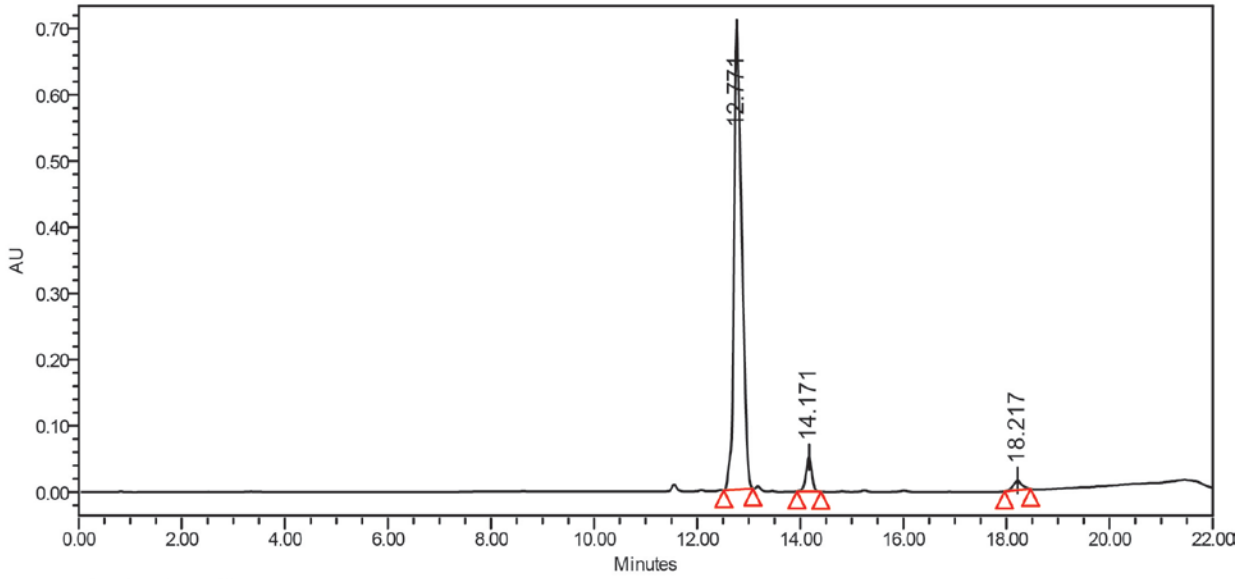

Peak Results

	RT	Area	Height	% Area
1	12.771	7420286	696755	92.62
2	14.171	420800	51896	5.25
3	18.217	170484	14655	2.13

User Spectra

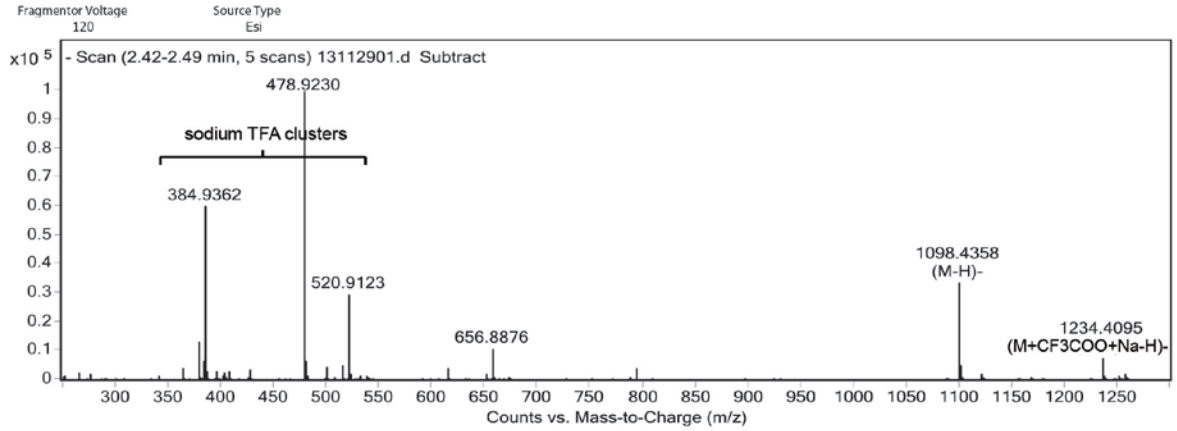

Formula Calculator Results

Formula	Ion Species	m/z	Calc. m/z	Diff (mDa)	Diff (ppm)	DBE	Ion	Score
C43 H65 N13 O21	C43 H64 N13 O21	1098.4358	1098.4345	-1.3	-1.18	18	(M-H)-	95.69
C45 H65 F3 N13 Na O23	C45 H64 F3 N13 Na O23	1234.4095	1234.4093	0.15	0.12	18		95.22

--- End Of Report ---

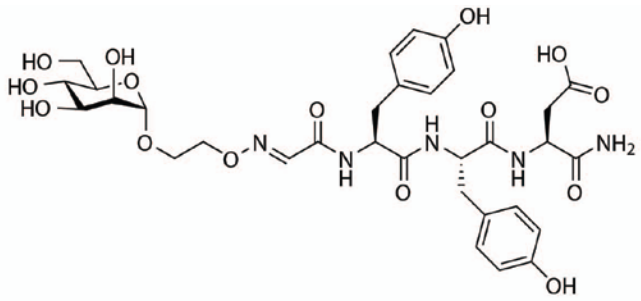

Man-YYD (L13)

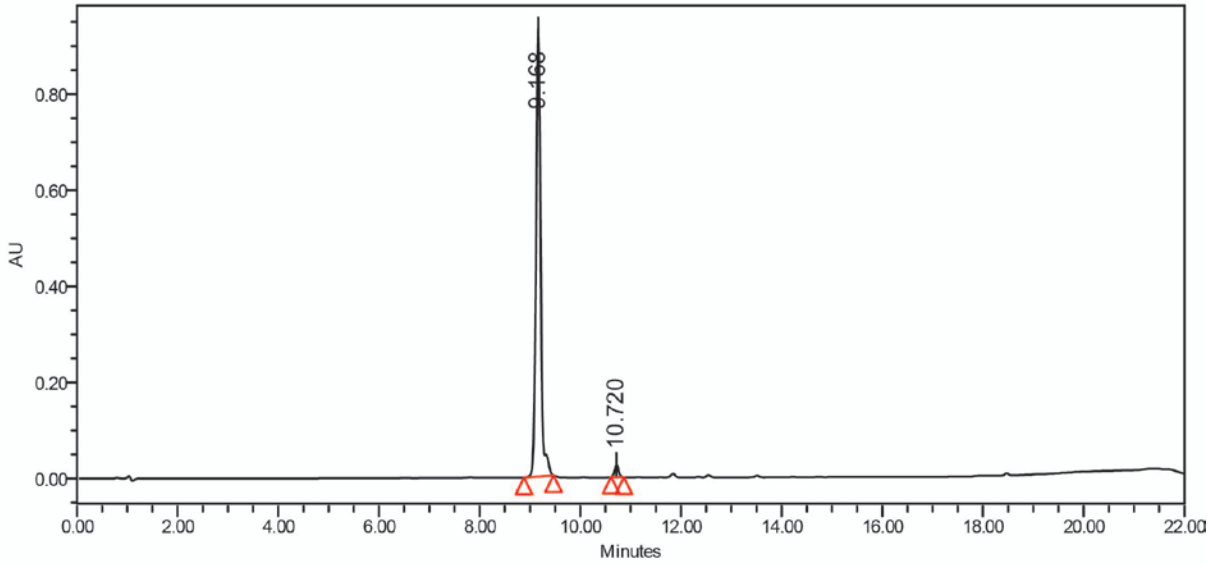

Peak Results

	RT	Area	Height	% Area
1	9.168	6129171	926489	97.80
2	10.720	137662	24391	2.20

User Spectra

Fragmentor Voltage 200 Source Type Esi

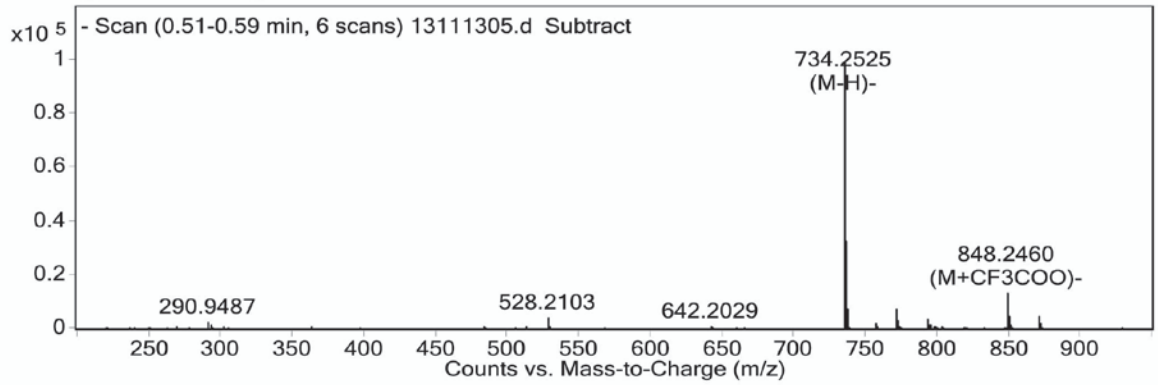

Formula Calculator Results

Formula	Ion Species	m/z	Calc. m/z	Diff (mDa)	Diff (ppm)	DBE	Ion	Score
C32 H41 N5 O15	C32 H40 N5 O15	734.2525	734.2526	0.16	0.22	15	(M-H)-	96.86
C32 H41 N5 O15	C34 H41 F3 N5 O17	848.246	848.2455	-0.51	-0.69	15	(M+CF3COO)-	96.95
C32 H41 N5 O15	C32 H41 Cl N5 O15	770.2302	770.2293	-0.84	-1.15	15	(M+Cl)-	97.23

--- End Of Report ---

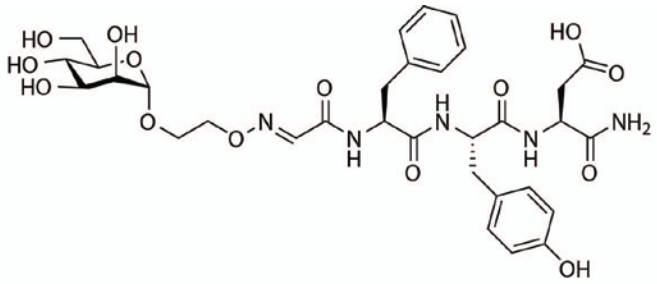

Man-FYD (L14)

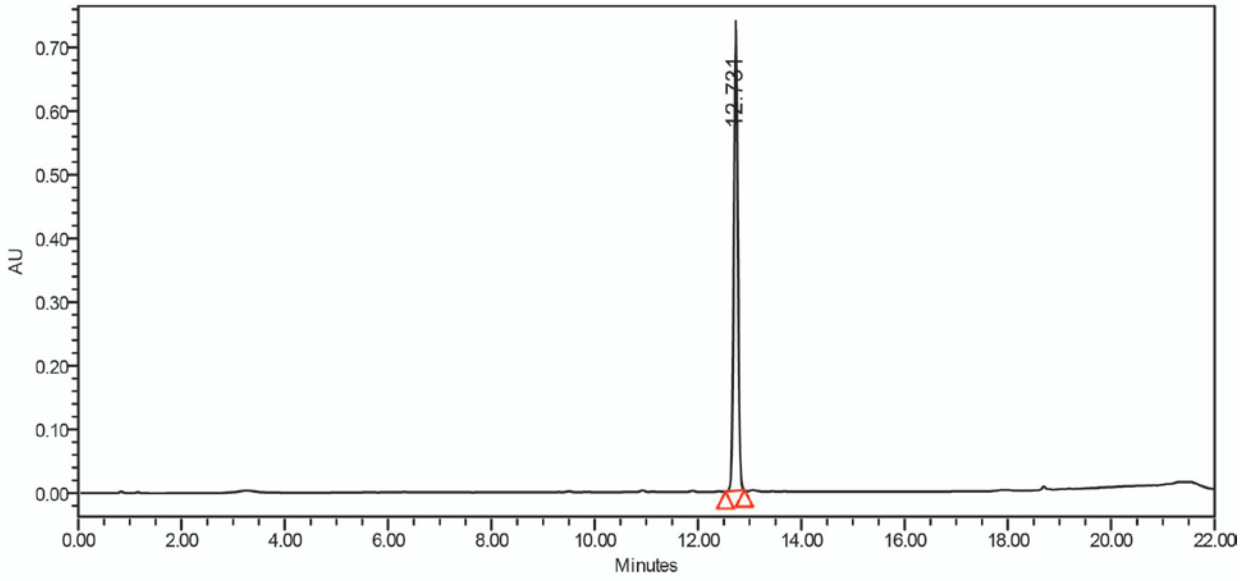

Peak Results

	RT	Area	Height	% Area
1	12.731	3978909	717857	100.00

User Spectra

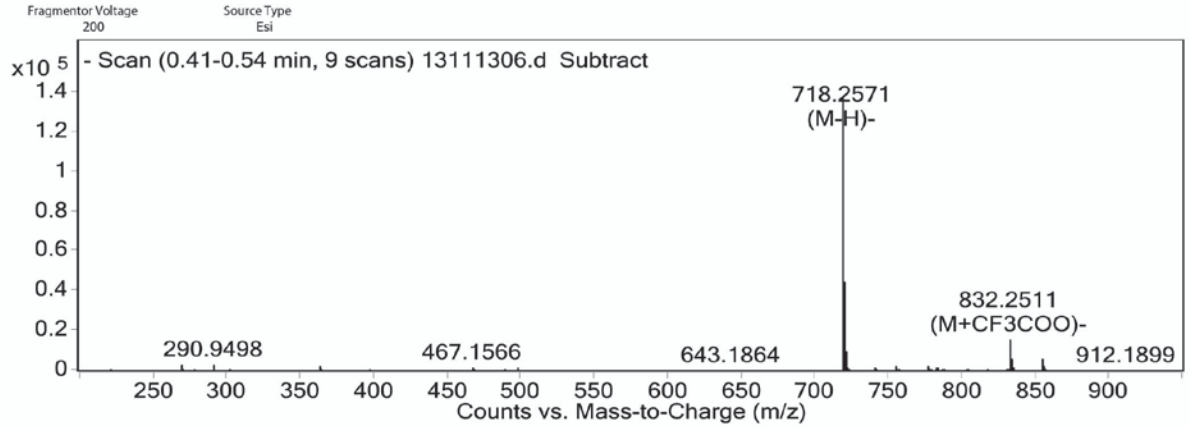

Formula Calculator Results

Formula	Ion Species	m/z	Calc. m/z	Diff (mDa)	Diff (ppm)	DBE	Ion	Score
C32 H41 N5 O14	C32 H40 N5 O14	718.2571	718.2577	0.61	0.85	15	(M-H)-	94.31
C32 H41 N5 O14	C34 H41 F3 N5 O16	832.2511	832.2506	-0.53	-0.74	15	(M+CF3COO)-	96.63

--- End Of Report ---

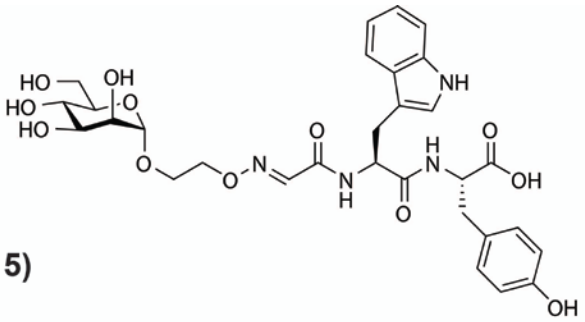

Man-WY-CO_2H (L15)

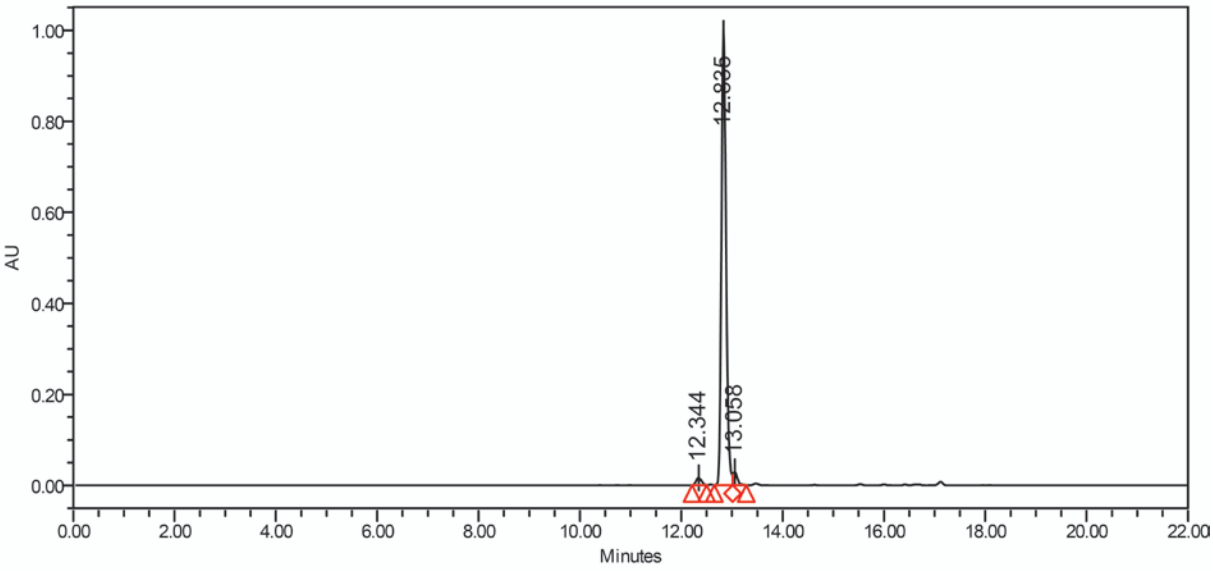

Peak Results

	RT	Area	Height	% Area
1	12.344	114443	15687	1.70
2	12.835	6440675	994444	95.81
3	13.058	166967	29830	2.48

User Spectra

Fragmentor Voltage 200 Source Type Esi

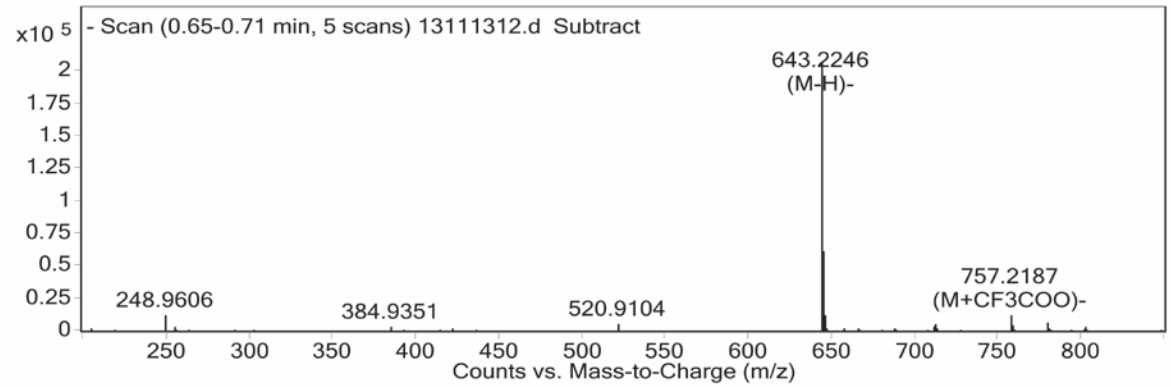

Formula Calculator Results

Formula	Ion Species	m/z	Calc. m/z	Diff (mDa)	Diff (ppm)	DBE	Ion	Score
C30 H36 N4 O12	C30 H35 N4 O12	643.2246	643.2257	1.01	1.57	15	(M-H)-	88.51
C30 H36 N4 O12	C32 H36 F3 N4 O14	757.2187	757.2186	-0.18	-0.28	15	(M+CF3COO)-	97.53

--- End Of Report ---

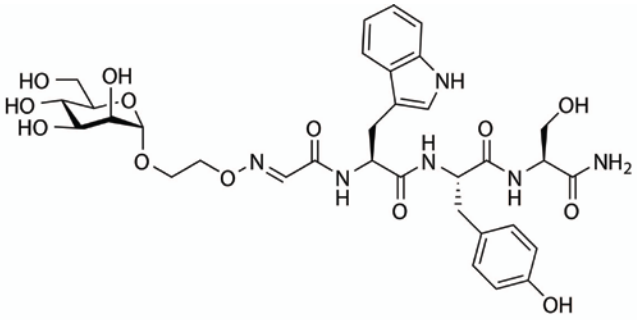

Man-WYS (L16)

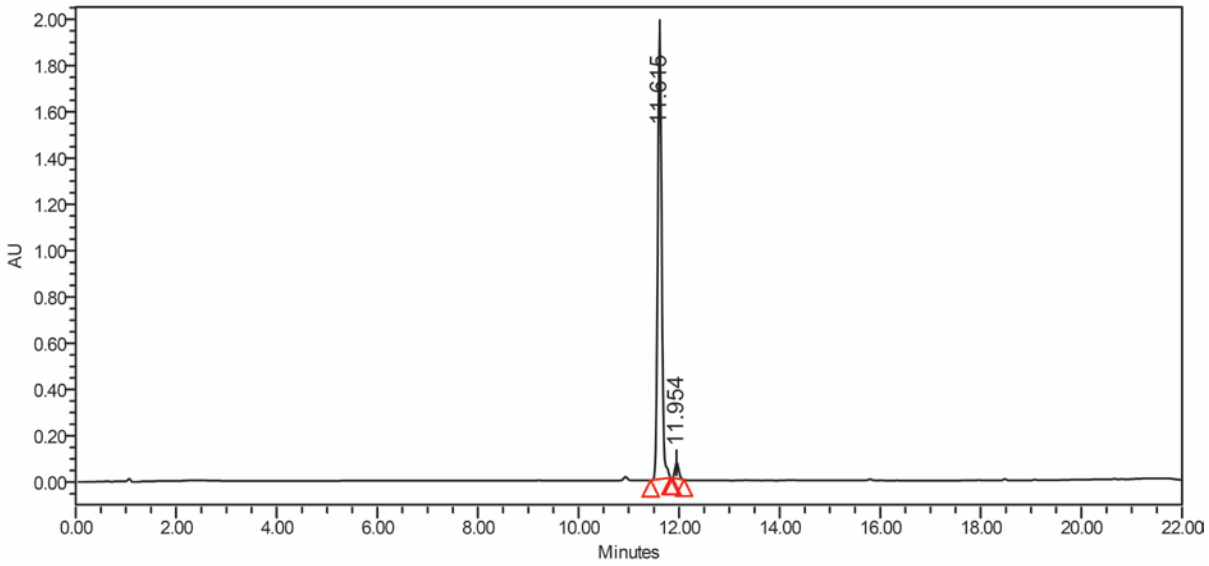

Peak Results

	RT	Area	Height	% Area
1	11.615	10830451	1923518	96.63
2	11.954	377249	69342	3.37

User Spectra

Fragmentor Voltage 150 Source Type Esi

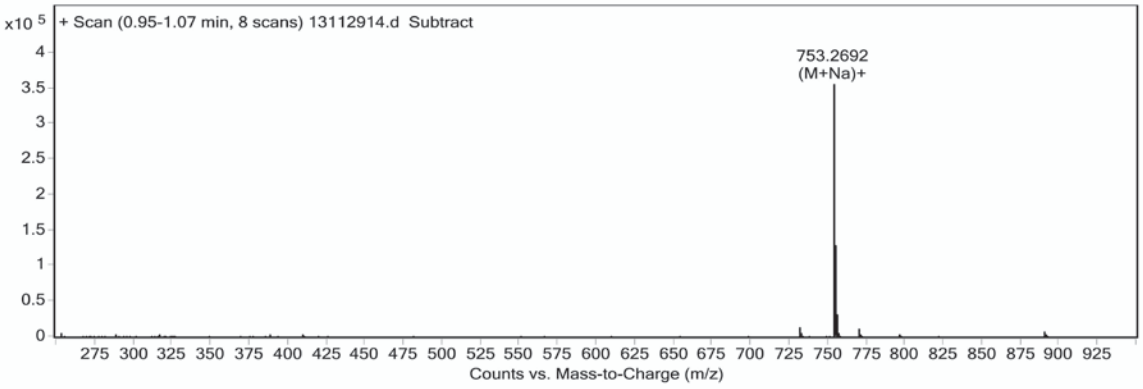

Formula Calculator Results

Formula	Ion Species	m/z	Calc. m/z	Diff (mDa)	Diff (ppm)	DBE	Ion	Score
C33 H42 N6 O13	C33 H43 N6 O13	731.2882	731.2883	0.04	0.06	16	(M+H)+	97.82
C33 H42 N6 O13	C33 H42 N6 Na O13	753.2692	753.2702	1.03	1.41	16	(M+Na)+	95.31
C33 H42 N6 O13	C33 H42 K N6 O13	769.2444	769.2441	-0.27	-0.37	16	(M+K)+	97.46

--- End Of Report ---

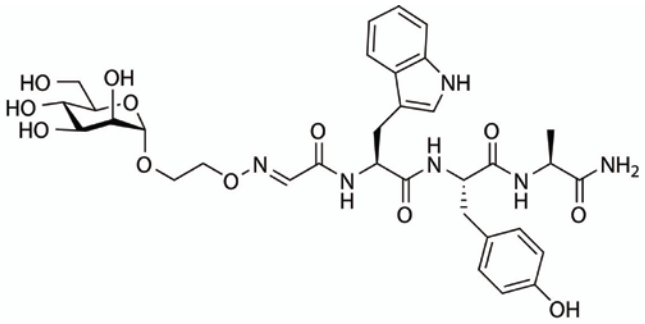

Man-WYA (L17)

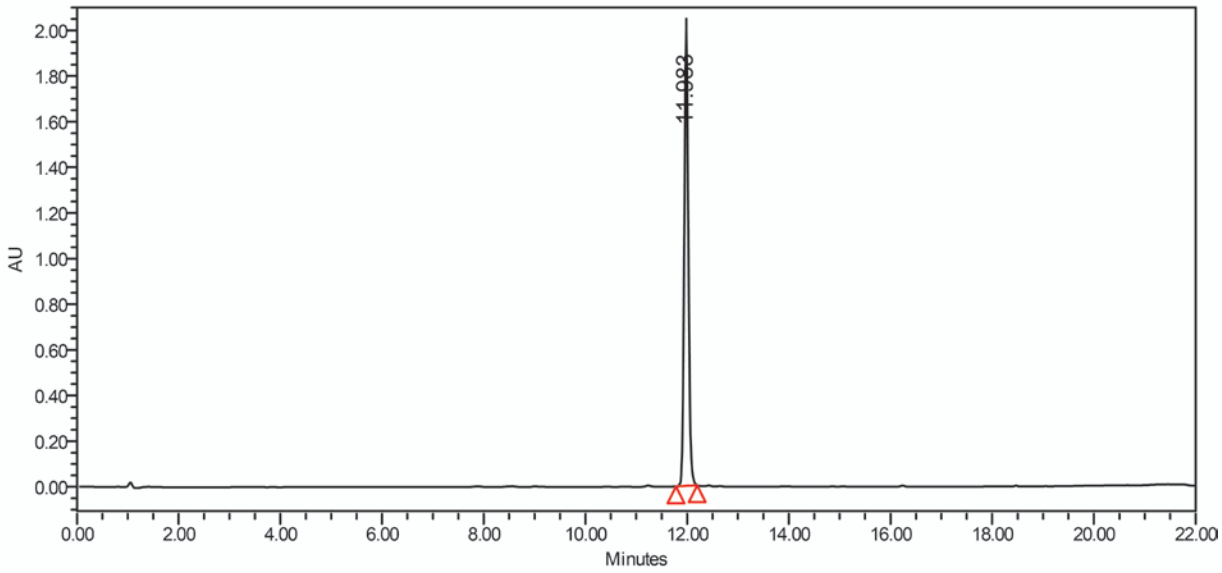

Peak Results

	RT	Area	Height	% Area
1	11.983	11425101	1977217	100.00

User Spectra

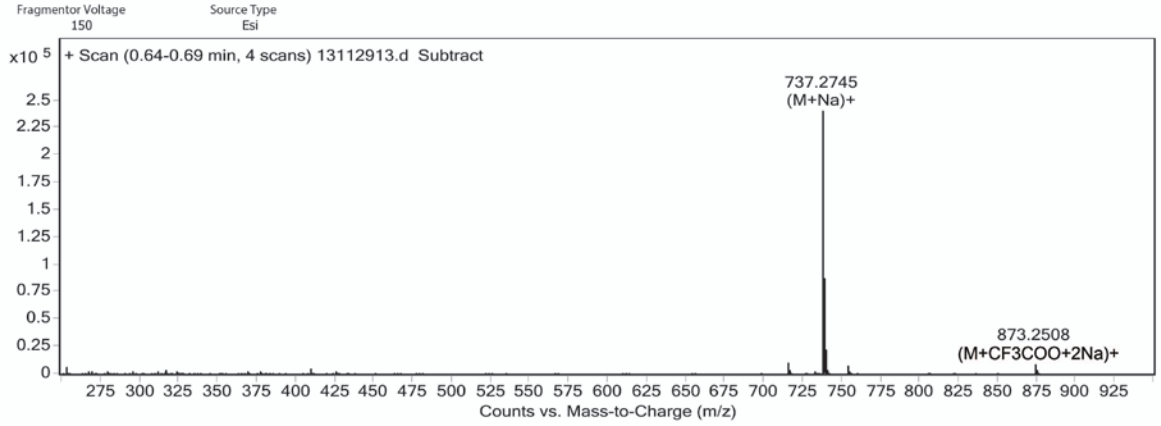

Formula Calculator Results

Formula	Ion Species	m/z	Calc. m/z	Diff (mDa)	Diff (ppm)	DBE	Ion	Score
C33 H42 N6 O12	C33 H42 N6 Na O12	737.2745	737.2753	0.78	1.09	16	(M+Na)+	96.15
C35 H42 F3 N6 Na O14	C35 H42 F3 N6 Na2 O14	873.2508	873.2501	-0.62	-0.73	16		95.63
C33 H42 N6 O12	C33 H43 N6 O12	715.2946	715.2933	-1.28	-1.79	16	(M+H)+	87.05
C33 H42 N6 O12	C33 H42 K N6 O12	753.2506	753.2492	-1.37	-1.92	16	(M+K)+	90.82

--- End Of Report ---

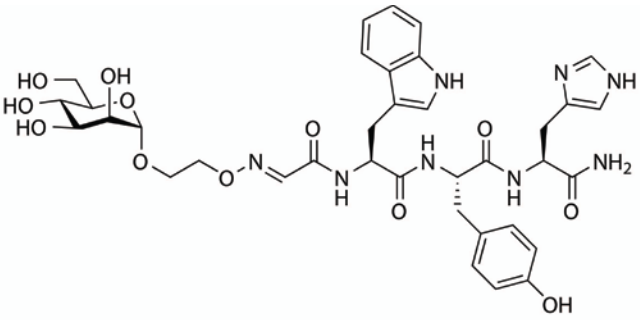

Man-WYH (L18)

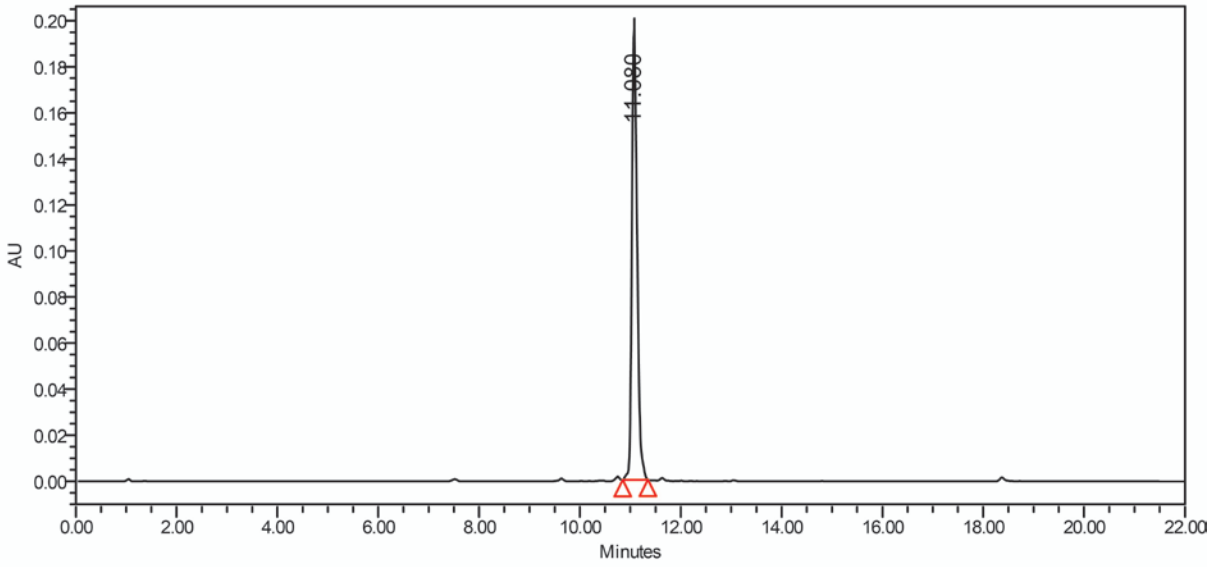

Peak Results

	RT	Area	Height	% Area
1	11.08(	1399084	195695	100.00

User Spectra

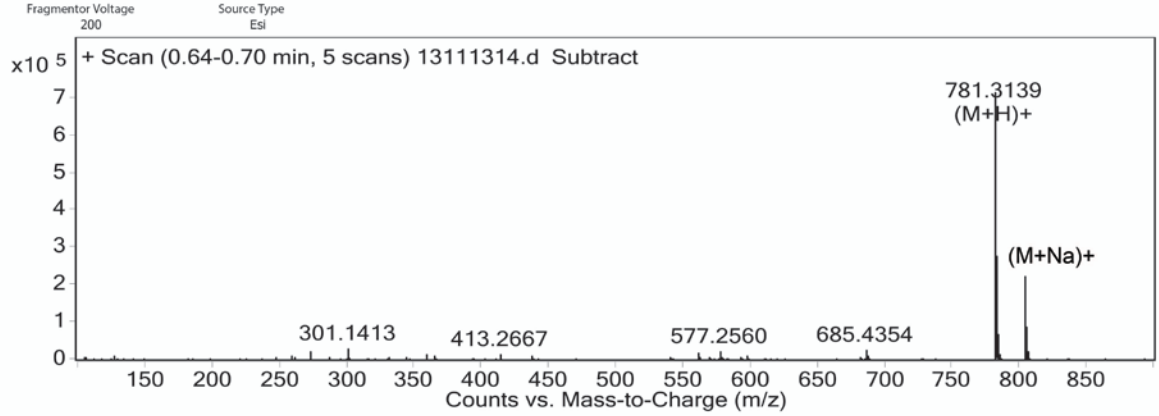

Formula Calculator Results

Formula	Ion Species	m/z	Calc. m/z	Diff (mDa)	Diff (ppm)	DBE	Ion	Score
C36 H44 N8 O12	C36 H45 N8 O12	781.3139	781.3151	1.26	1.62	19	(M+H)+	94.15
C36 H44 N8 O12	C36 H44 N8 Na O12	803.2963	803.2971	0.78	1	19	(M+Na)+	97.48

--- End Of Report ---

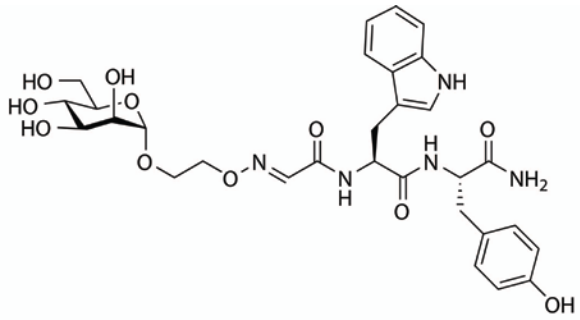

Man-WY (L19)

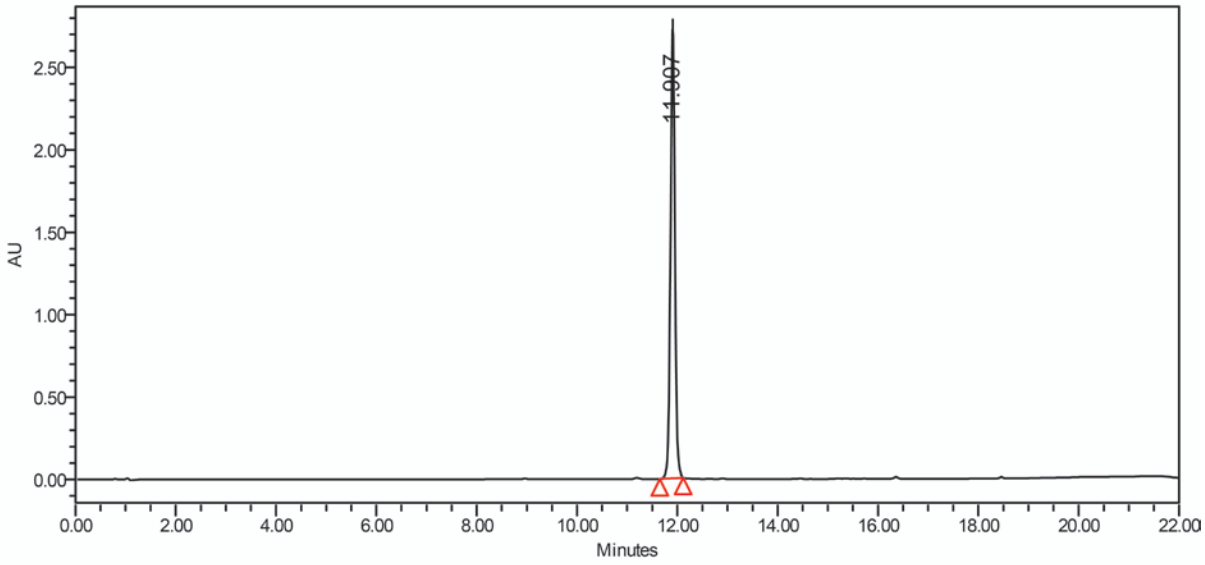

Peak Results

	RT	Area	Height	% Area
1	11.907	1680411€	2735998	100.00

User Spectra

Fragmentor Voltage 150 Source Type Esi

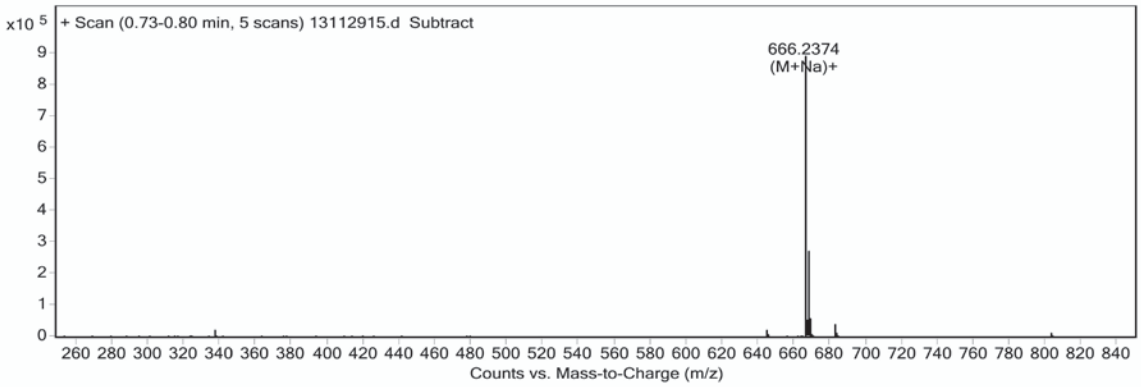

Formula Calculator Results

Formula	Ion Species	m/z	Calc. m/z	Diff (mDa)	Diff (ppm)	DBE	Ion	Score
C30 H37 N5 O11	C30 H38 N5 O11	644.2563	644.2562	-0.11	-0.17	15	(M+H)+	97.41
C30 H37 N5 O11	C30 H37 N5 Na O11	666.2374	666.2382	0.77	1.19	15	(M+Na)+	95.83
C30 H37 N5 O11	C30 H37 K N5 O11	682.2122	682.2121	-0.09	-0.14	15	(M+K)+	98.9

--- End Of Report ---

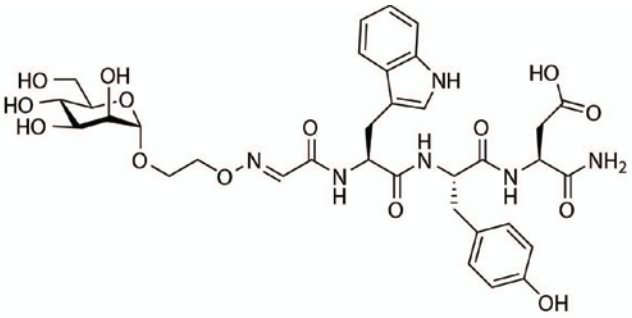

Man-WYD (L20)

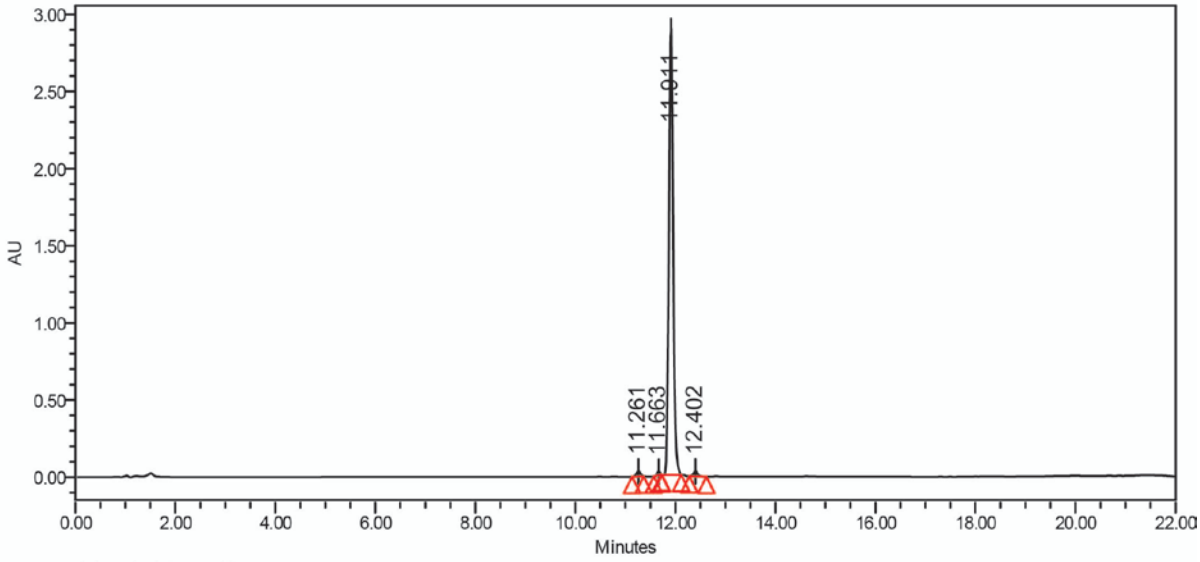

Peak Results

	RT	Area	Height	% Area
1	11.261	200615	34278	1.13
2	11.663	92683	22492	0.52
3	11.911	17312452	2899253	97.30
4	12.402	186709	32753	1.05

User Spectra

Fragmentor Voltage 200 Source Type Esi

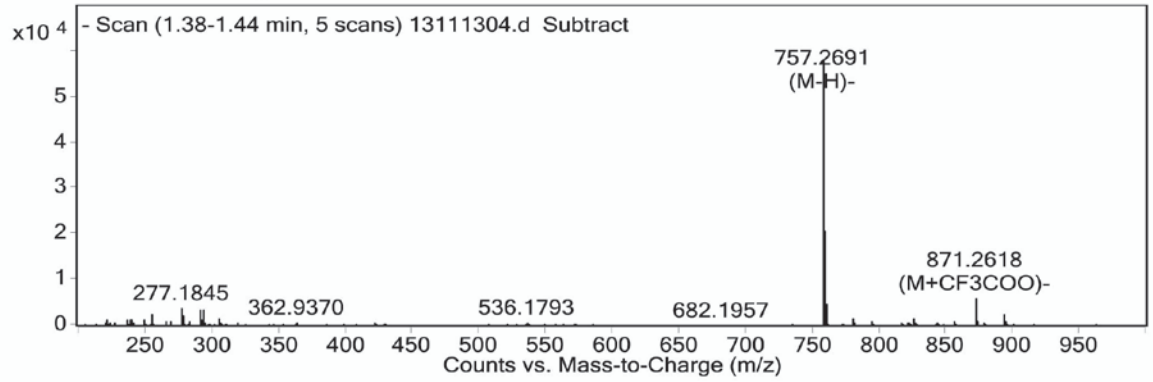

Formula Calculator Results

Formula	Ion Species	m/z	Calc. m/z	Diff (mDa)	Diff (ppm)	DBE	Ion	Score
C34 H42 N6 O14	C34 H41 N6 O14	757.2691	757.2686	-0.51	-0.68	17	(M-H)-	96.91
C34 H42 N6 O14	C36 H42 F3 N6 O16	871.2618	871.2615	-0.23	-0.3	17	(M+CF3COO)-	99

--- End Of Report ---

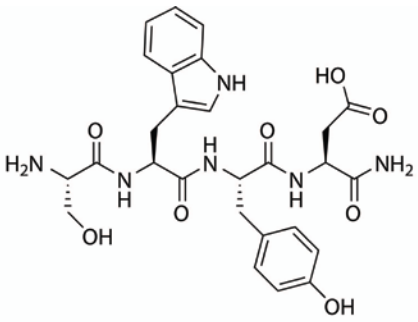

SWYD (L20.1)

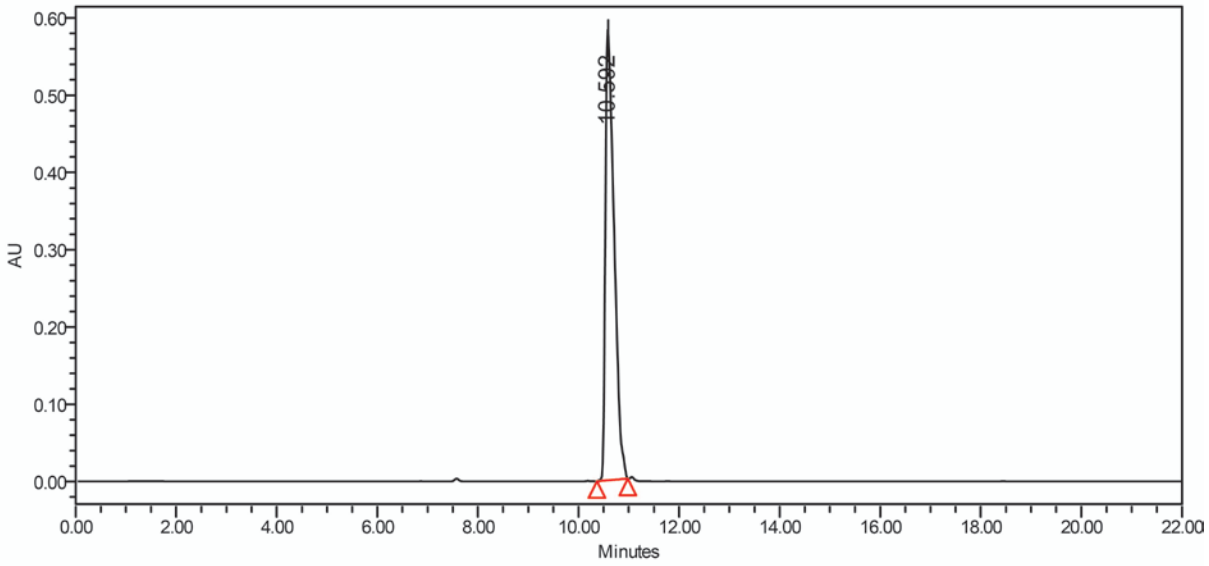

Peak Results

	RT	Area	Height	% Area
1	10.592	6932608	588590	100.00

User Spectra

Fragmentor Voltage 110 Source Type Esi

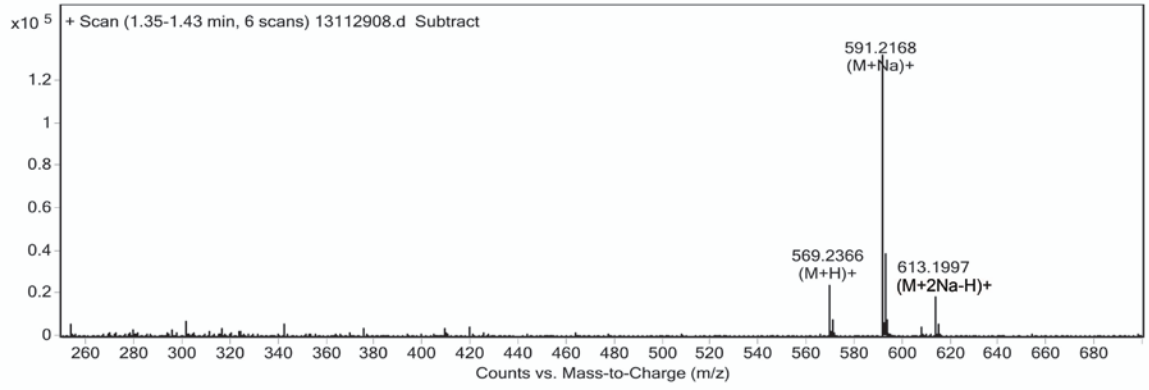

Formula Calculator Results

Formula	Ion Species	m/z	Calc. m/z	Diff (mDa)	Diff (ppm)	DBE	Ion	Score
C27 H32 N6 O8	C27 H33 N6 O8	569.2366	569.2354	-1.16	-2.05	15	(M+H)+	84.66
C27 H32 N6 O8	C27 H32 N6 Na O8	591.2168	591.2174	0.52	0.92	15	(M+Na)+	95.63
C27 H30 N6 Na2 O8	C27 H31 N6 Na2 O8	613.1997	613.1993	-0.35	-0.57	15	(M+2Na-H)+	97.98
C27 H32 N6 O8	C27 H32 K N6 O8	607.1925	607.1913	-1.12	-1.98	15	(M+K)+	49.21

--- End Of Report ---

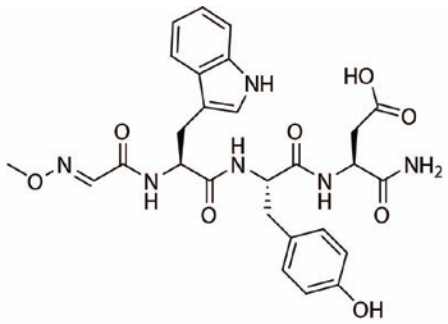

Me-WYD (L20.2)

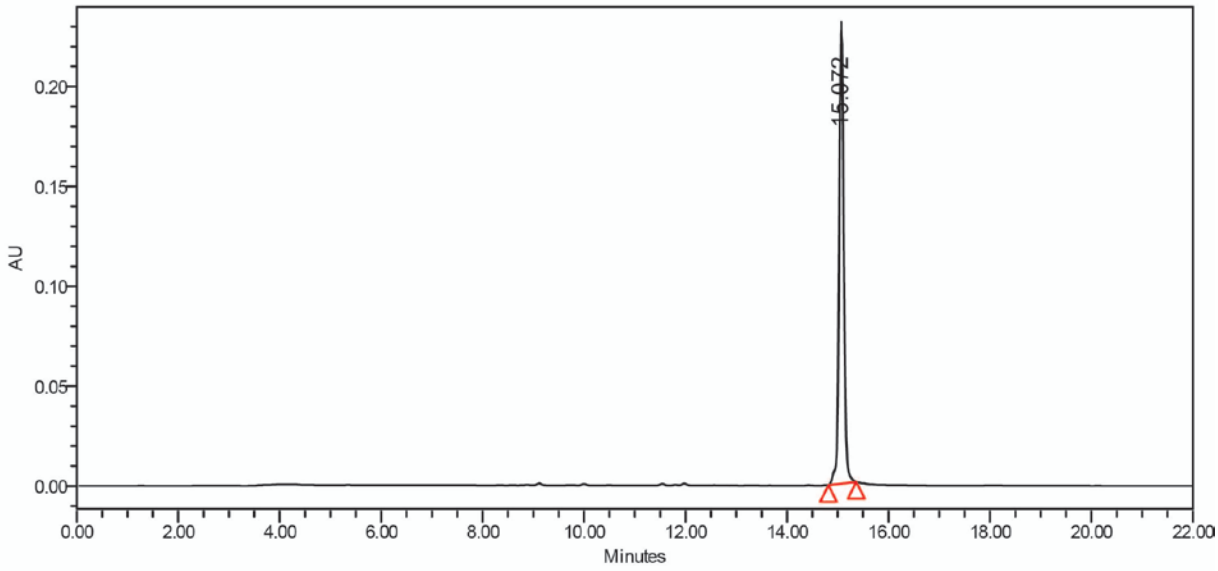

Peak Results

	RT	Area	Height	% Area
1	15.072	1428300	226982	100.00

User Spectra

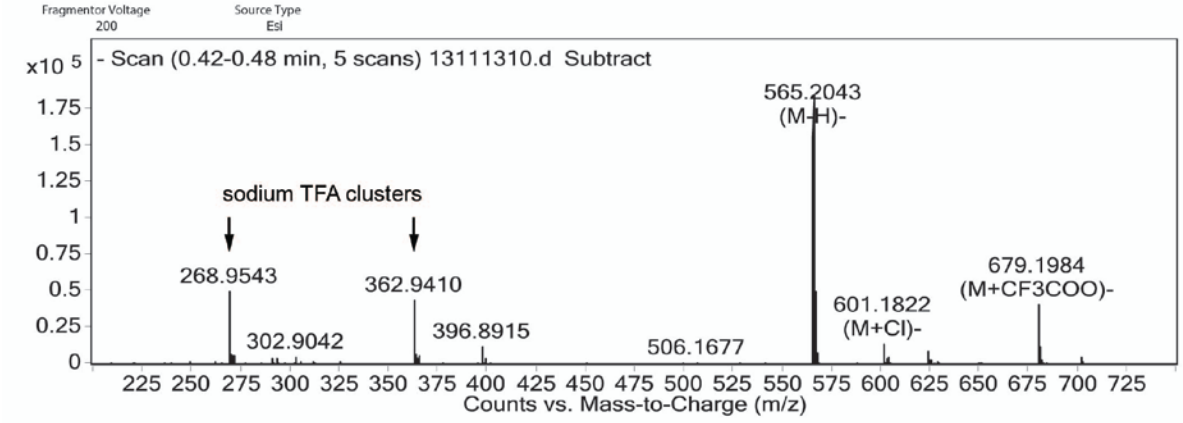

Formula Calculator Results

Formula	Ion Species	m/z	Calc. m/z	Diff (mDa)	Diff (ppm)	DBE	Ion	Score
C27 H30 N6 O8	C27 H29 N6 O8	565.2043	565.2052	0.91	1.61	16	(M-H)-	87.92
C27 H30 N6 O8	C27 H30 Cl N6 O8	601.1822	601.1819	-0.27	-0.47	16	(M+Cl)-	97.74
C27 H30 N6 O8	C29 H30 F3 N6 O10	679.1984	679.1981	-0.33	-0.58	16	(M+CF3COO)-	86.51

--- End Of Report ---

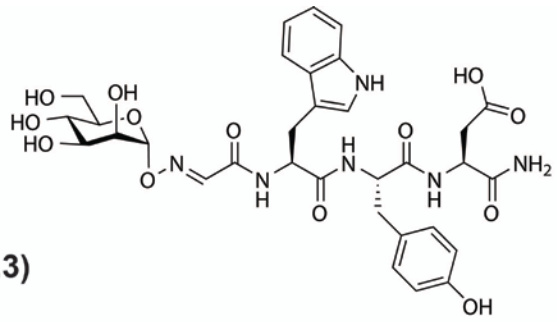

Man-NL-WYD (L20.3)

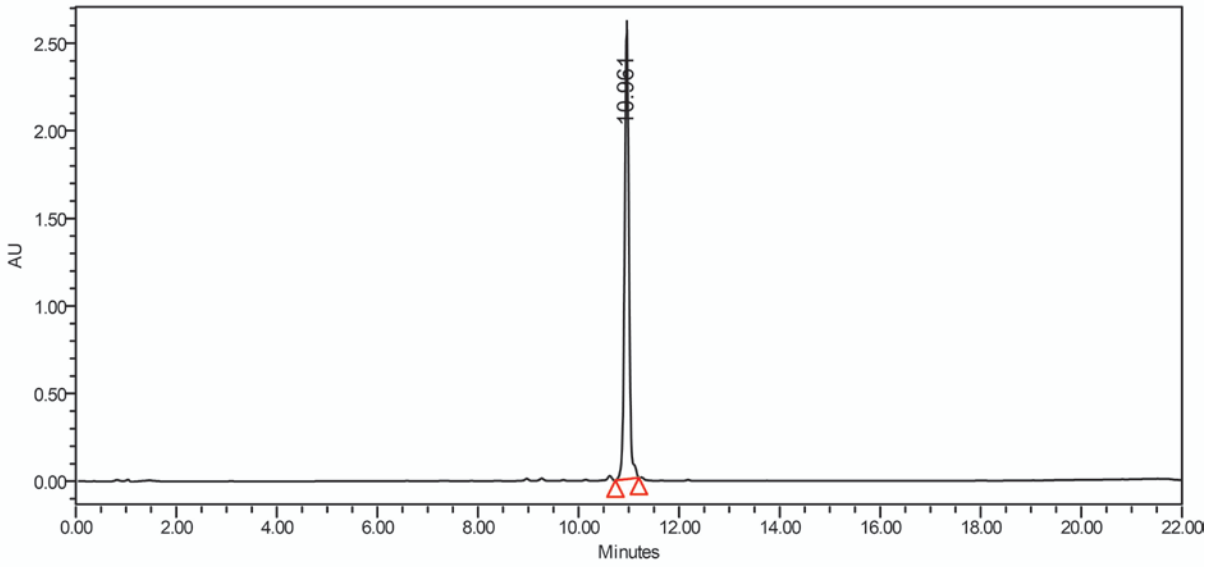

Peak Results

	RT	Area	Height	% Area
1	10.961	15837810	2565719	100.00

User Spectra

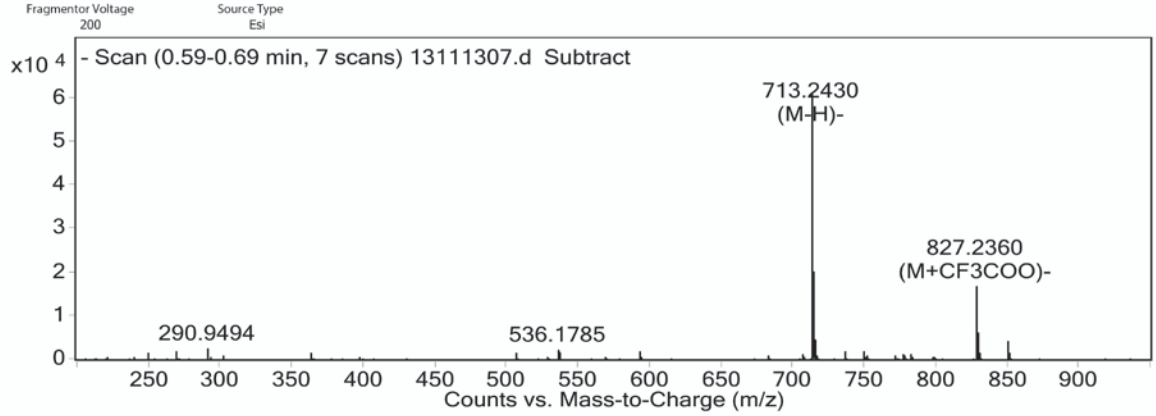

Formula Calculator Results

Formula	Ion Species	m/z	Calc. m/z	Diff (mDa)	Diff (ppm)	DBE	Ion	Score
C32 H38 N6 O13	C32 H37 N6 O13	713.243	713.2424	-0.65	-0.91	17	(M-H)-	95.49
C32 H38 N6 O13	C34 H38 F3 N6 O15	827.236	827.2353	-0.75	-1.05	17	(M+CF3COO)-	96.67

--- End Of Report ---

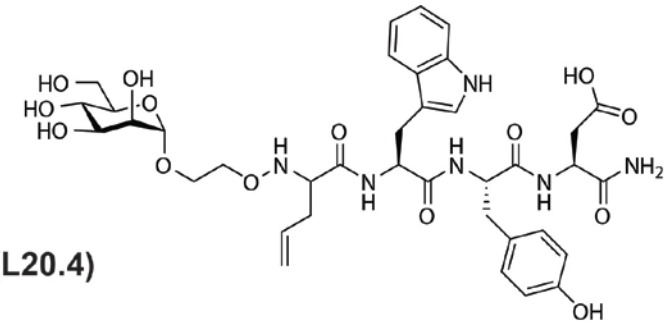

Man-ally-WYD (L20.4)

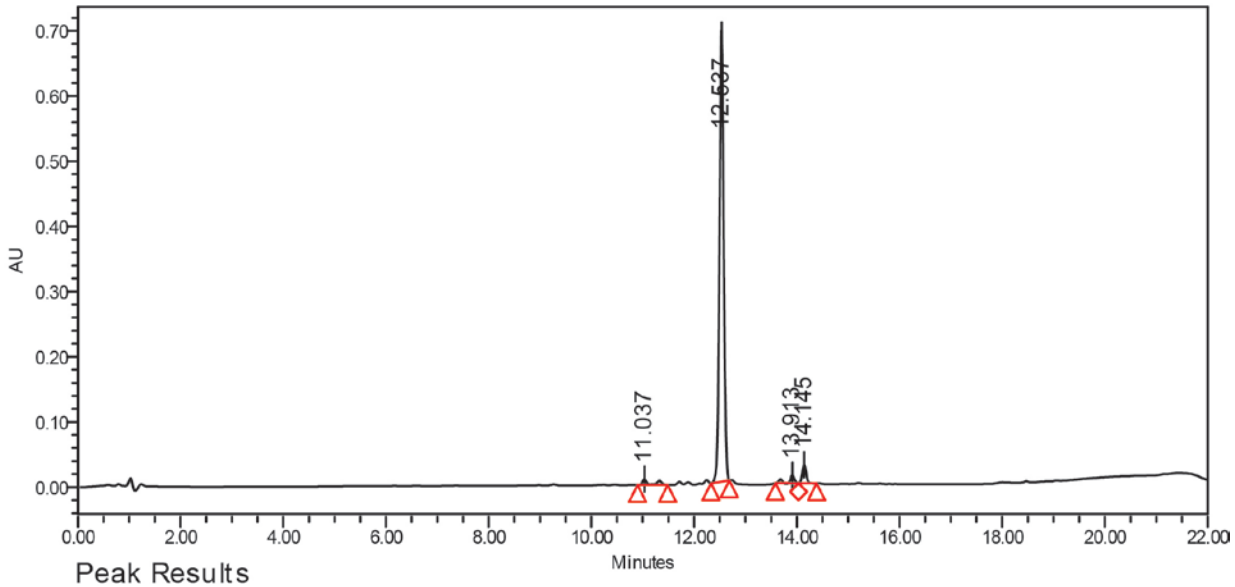

Peak Results

	RT	Area	Height	% Area
1	11.037	100350	9005	2.32
2	12.537	3972000	688752	91.85
3	13.913	96922	12178	2.24
4	14.145	155090	28374	3.59

User Spectra

Fragmentor Voltage: 200 Source Type: Esi

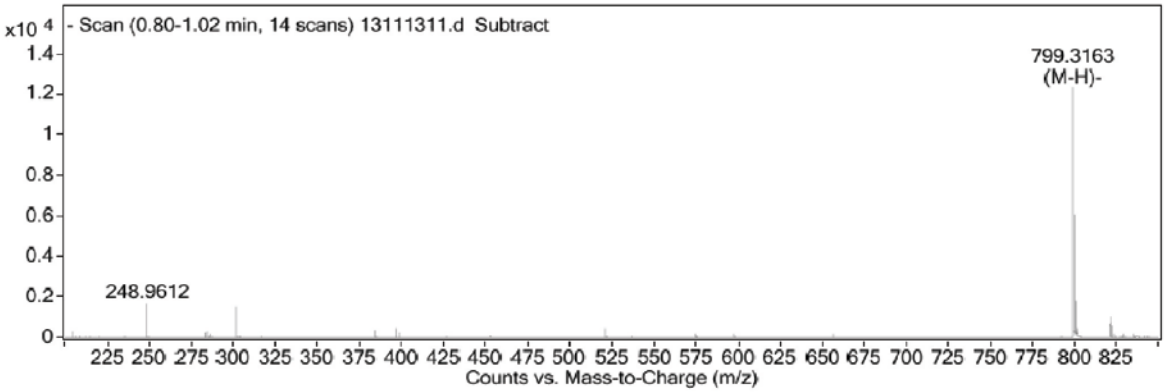

Formula Calculator Results

Formula	Ion Species	m/z	Calc. m/z	Diff (mDa)	Diff (ppm)	DBE	Ion	Score
C37 H48 N6 O14	C37 H47 N6 O14	799.3163	799.3156	-0.72	-0.9	17	(M-H)-	95.44

--- End Of Report ---

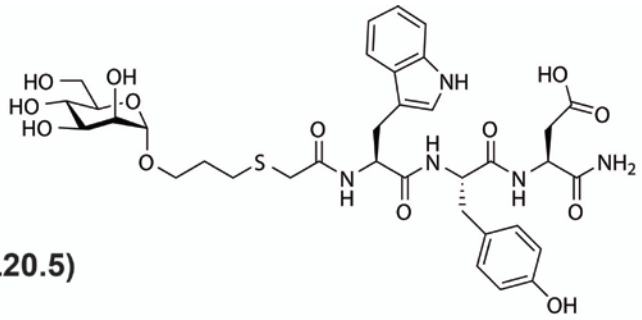

Man-SL-WYD (L20.5)

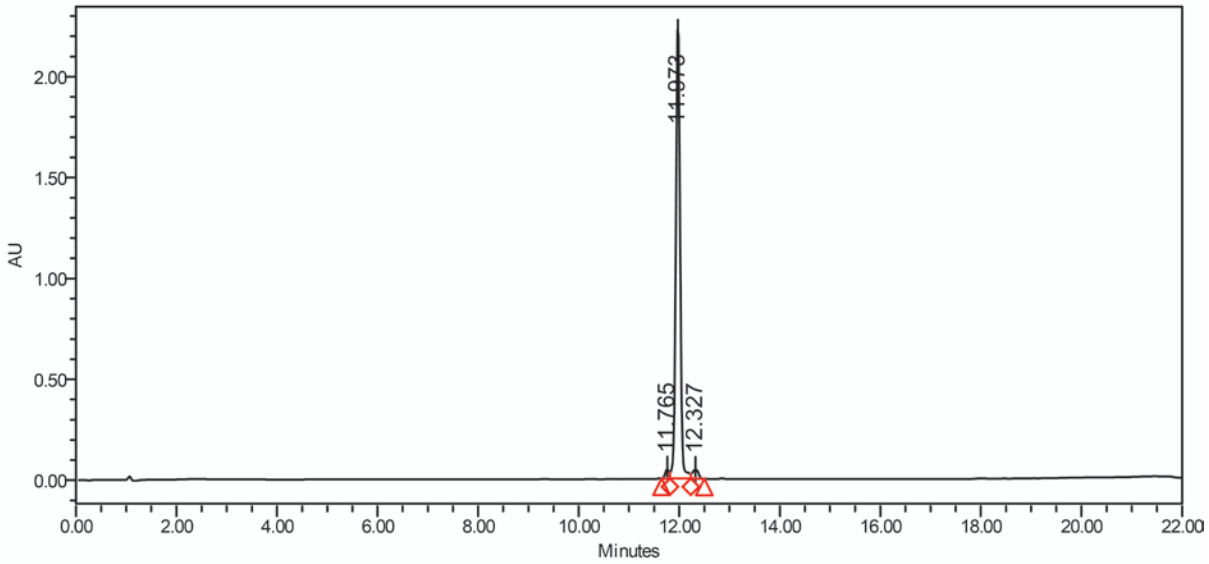

Peak Results

	RT	Area	Height	% Area
1	11.765	246631	45756	1.75
2	11.973	13460533	2235087	95.62
3	12.327	370512	45949	2.63

User Spectra

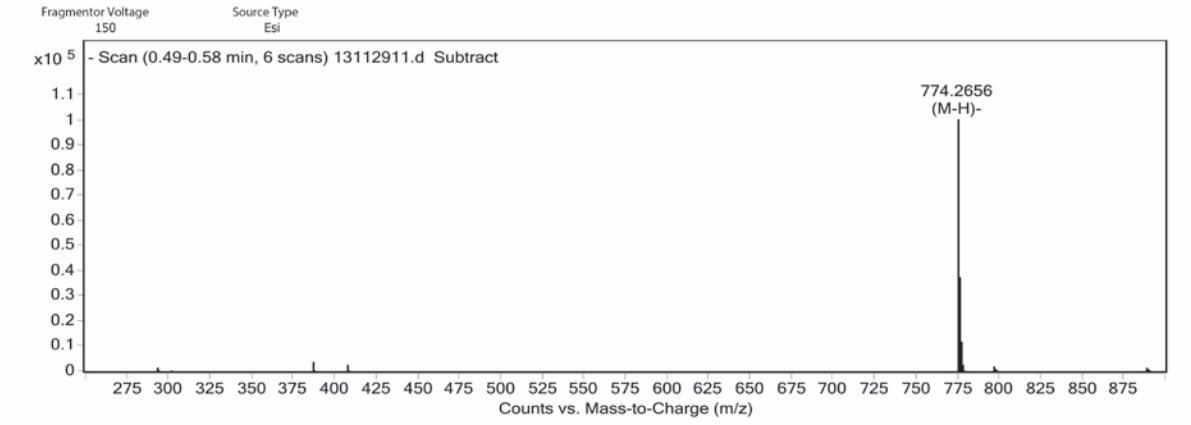

Formula Calculator Results

Formula	Ion Species	m/z	Calc. m/z	Diff (mDa)	Diff (ppm)	DBE	Ion	Score
C35 H45 N5 O13 S	C35 H44 N5 O13 S	774.2656	774.2662	0.55	0.71	16	(M-H)-	94.09

--- End Of Report ---

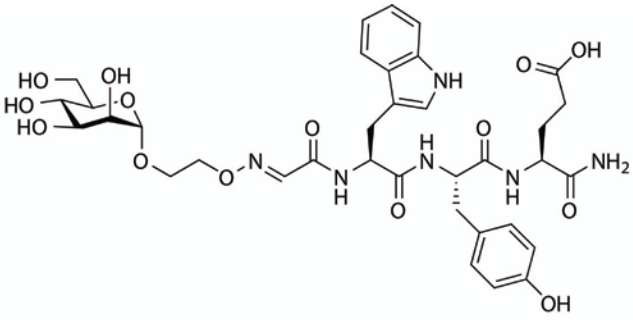

Man-WYE (L21)

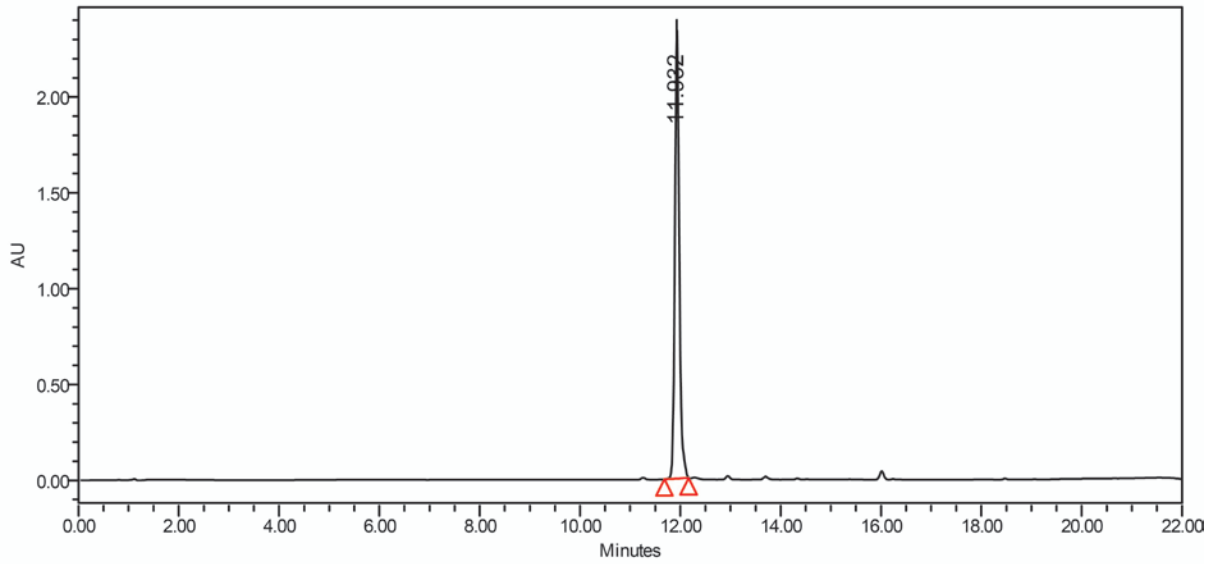

Peak Results

	RT	Area	Height	% Area
1	11.932	14570442	2323515	100.00

User Spectra

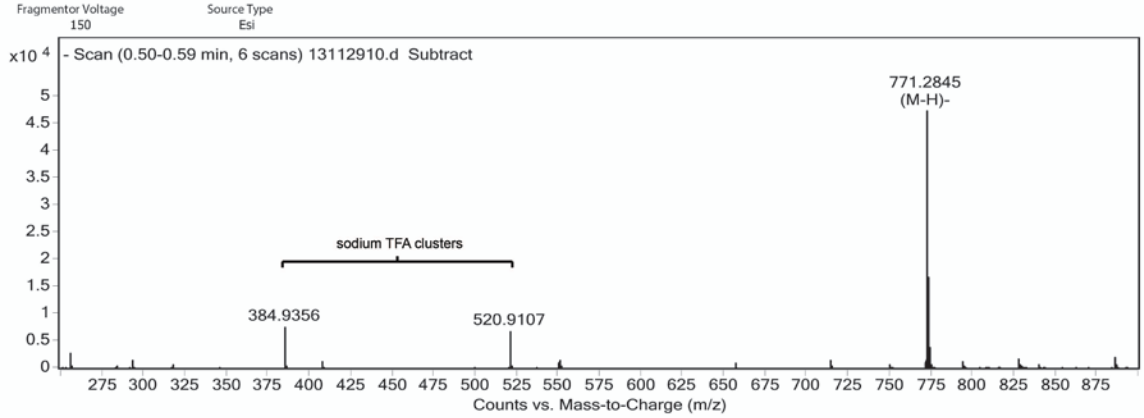

Formula Calculator Results

Formula	Ion Species	m/z	Calc. m/z	Diff (mDa)	Diff (ppm)	DBE	Ion	Score
C35 H44 N6 O14	C35 H43 N6 O14	771.2845	771.2843	-0.23	-0.3	17	(M-H)-	96.25

--- End Of Report ---

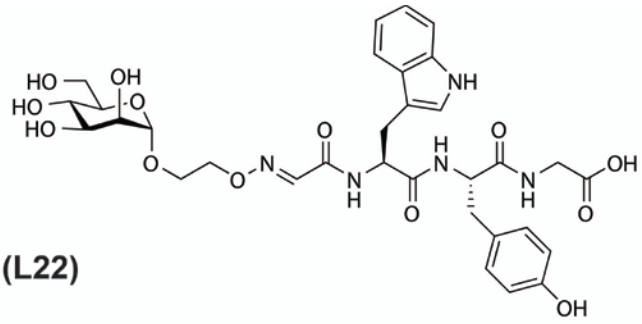

Man-WYG-CO_2H (L22)

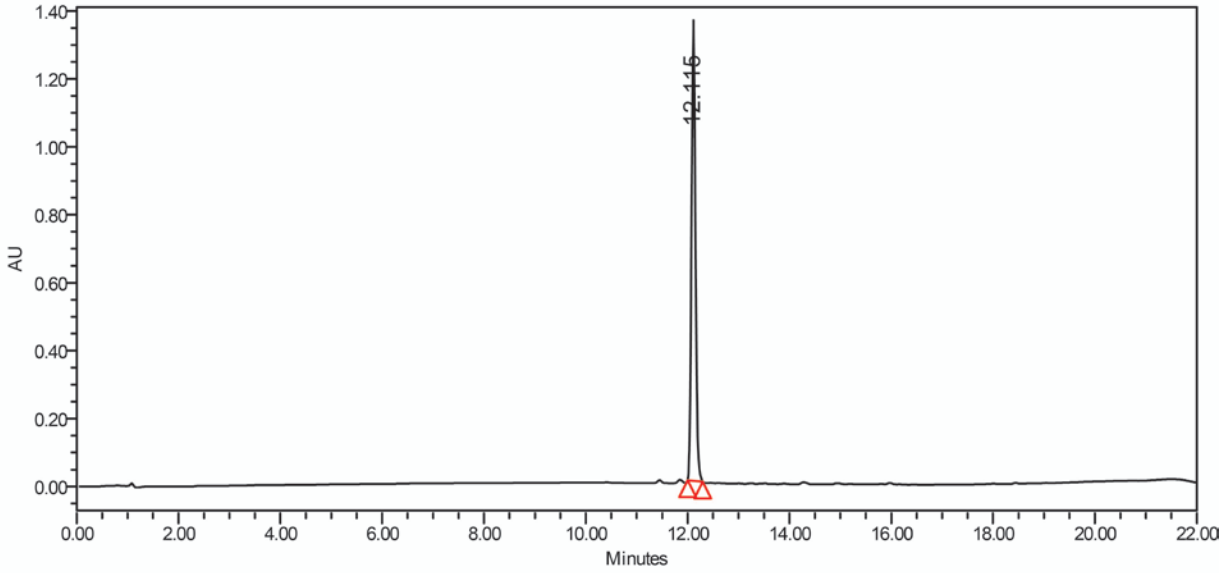

Peak Results

	Name	RT	Area	Height	% Area
1		12.115	7405346	1314804	100.00

User Spectra

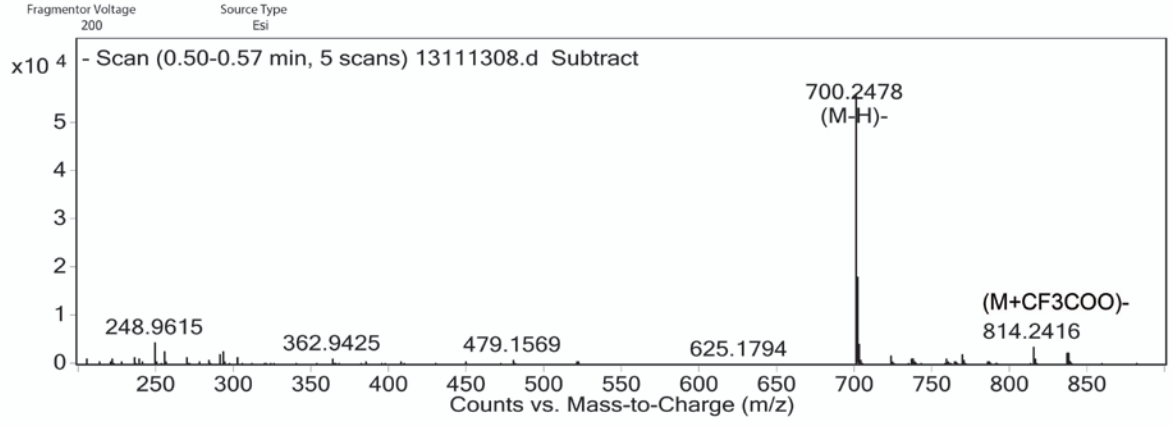

Formula Calculator Results

Formula	Ion Species	m/z	Calc. m/z	Diff (mDa)	Diff (ppm)	DBE	Ion	Score
C32 H39 N5 O13	C32 H38 N5 O13	700.2478	700.2472	-0.64	-0.91	16	(M-H)-	95.17

--- End Of Report ---

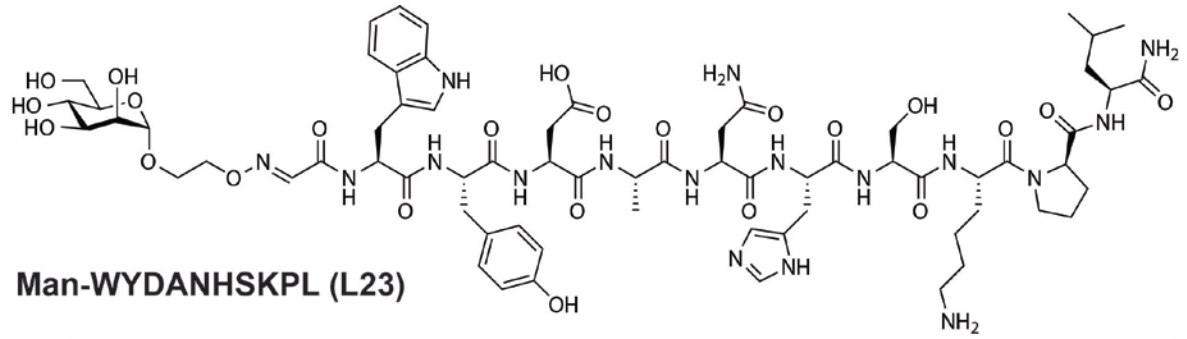

Man-WYDANHSKPL (L23)

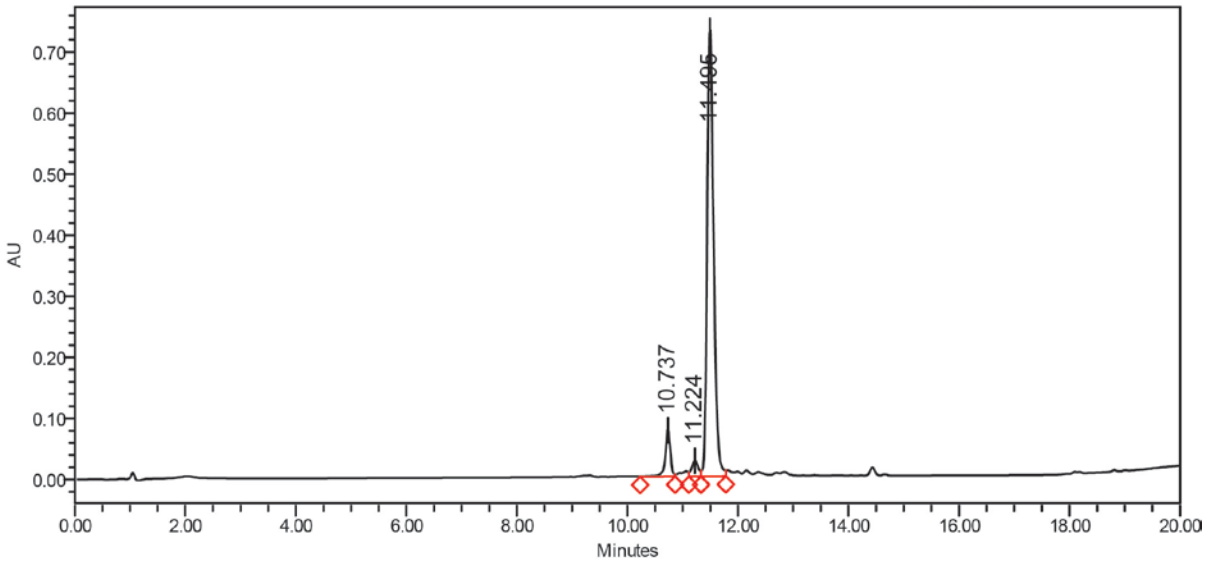

Peak Results

	RT	Area	Height	% Area
1	10.737	502723	76258	7.45
2	11.224	210967	25899	3.12
3	11.495	6038491	733262	89.43

User Spectra

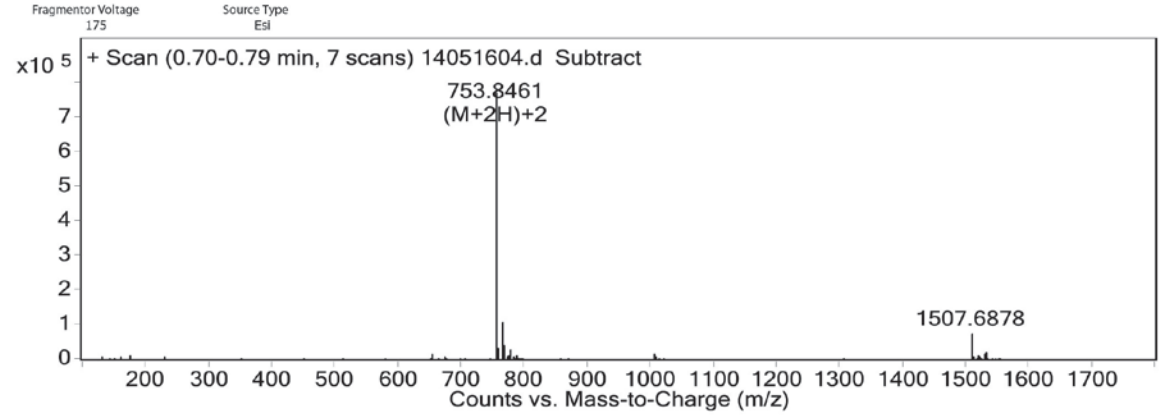

Formula Calculator Results

Formula	Ion Species	Mass	Calc. Mass	m/z	Calc. m/z	Diff (mDa)	Diff(ppm)	DBE	Ion	Score
C67 H95 N17 O23	C67 H97 N17 O23	1505.6774	1505.6787	753.8461	753.8466	1.3	0.86	29	(M+2H)+2	98.15

--- End Of Report ---

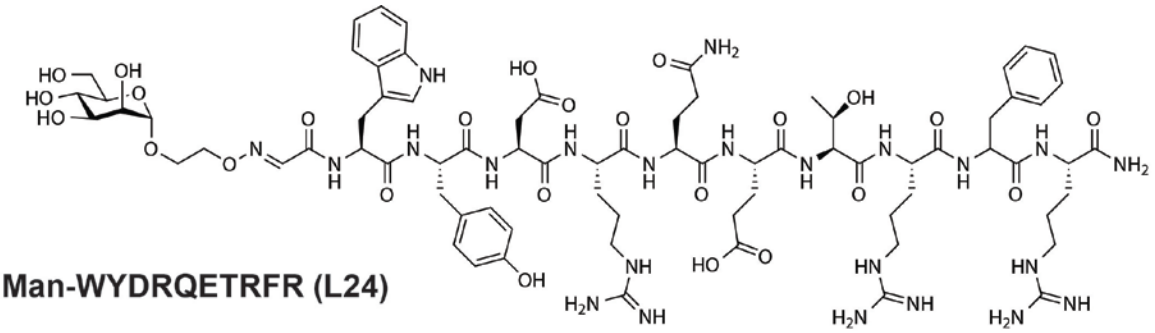

Man-WYDRQETRFR (L24)

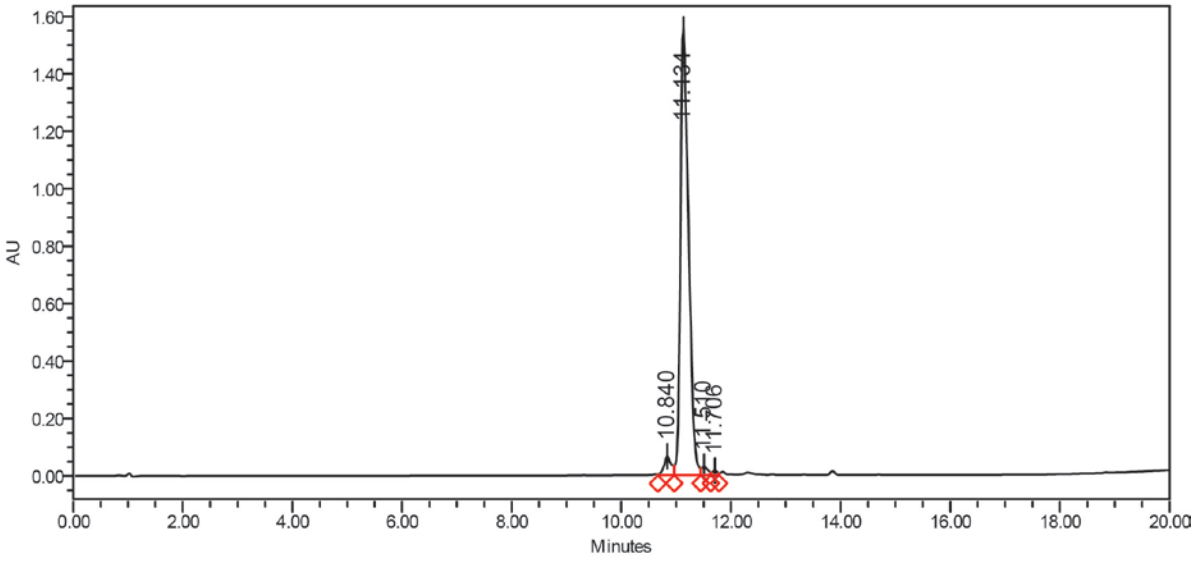

Peak Results

	RT	Area	Height	% Area
1	10.840	623620	66282	3.64
2	11.134	16143207	1554547	94.29
3	11.510	243575	29638	1.42
4	11.708	109879	16241	0.64

User Spectra

Fragmentor Voltage 175 Source Type Esi

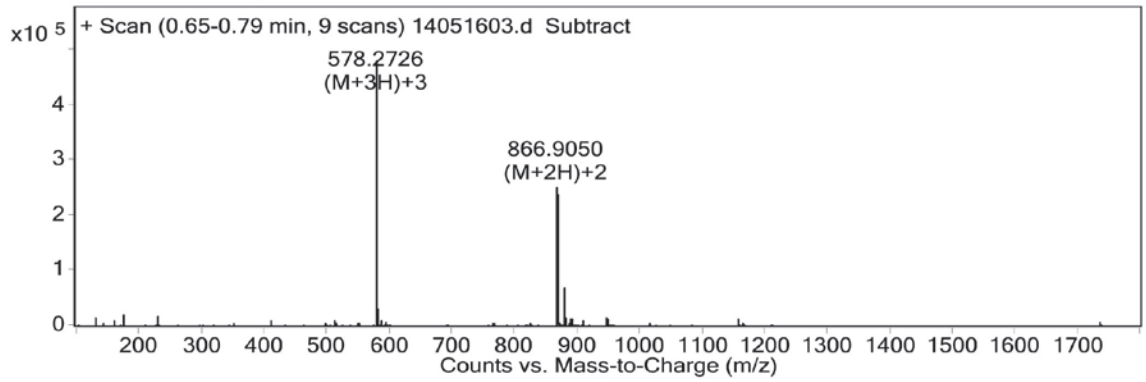

Formula Calculator Results

Formula	Ion Species	Mass	Calc. Mass	m/z	Calc. m/z	Diff (mDa)	Diff(ppm)	DBE	Ion	Score
C75 H109 N23 O25	C75 H112 N23 O25	1731.796	1731.7965	578.2726	578.2728	0.53	0.3	33	(M+3H)+3	99.4
C75 H109 N23 O25	C75 H111 N23 O25	1731.7953	1731.7965	866.905	866.9055	1.21	0.7	33	(M+2H)+2	98.52

--- End Of Report ---

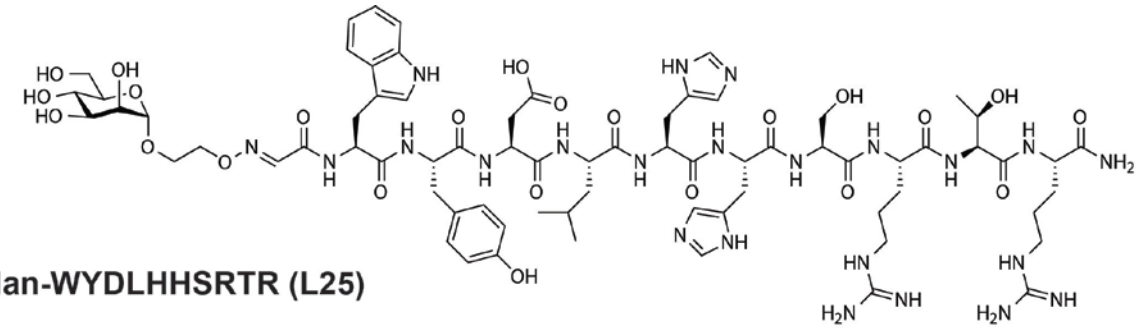

Man-WYDLHHSRTR (L25)

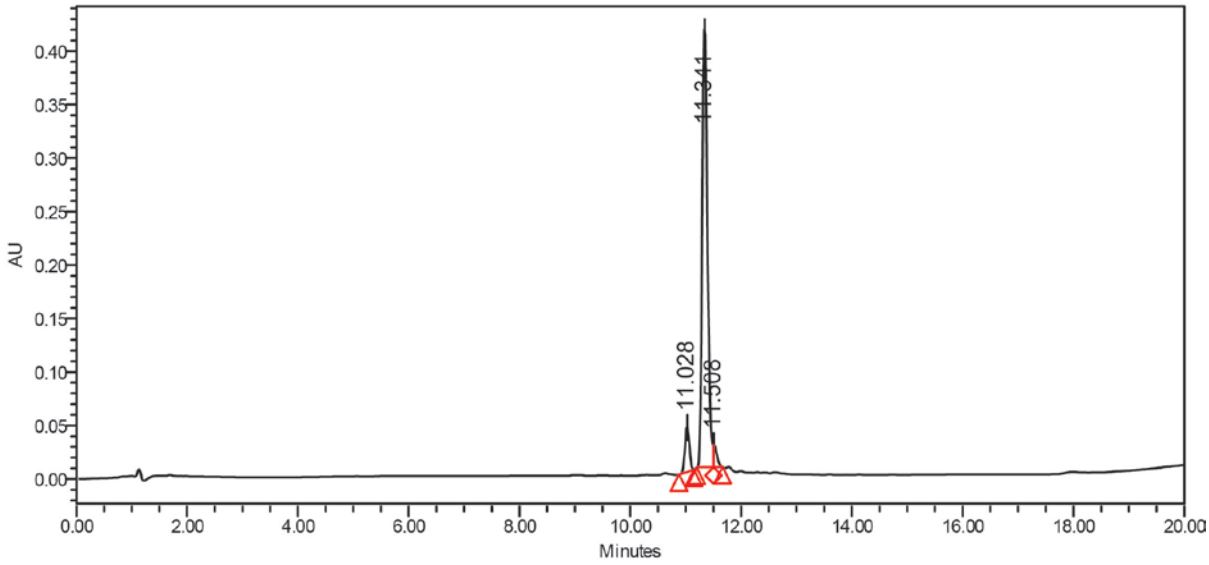

Peak Results

	RT	Area	Height	% Area
1	11.028	235217	41881	7.66
2	11.341	2746172	413130	89.38
3	11.508	91171	20455	2.97

User Spectra

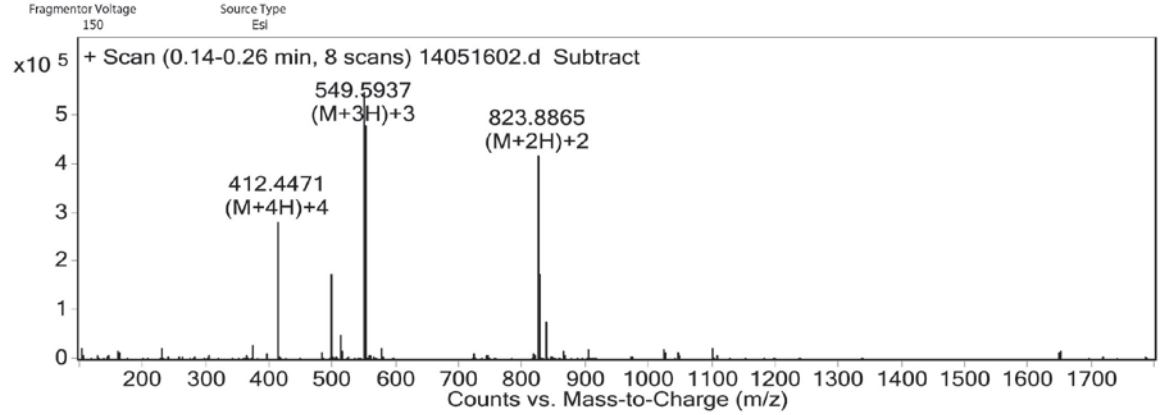

Formula Calculator Results

Formula	Ion Species	Mass	Calc. Mass	m/z	Calc. m/z	Diff (mDa)	Diff(ppm)	DBE	Ion	Score
C71 H103 N23 O23	C71 H105 N23 O23	1645.7581	1645.7597	823.8865	823.8871	1.61	0.98	32	(M+2H)+2	97.75
C71 H103 N23 O23	C71 H106 N23 O23	1645.7591	1645.7597	549.5937	549.5938	0.6	0.36	32	(M+3H)+3	99.25
C71 H103 N23 O23	C71 H107 N23 O23	1645.759	1645.7597	412.4471	412.4472	0.69	0.42	32	(M+4H)+4	98.86

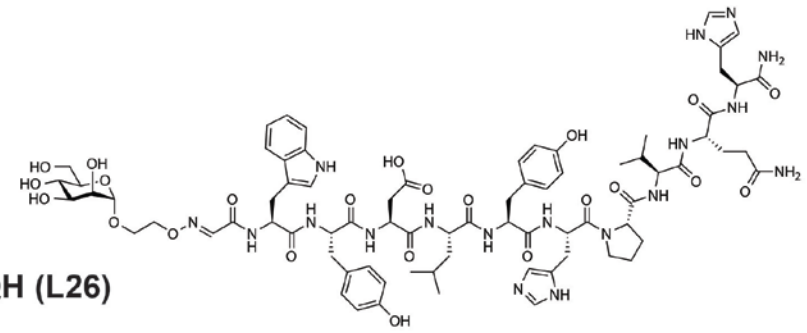

Man-WYDLYHPVQH (L26)

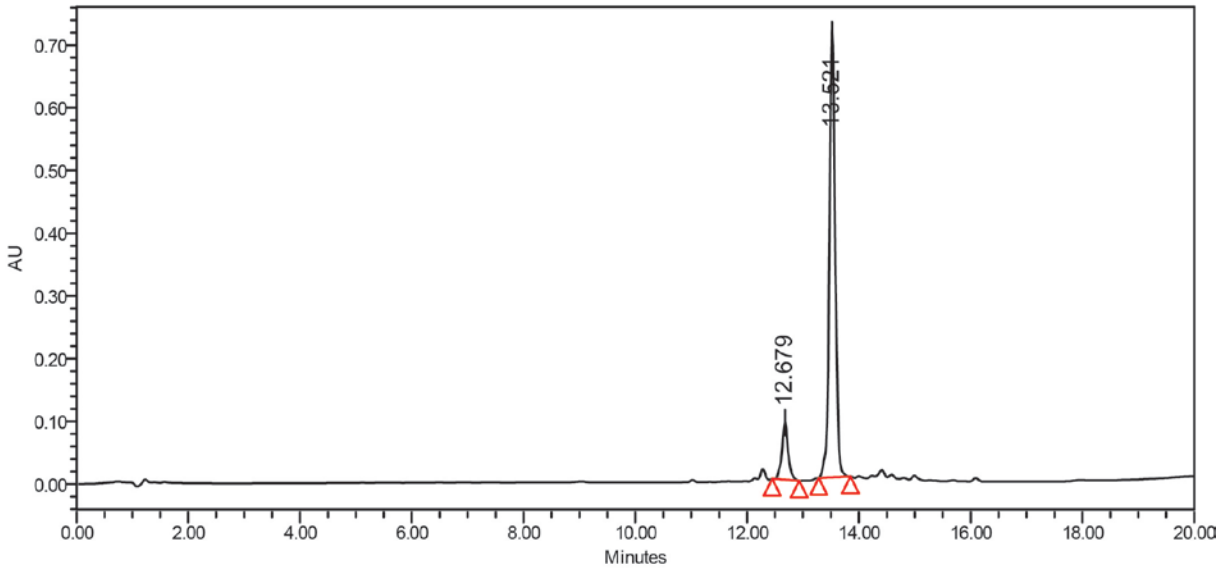

Peak Results

	RT	Area	Height	% Area
1	12.679	714360	91540	12.06
2	13.521	5206632	714136	87.94

User Spectra

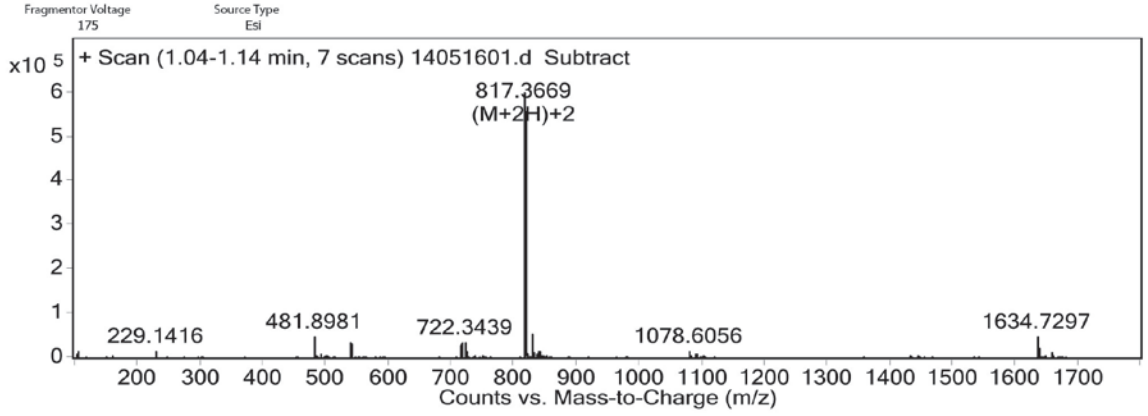

Formula Calculator Results

Formula	Ion Species	Mass	Calc. Mass	m/z	Calc. m/z	Diff (mDa)	Diff(ppm)	DBE	Ion	Score
C76 H100 N18 O23	C76 H102 N18 O23	1632.7191	1632.7209	817.3669	817.3677	1.79	1.09	36	(M+2H)+2	97.44

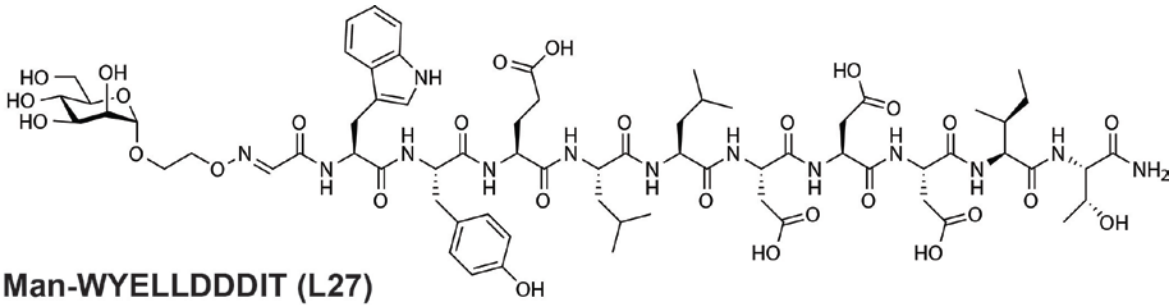

Man-WYELLDDDIT (L27)

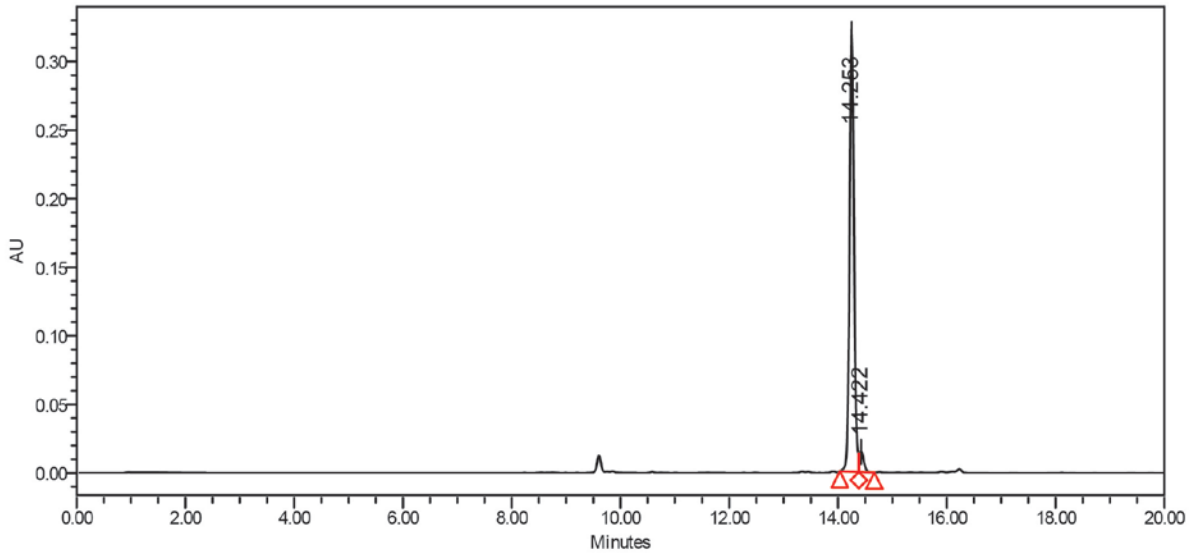

Peak Results

	RT	Area	Height	% Area
1	14.253	1856243	320454	95.50
2	14.422	87483	14853	4.50

User Spectra

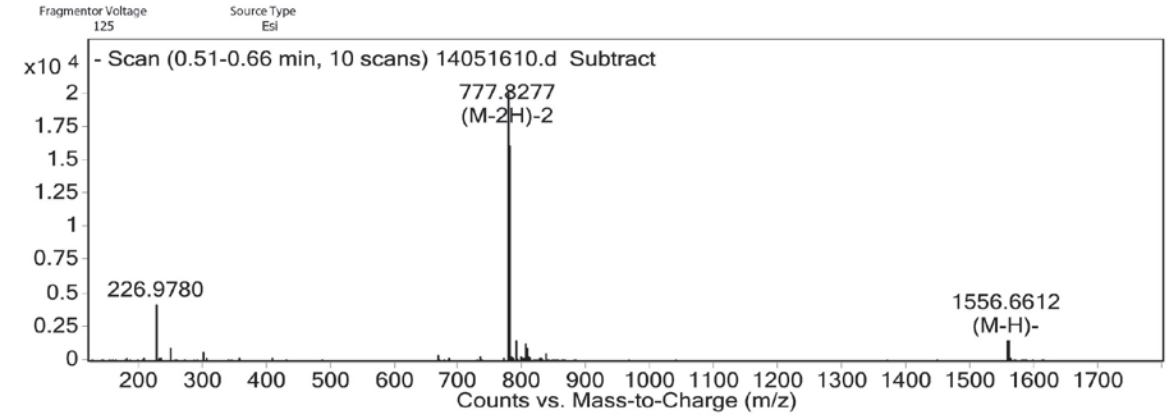

Formula Calculator Results

Formula	Ion Species	Mass	Calc. Mass	m/z	Calc. m/z	Diff (mDa)	Diff(ppm)	DBE	Ion	Score
C69 H99 N13 O28	C69 H97 N13 O28	1557.6696	1557.6722	777.8277	777.8288	2.63	1.69	27	(M-2H)-2	92.87
C69 H99 N13 O28	C69 H98 N13 O28	1557.669	1557.6722	1556.6612	1556.665	3.24	2.08	27	(M-H)-	87.35

--- End Of Report ---

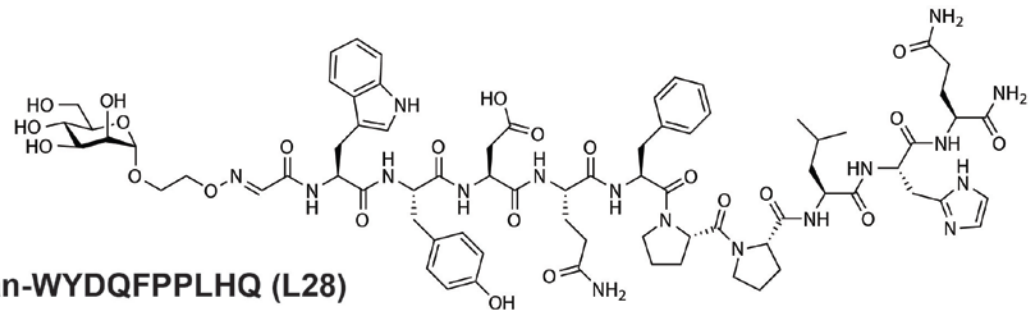

Man-WYDQFPPLHQ (L28)

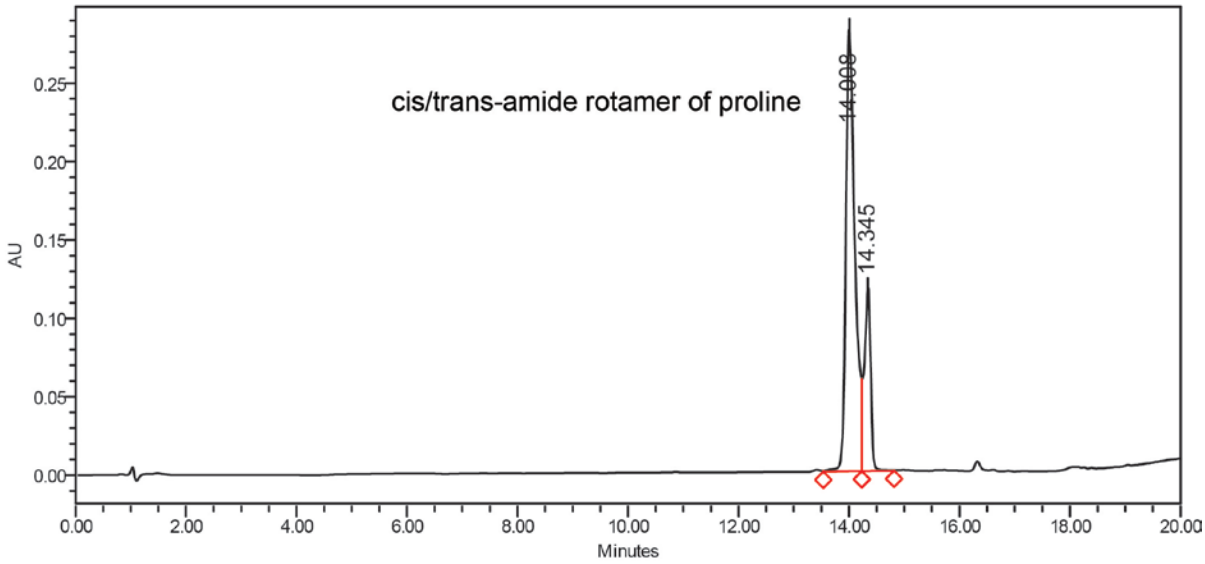

Peak Results

	RT	Area	Height	% Area
1	14.008	3206737	283373	77.29
2	14.345	942389	116218	22.71

User Spectra

Fragmentor Voltage 175 Source Type Esi

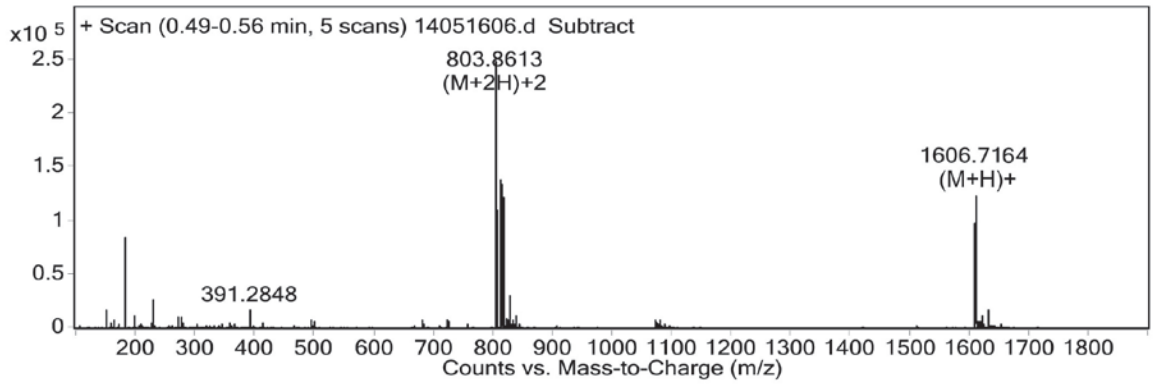

Formula Calculator Results

Formula	Ion Species	Mass	Calc. Mass							
C75 H99 N17 O23	C75 H101 N17 O23	1605.7081	1605.71							

--- End Of Report ---

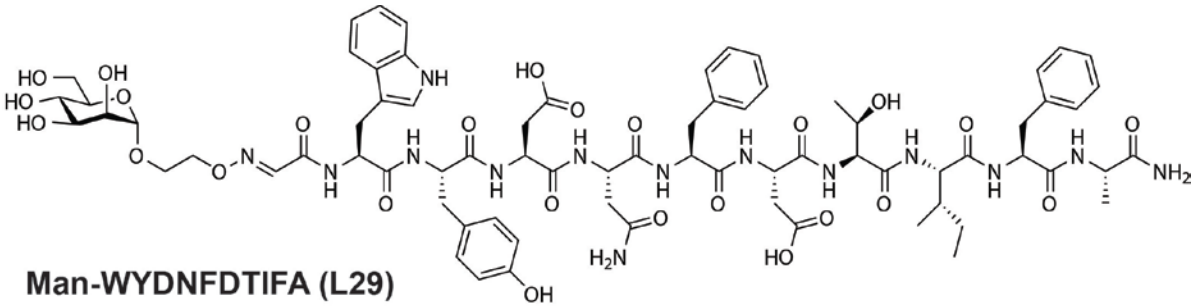

Man-WYDNFDTIFA (L29)

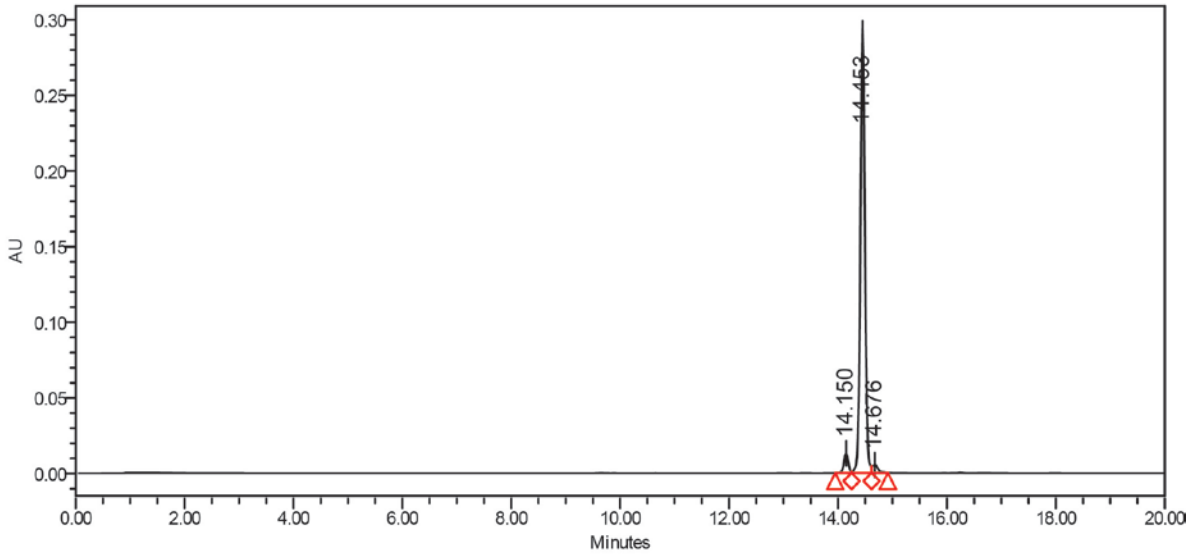

Peak Results

	RT	Area	Height	% Area
1	14.150	71969	12840	3.90
2	14.453	1731169	291871	93.92
3	14.676	40177	5200	2.18

User Spectra

Fragmentor Voltage 125 Source Type Esi

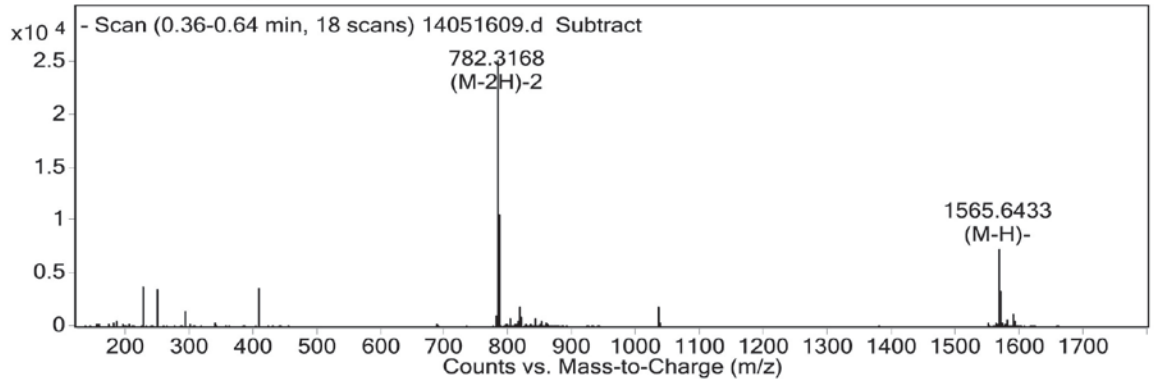

Formula Calculator Results

Formula	Ion Species	Mass	Calc. Mass	m/z	Calc. m/z	Diff (mDa)	Diff(ppm)	DBE	Ion	Score
C73 H94 N14 O25	C73 H92 N14 O25	1566.6482	1566.6515	782.3168	782.3185	3.3	2.1	34	(M-2H)-2	89.93
C73 H94 N14 O25	C73 H93 N14 O25	1566.6505	1566.6515	1565.6433	1565.6442	0.91	0.58	34	(M-H)-	96.6

--- End Of Report ---

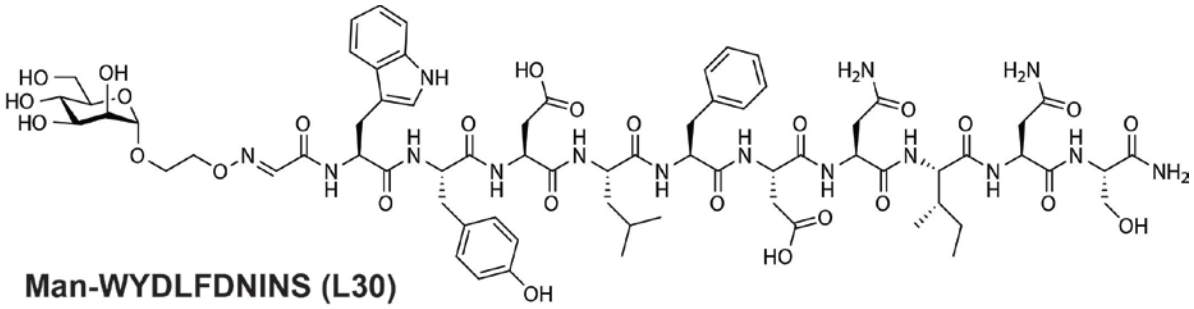

Man-WYDLFDNINS (L30)

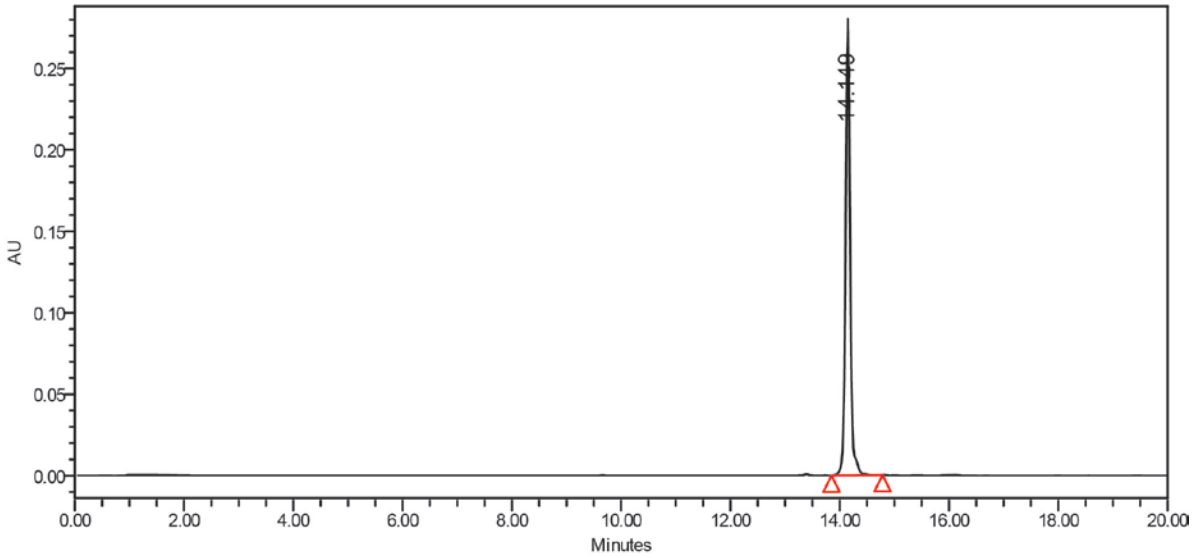

Peak Results

	RT	Area	Height	% Area
1	14.149	1650877	271689	100.00

User Spectra

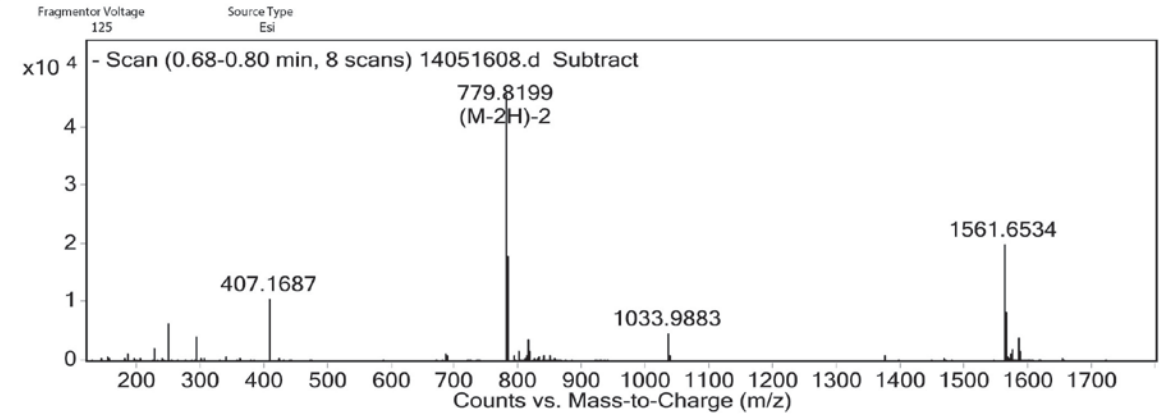

Formula Calculator Results

Formula	Ion Species	Mass	Calc. Mass	m/z	Calc. m/z	Diff (mDa)	Diff(ppm)	DBE	Ion	Score
C70 H95 N15 O26	C70 H93 N15 O26	1561.6544	1561.6573	779.8199	779.8214	2.82	1.81	31	(M-2H)-2	92.45

--- End Of Report ---

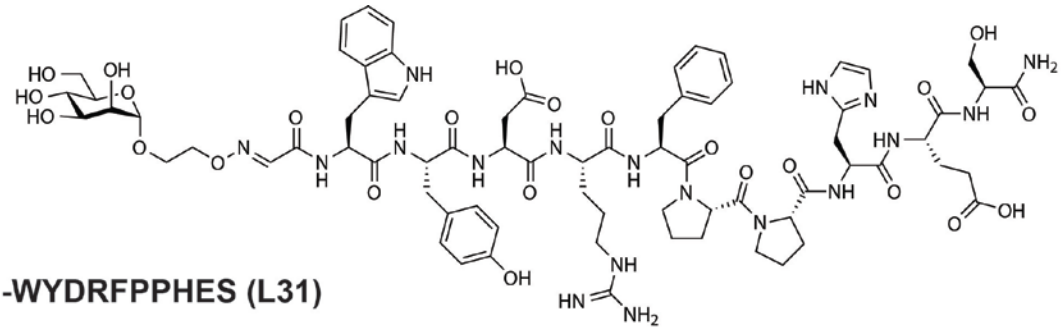

Man-WYDRFPPHES (L31)

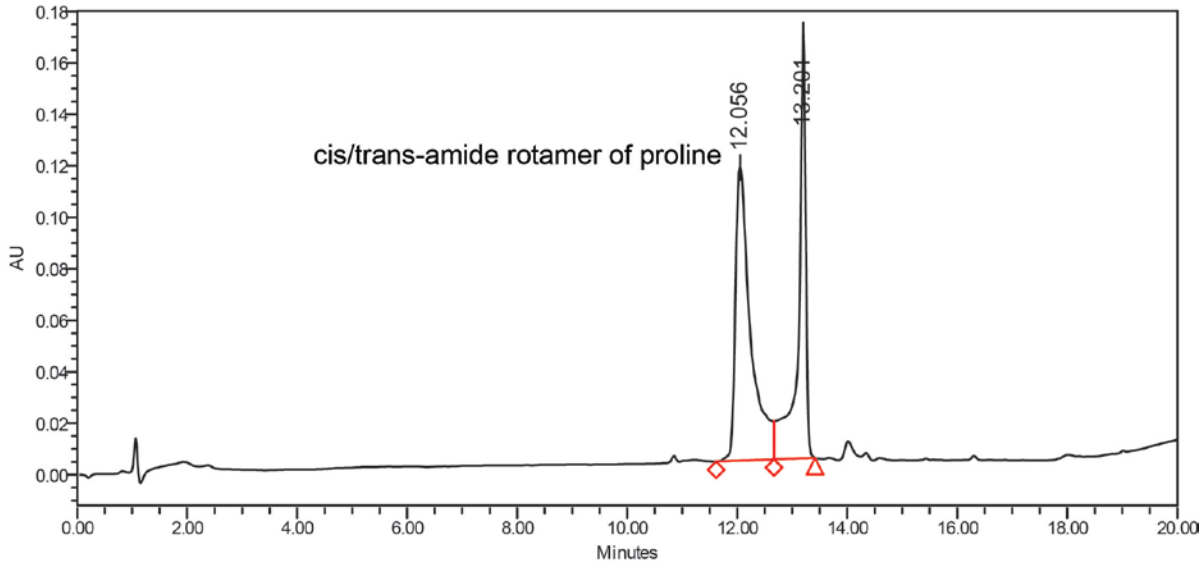

Peak Results

	RT	Area	Height	% Area
1	12.056	2202027	114303	58.26
2	13.201	1577683	163947	41.74

User Spectra

Fragmentor Voltage 175 Source Type Esi

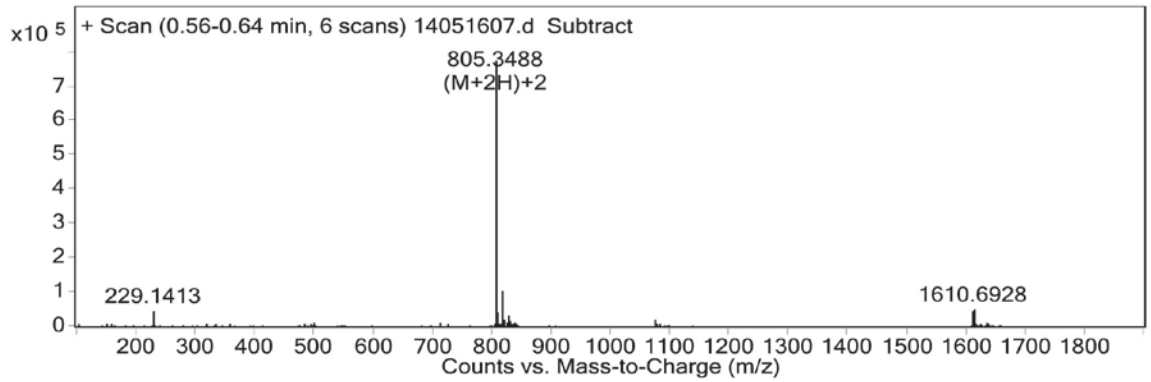

Formula Calculator Results

Formula	Ion Species	Mass	Calc. Mass	m/z	Calc. m/z	Diff (mDa)	Diff(ppm)	DBE	Ion	Score
C73 H96 N18 O24	C73 H98 N18 O24	1608.683	1608.6845	805.3488	805.3495	1.52	0.95	35	(M+2H)+2	97.59

--- End Of Report ---

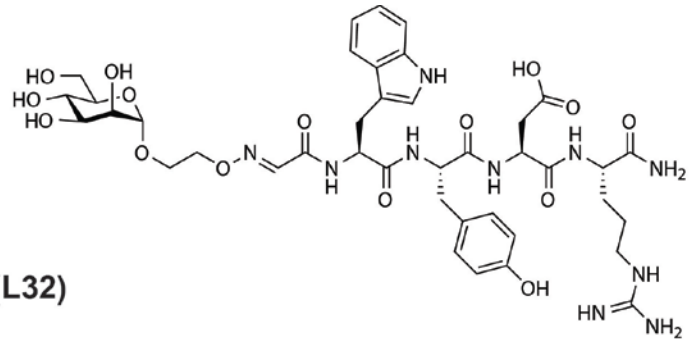

Man-WYDR (L32)

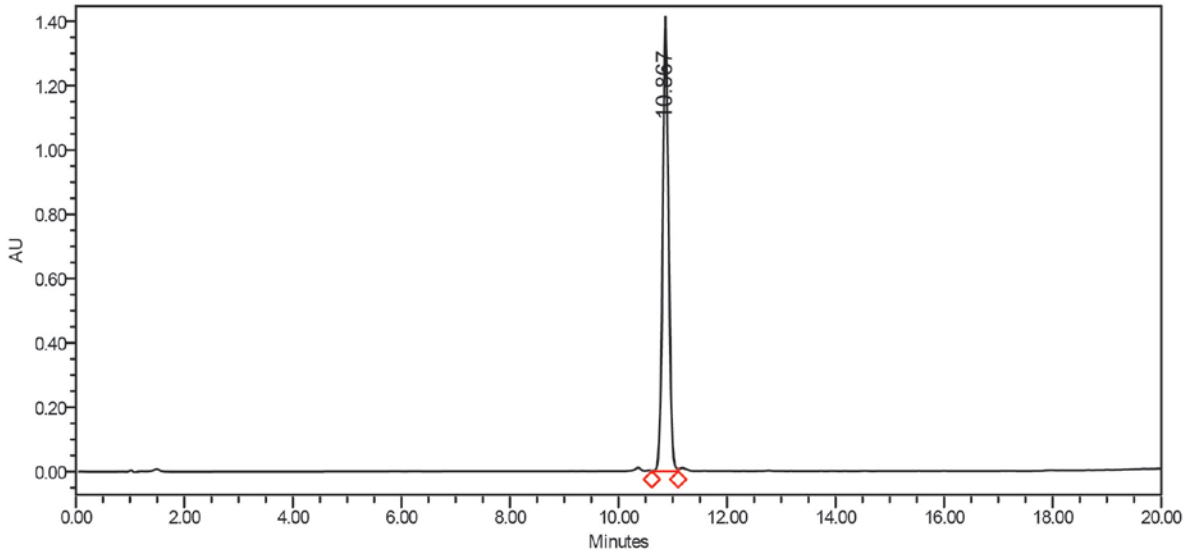

Peak Results

	RT	Area	Height	% Area
1	10.867	10522412	1371658	100.00

User Spectra

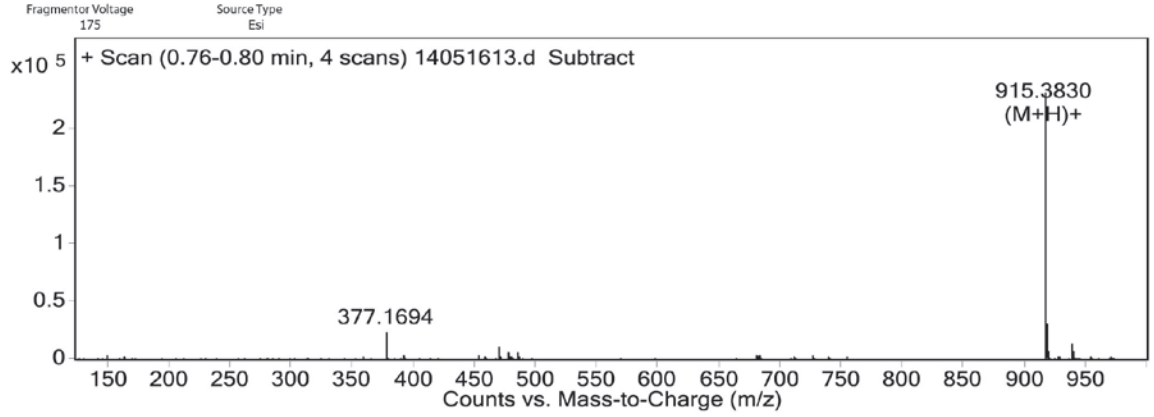

Formula Calculator Results

Formula	Ion Species	Mass	Calc. Mass	m/z	Calc. m/z	Diff (mDa)	Diff(ppm)	DBE	Ion	Score
C40 H54 N10 O15	C40 H55 N10 O15	914.3757	914.377	915.383	915.3843	1.28	1.4	19	(M+H)+	95.11
C40 H54 N10 O15	C40 H54 N10 Na O15	914.3771	914.377	937.3664	937.3662	-0.07	-0.08	19	(M+Na)+	90.82

--- End Of Report ---

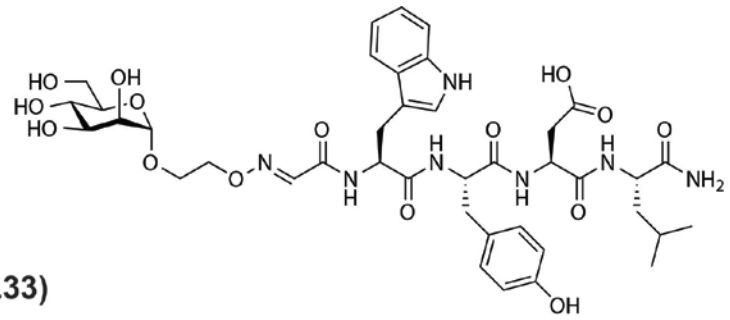

Man-WYDL (L33)

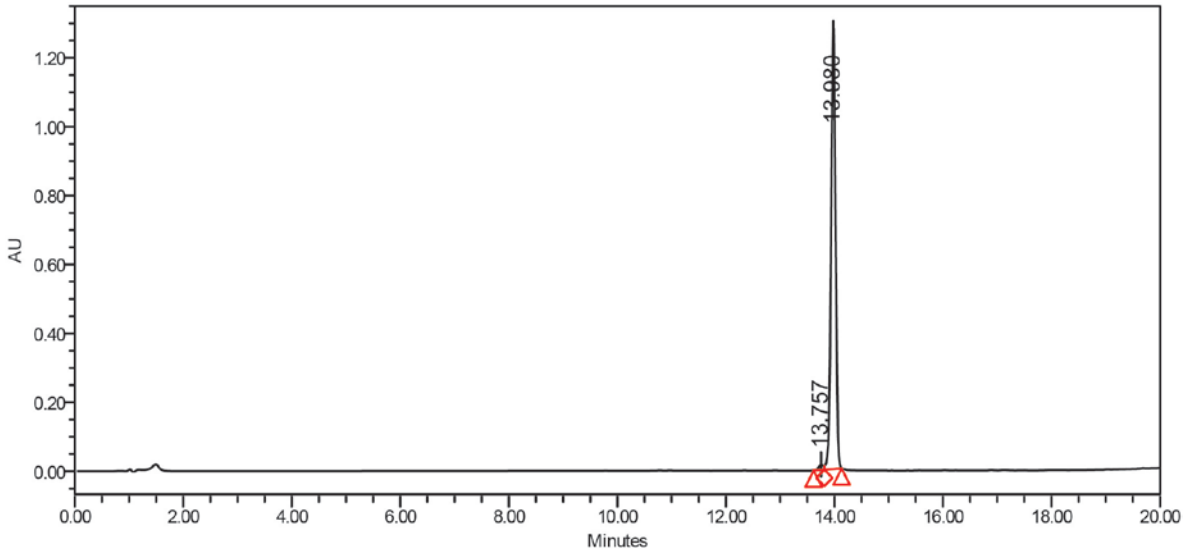

Peak Results

	RT	Area	Height	% Area
1	13.757	92139	15695	1.23
2	13.980	7402957	1272477	98.77

User Spectra

Fragmentor Voltage 175 Source Type Esi

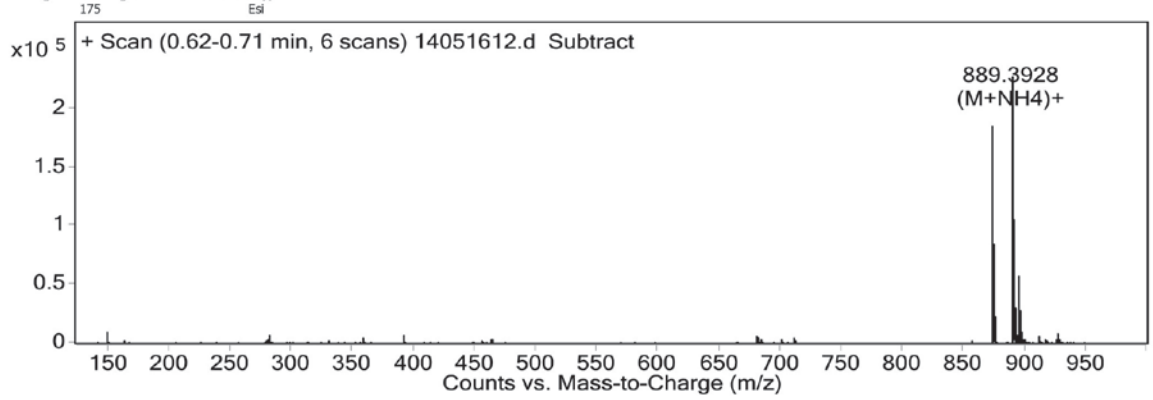

Formula Calculator Results

Formula	Ion Species	Mass	Calc. Mass	m/z	Calc. m/z	Diff (mDa)	Diff(ppm)	DBE	Ion	Score
C40 H53 N7 O15	C40 H54 N7 O15	871.3592	871.36	872.3665	872.3672	0.73	0.84	18	(M+H)+	97.25
C40 H53 N7 O15	C40 H57 N8 O15	871.359	871.36	889.3928	889.3938	0.95	1.09	18	(M+NH4)+	96.87
C40 H53 N7 O15	C40 H53 N7 Na O15	871.3594	871.36	894.3486	894.3492	0.55	0.63	18	(M+Na)+	95.86

--- End Of Report ---

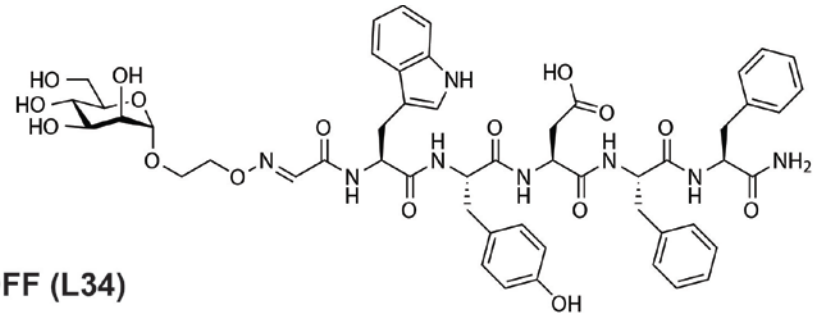

Man-WYDFF (L34)

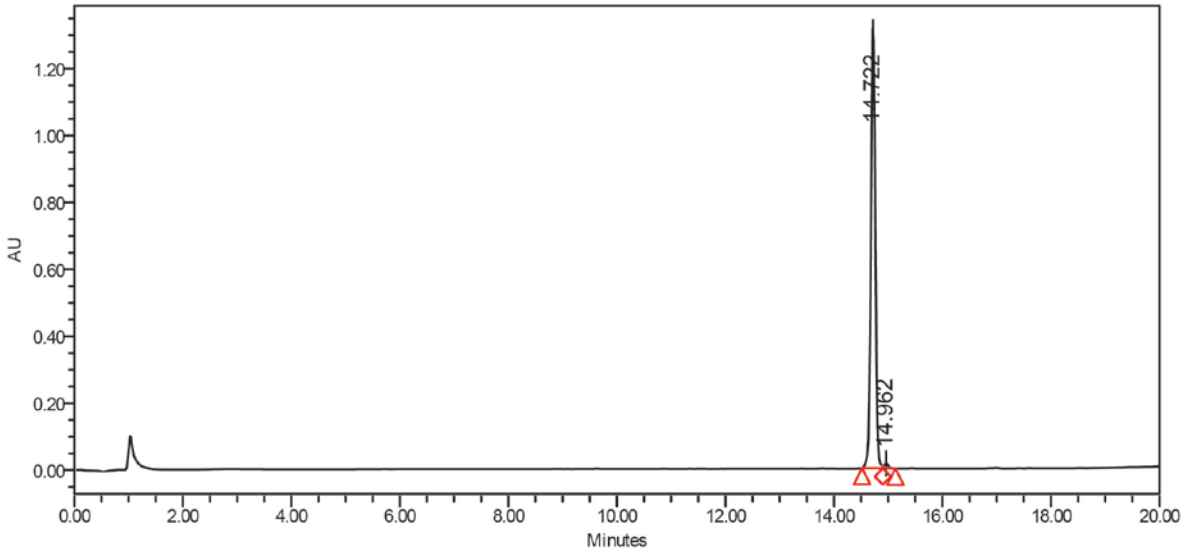

Peak Results

	RT	Area	Height	% Area
1	14.722	7441866	1314655	98.86
2	14.962	85621	14614	1.14

User Spectra

Fragmentor Voltage 175 Source Type Esi

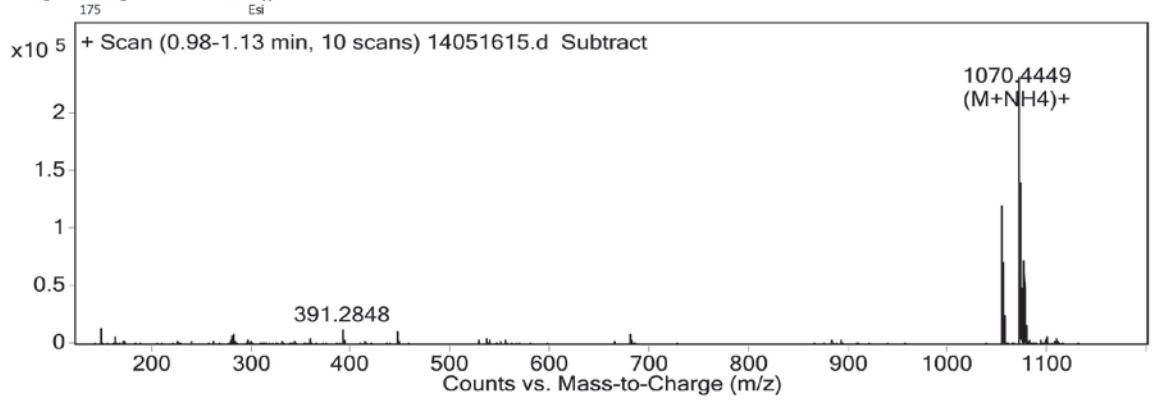

Formula Calculator Results

Formula	Ion Species	Mass	Calc. Mass	m/z	Calc. m/z	Diff (mDa)	Diff(ppm)	DBE	Ion	Score
C52 H60 N8 O16	C52 H61 N8 O16	1052.4119	1052.4127	1053.4191	1053.42	0.84	0.79	27	(M+H)+	98.43
C52 H60 N8 O16	C52 H64 N9 O16	1052.4111	1052.4127	1070.4449	1070.4466	1.63	1.54	27	(M+NH4)+	94.59
C52 H60 N8 O16	C52 H60 N8 Na O16	1052.4118	1052.4127	1075.401	1075.4019	0.9	0.86	27	(M+Na)+	97.01

--- End Of Report ---

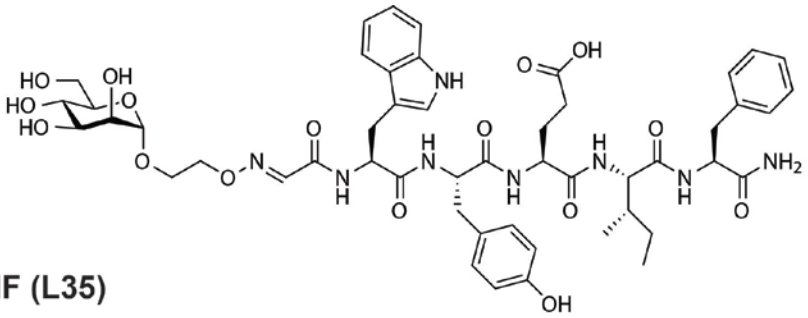

Man-WYEIF (L35)

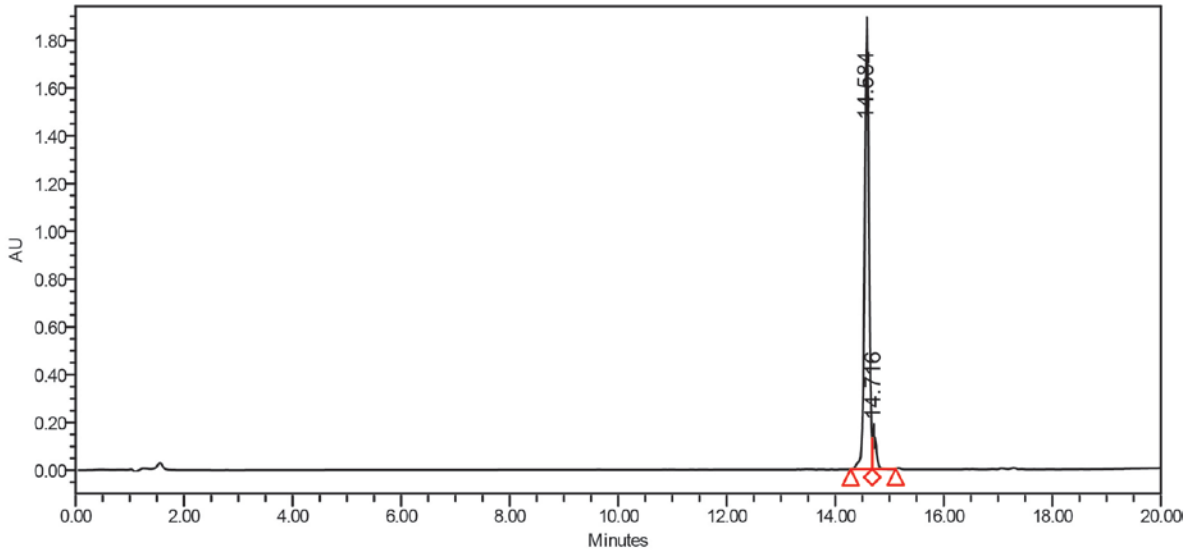

Peak Results

	RT	Area	Height	% Area
1	14.584	10462628	1826071	93.66
2	14.716	708711	137772	6.34

User Spectra

Fragmentor Voltage 175 Source Type Esi

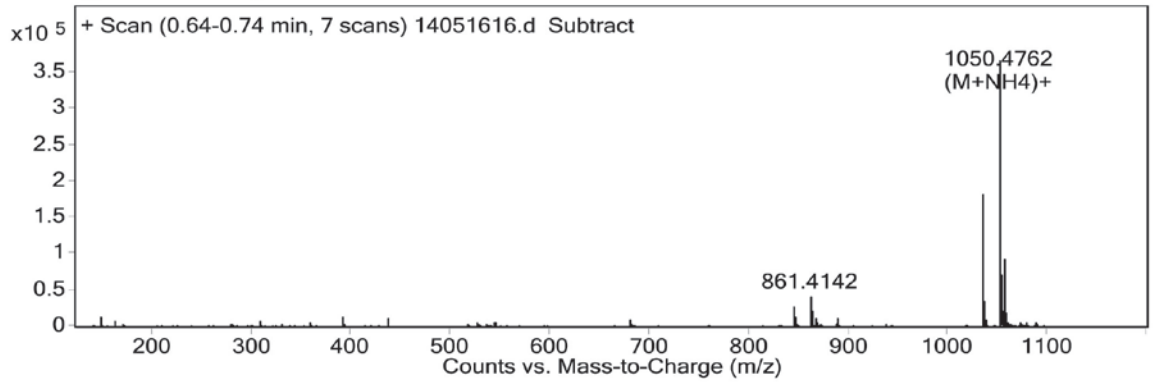

Formula Calculator Results

Formula	Ion Species	Mass	Calc. Mass	m/z	Calc. m/z	Diff (mDa)	Diff(ppm)	DBE	Ion	Score
C50 H64 N8 O16	C50 H65 N8 O16	1032.4427	1032.444	1033.4499	1033.4513	1.34	1.3	23	(M+H)+	95.67
C50 H64 N8 O16	C50 H68 N9 O16	1032.4424	1032.444	1050.4762	1050.4779	1.63	1.58	23	(M+NH4)+	94.19
C50 H64 N8 O16	C50 H64 N8 Na O16	1032.4433	1032.444	1055.4325	1055.4332	0.74	0.72	23	(M+Na)+	97.18

--- End Of Report ---

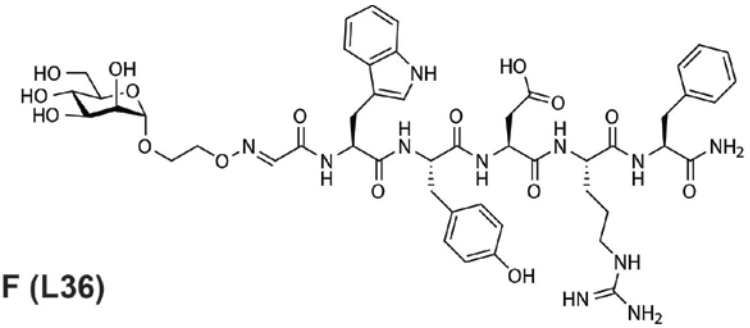

Man-WYDRF (L36)

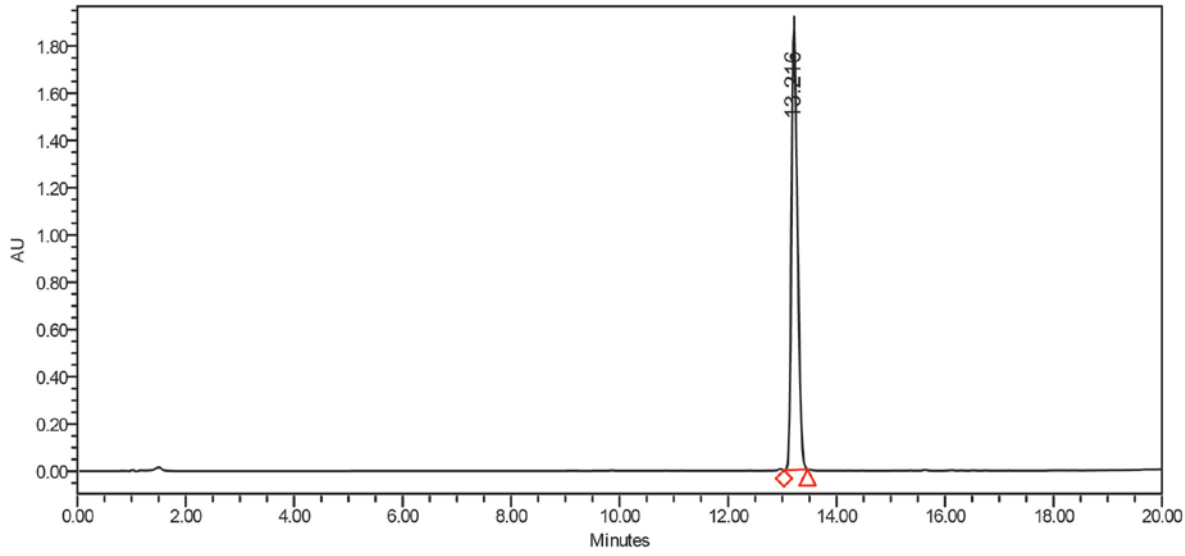

Peak Results

	RT	Area	Height	% Area
1	13.216	14523798	1864500	100.00

User Spectra

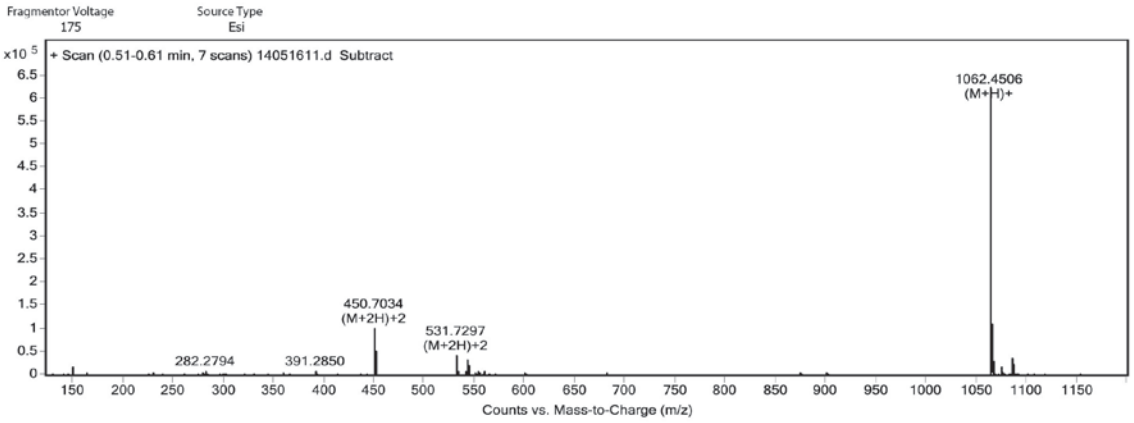

Formula Calculator Results

Formula	Ion Species	Mass	Calc. Mass	m/z	Calc. m/z	Diff (mDa)	Diff(ppm)	DBE	Ion	Score
C49 H63 N11 O16	C49 H65 N11 O16	1061.445	1061.4454	531.7297	531.73	0.47	0.44	24	(M+2H)+2	98.77
C49 H63 N11 O16	C49 H64 N11 O16	1061.4434	1061.4454	1062.4506	1062.4527	2.05	1.93	24	(M+H)+	91.33
C43 H53 N11 O11	C43 H55 N11 O11	899.3923	899.3926	450.7034	450.7036	0.27	0.3	23	(M+2H)+2	99.36

--- End Of Report ---

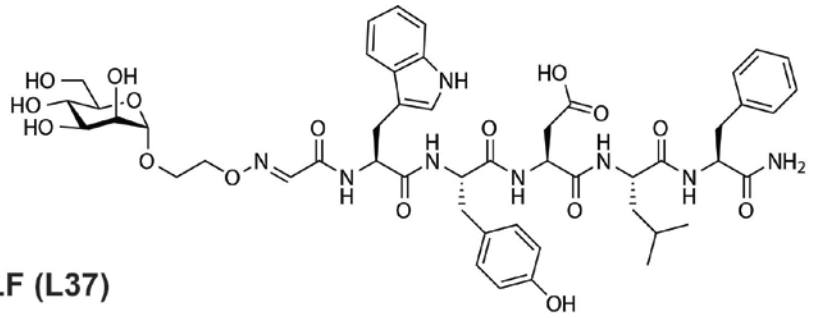

Man-WYDLF (L37)

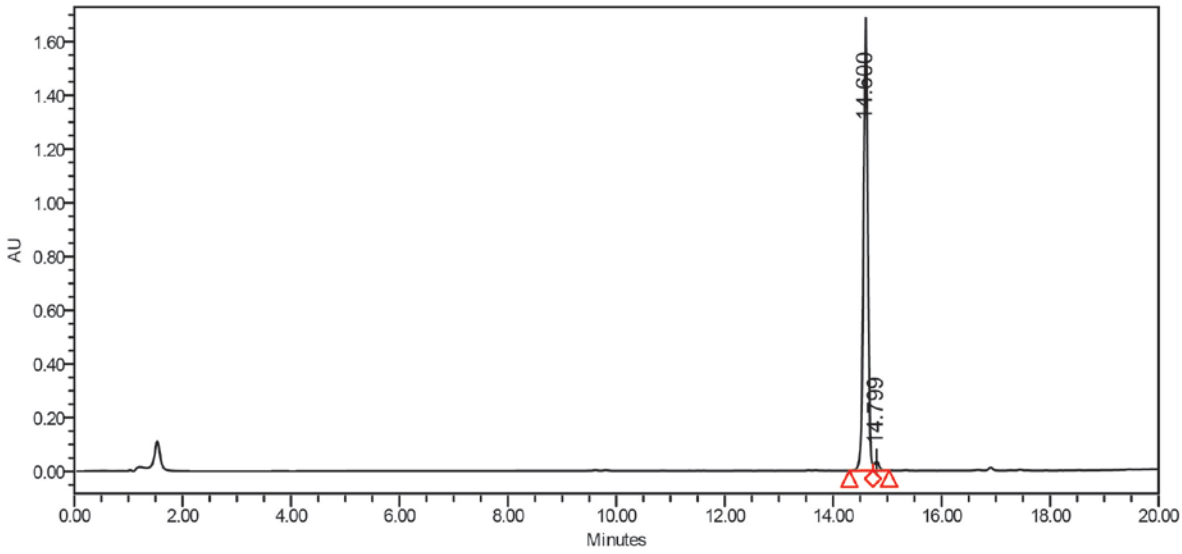

Peak Results

	RT	Area	Height	% Area
1	14.600	9269927	1627337	97.71
2	14.799	216819	33477	2.29

User Spectra

Fragmentor Voltage 175 Source Type Esi

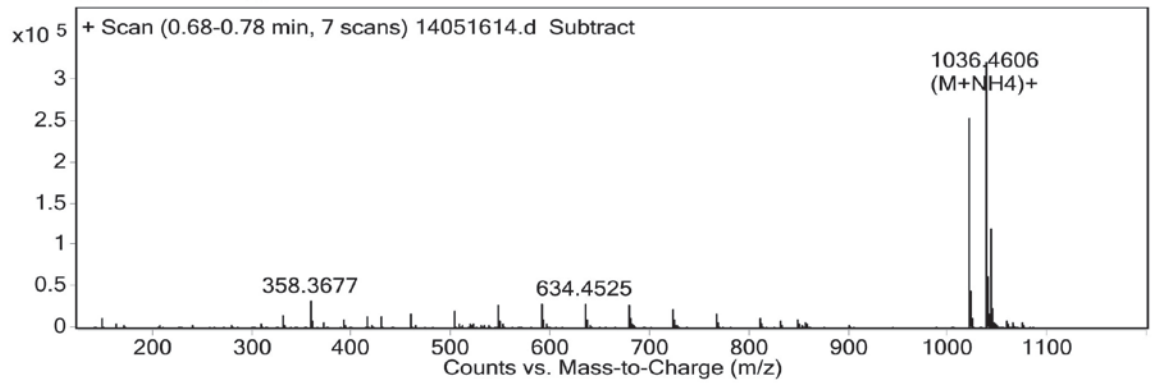

Formula Calculator Results

Formula	Ion Species	Mass	Calc. Mass	m/z	Calc. m/z	Diff (mDa)	Diff(ppm)	DBE	Ion	Score
C49 H62 N8 O16	C49 H63 N8 O16	1018.4271	1018.4284	1019.4343	1019.4357	1.29	1.27	23	(M+H)+	95.97
C49 H62 N8 O16	C49 H66 N9 O16	1018.4268	1018.4284	1036.4606	1036.4622	1.58	1.55	23	(M+NH4)+	94.42
C49 H62 N8 O16	C49 H62 N8 Na O16	1018.4274	1018.4284	1041.4165	1041.4176	1.01	0.99	23	(M+Na)+	96.81

--- End Of Report ---

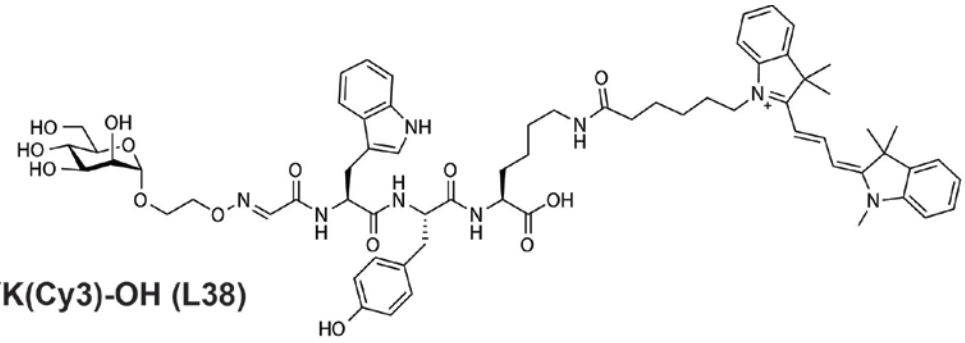

Man-WYK(Cy3)-OH (L38)

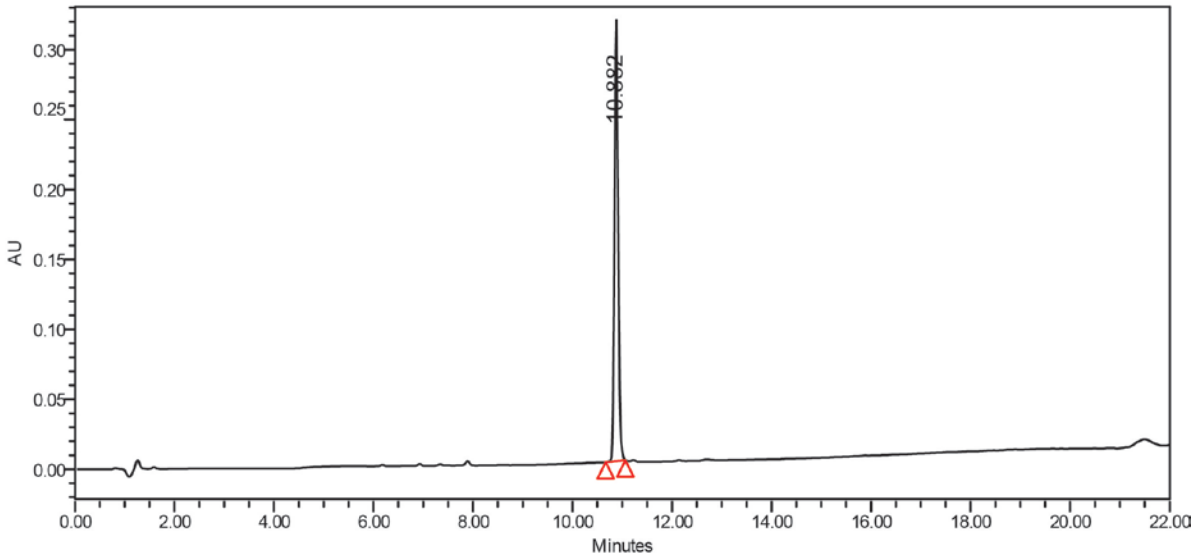

Peak Results

	RT	Area	Height	% Area
1	10.882	1621845	305123	100.00

User Spectra

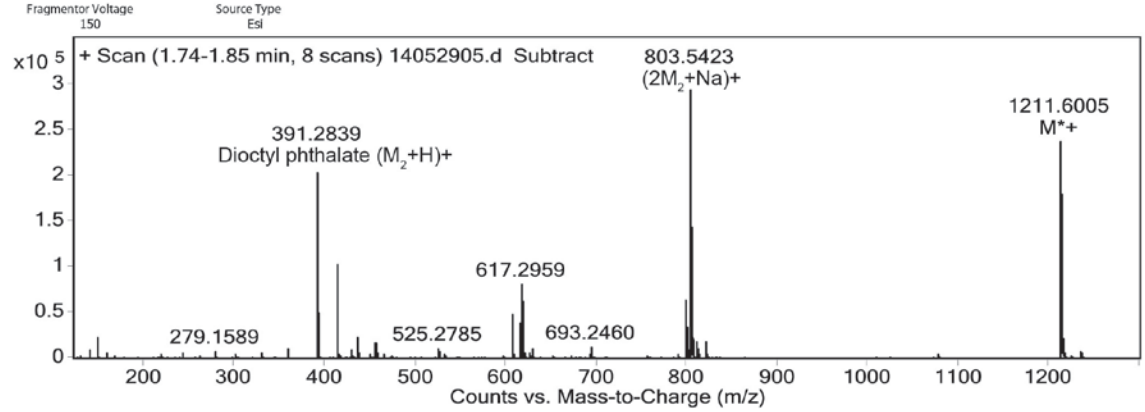

Formula Calculator Results

Formula	Ion Species	Mass	Calc. Mass	m/z	Calc. m/z	Diff (mDa)	Diff(ppm)	DBE	Ion	Score
C66 H83 N8 O14	C66 H83 N8 O14	1211.6011	1211.6029	1211.6005	1211.6023	1.81	1.5	29.5	M*+	94.82

--- End Of Report ---

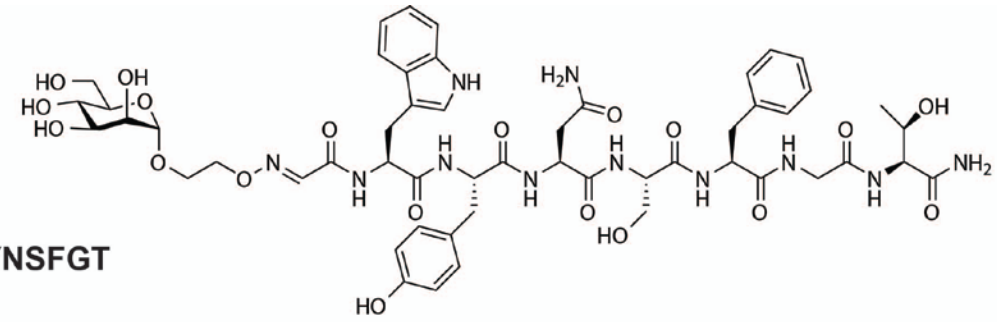

Man-WYNSFGT

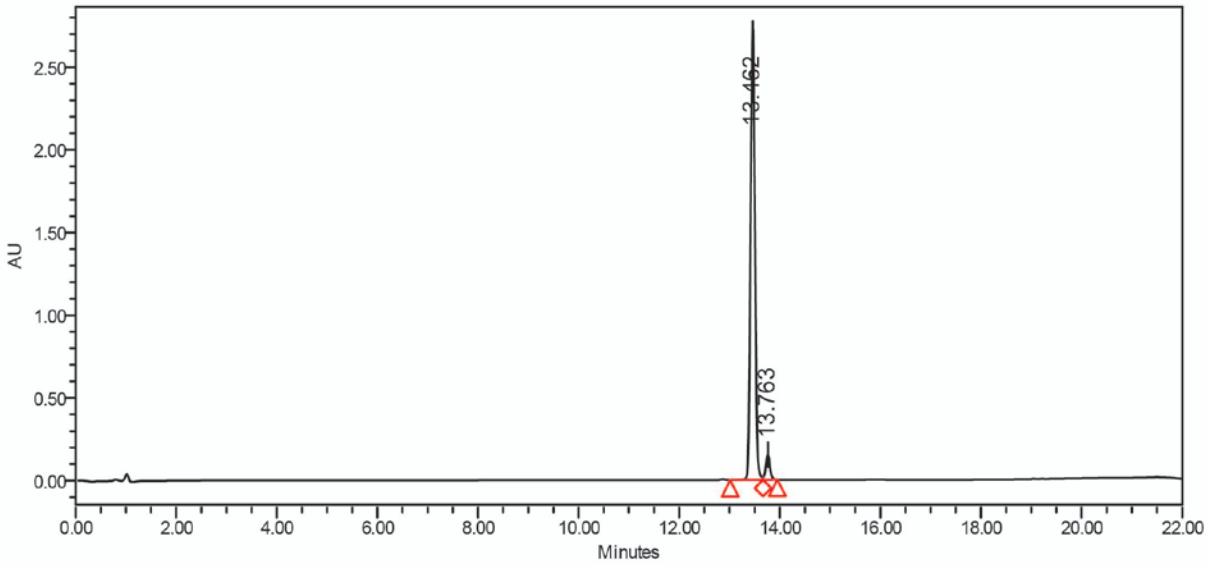

Peak Results

	RT	Area	Height	% Area
1	13.462	16117945	2720056	94.79
2	13.763	885592	152755	5.21

User Spectra

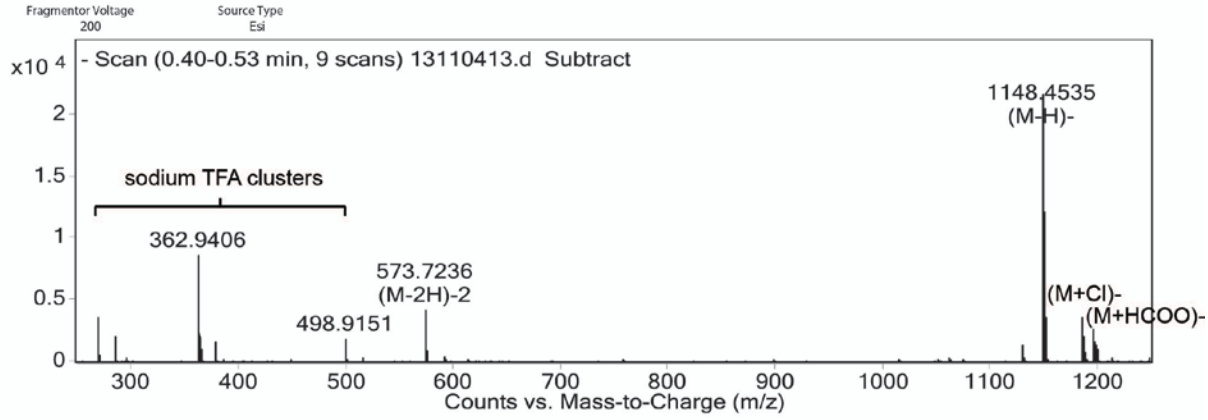

Formula Calculator Results

Formula	Ion Species	m/z	Calc. m/z	Diff (mDa)	Diff (ppm)	DBE	Ion	Score
C52 H67 N11 O19	C52 H65 N11 O19	573.7236	573.7235	-0.28	-0.24	25	(M-2H)-2	99.45
C52 H67 N11 O19	C52 H66 N11 O19	1148.4535	1148.4542	0.76	0.66	25	(M-H)-	94.5

--- End Of Report ---

SWYNSFGT

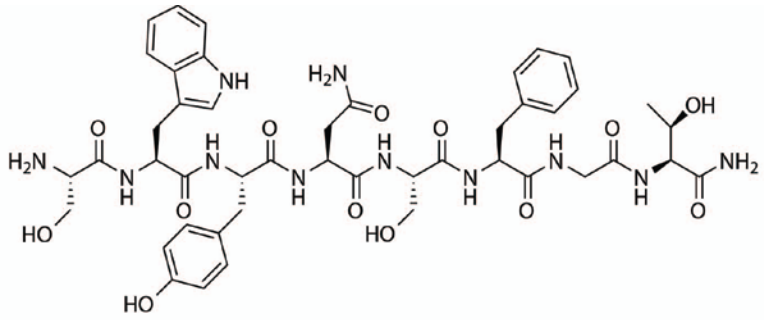

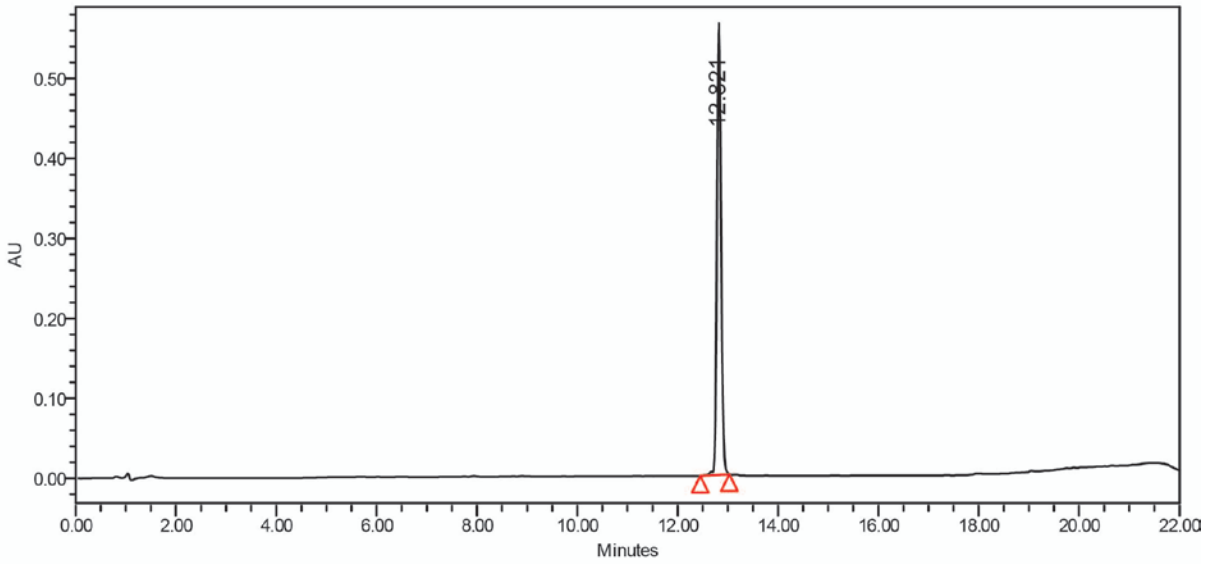

Peak Results

	RT	Area	Height	% Area
1	12.821	3267927	555411	100.00

User Spectra

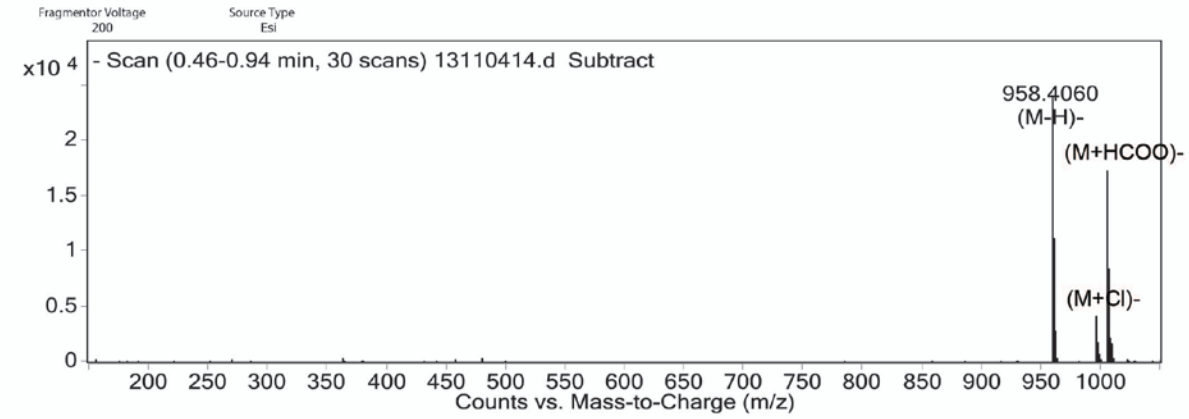

Formula Calculator Results

Formula	Ion Species	m/z	Calc. m/z	Diff (mDa)	Diff (ppm)	DBE	Ion	Score
C45 H57 N11 O13	C45 H56 N11 O13	958.406	958.4065	0.47	0.49	23	(M-H)-	94.32
C45 H57 N11 O13	C46 H58 N11 O15	1004.4111	1004.4119	0.85	0.89	23	(M+COOH)-	92.38
C45 H57 N11 O13	C45 H57 Cl N11 O13	994.3816	994.3831	1.56	1.63	23	(M+Cl)-	53.06

--- End Of Report ---

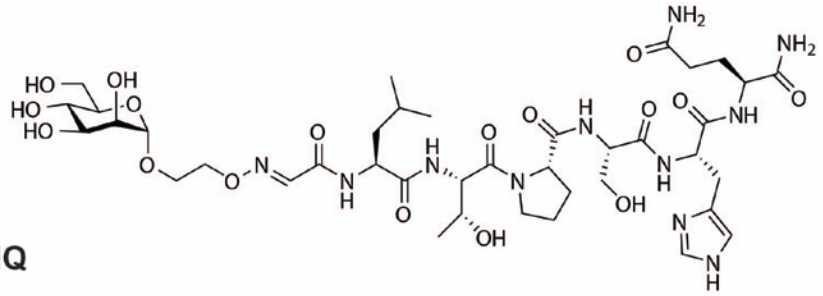

Man-LTPSHQ

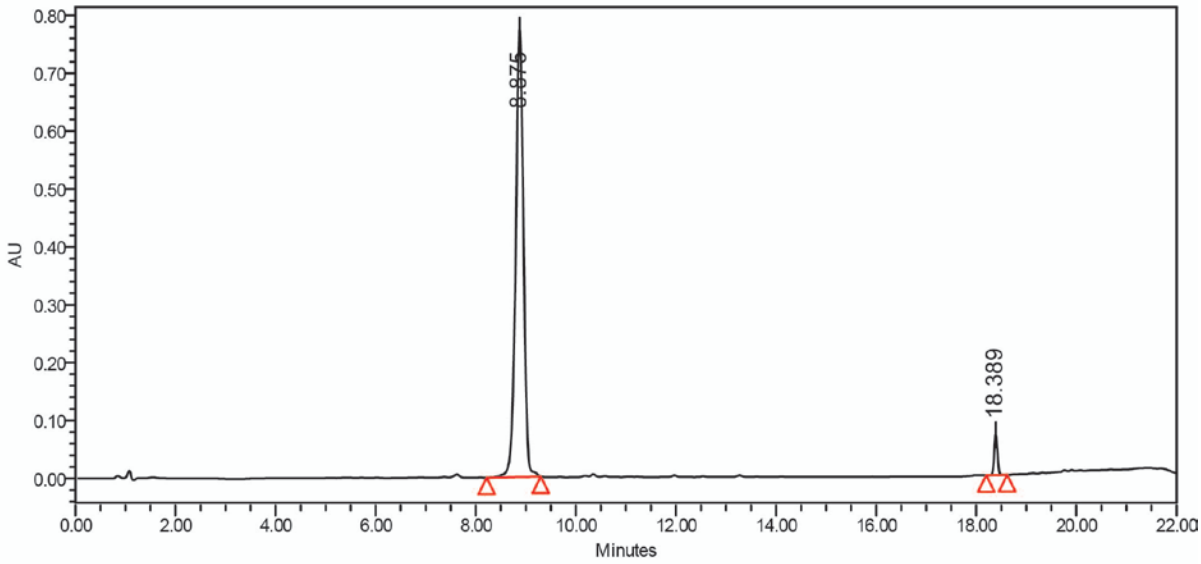

Peak Results

	RT	Area	Height	% Area
1	8.875	8290916	776943	96.25
2	18.389	323231	70076	3.75

User Spectra

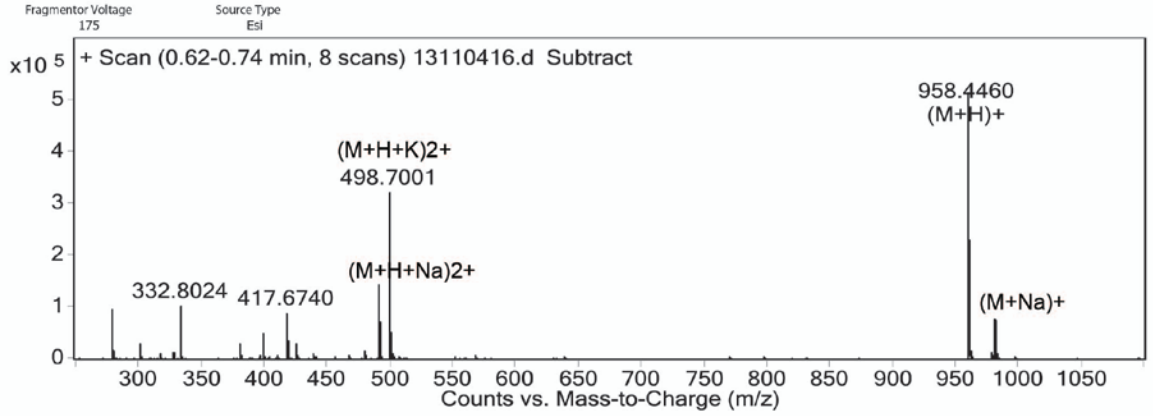

Formula Calculator Results

Formula	Ion Species	m/z	Calc. m/z	Diff (mDa)	Diff (ppm)	DBE	Ion	Score
C39 H63 N11 O17	C39 H64 N11 O17	958.446	958.4476	1.59	1.66	14	(M+H)+	94.07
C39 H63 N11 O17	C39 H63 N11 Na O17	980.429	980.4296	0.47	0.49	14	(M+Na)+	98.78

--- End Of Report ---

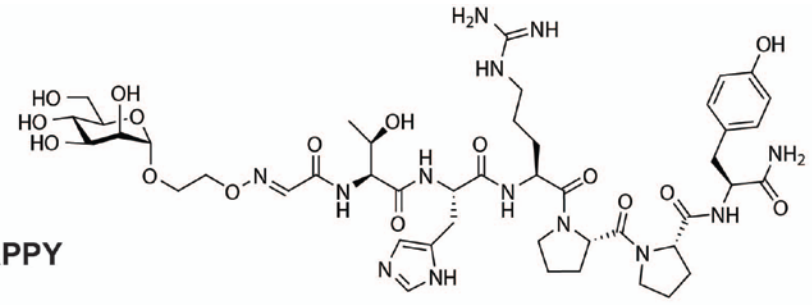

Man-THRPPY

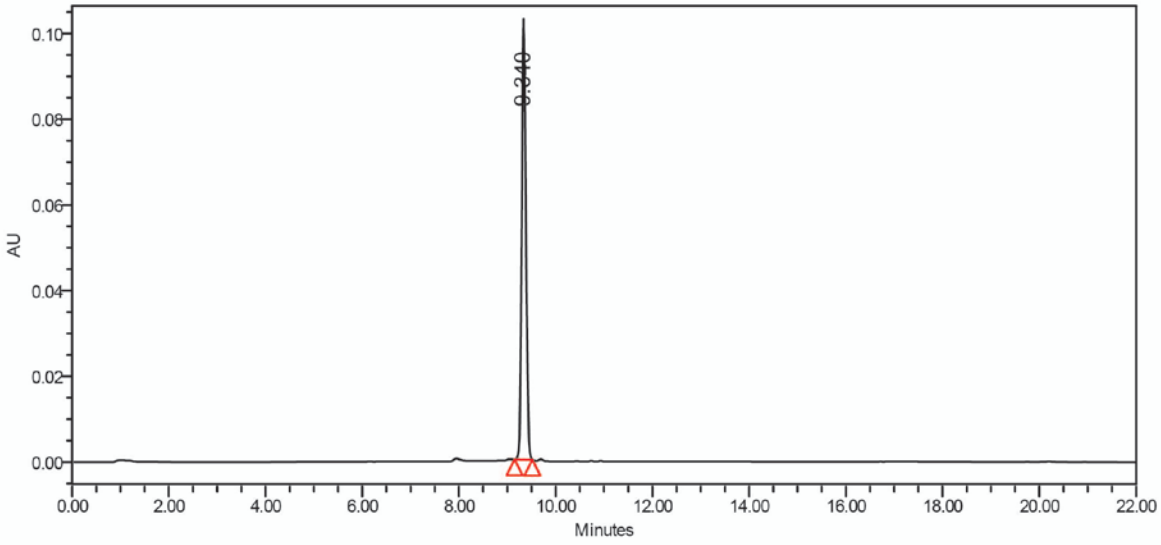

Peak Results

	RT	Area	Height	% Area
1	9.340	610375	101284	100.00

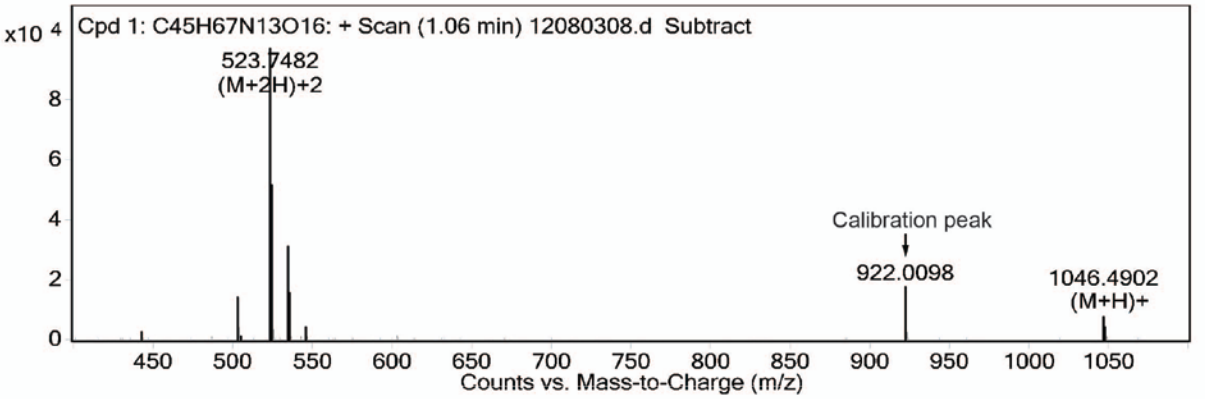

MS Spectrum Peak List

m/z	*Calc m/z*	Diff(ppm)	z	Abund	Formula	Ion
523.7482	523.7487	-1.05	1	96980	C45 H69 N13 O16	(M+2H)+2
1046.4902	1046.4901	0.08	1	7593	C45 H68 N13 O16	(M+H)+

--- End Of Report ---

Supporting information references

[1] M. Mayer, B. Meyer, *Angew. Chem. Int. Ed.* **1999**, *38*, 1784-1788.

[2] M. Liu, X.-a. Mao, C. Ye, H. Huang, J. K. Nicholson, J. C. Lindon, *J. Magn. Reson.* **1998**, *132*, 125-129.

[3] H. McWilliam, W. Li, M. Uludag, S. Squizzato, Y. M. Park, N. Buso, A. P. Cowley, R. Lopez, *Nucleic Acids Res.* **2013**, *41*, W597-W600.

[4] F. P. Schwarz, K. D. Puri, R. G. Bhat, A. Surolia, *J. Biol. Chem.* **1993**, *268*, 7668-7677.

[5] D. K. Mandal, C. F. Brewer, *Biochemistry* **1993**, *32*, 5116-5120.

[6] S. Ng, M. R. Jafari, W. L. Matochko, R. Derda, *ACS Chem. Biol.* **2012**, *7*, 1482-1487.

[7] O. Renaudet, P. Dumy, *Tetrahedron Lett.* **2001**, *42*, 7575-7578.

[8] K. A. Noren, C. J. Noren, *Methods* **2001**, *23*, 169-178.

[9] W. L. Matochko, S. Cory Li, S. K. Y. Tang, R. Derda, *Nucleic Acids Res.* **2014**, *42*, 1784-1798.

[10] T. D. Schneider, R. M. Stephens, *Nucleic Acids Res.* **1990**, *18*, 6097-6100.

[11] W. Kabsch, *Acta Crystallogr., Sect. D: Biol. Crystallogr.* **2010**, *66*, 125-132.

[12] N. Collaborative Computational Project, *Acta Crystallogr., Sect. D: Biol. Crystallogr.* **1994**, *50*, 760-763.

[13] P. D. Adams, P. V. Afonine, G. Bunkoczi, V. B. Chen, I. W. Davis, N. Echols, J. J. Headd, L.-W. Hung, G. J. Kapral, R. W. Grosse-Kunstleve, A. J. McCoy, N. W. Moriarty, R. Oeffner, R. J. Read, D. C. Richardson, J. S. Richardson, T. C. Terwilliger, P. H. Zwart, *Acta Crystallogr., Sect. D: Biol. Crystallogr.* **2010**, *66*, 213-221.

[14] I. W. Davis, A. Leaver-Fay, V. B. Chen, J. N. Block, G. J. Kapral, X. Wang, L. W. Murray, W. B. Arendall, J. Snoeyink, J. S. Richardson, D. C. Richardson, *Nucleic Acids Res.* **2007**, *35*, W375-W383.

[15] R. Kadirvelraj, B. L. Foley, J. D. Dyekjær, R. J. Woods, *J. Am. Chem. Soc.* **2008**, *130*, 16933-16942.

[16] M. O. Sinnokrot, E. F. Valeev, C. D. Sherrill, *J. Am. Chem. Soc.* **2002**, *124*, 10887-10893.

[17] M. G. Ford, T. Weimar, T. Köhli, R. J. Woods, *Proteins: Structure, Function, and Bioinformatics* **2003**, *53*, 229-240.

[18] D. A. Case, T. A. Darden, T. E. Cheatham, C. L. Simmerling, J. Wang, R. E. Duke, R. Luo, R. C. Walker, W. Zhang, K. M. Merz, B. Roberts, S. Hayik, A. Roitberg, G. Seabra, J. Swails, A. W. Goetz, I. Kolossváry, K. F. Wong, F. Paesani, J. Vanicek, R. M. Wolf, J. Liu, X. Wu, S. R. Brozell, T. Steinbrecher, H. Gohlke, Q. Cai, X. Ye, J. Wang, M.-J. Hsieh, G. Cui, R. D.R., M. D.H., S. M.G., R. Salomon-Ferrer, C. Sagui, V. Babin, T. Luchko, S. Gusarov, K. A., P. A. Kollman, *AMBER 12* **2012**, University of California, San Francisco.

[19] A. W. Götz, M. J. Williamson, D. Xu, D. Poole, S. Le Grand, R. C. Walker, *J. Chem. Theory Comput.* **2012**, *8*, 1542-1555.

[20] J.-P. Ryckaert, G. Ciccotti, H. J. C. Berendsen, *J. Comput. Phys.* **1977**, *23*, 327-341.

[21] T. Darden, D. York, L. Pedersen, *J. Chem Phys.* **1993**, *98*, 10089-10092.

[22] S. J. Hubbard, J. M. Thornton, *'NACCESS'* **1993**, Computer Program, Department of Biochemistry and Molecular Biology, University College London.

[23] A. Onufriev, D. Bashford, D. A. Case, *Proteins: Structure, Function, and Bioinformatics* **2004**, *55*, 383-394.

[24] K. T. Pilobello, P. Agrawal, R. Rouse, L. K. Mahal, *Curr. Protoc. Chem. Biol.* **2013**, *5*, 1-23.

[25] C. Cheadle, M. P. Vawter, W. J. Freed, K. G. Becker, *J. Mol. Diagn.* **2003**, *5*, 73-81.

[26] a) J. Sun, E. N. Kitova, W. Wang, J. S. Klassen, *Anal. Chem.* **2006**, *78*, 3010-3018; b) L. Deng, N. Sun, E. N. Kitova, J. S. Klassen, *Anal. Chem.* **2010**, *82*, 2170-2174.

[27] I. Coin, M. Beyermann, M. Bienert, *Nat. Protocols* **2007**, *2*, 3247-3256.

[28] Y.-W. Kim, T. N. Grossmann, G. L. Verdine, *Nat. Protocols* **2011**, *6*, 761-771.

NMR spectra of synthesized compounds

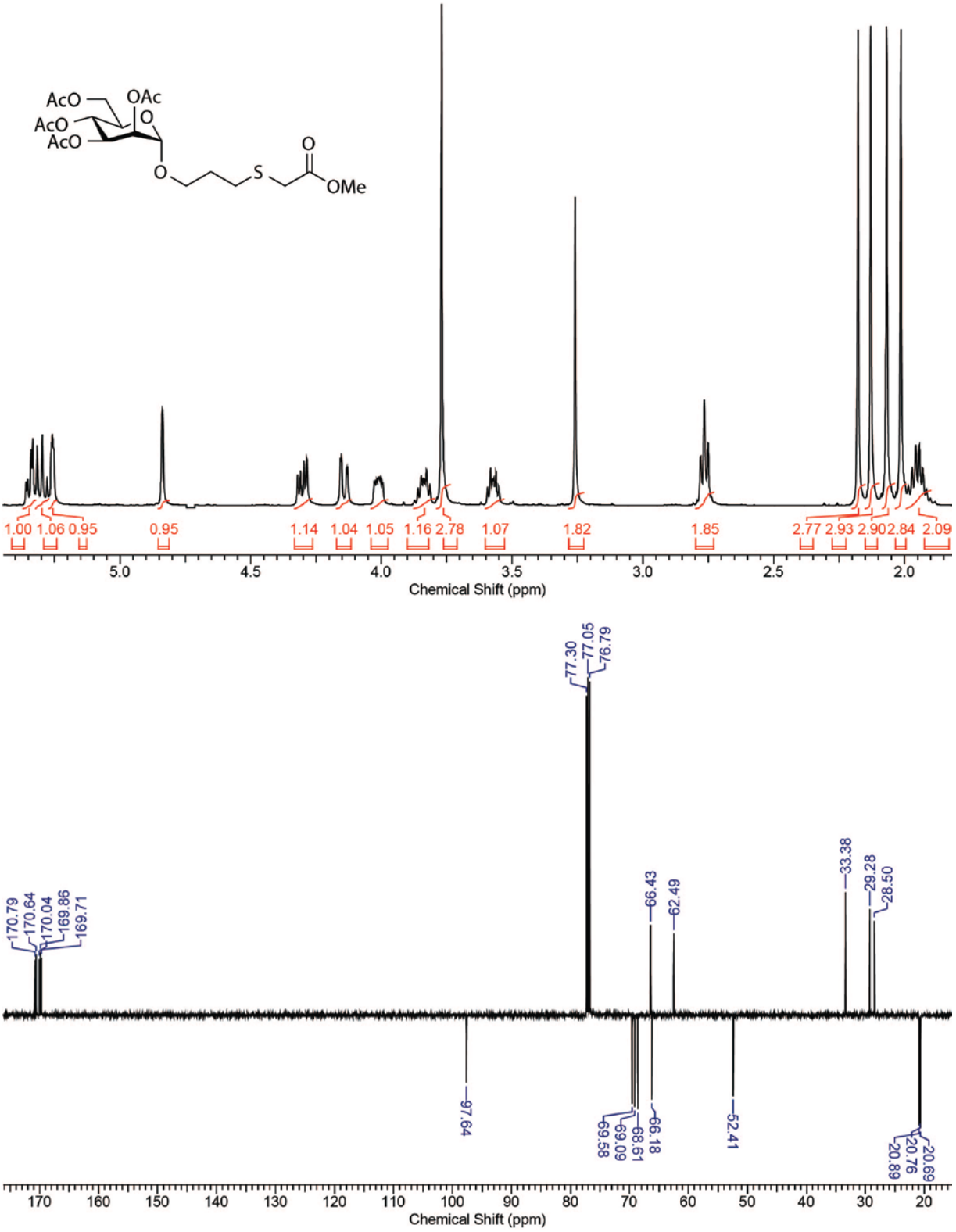

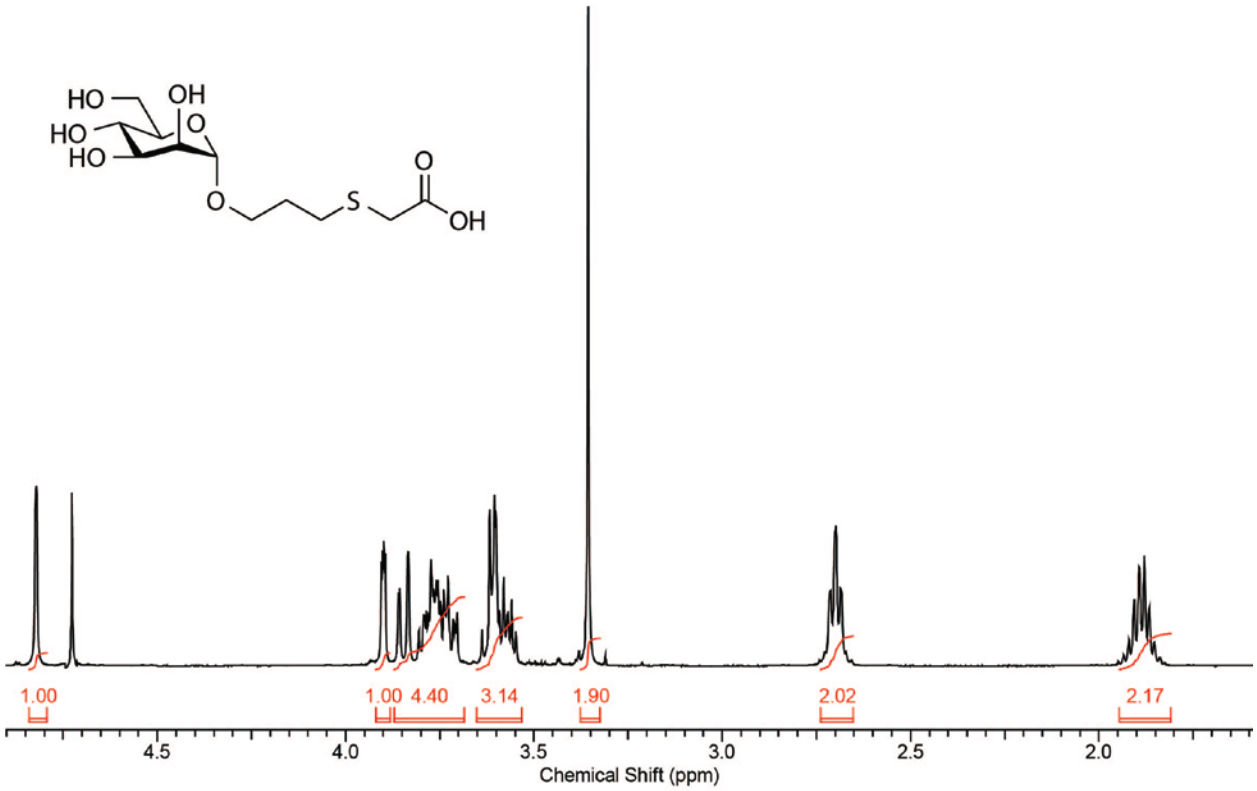
HO
OH
HO
O
HO
O
S
O
OH
1.00
1.00
4.40
3.14
1.90
2.02
2.17
4.5
4.0
3.5
3.0
2.5
2.0
Chemical Shift (ppm)

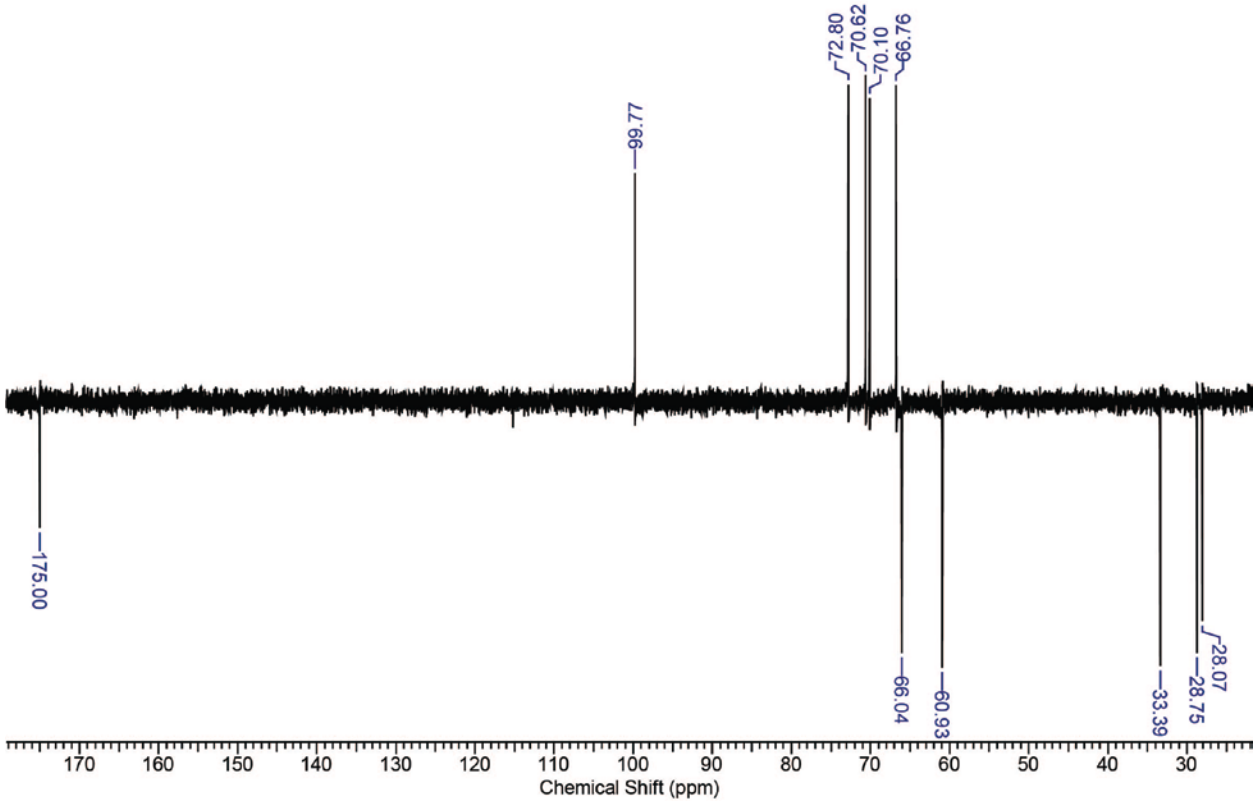
72.80
70.62
70.10
66.76
99.77
175.00
66.04
60.93
33.39
28.75
28.07
170
160
150
140
130
120
110
100
90
80
70
60
50
40
30
Chemical Shift (ppm)

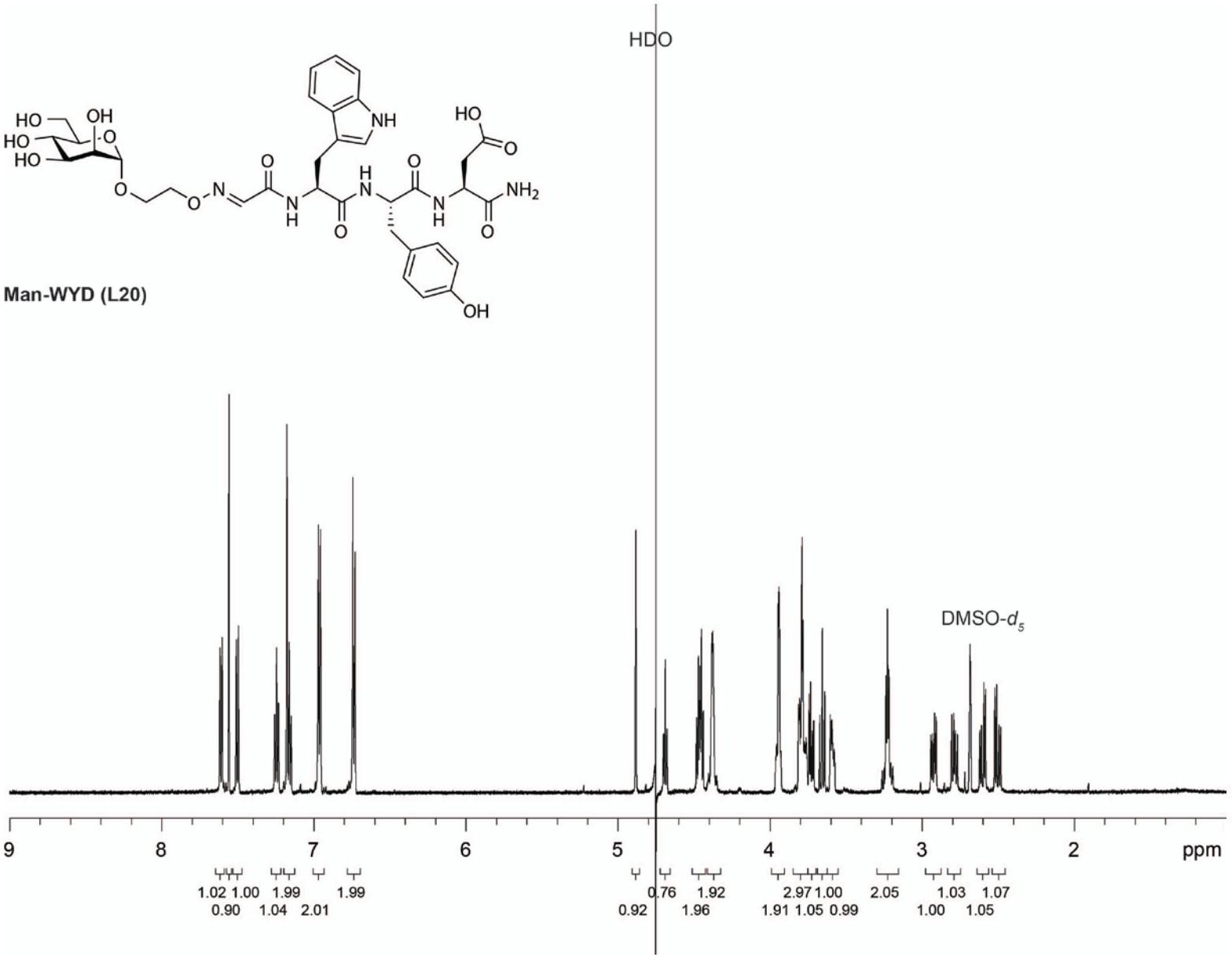
HDO
Man-WYD (L20)
DMSO-d_5
9
8
7
6
5
4
3
2
ppm
1.02 1.00 1.99 1.99
0.90 1.04 2.01
0.92 0.76 1.92
1.96
1.91 2.97 1.05 1.00 0.99
2.05
1.00 1.03 1.07
1.05

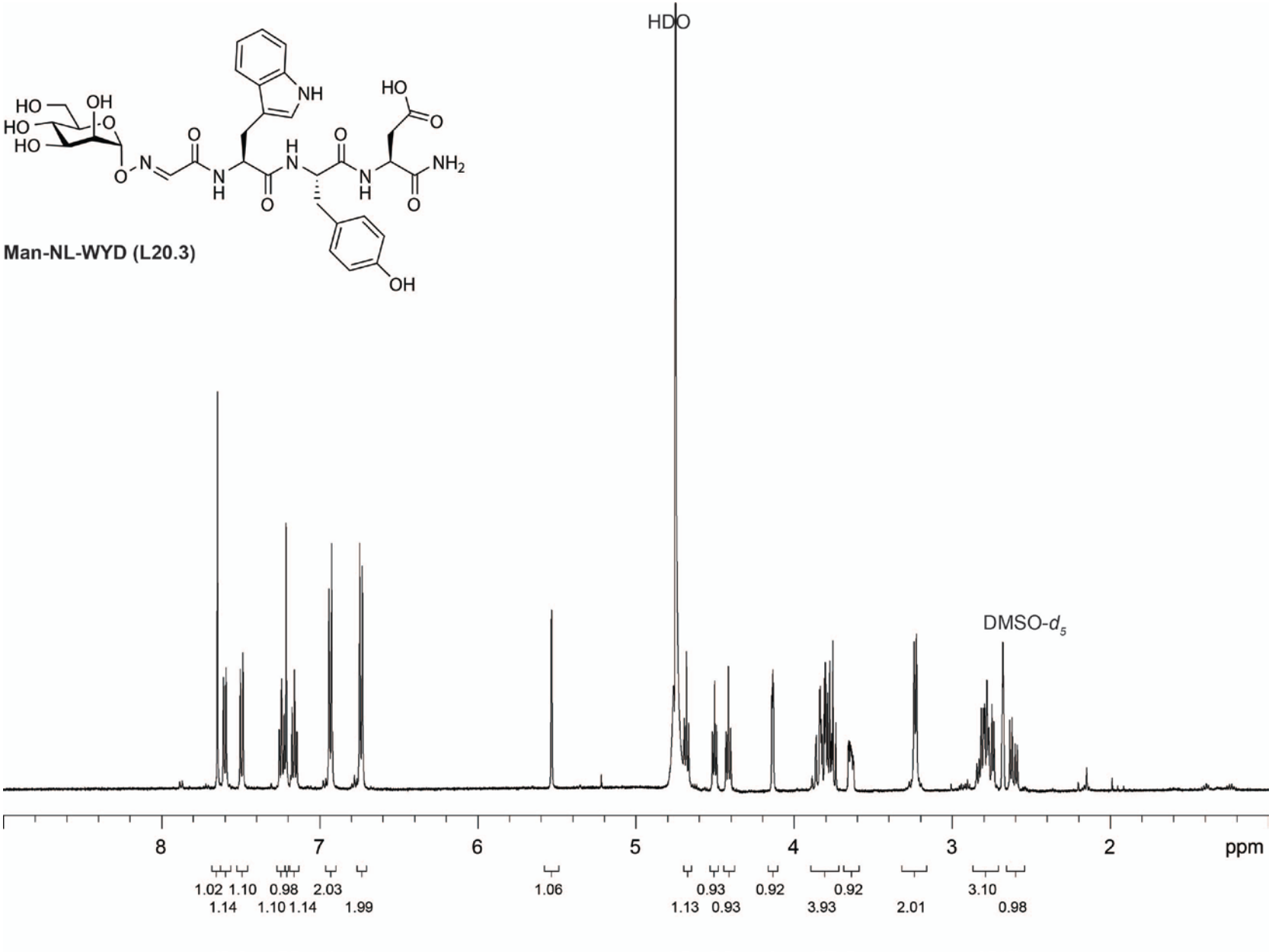
HDO
DMSO-d_5
Man-NL-WYD (L20.3)
8
7
6
5
4
3
2
ppm
1.02 1.10 0.98 2.03
1.14 1.10 1.14 1.99
1.06
0.93 0.92 0.92
1.13 0.93 3.93 2.01
3.10
0.98

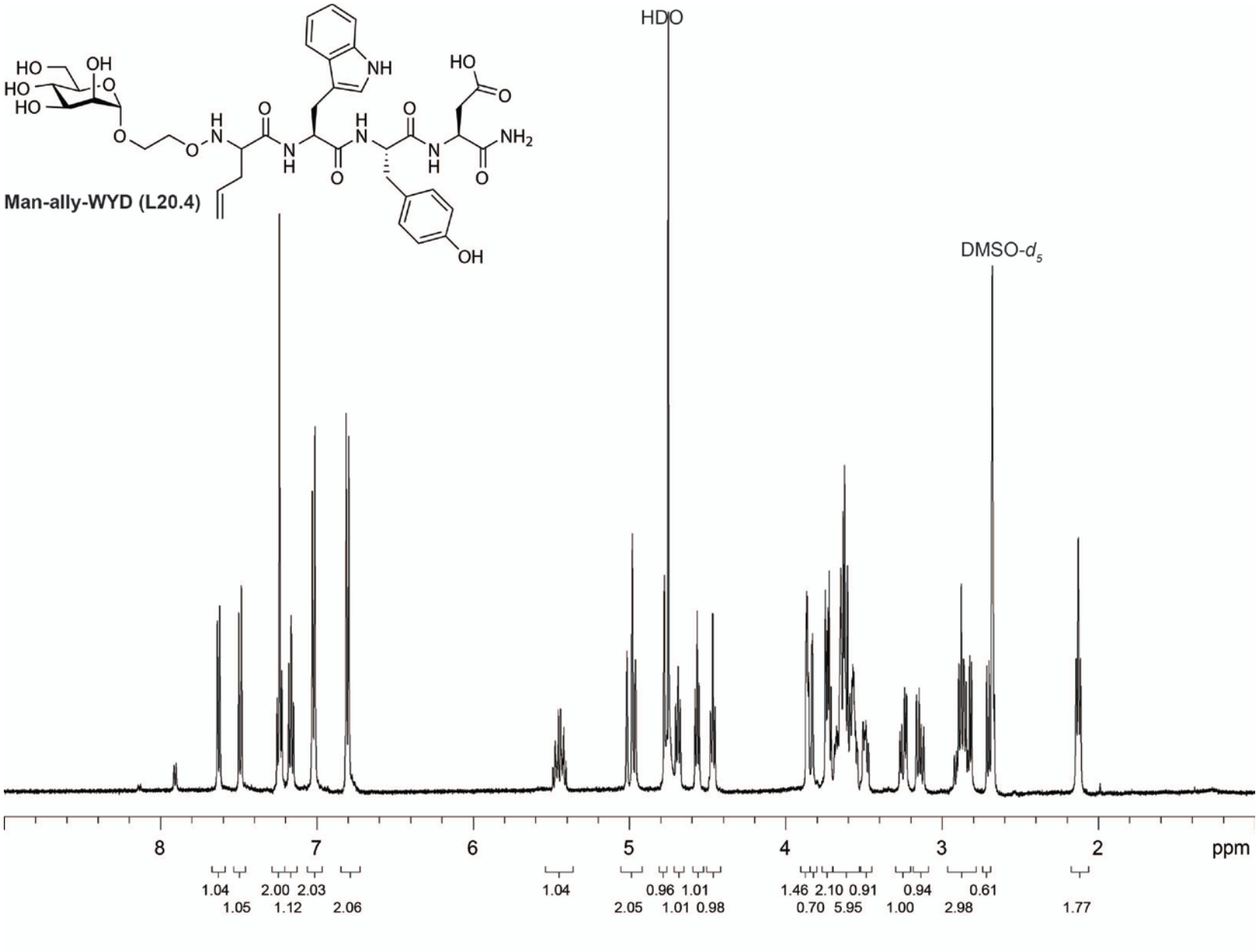
Man-ally-WYD (L20.4)
HDO
DMSO-d_5
8
7
6
5
4
3
2
ppm
1.04 1.05
2.00 1.12
2.03
2.06
1.04
2.05
0.96
1.01 0.98
1.01
1.46 0.70
2.10 5.95
0.91
0.94 1.00
2.98
0.61
1.77

^{1}H NMR Spectra in $CDCl_3$, 400

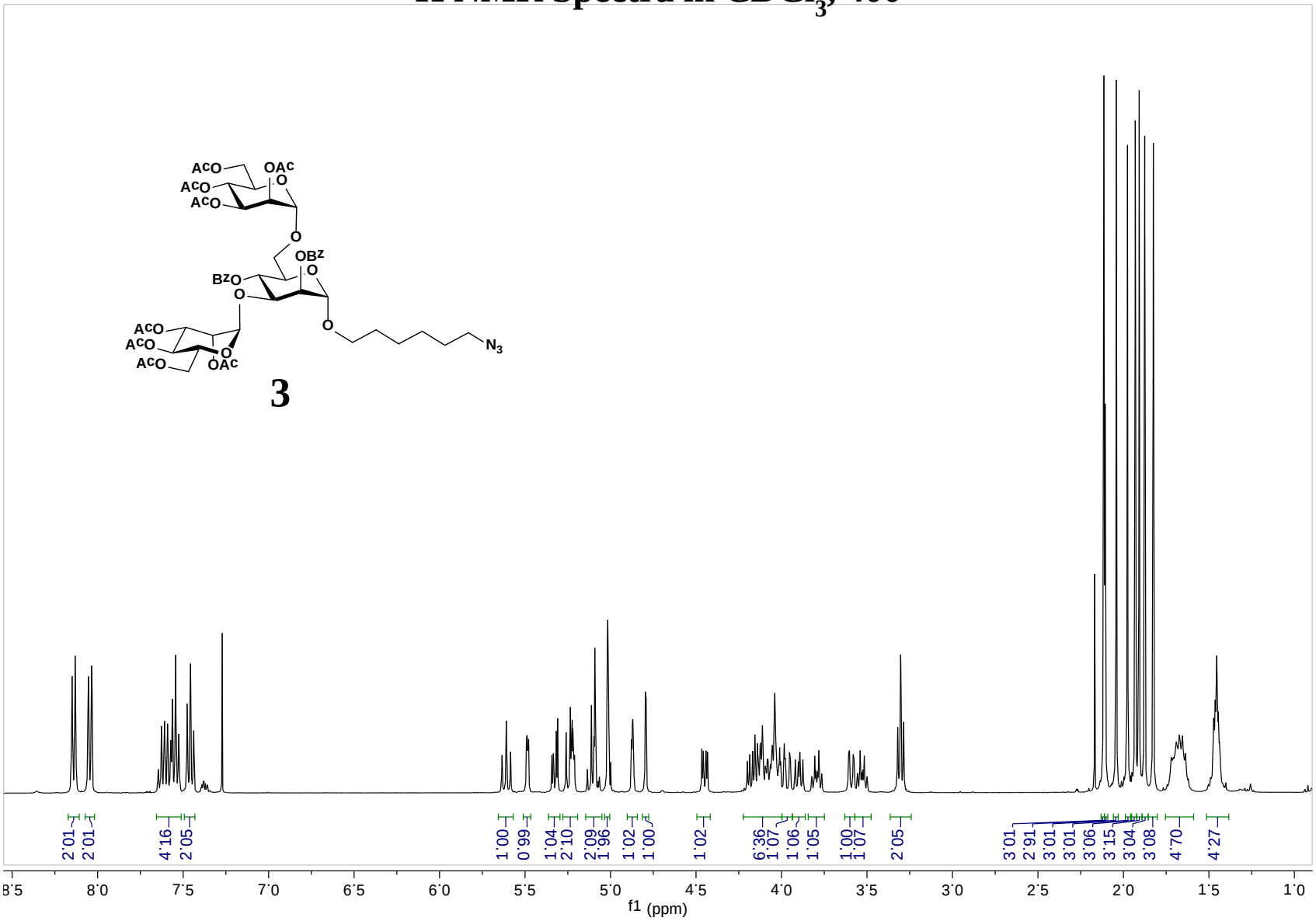

^{13}C DEPTQ NMR Spectra in $CDCl_3$, 100

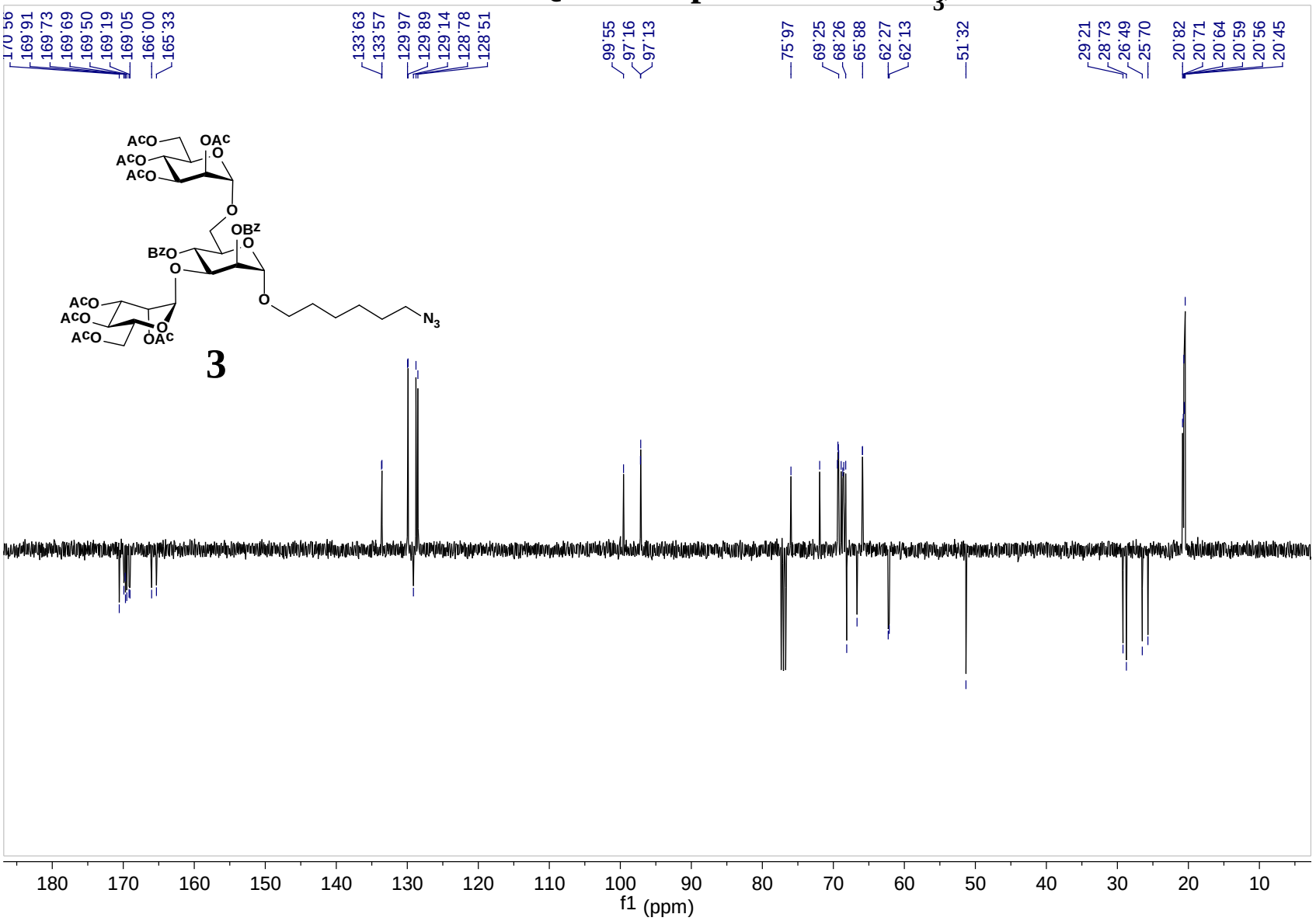

^{1}H-^{1}H GCOSY NMR Spectra in $CDCl_3$, 400 MHz

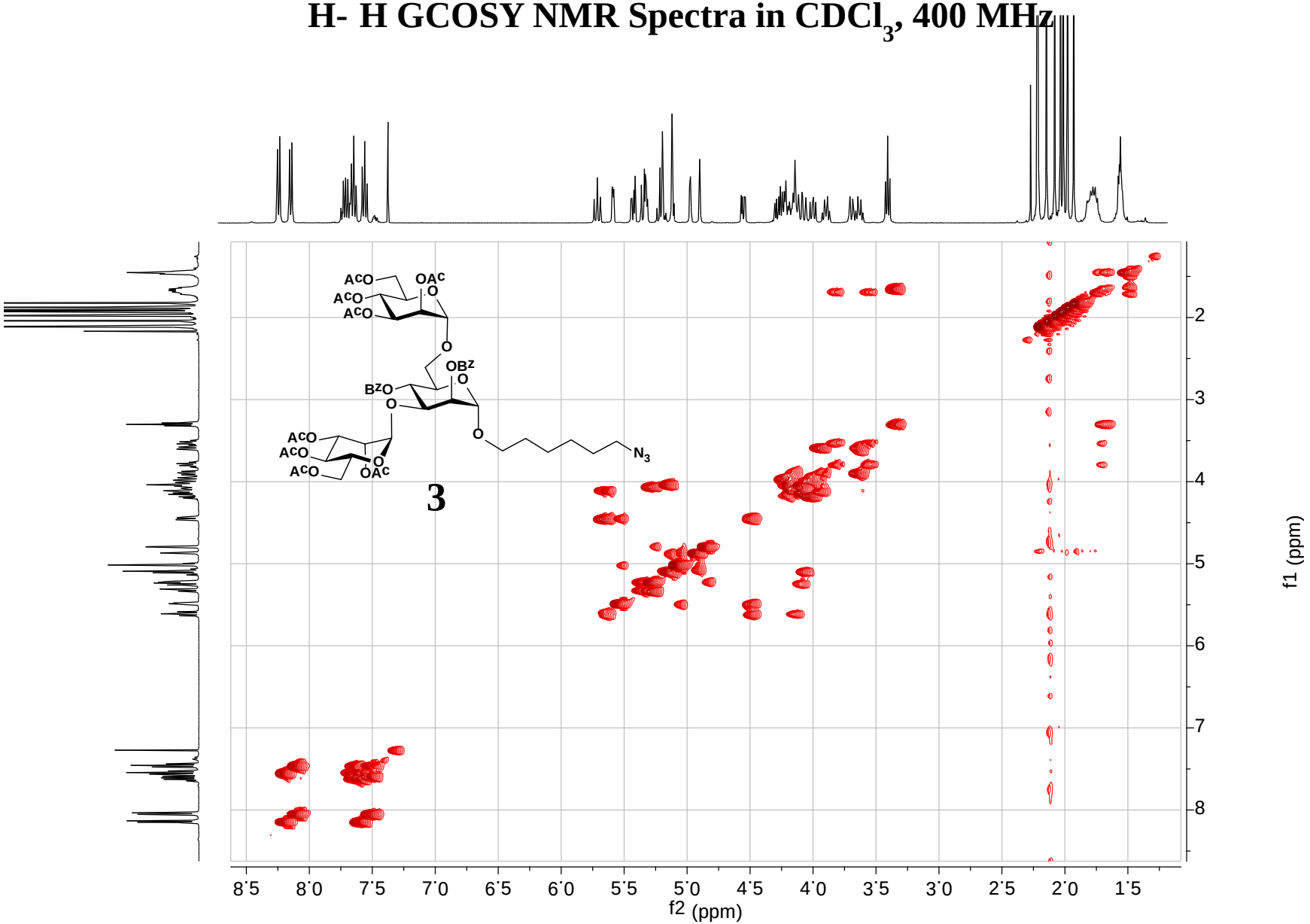

^{1}H-^{13}C HSQC NMR Spectra in $CDCl_3$, 400 MHz

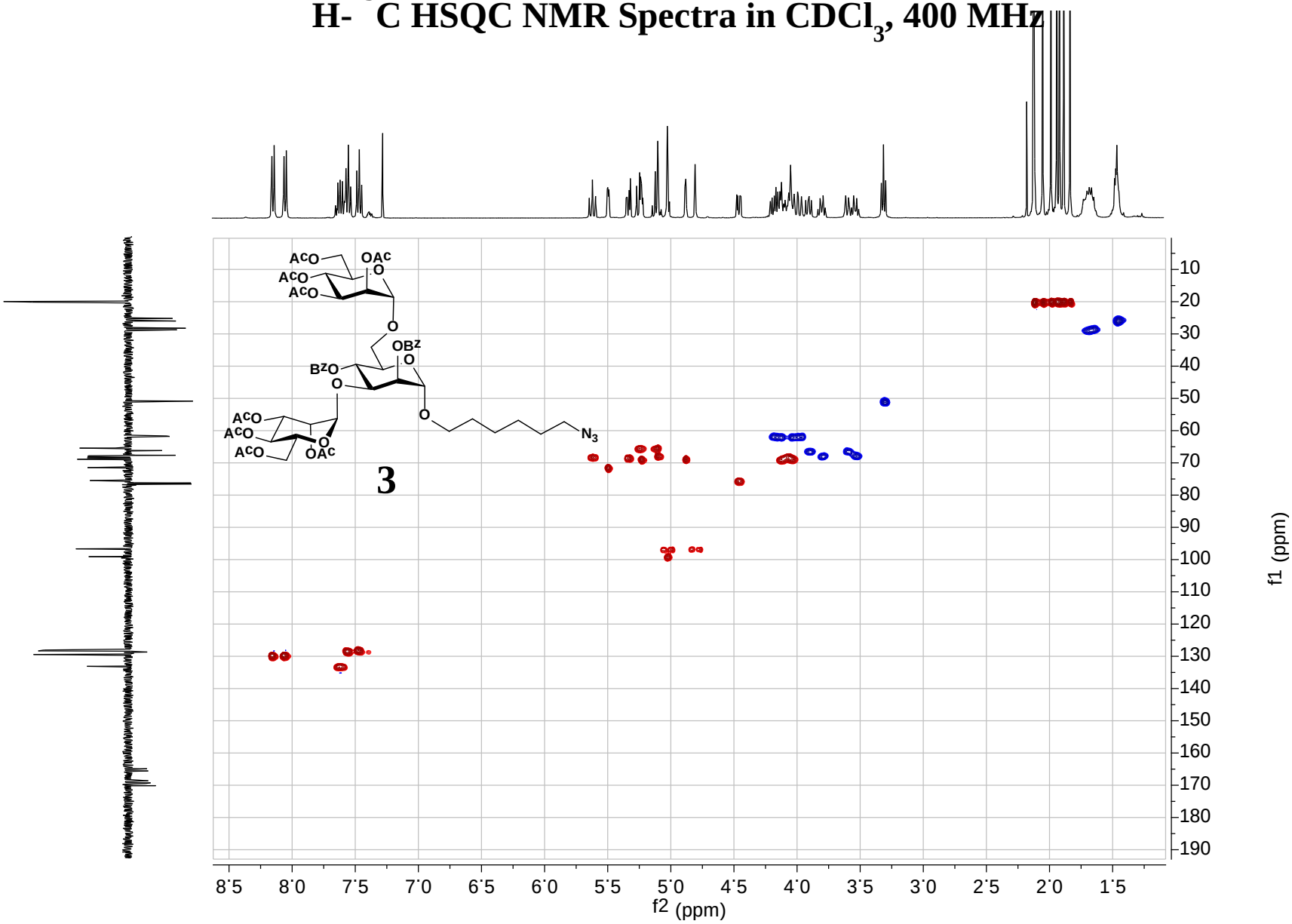

^{1}H NMR Spectra in D_2O, 600 MHz

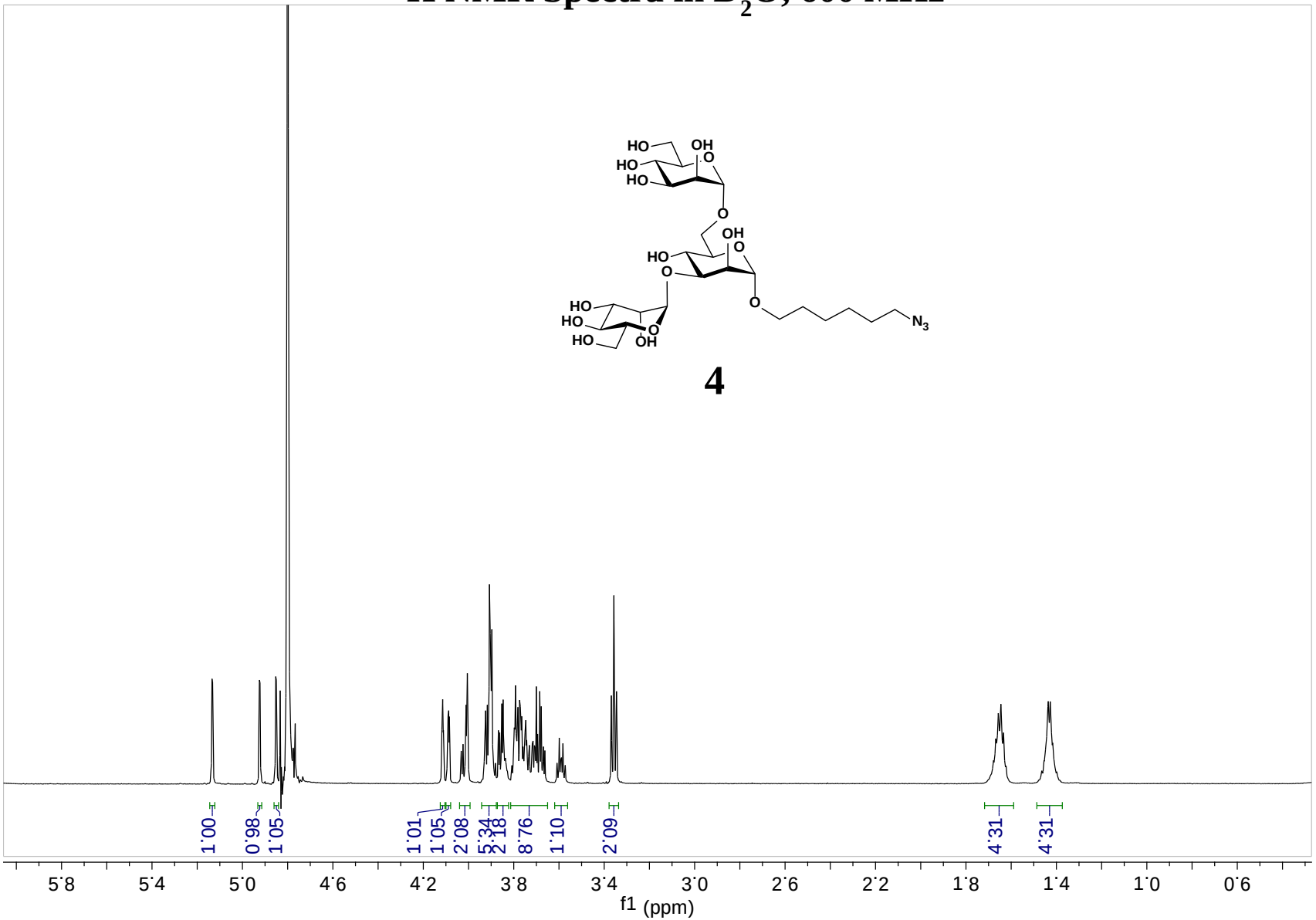

^{13}C DEPTQ NMR Spectra in D_2O, 150 MHz

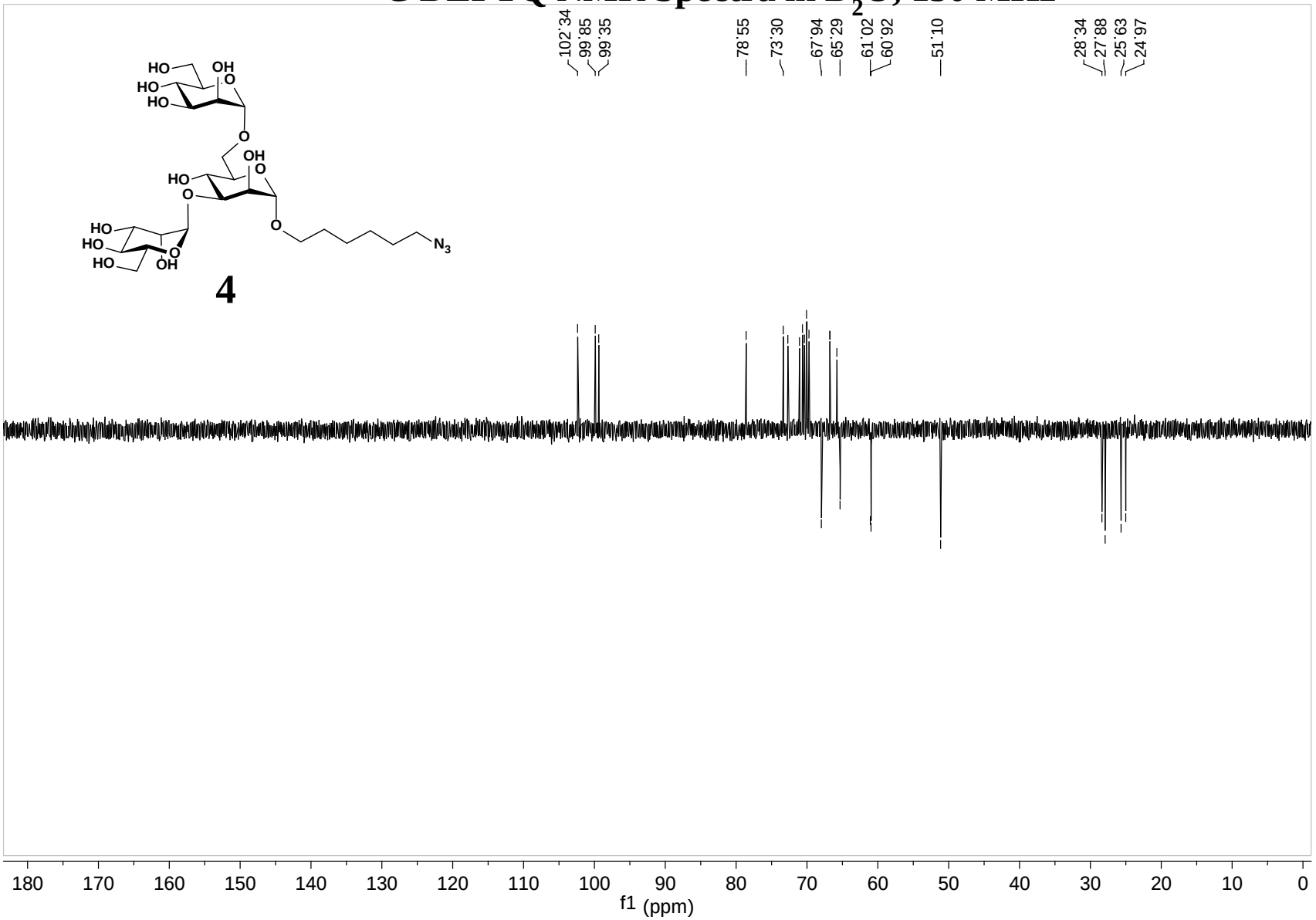

^{1}H-^{1}H GCOSY NMR Spectra in D_2O, 600 MHz

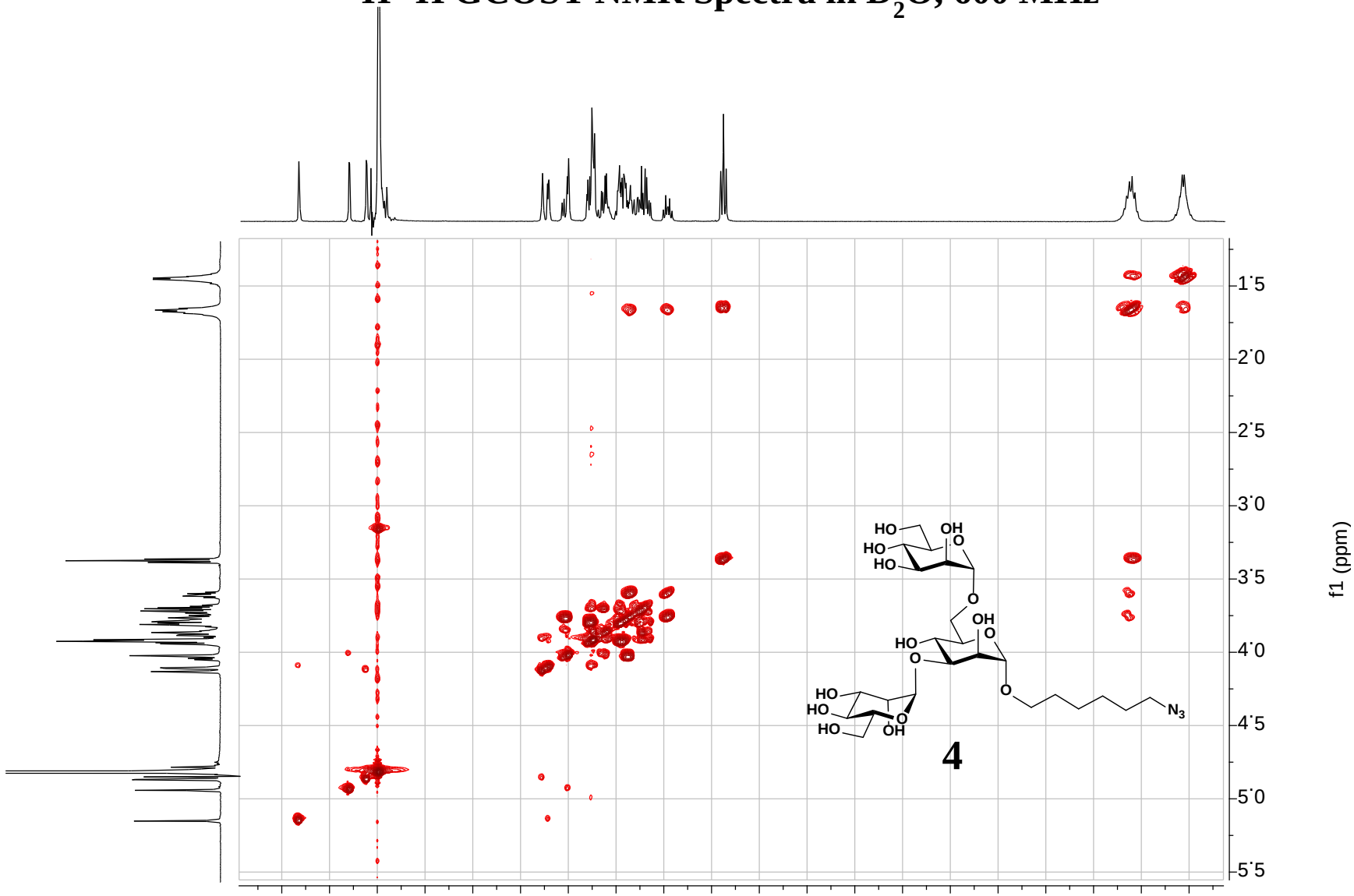

^{1}H-^{13}C HSQC NMR Spectra in D_2O, 600 MHz